АКУСТИЧЕСКИЙ ЖУРНАЛ

АКАДЕМИЯ НАУК СССР

SOVIET PHYSICS

Acoustics

VOLUME 1 NOS. 3 AND 4

A Translation

of the

Journal of Acoustics

of the

Academy of Sciences of the USSR

Published by the

AMERICAN INSTITUTE OF PHYSICS

INCORPORATED

SOVIET PHYSICS

Acoustics

A translation of the "Journal of Acoustics" of the USSR.

A publication of the

AMERICAN INSTITUTE OF PHYSICS

Governing Board

ALLEN V. ASTIN
WALTER S. BAIRD
JESSE W. BEAMS
HANS A. BETHE
RAYMOND T. BIRGE
RICHARD H. BOLT
FRANKLIN D. DEKTER
IRVINE C. GARDNER
SAMUEL A. GOUDSMIT
CHARLES KITTEL
HUGH S. KNOWLES
WINSTON E. KOCK
R. BRUCE LINDSAY
WILLIAM F. MEGGERS
WALTER C. MICHELS
R. RONALD PALMER
ROBERT F. PATON
JOSEPH B. PLATT
RALPH A. SAWYER
HENRY D. SMYTH
MARK W. ZEMANSKY

Officers and Staff

FREDERICK SEITZ
Chairman, Governing Board
ELMER HUTCHISSON
Director
HENRY A. BARTON
Associate Director
WALLACE WATERFALL
Executive Secretary
MARK W. ZEMANSKY
Treasurer
THEODORE VORBURGER
Advertising Manager
RUTH P. BRYANS
Publication Manager
KATHRYN SETZE
Assistant Treasurer
ALICE MASTROPIETRO
Circulation Manager
EUGENE E. KOHN
Director of Public Relations

American Institute of Physics Advisory Board on Russian Translations

ELMER HUTCHISSON, *Chairman*

DWIGHT GRAY, MORTON HAMERMESH, VLADIMIR ROJANSKY, VICTOR WEISSKOPF

"Soviet Physics—Acoustics" is published by the American Institute of Physics for the purpose of making available in English reports of current Soviet research in acoustics as contained in the "Journal of Acoustics" of the Academy of Sciences of the USSR, and will regularly consist of four issues per year.

Transliteration of the names of Russian authors follows the system employed by the Library of Congress.

This translating and publishing project was undertaken by the Institute in the conviction that dissemination of the results of research everywhere in the world is invaluable to the advancement of science. The National Science Foundation of the United States and the Office of Naval Research encouraged the project initially and are supporting it in large part by a grant. Translation and printing are being handled by Consultants Bureau, Inc.

The American Institute of Physics and its translators propose to translate faithfully all the scientific material in the "Journal of Acoustics" of the Academy of Sciences of the USSR appearing after January 1, 1955, the first year of its publication. The views expressed in the translated material, therefore, are intended to be those expressed by the original authors, and not those of the translators nor of the American Institute of Physics.

One volume is published annually. Volume 1 will contain all of the scientific material published in the original Russian journal during the calendar year 1955, and Volume 2 will contain all of the scientific material published in the original Russian journal during the calendar year 1956.

Subscription Prices:

Per year, beginning with Volume 2 (4 issues)	
United States and Canada	$20.00
Elsewhere	22.00
*Back Numbers (beginning with Volume 2)	
Single copies	$ 6.00

*Volume 1, consisting of two issues, is available only as a set at the yearly rates quoted above.

Subscriptions should be addressed to the American Institute of Physics, 335 East 45th Street, New York 17, New York.

Copyright by American Institute of Physics 1957

SOVIET PHYSICS

Acoustics

SOVIET PHYSICS – ACOUSTICS VOLUME 1, NUMBERS 3 AND 4

N. N. ANDREEV

(On his 75th birthday)

June 28, 1955 marks the 75th birthday of the great Soviet acoustic scientist, Academician Nikolai Nikolaevich Andreev. One cannot overestimate the value of Nikolai Nikolaevich's investigations in the field of physics and technical acoustics to the Soviet national economy and to the development of the theoretical foundations of acoustic science.

Scientific and pedagogical activity of N. N. Andreev began 55 years ago, when as an auditor in the first year of the Moscow University (1900-1901) he served as assistant to mathematics professor N. V. Bugaev. He continued his education in Germany (1904-1909), first in Goettingen, then in Basel, frequently returning to his fatherland, where he carried out various engineering projects which served as his source of income.

His first scientific work was "Theoretical and experimental investigation of the effect of temperature on the dispersion of light," for which the Basel University awarded him in 1909 the degree of Doctor of Philosophy cum laude.

Returning to the fatherland after graduation, N. N. Andreev taught physics for some time (1909-1917) in Moscow schools. Dating from approximately the same period is the publication of many articles, brochures, and papers which popularized the accomplishments of science and engineering: acoustics, theory of relativity, wave mechanics, thermodynamics, and electrodynamics. In 1922, the first scientific-popular journal "Iskra" was founded in the Soviet Union through N. N. Andreev's initiative and with active participation.

N. N. Andreev's scientific activity developed in parallel with his school teaching. Working as a laboratory assistant in the Moscow University (1912-1914), N. N. Andreev passed his Magister's examinations, receiving the title of Lecturer and defending a Master's thesis on "Electric oscillations and their spectra" (1917). Problems in oscillations became the backbone of N. N. Andreev's fruitful scientific work in 1909-1919. Worthy of particular notice is the exceedingly clear and profound analysis "Grating, prism, resonator" (1915), in which he considers the spectra of damped waves and the effect of a diffraction grating, resonator, and a refracting prism on such waves. These works retain their significance to the present day.

Closely related to N. N. Andreev's scientific activity is his teaching work. The young scientist became professor of physics in the Omsk Polytechnic and Omsk Agricultural Institutes (1918-1920), having already gained experience in delivering a series of lectures in the Moscow University on the electron theory of dielectrics, on statistical mechanics, on the theory of relativity, and on tensor analysis (1914-1917). The principal field of

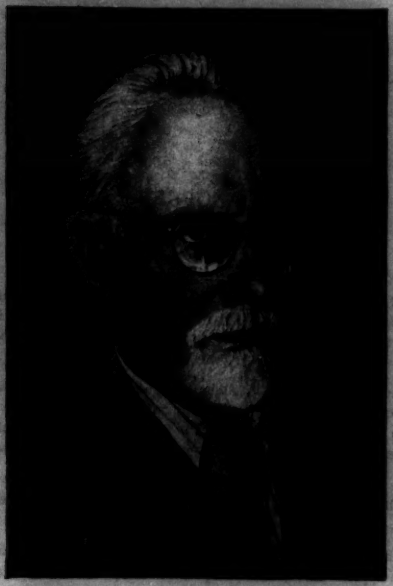

N. N. Andreev

N. N. Andreev's scientific interest took form in the 1920-1926 period. During these years he organized the Acoustical Laboratory of the State Experimental Electrotechnical Institute in Moscow, which he headed until he moved to Leningrad (1926), where he organized the Acoustical Laboratory of the Leningrad Physical-Technical Institute (LFTI). There N. N. Andreev collected and trained a large group of young Soviet acoustic scientists, who performed under his leadership many interesting and important investigations on theoretical and technical acoustics. The cadres of this laboratory went on later to organize research on acoustics in many scientific-research institutes.

When he undertook research in the field of acoustics, N. N. Andreev was faced with the need of calling principal attention to the method of acoustic measurements and to the acoustic experimental techniques. The vigorous development of Soviet radio broadcasting and communication engineering and the need for investigating and developing new types of telephones, microphones, and loudspeakers, called for improvements in methods of testing acoustic apparatus and for new methods of measuring acoustic quantities. The investigations of Russian scientists P. N. Lebedev, V. D. Zernov, and V. Al'tberg were successfully applied and improved on by N. N. Andreev and his co-workers.

In addition, Nikolai Nikolaevich himself created many original and yet simple methods for acoustic measurements. It is enough to mention here the elegant and precise method for absolute measurement of amplitudes of mechanical vibrations of solids – the fine-sand method. The "technical amplitude meter" suggested by Nikolai Nikolaevich made it possible to measure vibration amplitudes of solids with great accuracy and over a wide frequency range. Using this instrument, N. N. Andreev and N. N. Riabinina investigated all details of vibrations of telephone membranes and studied the properties of a single-contact carbon microphone. N. N. Andreev's amplitude meter was also used by A. L. Belov to study the directivity of radiation from loudspeakers. Under the direction of N. N. Andreev and using one of his ideas, M. L. Rodman developed an improved method for automatic frequency analysis of electric and acoustic oscillations. Many such instruments were built and used in acoustic investigation in many institutes and laboratories of the Soviet Union. Analyzers of this type are even now considered the better instrument for automatic analysis. N. N. Andreev and A. L. Belov developed methods for measuring acoustic impedances and methods for investigating acoustic filters. Mention should be made of work on design of noise meters (L. S. Freiman, A. L. Bronshtein) and work on design of a reverberation meter, carried out under the initiative of N. N. Andreev. N. N. Andreev's work on the theory of acoustic four-terminal networks as applied to mufflers for internal combustion engines has been a great contribution to technical acoustics.

It should be noted that the theory of propeller sound was developed by N. N. Andreev with his co-workers in 1933, before such work was done abroad. In the field of atmospheric acoustics N. N. Andreev developed the theory of propagation of sound near the earth's surface. In the winter of 1932-1933 he participated directly in planning and carrying out experiments on the sounding of the stratosphere in polar latitudes. Together with I. G. Rusakov, N. N. Andreev developed the basic premises of the acoustics of moving media.

Soviet-Union development of piezoelectric apparatus was greatly dependent on the fundamental work by N. N. Andreev, "Equilibrium and oscillations of piezoelectric crystals" (1928).

N. N. Andreev was the first to propose the widely-used bimorphous element of Rochelle salt. The research performed by the Soviet scientist G. D. Shul'vas-Sorokina on the properties of Rochelle salt were started under his leadership and at his initiative, as were the works performed by V. N. Fedorovich on piezoelectric sound pickups for phonograph records.

N. N. Andreev and his students stated and solved many problems in nonlinear acoustic oscillations and the related effects of sound pressure (radiation pressure), sonic wind, and also the problems of hydrodynamic sound formation. It is necessary to mention here the work by I. G. Rusakov (on sonic wind) and the work by N. N. Andreev, B. P. Konstantinov, and A. L. Bronshtein, who have clarified many difficult problems in nonlinear acoustic oscillations.

The first specialized Scientific-Research Institute for the Musical Industry (NIIMP) in the world was organized in 1931. Its founder and scientific leader was N. N. Andreev. The Soviet musical industry was confronted by important problems – freedom from the need of importing high quality lumber (so-called "resonant fir"), and

development of the physical research and quality control of musical instruments. N. N. Andreev resolved radically the problem of obtaining Russian wood for musical instruments by studying the physical and mechanical properties of wood and by formulating acoustic requirements with respect to these properties. The problem of building different musical instruments and of so-called "tempering" to determine the rational dimensions of vibrators and musical instruments (strings, accordion reeds, brass horns and wooden musical instruments) were successfully solved at the NIIMP by A. I. Belov, B. P. Konstantinov, and A. V. Rimskii-Korsakov with N. N. Andreev directly participating. Of particular interest is the work by B. P. Konstantinov and A. V. Rimskii-Korsakov on sound formation in string and wind instruments, initiated by N. N. Andreev while still at the LFTI and finally solved at the NIIMP. At the initiative of Nikolai Nikolaevich, A. A. Kharkevich designed at the same institute apparatus for reproducing phonograph records, and also prepared an original and profound exposition on the theory of electroacoustic apparatus.

Nikolai Nikolaevich's scientific activity in Leningrad continued to be closely related with his pedagogical work. There he became prominent as a teacher of special theories, and as Professor at the M. I. Kalinin Leningrad Polytechnic Institute (1926-1938), and later in charge of the Acoustics Department (1936-1938), he trained many Soviet acoustical engineers. Later on Nikolai Nikolaevich was the chief of the department and of the acoustics laboratory organized by him in the Budenny Military Electrotechnic Academy of Communications. After he left the Academy of Communications, the acoustical laboratory was named the "Professor N. N. Andreev Laboratory of Electroacoustics." During that time Nikolai Nikolaevich prepared an original course of lectures on general acoustics.

In 1933, N. N. Andreev was chosen associate member of the U.S.S.R. Academy of Sciences. In 1936 he organized at the U.S.S.R. Academy of Sciences an Acoustics Commission, which to this day organizes conferences and meetings on various scientific-technical problems. The commission has published eight collections. These collections contain many works by N. N. Andreev, partly co-authored by E. E. Lysenko, on problems of sound absorption. Starting with 1955, the Proceedings of the Acoustics Commission were superseded at Nikolai Nikolaevich's initiative, by the "Journal of Acoustics of the U.S.S.R. Academy of Sciences."

The Leningrad period of N. N. Andreev's activity lasted until to 1940 when he assumed work at the Academy of Sciences and became in charge of the acoustic laboratory of the P. N. Lebedev Physics Institute of the U.S.S.R. Academy of Sciences in Moscow (FIAN), in which he carries on his principal scientific activity.

As early as 1937, N. N. Andreev started solving problems in architectural acoustics, arising in connection with the design of the Palace of the Soviets in Moscow. At his initiative, cadres of scientific workers in architectural acoustics and electroacoustics were organized into an acoustics sector during the construction of the Palace of the Soviets. Here, in Moscow, Nikolai Nikolaevich again comes forth as an organizer and inspirer of a large creative group of acoustical scientists. Thus, for example, G.D. Maliuzhinets solves problems in sound absorption, L. D.Rozenberg carries out work on the investigation of distributed sound-amplifier and sound-reproducing systems, G. A. Gol'derg performs calculations on the investigation of acoustic feedback in complex systems, Iu. M. Sukharevskii works on experimental and theoretical studies of concentrated sound-amplifying systems, V. S. Grigor'ev works on electroacoustic apparatus and procedures for architectural-acoustic measurements, and M. S. Antsiferov works in the field of research on sound and vibration insulation. The above research was the foundation for Soviet architectural acoustics and sound distribution.

To exercise control over the scientific phases of the above works, N. N. Andreeve created a special brigade at the Acoustics Commission of the Academy of Sciences, the work of which was pointed out many times an example of successful combination of science and engineering practice.

During the great war of the fatherland, the FIAN laboratory under the leadership of N. N. Andreev carried out many important tasks. He and a group of his coworkers spent much time directly at the front, solving energetically on location problems of great significance for the Navy. For these activities Nikolai Nikolaevich was awarded the Order of the Red Banner of Labor (1944).

In the post-war years, the laboratory has continusouly grown and developed under the leadership of Nikolai Nikolaevich and by the end of 1953 it was reorganized as the Acoustics Institute of the U.S.S.R. Academy of Sciences. Always attaching great significance to theory, Nikolai Nikolaevich contributed to the development

of the theoretical section of the FIAN acoustics laboratory. At the present time the theoretical division of the Acoustics Institute, which has grown out of this section, and which is now headed by Associate Member of the U.S.S.R. Academy of Sciences L. M. Brekhovskikh, is a strong center of theoretical acoustics with a staff of prominent acoustical theoreticians (M. A. Isakovich, G. D. Malinzhinets, and others).

From among the works of the post-war years performed by Nikolai Nikolaevich, mention must be made of the "Method of averaging in the solution of wave problems," in which he suggested a new and very elegant method of solving problems on the propagation of sound waves in a plane-parallel layer and in a wedge, and also the work "On the Lorenz-Lorentz equation for crystals," printed in a collection devoted to the memory of S. I. Vavilov, in which he gave, in addition to a critique of the wrong approaches to this problem, also an accurate expression for a crystal of any symmetry. Mention must also be made of the research done by Nikolai Nikolaevich and his co-workers (N. A. Roi, A. A. Ana'eva, and I. P. Goliamina) on the piezoelectric properties of polarized barium titanate ceramics, and also on radiators and receivers made of this material.

In the Acoustics Institute, N. N. Andreev is in charge of the laboratory in which many interesting problems in physical acoustics are being studied. Along with continuing research on piezoelectric properties of materials, he started investigation on magnetostriction and cavitation in liquids. Nikolai Nikolaevich is also solving problems in nonlinear acoustics, in which he has long been interested. Thus, his last work "On certain second-order quantities in acoustics," which contains a profound analysis of the density and flux of sound energy and of the momentum and pressure of sound radiation, is the beginning of a series of investigations he is planning in the field of nonlinear acoustics.

The great creative activity carried on by Nikolai Nikolaevich with tremendous energy for many years has not kept him, a physicist with an all-around education, from actively engaging in literary labor or from editing scientific journals. Nikolai Nikolaevich has been continuously a member of the editorial staff of the Journal of Technical Physics of the U.S.S.R. Academy of Sciences from the instant it was founded, and also edited the Proceedings of the Acoustics Commission, the Journal of the Theoretical and Experimental Physics of the U.S.S.R. Academy of Sciences, and now is the editor-in-chief of Journal of Acoustics of the U.S.S.R. Academy of Sciences. Nikolai Nikolaevich has written many sections in the general course in physics for higher schools, published under the editorship of Academician N. D. Papaleksi.

For fruitful and varied scientific, pedagogical, and scientific-organizational activity, N. N. Andreev was awarded many orders and medals, including two orders of Lenin and the Order of the Red Banner of Labor.

In 1953 Nikolai Nikolaevich was chosen a full member of the Academy of Sciences of the U.S.S.R.

Nikolai Nikolaerich Andreev has a lively interest in the scientific work of his co-workers and students. Rapidly grasping the essence of the arising problems, thanks to his wide erudition, thorough knowledge of the classical works on theoretical physics, and the latest advances in science, Nikolai Nikolaevich is always ready to give useful advice, to make a critical remark, or to point the necessary direction to be followed by a young scientific worker in his future work.

The invariable high spirits and high principles in science and in social life help Nikolai Nikolaevich still carry with distinction, in his 76th year, the calling of a Soviet scientist and outstanding man of our era. We wish Nikolai Nikolaevich Andreev many more years of health, vigor, and success in the matter to which he devoted his life — in science.

MOTION PICTURE THEATER LOUDSPEAKER WITH SCATTERING SOUND LENS

B. G. Belkin

Description of a duplex motion picture theater loudspeaker having a scattering sound-lens with variable index of refraction in its high frequency radiator.

A description of a scattering sound lens with a variable index of refraction, intended for operation in the range of audible frequencies is given in [1]. The "Kinap" motion-picture equipment plant of Leningrad has set up production of such lenses and these are now available under code number 5A-8 as part of the 30A-3 motion picture theater loudspeaker.

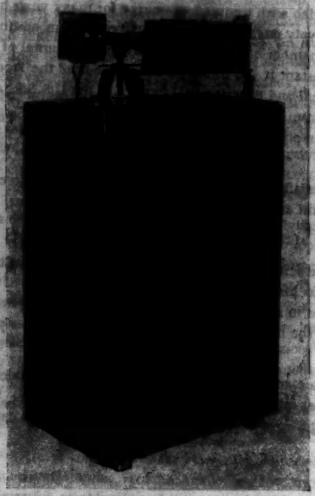

Fig. 1. 30A-3 motion picture theater loudspeaker with scattering sound lens.

The external view of the 30A-3 loudspeaker with sound lens is shown in Fig. 1. This is a duplex unit, intended for motion picture theaters of medium seating capacity. It consists of a low-frequency cone element 2A-9, mounted in a reflex cabinet, and a high frequency horn element operating with a sound lens. Two such loudspeakers are used with one 40-watt single-channel amplifier. The frequency division is by means of a cross-over filter, connected at the amplifier output; the cross-over frequency is 800 cycles.

Up to recently, the high frequency radiator of the 30A-3 loudspeaker employed a multicellular horn (code 5A-7), having quite satisfactory directivity characteristics; broadening these characteristics would result only in deteriorating the quality of the sound, owing to increased reflections from the side walls of the theater. The purpose of replacing the multicellular horn with a scattering lens was principally therefore not to broaden the directivity characteristics of the radiator, but to simplify and reduce the cost of the entire construction. It was possible at the same time to improve somewhat the directivity characteristics at high frequencies.

A sketch of the 5A-8 lens, indicating the basic dimensions, is shown in Fig. 2. This lens is made of 1.2 mm sheet steel. The individual plates are first stamped out and then welded into a single unit, which in turn is welded to the horn. It is easy to see that this lens converts the plane wavefronts into diverging

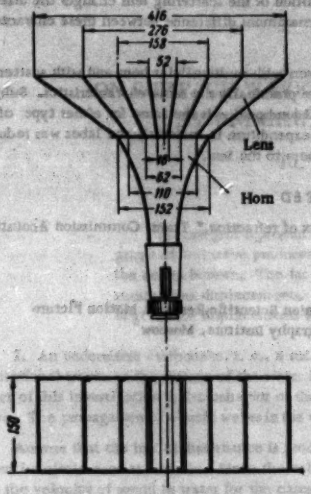

Fig. 2. Sketch of 5A-8 scattering sound lens.

cylindrical front, i. e., has a scattering effect only in the horizontal plane.

The directional properties of the loudspeaker in the vertical plane depend entirely on the horn that feeds the lens. Inasmuch as the 30A-3 loudspeaker is designed for use in medium motion picture theaters without balconies, a broad directivity pattern in the vertical plane is not only unnecessary, but is even not recommendable for evident reasons. The use of a cylindrical-type lens is therefore fully justified in this case. The focal distance of the 5A-8 lens is 30 cm, and the rated aperture angle is 35°. The area of the inlet opening is 15 x 15 cm^2, the outlet opening is 15 x 41.6 cm^2. The lens contains a total of eight plates, this number having been determined experimentally. Measurements have established that changing the number of plates from twenty-eight to eight hardly affects the properties of the lens, but that further reduction in the number of plates sharpens considerably the directivity pattern.

The calculated directivity characteristic of this lens is shown in Fig. 3.* The same figure shows the experimentally determined directivity characteristics of the multicellular 5A-7 horn and of the lens; these data hold for frequencies of 3 kc and above, for only

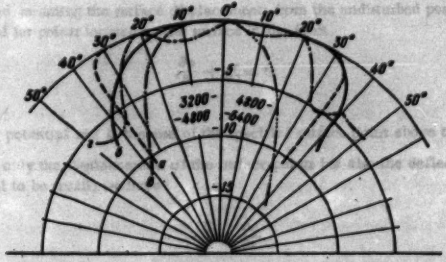

Fig. 3. Directivity characteristics of high-frequency radiator of 30A-3 loudspeaker. a) Calculated characteristic with scattering lens; b) experimental characteristic of radiator with scattering lens; c) experimental characteristic of radiator without scattering lens; d) experimental characteristic of radiator with multicellular horn.

at these frequencies does the scattering effect of the lens manifest itself. Measurements were made with semi-octave bands of white noise in free space; the distance from the radiator to the microphone was about 5 m. It is easily seen that at higher frequencies the directivity characteristics produced by the lens are not worse and are even better than those of the multicellular horn. We will not give the results of measurements made at

* [1] gives a simplified method for the calculation of the structural dimensions of lenses with variable index of refraction, as well as of their directivity characteristics.

lower frequencies (in the 800-3200 cycle range), for here the addition of the scattering lens changes the directivity characteristics of the exponential horn only slightly — the maximum difference between these characteristics does not exceed 3 db.

Measurements of the frequency characteristics of loudspeakers with multicellular horn and with scattering lens, performed under usual conditions, have shown that both have practically the same characteristics. Subjective tests have also confirmed that the sound quality of the 30A-3 loudspeaker is the same for either type of high-frequency radiator. In conclusion let us point out, that the expenditure in materials and labor was reduced by approximately one half by changing from the multi-cellular horn to the lens.

LITERATURE CITED

[1] B. G. Belkin, "Scattering sound lens with variable index of refraction," Trans. Commission Acoustics 8, 125-138 (1958).

Received January 25, 1965

All-Union Scientific Research Motion Picture Photography Institute, Moscow

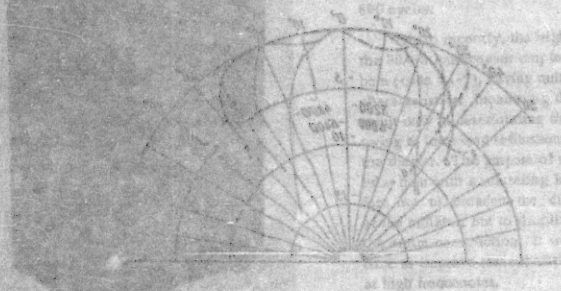

ON SURFACE WAVES LAUNCHED IN THE OCEAN BY UNDERWATER EARTHQUAKES

Iu. L. Gazarian

An integral representation was obtained for the potential of the gravitational wave produced by a piston-type displacement of part of the ocean bottom. The far wave was investigated for the case of instantaneous displacement. A criterion of the validity of these results is given for displacements lasting a finite time interval.

1. An underwater earthquake, i. e., a sudden displacement of a certain portion of the sea bottom, produces gravitational waves on the surface of the water in addition to elastic waves in the water and in the ground. The object of this investigation is the behavior of the gravitational waves at long distances from the site of the earthquake. The propagation of elastic waves in the water will be considered later.

Assume that the initial disturbance is produced by a rise in the bottom within a circle of radius a, where the entire circle rises as a whole. Since the velocity of propagation of surface waves is considerably smaller than the velocity of sound in water for the cases of interest to us, we can neglect the compressibility of the water. The resultant motion is derivable from a potential. We shall assume the layer of water to be infinite in the horizontal direction and to have a constant depth h in the undisturbed state. Passing the z axis of a cylindrical system of coordinates (z,r) vertically through the center of the circle, placing the $z = 0$ plane on the undisturbed surface of the water, and assuming the surface displacements from the undisturbed position to be small, we obtain the Cauchy integral for points located on the surface in the form

$$\frac{\partial \varphi}{\partial t} + g\zeta = 0, \tag{1}$$

where φ is the velocity potential and ζ the rise of the specified surface point above the plane $z = 0$.

If we assume not only the displacements of the surface points but also the deflections of the normals to the surface from the vertical to be small, we have

$$\frac{\partial \zeta}{\partial t} = \frac{\partial \varphi}{\partial z}$$

and we obtain from (1) on the surface or, with accuracy to within small higher-order quantities, on the plane $z = 0$ the following equation:

$$\text{at} \quad z = 0 \quad \frac{\partial^2 \varphi}{\partial t^2} + g\frac{\partial \varphi}{\partial z} = 0.$$

Denoting the speed of the rise of the circle by $w(t)$ and assuming the bottom to be stationary for $r > a$, we obtain the following conditions at the bottom:

$$\text{at } z = -h, \quad \frac{\partial \varphi}{\partial z} = \begin{cases} w(t) & \text{for } r < a, \\ 0 & \text{for } r > a. \end{cases} \tag{2}$$

The velocity potential inside the water layer satisfies the following equation

$$\frac{1}{r}\frac{\partial}{\partial r}\left(r\frac{\partial \varphi}{\partial r}\right)+\frac{\partial^2 \varphi}{\partial z^2}=0.$$

Furthermore, assuming w and dw/dt to vanish as $t \to -\infty$, i.e., that $\partial\varphi/\partial t$ and φ vanish.

2. We shall not justify the transformations made below in the solution of the problem; having obtained the solution, it will be possible to check its validity by direct verification.

Let $\varphi^{(1)}$ be the temporal Fourier transform of the function φ, i.e.,

$$\varphi^{(1)}=\int_{-\infty}^{+\infty}\varphi \exp(i\omega t)\,dt, \qquad \varphi=\frac{1}{2\pi}\int_{-\infty}^{+\infty}\varphi^{(1)}\exp(-i\omega t)\,d\omega. \tag{3}$$

The operator $\frac{\partial^2}{\partial t^2}$ for φ is equivalent to the factor $-\omega^2$ for $\varphi^{(1)}$. The equations of motion and the boundary conditions for $\varphi^{(1)}$ are obtained by multiplying by $\exp(i\omega t)$ and by integrating the corresponding equations for φ with respect to time

$$\frac{1}{r}\frac{\partial}{\partial r}\left(r\frac{\partial \varphi^{(1)}}{\partial r}\right)+\frac{\partial^2 \varphi^{(1)}}{\partial z^2}=0,$$

$$\text{at } z=0, \quad -\omega^2\varphi^{(1)}+g\frac{\partial \varphi^{(1)}}{\partial z}=0,$$

$$\text{at } z=-h, \quad \frac{\partial \varphi^{(1)}}{\partial z}=\begin{cases}\displaystyle\int_{-\infty}^{+\infty} w(t)\exp(i\omega t)\,dt & \text{for } r<a,\\ 0 & \text{for } r>a.\end{cases}$$

Furthermore, let $\varphi^{(2)}$ be the Fourier-Bessel transform of the function $\varphi^{(1)}$ with respect to the coordinate r, i.e.,

$$\varphi^{(2)}=\int_0^\infty \varphi^{(1)} J_0(\xi r)\,r\,dr, \qquad \varphi^{(1)}=\int_0^\infty \varphi^{(2)} J_0(\xi r)\,\xi\,d\xi. \tag{4}$$

The operation $\frac{1}{r}\frac{\partial}{\partial r}\left(r\frac{\partial}{\partial r}\right)$ is equivalent to multiplying by $-\xi^2$. The equations for $\varphi^{(2)}$ will be

$$-\xi^2\varphi^{(2)}+\frac{d^2\varphi^{(2)}}{dz^2}=0,$$

$$\text{at } z=0, \quad -\omega^2\varphi^{(2)}+g\frac{d\varphi^{(2)}}{dz}=0,$$

$$\text{at } z=-h, \quad \frac{d\varphi^{(2)}}{dz}=\int_0^a J_0(\xi r)\,r\,dr\int_{-\infty}^{+\infty} w(t)\exp(i\omega t)\,dt=$$

$$=\frac{aJ_1(\xi a)}{\xi}\int_{-\infty}^{+\infty} w(t)\exp(i\omega t)\,dt.$$

Having thus obtained $\varphi^{(1)}$ and using Relationships (3) and (4), we get *

$$\varphi = \frac{a}{2\pi}\int_{-\infty}^{+\infty}\exp(-i\omega t)\,d\omega\int_0^{\infty}\frac{\omega^2\operatorname{sh}\xi z+g\xi\operatorname{ch}\xi z}{\omega^2\operatorname{ch}\xi\lambda-g\xi\operatorname{sh}\xi\lambda}\frac{J_1(\xi a)}{\xi}J_0(\xi r)\,d\xi\int_{-\infty}^{+\infty}w(\tau)\exp(i\omega\tau)\,d\tau. \tag{5}$$

In this expression we encounter poles of the integrand on the path of the integration; let us agree to bypass these poles in the complex plane. This can be done because the poles vanish from the path of integration in the presence of a small amount of attenuation, and our solution should represent the limit obtained as the attenuation approaches zero. Introducing the attenuation, it would be possible to determine in which direction to bypass the poles; we shall solve this problem later in a different manner. To calculate (5) it is desirable to interchange the order of integration and to perform the first integration with respect to ω, but the corresponding integrand will not diminish as ω approaches $\pm\infty$ and the integral becomes meaningless. To avoid this, let us first integrate the last integral in (5) by parts:

$$\int_{-\infty}^{+\infty}w(\tau)\exp(i\omega\tau)\,d\tau=\frac{i}{\omega}\int_{-\infty}^{+\infty}w'(\tau)\exp(i\omega\tau)\,d\tau.$$

It is possible next to change the order of integration

$$\varphi=\frac{ai}{2\pi}\int_{-\infty}^{+\infty}w'(\tau)\,d\tau\int_0^{\infty}\frac{J_1(\xi a)}{\xi}J_0(\xi r)\,d\xi\int_{-\infty}^{+\infty}\exp(i\omega(\tau-t))\frac{\omega^2\operatorname{sh}\xi z+g\xi\operatorname{ch}\xi z}{\omega^2\operatorname{ch}\xi\lambda-g\xi\operatorname{sh}\xi\lambda}\frac{d\omega}{\omega}.$$

The latter integral is equal here, with an accuracy to within a factor of $2\pi i$, to the sum of the residues at the poles located above the path of integration if $\tau-t>0$, and to the sum of the residues of poles located under the path of integration if $\tau-t<0$. It is now easy to determine in what direction to go around the pole. There are three poles in the entire complex plane

$$\omega=0,\ \omega=\pm\sqrt{g\xi\tanh\xi\lambda}.$$

Were the initial disturbance to act only at the instant $t=0$ (i. e., $w'(\tau)=0$ at $\tau\neq 0$), it would be enough to calculate the integral with respect to ω at $\tau=0$. Then there should be no field at $t<0$, i. e., in this case the integral should vanish and consequently there should not be a single pole above the path of integration. We conclude from this that for an arbitrary initial disturbance the path of integration must pass above the poles when integrating with respect to ω. Calculating the integral with respect to ω, we obtain the following expression for

$$\varphi=a\int_{-\infty}^{t}w'(\tau)\,d\tau\int_0^{\infty}\frac{J_1(\xi a)}{\xi}J_0(\xi r)\left[\frac{\operatorname{ch}\xi(z+\lambda)}{\operatorname{sh}\xi\lambda\operatorname{ch}\xi\lambda}\cos\left((t-\tau)\sqrt{g\xi\operatorname{th}\xi\lambda}\right)-\frac{\operatorname{ch}\xi z}{\operatorname{sh}\xi\lambda}\right]d\xi.$$

Integrating by parts with respect to τ, we obtain finally

$$\varphi=aw(t)\int_0^{\infty}\frac{J_1(\xi a)}{\xi}J_0(\xi r)\frac{\operatorname{sh}\xi z}{\operatorname{ch}\xi\lambda}\,d\xi-$$

$$-a\sqrt{g}\int_{-\infty}^{t}w(\tau)\,d\tau\int_0^{\infty}\frac{\operatorname{ch}\xi(z+\lambda)}{\operatorname{ch}\xi\lambda}\frac{\sin\left((t-\tau)\sqrt{g\xi\operatorname{th}\xi\lambda}\right)}{\sqrt{\xi\operatorname{th}\xi\lambda}\operatorname{ch}\xi\lambda}J_1(\xi a)J_0(\xi r)\,d\xi.$$

* [In the following equations 'sh' = 'sinh', 'ch' = 'cosh', 'th' = 'tanh' — editor's note.]

It is now easy to verify directly that the expression obtained is actually a solution to the problem.

Using (1), we obtain an expression for the form of a surface ζ:

$$\zeta = a \int_{-\infty}^{t} w(\tau)\, d\tau \int_0^{\infty} \frac{J_1(\xi a)\, J_0(\xi r)}{\operatorname{ch} \xi h} \cos\left\{(t-\tau)\sqrt{g\xi \operatorname{th} \xi h}\right\} d\xi. \tag{6}$$

The same expression could be obtained by finding ζ directly from (5), changing the order of integration, and integrating with respect to ω. The latter turns out to be possible, for now the integral with respect to ω exists at $z = 0$.

3. Let us now investigate the solution resulting for the case when $w(t)$ is a delta function. We then obtain from (6) that $\zeta = 0$ when $t < 0$, and that at $t > 0$

$$\zeta = a \int_{-\infty}^{+\infty} w(\tau)\, d\tau \int_0^{\infty} \frac{J_1(\xi a)\, J_0(\xi r)}{\operatorname{ch} \xi h} \cos\left(t\sqrt{g\xi \operatorname{th} \xi h}\right) d\xi,$$

Let us put

$$Z = \int_{-\infty}^{+\infty} w(\tau)\, d\tau.$$

Z is the total rise of the bottom during the entire time interval. Let us next introduce in lieu of r and t the following dimensionless quantities

$$\rho = \frac{r}{h}, \qquad \tau = t\sqrt{\frac{g}{h}}.$$

In dimensionless quantities the velocity of propagation $\sqrt{gh}$ of an infinitely long harmonic surface wave is unity. Changing variables and introducing the exponential in lieu of the cosine, we finally get

$$\zeta = \operatorname{Re}\left\{\frac{aZ}{h} \int_0^{\infty} \exp\left(i\tau\sqrt{\xi \operatorname{th} \xi}\right) J_0(\xi\rho)\, \frac{J_1\left(\xi \frac{a}{h}\right)}{\operatorname{ch} \xi}\, d\xi\right\}. \tag{7}$$

We are interested in the behavior of ζ for certain large values of ρ, when τ varies from zero to infinity. We shall seek the principal term of the asymptotic expansion of ζ in negative powers of ρ. Restricting ourselves temporarily to the case when τ is of the same order of or greater than ρ, let us investigate the integral in the right half using the steepest-descent method. For this purpose let us replace the zero Bessel function with the first term of its asymptotic expansion. This replacement is valid for $\xi = 0$, but in this case the integrand vanishes both before and after the replacement. * Thus we obtain

* The error due to replacing the exact integrand by an approximate one may become substantial if the principal contribution to the integral is obtained from the path of integration near the point $\xi = 0$; such a case is considered in Section 4. In this case the order of magnitude of the error does not exceed the sum of the exact and approximate integrals over the section of the path, where the asymptotic representation of the Bessel function does not hold, i. e., with an accuracy along the section to an order of $0 \le \xi \le 1/\rho$. Upon calculation we find that the order of this error does not exceed ρ^{-1}, while the integral, as shown in Section 4, is of the order ρ^{-1}, i. e., replacing the Bessel function by the first term of the asymptotic expansion is permissible also in this case.

$$\frac{e^{-i\frac{\pi}{4}}}{\sqrt{2\pi\rho}}\int_0^\infty \exp[i(\tau\sqrt{\xi\operatorname{th}\xi}+\xi\rho)]\,\frac{J_1\left(\xi\frac{a}{h}\right)}{\sqrt{\xi\operatorname{ch}\xi}}\,d\xi + \tag{8}$$

$$+\frac{e^{i\frac{\pi}{4}}}{\sqrt{2\pi\rho}}\int_0^\infty \exp[i(\tau\sqrt{\xi\operatorname{th}\xi}-\xi\rho)]\,\frac{J_1\left(\xi\frac{a}{h}\right)}{\sqrt{\xi\operatorname{ch}\xi}}\,d\xi.$$

We shall assume that a/h is small compared with ρ, i. e., $a \ll r$. Then the exponent in (8) varies rapidly relative to the remaining factors and the saddle-point method can be employed. Let us first investigate the behavior of the function $f(\xi)=\sqrt{\xi\tanh\xi}$ along the path of integration. We have

$$f'(\xi)=\frac{1}{2}\left\{\sqrt{\frac{\operatorname{th}\xi}{\xi}}+\sqrt{\frac{\xi}{\operatorname{th}\xi}}\cdot\frac{1}{\operatorname{ch}^2\xi}\right\},$$

$$f''(\xi)=-\frac{4\xi^2\operatorname{sh}^2\xi+(\operatorname{sh}\xi\operatorname{ch}\xi-\xi)^2}{4\xi\operatorname{sh}\xi\operatorname{ch}^3\xi\sqrt{\xi\operatorname{th}\xi}}.$$

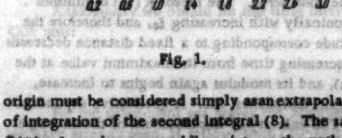

Fig. 1.

It follows from this that as ξ varies from zero to infinity, $f'(\xi)$ decreases monotonically from unity to zero, with $f''(0)=0$. A plot of $f'(\xi)$ is shown in Fig. 1. The condition $f''(0)=0$ denotes that if the saddle point is at the origin, the ordinary equations of the steepest-descent method are not valid (this is the case of two coinciding saddle points). We shall not treat this case separately here, and will defer its consideration to Section 4. The use of the equations obtained below for the case of a saddle point at the origin must be considered simply as an extrapolation of the result. Let us now find the saddle points on the path of integration of the second integral (8). The saddle point is determined from the equation $f'(\xi)=\rho/\tau$. Since $f'(\xi)\leq 1$, we have no saddle points on the path of integration if $\tau<\rho$ and a single saddle point if $\tau>\rho$. For the first integral in (8) there are never any saddle points on the path of integration. If there are no saddle points on the real axis, the paths of the integrals under consideration can be deformed in the complex plane so as to make the integrand decrease rapidly away from the origin and the initial portion of the path makes the principal contribution to the integral. If there is a saddle point on the real axis, it is necessary to add the contribution from the section in the vicinity of the saddle point. The integral along the initial portion, which can be calculated by the method of steepest descents, is considerably smaller than the integral in the saddle-point region and differs from it at least by a factor on the order of $\rho^{-1/2}$; we shall obtain a more accurate estimate below. When deforming the path, there is no danger of encountering poles and other singularities for the latter lie in the region $|\operatorname{Im}\xi|\geq\pi/2$ and the corresponding portions of the integration path give a value that diminishes exponentially with increasing ρ. Thus, if we take into consideration only the terms of the lowest order of $1/\rho$ in the asymptotic expansion of the integral, it is possible to assume that the surface of the water is stationary, as long as $\tau<\rho$, and consequently, the leading front of the wave arrives at the instant $\tau=\rho$. This corresponds to the leading front propagating at the same velocity as an infinitely long harmonic surface wave. The value of ζ at $\tau>\rho$, which can be obtained by using, for example, the equation from [1], will be

$$\zeta\sim\frac{aZ}{h}\,\frac{f'(\xi_0)\xi_0}{-f''(\xi_0)\cosh^2\xi_0}\cdot\frac{J_1\left(\xi_0\frac{a}{h}\right)}{\xi_0}\cdot\cos\left(\tau\,\xi_0\tanh\xi_0-\xi_0\rho\right)\frac{}{\rho},$$

where ξ_0 is the saddle point; it can be obtained from Fig. 1. At $\tau=\rho$, we have $\xi_0=0$. If ρ is fixed, ξ_0 increases with time.

Let us introduce the quantity

$$K(\xi_0) = \sqrt{\frac{f(\xi_0)}{-f'(\xi_0)}} \cdot \frac{\sqrt{\xi_0}}{\operatorname{ch} \xi_0}. \tag{9}$$

A plot of $K(\xi_0)$ is given in Fig. 2. We have

$$\zeta \sim \frac{aZ}{h} K(\xi_0) \cdot \frac{J_1\left(\xi_0 \frac{a}{h}\right)}{\xi_0} \cdot \frac{\cos\left\{\tau\sqrt{\xi_0 \tanh \xi_0} - \xi_0 \rho\right\}}{\rho}. \tag{10}$$

Expression (10) describes a cosine wave modulated in time and distance. Its amplitude will be

$$\frac{aZ}{h\rho} K(\xi_0) \frac{J_1\left(\xi_0 \frac{a}{h}\right)}{\xi_0};$$

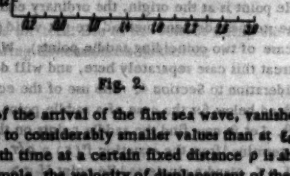

Fig. 2.

Since the amplitudes corresponding to distances and instants of time for which $\xi_0 = \text{const}$ differ from differ from each other only by the slowly-varying factor $\frac{1}{\rho}$, the deformation of the envelope wave can be neglected for relatively small changes in the distance, and only the velocity of propagation of the envelope need be considered. The factor $K(\xi_0)$ diminishes monotonically with increasing ξ_0, and therefore the amplitude corresponding to a fixed distance decreases with increasing time from its maximum value at the instant of the arrival of the first sea wave, vanishes with $J_1(\xi_0 a/h)$, and its modulus again begins to increase, but only to considerably smaller values than at $\xi_0 = 0$; it then again diminishes, etc. A qualitative dependence of ζ with time at a certain fixed distance ρ is shown in Fig. 3. The velocity of displacement of the envelope (for example, the velocity of displacement of the zero of the Bessel function), is obtained from the condition $\xi_0 = \text{const}$. Using the relationship

$$\tau f'(\xi_0) - \rho = 0, \tag{11}$$

we obtain for this velocity

$$\frac{\partial \rho}{\partial \tau} = f'(\xi_0).$$

The velocity of the individual sea wave is determined from the condition

$$\tau\sqrt{(\xi_0)} - \xi_0 \rho = \text{const},$$

which yields, using (11),

$$\frac{\partial \rho}{\partial \tau} = \frac{f(\xi_0)}{\xi_0} = \frac{\int_0^{\xi_0} f'(\xi)\, d\xi}{\int_0^{\xi_0} d\xi}.$$

Inasmuch as $f'(\xi)$ decreases monotonically, the velocity of the individual sea wave is greater than the velocity of the envelope (except if $\tau = \rho$, when $\xi_0 = 0$ and both velocities are equal). Let us find further the distance $\frac{L}{2}$ from the crest of the first sea wave to the nearest trough. Let the first maximum arrive at point ρ at the instant $\tau = \rho$; then the nearest trough is located at the same instant at the point $\rho - \frac{L}{2}$. For the point $\rho - \frac{L}{2}$ we have:

$$\varphi'(\xi_0) - \xi_0(\rho - L/2) = \pi.$$

In addition, we obtain from (11)

$$\varphi'(\xi_0) - (\rho - L/2) = 0.$$

Replacing f and f' by the first terms of the expansion about zero, retaining terms with ξ^3, and taking into account that $\tau = \rho$, we obtain

$$-\rho\frac{\xi_0^3}{6} + \xi_0\frac{L}{2} = \pi, \quad -\rho\frac{\xi_0^2}{2} + \frac{L}{2} = 0,$$

i. e., for the first sea wave $\frac{L}{2} = \frac{(3\pi)^{2/3}}{2}\rho^{1/3}$, or in dimensional units

$$\frac{L}{2} = \left(\frac{9}{8}\right)^{1/3}(gh)^{2/3}\rho^{1/3} \approx 2.2\,h^{2/3}\rho^{1/3}.$$

Analogously we obtain for the time interval T between the arrival of the first and second crests, using CGS units

$$T \approx 0.11\,h^{1/3}\rho^{1/3}.$$

For the subsequent sea waves the argument of the cosine will vary faster, and L and T will decrease. As we have already seen, it follows from (10) that at a fixed distance the maximum displacement will occur at the instant of arrival of the first sea wave, when $\xi_0 = 0$. This displacement is

$$\zeta_{max} = \frac{a^2Z}{2h^2\rho} = \frac{a^2Z}{2h^2}.$$

Introducing $V = \pi a^2 Z$, where V is the total volume displaced by the rise of the bottom, we get

$$\zeta_{max} = \frac{V}{2\pi h^2}. \tag{12}$$

Thus, the maximum amplitude is the ratio of the total volume displaced to the cylindrical area of the intenection between the layer of water and the cylinder passing through the point of observation coaxial with the z axis. Equation (12) is correct not only in absolute magnitude, but also in sign, i. e., if V is negative, the maximum displacement will also be negative.

In view of the linearity of the equation in the problem, it is possible to obtain ζ for the case when the rising bottom is not a circle but a ring of radius a and width δa, by merely replacing in Expression (10)

$$aJ_1\left(\xi_0\frac{a}{h}\right) \text{ by } \delta\left\{aJ_1\left(\xi_0\frac{a}{h}\right)\right\} = \frac{\xi_0 a\,\delta a}{h}J_0\left(\xi_0\frac{a}{h}\right),$$

i. e., in this case ζ will be proportional to the quantity

$$\frac{\delta V}{2\pi\sigma h} J_0\left(\xi_0 \frac{a}{h}\right) K(\xi_0). \tag{13}$$

Let us now explain the physical meaning of the results obtained. The expression

$$\cos\{t\sqrt{g\xi \operatorname{th} \xi h}\}\, J_0(\xi r)$$

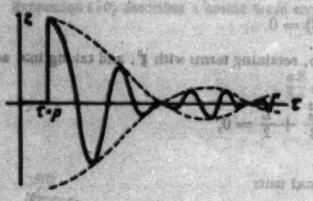

Fig. 3.

describes a cylindrical harmonic gravitational wave, which becomes a plane wave with wave number ξ at large values of ξr. Its phase velocity $\sqrt{\frac{g}{\xi}\tanh \xi h}$ has a maximum for infinitely long waves ($\xi = 0$) and diminishes to zero as ξ increases. The group velocity equals the phase velocity for infinitely long waves, but diminishes and becomes smaller than the phase velocity for shorter waves. Expression (7) represents a superposition of harmonic waves with all possible wave numbers. At $\tau < \rho$ all these waves interfere with each other and the resultant amplitude is zero to within higher-order terms. Once τ exceeds ρ, integral (7) starts differing from zero, and its principal part is produced by waves having wave numbers close to ξ_0. This means that at the instant τ, related to ξ_0 by Eq. (11), the components with wave numbers close to ξ_0 become so phased as to give a nonvanishing surface displacement, while the remaining components, interfering with each other, continue to give a zero contribution. As is readily seen from (11), the surface displacement resulting from this phasing propagates in space with a corresponding group velocity. The displacements arriving in the first instant are those caused by the infinitely-long waves. Taking Expression (13) for near-zero values of ξ_0 and considering that $J_0(0) = K(0) = 1$, we see, as expected, that all the surface displacements caused by very long waves, produced by individual portions of the circle, arrive in phase and that the resulting amplitude is obtained by summing terms of equal sign. As τ increases, the arriving displacements are caused by shorter waves, and waves originating in different parts of the circle will produce out of phase displacements, by virtue of the accumulation of phases due to the path differences (this phase accumulation becomes particularly strong when the wavelength becomes comparable with the radius of the circle). If the radius a of the circle is assumed small, the physical meaning of the coefficient $K(\xi_0)$ becomes clear from (10); it represents the ratio of the amplitude of a displacement due to a wave with wave number ξ_0 launched by the rise of an infinitely small area, to the displacement due to an infinitely-long wave launched by the same rise. As can be seen from (9), the value of $K(\xi_0)$ depends on two factors: the first factor expresses the dependence of the resultant displacement on the character of the superposition of the waves with adjacent wave numbers, while the second represents the contribution to (7) made by waves having a wave number ξ_0.

From the consideration given above one can also draw certain conclusions concerning a more general type of initial disturbance. It is clear first of all that the assumed circular symmetry does not affect substantially the character of the first arriving sea waves. One can also readily visualize a case in which some sections of the bottom rise and others drop. For example, if the rise and drop occur in such a way, that the total volume displaced is zero, the displacements due to the infinitely-long waves, arriving with positive amplitudes from the site of rise and with negative amplitudes from the site of drop, will result in a zero total amplitude. But if the arriving displacements are due to shorter waves the total amplitude, under favorable interference conditions, may rise sharply, without exceeding, however, the amplitude corresponding to the arithmetic sum of the volumes displaced. As a result, the leading front of the disturbance will arrive with zero amplitude, and the sea waves will reach a maximum amplitude only at $\tau > \rho$.

It is easy to obtain the exact result for any type of cylindrical symmetrical instantaneous rise of the bottom. In particular, (12) is valid when one takes jointly with (2) the following condition

$$\text{at } z = -h \quad \frac{\partial \eta}{\partial t} = F(r)\,w(t),$$

where $w(t)$, as in the case above, is a delta function. It is merely necessary that the radius of the region of noticeable displacement of the bottom be much smaller than the distance to the point of observation. If, for example, we put $F(r) = e^{-\alpha r}$, then

$$\zeta \sim ZK(\xi_0)\frac{\alpha h}{(\alpha^2 h^2 + \xi_0^2)^{3/2}} \cdot \frac{\cos\left\{\tau\sqrt{\xi_0 \tanh \xi_0} - \xi_0\rho\right\}}{\rho}. \tag{14}$$

Let us remark, finally, that the smoother the rise of the bottom varies with distance, the more pronounced is the time variation of the amplitude of the arriving wave, and vice versa. For example, at large values of a and at small values of α, respectively, the amplitude in Expressions (10) and (14) diminishes very rapidly with increasing ξ_0. This results from the general properties of the Fourier transform. The physical explanation lies in the fact that if the rise of the bottom is smooth, the waves excited are principally long, while if the irregularities of the bottom are sharp, the shorter waves also appear.

4. As already remarked, there is one flaw in the arguments of Section 3. The equation cited from [1], which we used, is not valid when $f''(\xi_0)$ is close to zero. In our case, however, we have $f''(\xi_0) = 0$ at $\xi_0 = 0$. Thus, the entire initial portion of the leading front of the arriving wave was inaccurately determined. It is therefore necessary to calculate the second integral in Eq. (8) when the saddle point is close to $\xi = 0$, i. e., when τ is close to ρ. We employ for this purpose the following argument. As before, an important role is played only by that segment of the path of integration, lying near the saddle point, i. e., near the origin. But in that case the factor preceding the exponent in the expression for $\sqrt{\xi \tanh \xi}$ can be replaced by the first terms of its expansions about $\xi = 0$ and the resultant integral can then be calculated by the method of steepest descent. Performing the above operations, we obtain for our integral the following expression:

$$\frac{a}{2\lambda}\int_0^\infty \exp\left\{i\left[(\tau-\rho)\xi - \tau\frac{\xi^3}{6}\right]\right\}\xi^{\frac{1}{3}}\,d\xi.$$

The integral along the real axis equals the integral along the line

$$\xi = \eta \exp\left(-i\frac{\pi}{6}\right), \quad 0 < \eta < \infty.$$

Since τ is close to ρ, the last integral can be calculated by expanding $\exp[i(\tau - \rho)\xi]$ in a series. We thus obtain for ζ the following expression:

$$\zeta \sim \mathrm{Re}\left\{\frac{a^2 Z}{2\lambda^2}\frac{1}{\sqrt{3\tau\rho}}\sum_{k=0}^{\infty}\frac{\Gamma\left(\frac{k}{3}+\frac{1}{2}\right)}{\sqrt{\pi}\,k!}\exp\left(-i\frac{2k\pi}{3}\right)\left[\frac{\rho-\tau}{(\tau/6)^{\frac{1}{3}}}\right]^k\right\}. \tag{15}$$

In this manner we obtain for ζ at the instant of arrival of the leading front

$$\zeta \sim \frac{a^2 Z}{2\lambda^2 \rho\sqrt{3}} = \frac{V}{2\pi h}\cdot\frac{1}{\sqrt{3}},$$

which is approximately half the value given by Eq. (12) derived in the preceding section. Thus, even in this case of a general rise in the bottom, the amplitude of the first arriving sea wave is in general not the maximum and the amplitude of the second wave may be greater, without however exceeding the value given by (12).

5. We have already seen that for $\tau < \rho$ the displacements of the points on the water surface are at least $\sqrt{\rho}$ times smaller than for $\tau > \rho$. It is desirable to obtain the exact value of the first term of the asymptotic expansion of ζ for this case, so as to be able to follow the nature of the wave shortly prior to the arrival of the leading front. Replacing the Bessel function above by the first term of its asymptotic expansion and calculating the resulting integral does not lead to success here, for the resultant values are zero, and it is impossible to use the second term of the asymptotic expansion of the Bessel function owing to the divergence of the integral. One must therefore dispense here with replacing the Bessel function by its asymptotic value.

We have

$$\frac{h}{aZ}\zeta = \int_0^\infty \cos\left(\tau\sqrt{\xi \operatorname{th}\xi}\right) J_0(\xi\rho)\,\frac{J_1\left(\xi\frac{a}{h}\right)}{\operatorname{ch}\xi}\,d\xi =$$

$$= 2\sum_{s=0}^{\infty}(-1)^s \int_0^\infty \cos\left\{\tau\left(\xi - \frac{\xi^2}{6} + \ldots\right)\right\}\left\{\frac{\xi a}{2h} - \right.$$

$$\left. - \frac{\xi^3 a^3}{16h^3} + \ldots\right\} \exp\left[-(1+2s)\xi\right] J_0(\xi\rho)\,d\xi. \tag{16}$$

Noticing that

$$\int_0^\infty \exp(-A\xi)\,\xi^n J_0(\xi\rho)\,d\xi = \frac{\Gamma(n+1)\Gamma\left(-\frac{1}{2}\right)}{A^{n+1}\Gamma\left(\frac{n+1}{2}\right)\Gamma\left(-\frac{n}{2}\right)}\left(\frac{A}{\rho}\right)^{n+1} \times$$

$$\times F\left(\frac{n+2}{2}, \frac{n+2}{2}; \frac{3}{2}; -\frac{A^2}{\rho^2}\right) +$$

$$+ \frac{\Gamma(n+1)\Gamma\left(\frac{1}{2}\right)}{A^{n+1}\Gamma\left(\frac{n+2}{2}\right)\Gamma\left(\frac{1-n}{2}\right)}\left(\frac{A}{\rho}\right)^{n+1} F\left(\frac{n+1}{2}, \frac{n+1}{2}; \frac{1}{2}; -\frac{A^2}{\rho^2}\right), \tag{17}$$

which follows from [2] upon transforming the expression for the hypergeometric function, we see that after expanding the first two factors under the integral sign in (16) into a power series in ξ, the terms containing ξ^n will yield upon integration terms on the order of $1/\rho^{n+1}$. Taking into account the fact that we are interested also in cases when $\tau \sim \rho$, and that the terms of the form $(\xi\tau)^n\xi$ will yield upon integration τ^n/ρ^{n+1}, we find that the principal terms of the expansion are of the order $\frac{1}{\rho^2}$ (for the second term in the right half of (17) vanishes for n = 1) and to calculate this term it is necessary to retain the terms containing $(\tau\xi)^n$, retaining only the first term in the second multiplier.

The first term of the integral of interest to us is thus the same as the principal term of the asymptotic expansion of the following integral

$$\int_0^\infty \cos\tau\xi\,\frac{\xi a}{2h}\exp\left[-(1+2s)\xi\right] J_0(\xi\rho)\,d\xi =$$

$$= \operatorname{Re}\left\{\frac{a}{2h}\int_0^\infty \exp\left[-(1+2s+i\tau)\xi\right] J_0(\xi\rho)\,\xi d\xi\right\},$$

which can be readily calculated (see, for example, [2]). From this we obtain

$$\zeta \sim \mathrm{Re}\left\{\frac{a^2 Z}{h^2}\sum_{s=1}^{\infty}(-1)^s \frac{1+2s+i\tau}{[\rho^2+(1+2s+i\tau)^2]^{3/2}}\right\}. \tag{18}$$

If $\tau \gg 1$ and the series converges rapidly enough, then neglecting unity compared with $\frac{\tau}{(1+2s)}$, this expression can be simplified to:

$$\zeta \sim \frac{a^2 Z}{h^2}\frac{1}{2\sqrt{2\tau}}\sum_{s=0}^{\infty}\frac{(-1)^s}{(1+2s)^{\frac{5}{2}}}\cos\left\{\frac{3}{2}\arctan\left[\frac{\rho^2-\tau^2}{2\tau(1+2s)}\right]-\frac{\pi}{4}\right\}\Big/\left\{1+\left[\frac{\rho^2-\tau^2}{2\tau(1+2s)}\right]^2\right\}^{3/4}. \tag{19}$$

From the above expressions it is seen that at $\tau \ll \rho$, ζ is of the order of $\frac{1}{\rho^3}$. For values of τ close to ρ we obtain a value of ζ that is clearly too high, on the order of $\frac{1}{\rho}$. The reason is readily understood: at $\tau = \rho$ the cosine and the zero Bessel function have the same phase when the argument of the cosine is replaced by $\xi\tau$ in Expression (16), and the sign of the integrand no longer changes rapidly for large values of ξ. To be able to evaluate the phase difference between the cosine and the Bessel function it is necessary to retain the second term in the expansion of the argument of the cosine, as was done in Section 4. Expression (18) is thus suitable for values of τ not too close to ρ. Let us note, that Expression (18) is suitable for evaluation of the portion of the integral corresponding to the initial segment of integration path, not only at $\tau < \rho$, but also at $\tau > \rho$. We thus see that discarding the integral along the initial portion of the path in the derivation of Equation (10) causes an error on the order of $1/\rho^3$. Let us further remark that it follows from the resultant expression that the initial disturbance propagates instantaneously. This is a consequence of ignoring the compressibility of water. Allowance for the compressibility would result in propagation of the disturbance with the velocity of sound and would change Expression (18) for values of τ close to zero.

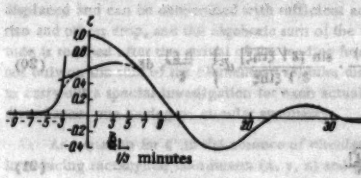

Fig. 4.

The investigation performed makes it possible to determine ζ for large values of ρ for all τ. It is necessary here to employ Eq. (18) for $\tau < \rho$, Eq. (15) for $\tau \sim \rho$, and Eq. (19) for $\tau > \rho$. Figure 4 shows the time dependence of ζ for the following actual case. It is assumed that r = 5000 km, h = 5 km, a = 70 km, and Z = = 10 m; here $\zeta_{max} = 1$ m, $L_{max}/2 = 110$ km, $T_{max} = 13$ minutes, and the leading front propagates at 220 m/sec. The abscissa represents the quantity $\Delta\tau = \tau - \rho$, where $\Delta\tau = 1$ represents 23 seconds in dimensional quantities. The solid lines show the three curves calculated from the equations derived above, while the dotted lines show the values assumed in the intermediate regions. Four terms of the series were calculated in Eq. (15). Nine terms of the series were calculated in Eq. (19), with the Cesaro method of summation being used here because of the poor convergence.

Let us remark that the displacements given by Eqs. (15) and (19) are proportional to the total volume displaced, with the proportionality coefficient independent of the radius a of the circle. The form of the leading front obtained by us is thus independent of a for a fixed value of volume displaced. To obtain this dependence it would be necessary to retain in the series the terms beyond the first one in the calculations made in connection with the expansion $J_1(\xi a)$.

6. We considered above an instantaneous rise of the bottom; actually, however, the rise always occurs within a finite time interval. Let us see how this affects the result and under what conditions is the representation of the velocity of the rise in the form of a delta function sufficiently accurate. Let $w(\tau)$ be defined in Eq. (6) as follows:

$$w(\tau) = \begin{cases} 0 & \text{at } |\tau| > \Delta, \\ W & \text{at } |\tau| < \Delta, \end{cases}$$

i. e., a portion of the bottom rises with a constant velocity W during a time interval 2Δ. Then for $t > \Delta$, we obtain from (6):

$$\zeta = \operatorname{Re}\left\{ aW \int_0^\infty \frac{J_1(\xi a) J_0(\xi r)}{\operatorname{ch} \xi h} \cdot \frac{2 \sin\left[\Delta \sqrt{g\xi \operatorname{th} \xi h}\right]}{\sqrt{g\xi \operatorname{th} \xi h}} \exp\left(it \sqrt{g\xi \operatorname{th} \xi h}\right) d\xi \right\} dt.$$

Introducing the total rise of the bottom $Z = 2\Delta W$, converting to dimensionless units, and denoting by 2δ the time of rise in dimensionless units

$$2\delta = 2\Delta \sqrt{g/h},$$

we get

$$\zeta = \operatorname{Re}\left\{ \frac{aZ}{h} \int_0^\infty e^{it\sqrt{\xi \operatorname{th} \xi}} J_0(\xi\rho) \frac{J_1(\xi \frac{a}{h})}{\operatorname{ch} \xi} \cdot \frac{\sin\left[\delta \sqrt{\xi \operatorname{th} \xi}\right]}{\delta \sqrt{\xi \operatorname{th} \xi}} d\xi \right\} \frac{h}{\xi} dt \qquad (20)$$

This expression differs from (7) only by an added factor

$$\frac{\sin\left[\delta \sqrt{\xi \tanh \xi}\right]}{\delta \sqrt{\xi \tanh \xi}} \qquad (21)$$

in the integrand. It is natural to restrict oneself to $\delta \ll \rho$, when an analysis of (20) can be carried out in analogy with that of (7). When we calculated (7) for the instants of time near the instant of arrival of the leading front, we expanded the integrand about the point $\xi = 0$ and retained only the principal term of the expansion. Since the principal term of Expansion (21) is unity, it follows that in this case the result is independent of δ, i. e., of the time of rise of the bottom. For $\tau > \rho$ we obtain in complete analogy with (10)

$$\zeta \sim \frac{aZ}{h} K(\xi_0) \frac{J_1(\xi_0 \frac{a}{h})}{\xi_0} \cdot \frac{\sin\left[\delta \sqrt{\xi_0 \operatorname{th} \xi_0}\right]}{\delta \sqrt{\xi_0 \operatorname{th} \xi_0}} \cdot \frac{\cos\left(\tau \sqrt{\xi_0 \operatorname{th} \xi_0} - \xi_0 \rho\right)}{\rho}.$$

Thus, the fact that the rise time interval is finite will begin to play a role only when Expression (21), calculated at the point ξ_0, begins to differ considerably from unity.

Expanding (21) in a series and requiring that the second term of the series be small compared with the first, we obtain the following condition for the duration of the rise to be insignificant:

$$1 \gg \frac{(\delta \sqrt{\xi_0 \tanh \xi_0})^2}{6}.$$

Since ξ_0 approaches infinity with increasing time, sooner or later this condition will be violated, but at sufficiently small values of δ it will always be satisfied for the sea waves of interest to us with large amplitudes and with large distances between crests. To clarify the physical meaning of the condition obtained, let us convert to dimensional units; we then obtain

$$\Delta \ll \frac{\sqrt{6}}{\sqrt{gk_0 \tanh hk_0}}.$$

Considering that the quantity

$$T_0 = \frac{2\pi}{\sqrt{gk_0 \tanh hk_0}},$$

represents the period of the superposition wave that causes the displacement of the surface at the instant under consideration, we get

$$2\Delta \ll \frac{\sqrt{6}}{\pi} T_0,$$

i. e., the rise can be assumed instantaneous as long as the arriving displacements are caused by waves having a period of oscillation large compared with the rise time. Thus, for the finite rise time discussed in the example at the end of Section 5 to play a substantial role even for the first sea waves, having crests 100 km apart, it is necessary that the rise time be on the order of several minutes.

7. We saw that if the individual sections of the bottom are all displaced in the same direction, the waves with the maximum amplitudes will be the very first ones; these amplitudes are proportional to the total volume displaced and can be determined with sufficient accuracy with Eq. (12). If, however, some parts of the bottom rise and others drop, and the algebraic sum of the volume displaced is nearly equal to zero, the maximum amplitude is reached after the arrival of the leading front of the wave. In this case the maximum amplitude depends not only on the sum of the elementary volumes displaced, but also on their spatial distribution and it is necessary to carry out a special investigation for each actual case. Let us consider a likely example of such an initial disturbance, one having no circular symmetry.

An equation for ζ in the absence of circular symmetry is not hard to derive in analogy with Section 2. Introducing rectangular coordinates (x, y, z) and placing the origin and the z axis as before, the only difference will be that instead of the Fourier-Bessel transform with respect to the r coordinate we deal with the Fourier transforms with respect to x and y. Replacing (2) by the condition that at $z = -h$ we have

$$\frac{\partial \varphi}{\partial z} = w(t) F(x, y), \tag{22}$$

we obtain in lieu of (6)

$$\zeta = \frac{1}{4\pi^2} \int_{-\infty}^{t} w(\tau)\, d\tau \int_{-\infty}^{+\infty}\int_{-\infty}^{+\infty} \exp[i(\xi x + \eta y)] \times \frac{\cos[(t-\tau)\sqrt{g\sqrt{\xi^2+\eta^2}\,\mathrm{th}\,(h\sqrt{\xi^2+\eta^2})}]}{\mathrm{ch}\,(h\sqrt{\xi^2+\eta^2})}\, d\xi\, d\eta \times$$
$$\times \int_{-\infty}^{+\infty}\int_{-\infty}^{+\infty} \exp[-i(\xi\mu + \eta\nu)]\, F(\mu, \nu)\, d\mu\, d\nu. \tag{23}$$

Let us now put

$$F(x, y) = \begin{cases} A_1 \exp(\alpha x - \beta^2 y^2) & \text{at } x < 0, \\ A_2 \exp(-\alpha x - \beta^2 y^2) & \text{at } x > 0. \end{cases}$$

Such an initial disturbance is a fault in the bottom along a segment parallel to the y axis. The parameters A_1 and A_2 characterize the rise (or drop) of the bottom on one side of the fault line or the other, B gives the length of the fault section, and α characterizes the smoothness of the rise of the bottom in a direction perpendicular to the direction of the fault. Choosing $w(t)$ in form of a delta function and considering that at $t > 0$ we have

$$A_1 \int_{-\infty}^{t} w(\tau)\, d\tau = A_1 \int_{-\infty}^{+\infty} w(\tau)\, d\tau = Z_1,$$

where Z_1 is the maximum rise in the half space $x < 0$, we obtain at $t > 0$, upon integration with respect to μ and ν and upon conversion to dimensionless quantities

$$\zeta = \frac{1}{4\pi\sqrt{\pi\beta\lambda}} \int_{-\infty}^{+\infty}\int_{-\infty}^{+\infty} \left(\frac{Z_1}{\lambda\alpha - i\xi} + \frac{Z_2}{\lambda\alpha + i\xi}\right) \times$$

$$\times \frac{\cos\left(\tau\left|\sqrt{\xi^2 + \eta^2}\,\mathrm{th}\,\sqrt{\xi^2 + \eta^2}\right|^{1/2}\right)}{\mathrm{ch}\,\sqrt{\xi^2 + \eta^2}} \exp\left[i\left(\xi\frac{x}{\lambda} + \eta\frac{y}{\lambda}\right) - \frac{\eta^2}{4\beta^2\lambda^2}\right] d\xi\, d\eta.$$

Introducing for convenience the polar coordinates

$$\xi = R\cos\Phi, \frac{x}{\lambda} = r\cos\varphi, \eta = R\sin\Phi, \frac{y}{\lambda} = r\sin\varphi$$

and taking into account the fact that the integration yields a real number, we can write the resultant expression as

$$\zeta = \mathrm{Re}\left\{\frac{1}{4\pi\sqrt{\pi\beta\lambda}} \int_{-\infty}^{+\infty}\int_{-\infty}^{+\infty} \left(\frac{Z_1}{\lambda\alpha - i\xi} + \frac{Z_2}{\lambda\alpha + i\xi}\right) \times\right.$$

$$\left. \times \frac{\exp\left(-\frac{\eta^2}{4\beta^2\lambda^2}\right)}{\mathrm{ch}\,R} \exp\left\{i\left[\sqrt{f(R)} + \xi\frac{x}{\lambda} + \eta\frac{y}{\lambda}\right]\right\} d\xi\, d\eta \right\}. \qquad (24)$$

Equation (24) is completely analogous with (7) and differs only in that it depends not only on the distance to the point of observation, but also on its azimuth, i. e., it takes into account the direction of the wave produced. From the above analysis of Eq. (7) it is clear that ζ can be calculated by restricting oneself to that portion of the integral in the neighborhood of the saddle point. In this case we obtain, using the same reasoning as used in [1], the following generalization of the equation given there. Consider the integral

$$\iint_S \varphi(\xi, \eta) \exp\left[if(\xi, \eta)\right] d\xi\, d\eta,$$

where f is a rapidly varying function. Then if f has a stationary point (ξ_0, η_0) in the integration region and if the discriminant of f at this point is D_0, the approximate value of the integral is given by the following expression

$$\frac{2\pi}{\sqrt{D_0}} \varphi(\xi_0, \eta_0) \exp\left\{i\left[f(\xi_0, \eta_0) \pm \frac{\pi}{2}\right]\right\},$$

provided $f(\xi, \eta)$ has a strict extremum at the stationary point; here the upper sign is taken for the maximum and the lower for the minimum, and the value of the integral is approximately

$$\frac{2\pi}{\sqrt{-D_0}} \varphi(\xi_0, \eta_0) \exp[if(\xi_0, \eta_0)], \tag{25}$$

if (ξ_0, η_0) is a saddle point for $f(\xi, \eta)$. Let us now find the saddle points of the integrand of (24). We have

$$\tau f'(R_0)\frac{\xi_0}{R_0} + \frac{x}{h} = r\cos\varphi, \qquad \tau f'(R_0)\frac{\eta_0}{R_0} + \frac{y}{h} = 0,$$

i. e.,

$$\tau f' \cos\Phi_0 + r\cos\varphi = 0, \quad \tau f' \sin\Phi_0 + r\sin\varphi = 0,$$

hence

$$\tau f' = r \text{ and } \Phi_0 = \varphi + \pi.$$

Thus, a single saddle point exists at $\tau > r$ but none exist at $\tau < r$, for $f'(R) < 1$. Consequently, as before, the forward front of the wave arrives at the instant $\tau = r$, i. e., it moves with the velocity of the infinitely long wave. It is furthermore clear, that this saddle point is also a saddle point for the function

$$\tau f(R) + \xi\frac{x}{h} + \eta\frac{y}{h}.$$

Actually, the curvature of the surface represented by this function has the same character as that of the surface represented by the function $f(R)$; the latter is a surface of revolution of the curve investigated in Section 3, and, as can be readily seen, has a negative curvature everywhere except at the origin. Using Eq. (25) and introducing the symbols previously defined, we obtain the following expression for ζ at $\tau > \rho$:

$$\zeta \sim \frac{K(\xi_0)}{2\pi\rho h^2}\exp\left(-\xi_0^3\frac{\sin^2\varphi}{4\rho^3 h^3}\right)\times$$
$$\times\frac{(V_1+V_2)\cos\{\tau f(\xi_0)-\rho\xi_0\}+(V_1-V_2)\dfrac{\xi_0}{\alpha h}\cos\varphi\sin\{\tau f(\xi_0)-\rho\xi_0\}}{1+\dfrac{\xi_0^2}{\alpha^2 h^2}\cos^2\varphi}.$$

Here ρ and τ are the dimensionless distance and time, φ is the azimuth of the point of observation, V_1 and V_2 are the total volumes displaced in the half spaces $x < 0$ and $x > 0$, respectively, taken with the proper signs, and ξ_0 is the root of the equation $f'(\xi) = \rho/\tau$. As to explaining the physical meaning of the expression obtained, the entire argument given in Section 3 can be repeated here. One must only add that while the result for infinitely long waves does not differ at all from that obtained in the case of a cylindrically-symmetrical disturbance, the asymmetry of the rising platform plays a substantial role in the case of short waves. The author expresses deep gratitude to M. A. Isakovich for evaluation of the problems touched upon above, and also thanks to L. M. Brekhovskikh and L. N. Sretenskii for many remarks.

LITERATURE CITED

[1] G. Lamb, Hydrodynamics (1947), p. 495 (Russian translation).

[2] I. M. Ryzhik and I. S. Gradshtein, Tables of Integrals (1951), p. 265.

Received March 15, 1955

Acoustics Institute, USSR Academy of Sciences, Moscow

CAPACITIVE ANALYZER FOR SOUND FIELD

V. A. Zverev, V. M. Bokov, and I. E. Lur'e

An experiment in which the sound field was investigated by determining the dependence of the dielectric constant on pressure is described. The experiment was performed in a liquid. At 5 mc, and using sound at 85 kc and a pressure on the order of 10^5 bars, the variation in the dielectric constant of water was found to be on the order of 10^{-6}.

In many problems in physical acoustics it is desirable to determine the sound field without distorting it. One way to solve this problem is to determine the sound field from the changes in properties of the medium caused by the propagation of the sound wave through the medium. Thus, for example, the change in the density of the medium, and with it the change in the index of refraction, are used for visual observation of sound in the

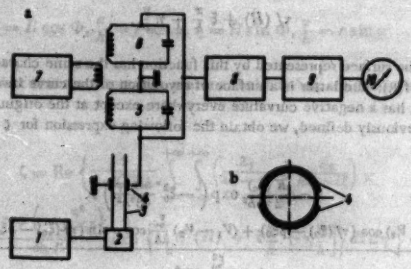

Fig. 1.

dark field method. In this investigation we propose to employ the changes produced by the sound field in the dielectric constant of the medium at radio frequencies. This makes it possible to study relatively low-frequency fields. The idea of the method is as follows: one measures the change in dielectric constant ε of the medium, caused by sound waves occurring at sonic frequencies, by determining the changes in a capacitance that uses the tested medium as a dielectric. The change in capacitance at some frequency can be determined quite accurately by radio-engineering methods. The upper limit of the sound-frequency band that can be investigated in this manner depends on the dimensions of the capacitor, which must be less than half the wavelength of the sound wave.

To evaluate experimentally the operation of the analyzer, the setup shown schematically in Fig. 1a was assembled. Voltage at a frequency f_1 = 85 kc is fed from generator 1 to radiator 2, which is the bottom of a tube 3, filled with the tested liquid. Electrodes 4 are glued on the tube as shown in Fig. 1b. The electrodes 4 form a capacitor C_0, the dielectric of which is the tested medium, disturbed by the sound field. The tube diameter

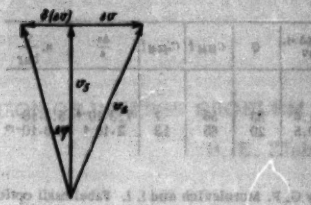

Fig. 2.

was approximately 3 cm, and the axial length of the capacitor electrodes was 0.5 cm, i. e., less than half the length of the sound wave produced by the radiator in the liquid. Capacitor C_0 is part of the capacitance of tank circuit 5, tuned to the frequency of generator 7, namely $f_2 = 5$ mc. Changing C_0 detunes tank circuit 5, thereby changing the phase of the oscillation induced in it by generator 7. An interference scheme, analogous to that used by L. L. Benshtein [1, 2] was used to detect the changes in phase and to measure the phase fluctuations of the generator. The oscillations at frequency f_2 add up as shown in the vector diagram of Fig. 2. The resultant voltage Δv will vary in amplitude whenever the angle between vectors v_1 and v_2 changes, as indeed occurs when the phase of v_2 changes. The output of detector 8 is a voltage of frequency f_1, which is measured at the output of amplifier 9 by means of meter 10.

The setup described was used to measure the value of $\Delta\epsilon$ at a certain sound pressure p. For a given Q of tank circuit 5 and for a given total capacitance C, the change in phase of the tank circuit due to a quasi-static variation in ϵ (as indeed occurs in our case) will be

$$\Delta\varphi = Q\frac{\Delta\epsilon}{\epsilon}\frac{C_0}{C}. \qquad (1)$$

If the phase of voltage v_2 varies periodically by an amount $\Delta\varphi$, one can obtain from the vector diagram of Fig. 2 an expression for the percentage modulation m of the voltage Δv

$$m = \frac{\delta(\Delta v)}{\Delta v} = \frac{v_1}{\Delta v}\Delta\varphi \qquad (2)$$

or

$$m = \frac{p}{\Delta v}Q\frac{\Delta\epsilon}{\epsilon}\frac{C_0}{C}. \qquad (3)$$

The value of m is determined by comparing the reading of meter 10 (Fig. 1) with the reading obtained when a voltage Δv is applied to the input of detector 8 from generator 7 at a known percentage modulation. The order of magnitude of ϵ is determined from the detuning introduced in tank circuit 5 by filling the tube 3 with water. The capacitance C_0 is taken to be that formed by the capacitor with electrodes 4 when tube 3 is filled.

Unfortunately, we were unable to measure the value of the sound pressure at the location of the capacitor electrodes. The pressure produced by the radiator was therefore estimated by us approximately from the value of the applied voltage and of the piezoelectric modulus (the crystal operated at a frequency considerably below resonance). An estimate of the pressure based on the power consumed in radiation on the electrical end yielded the same results. During the time of the experiment the liquid column in tube 3 was resonating at the frequency of generator 1, while a pressure antinode was formed at the location of the electrodes 4. It was therefore possible to assume that the pressure at the location of the plates was approximately the same as on the surface of the radiator. The results of the experiments are listed in the table. From these data we obtain for the quantity

$$\varkappa = \rho\left(\frac{\partial c}{\partial p}\right)$$

TABLE

Substance	Δp bar	s	v, V	$\delta(\Delta v)$, mv	Q	$C_{\mu\mu f}$	$C_{\mu\mu f}$	$\frac{\Delta\varepsilon}{\varepsilon}$	$\alpha, \frac{1}{\text{bar}}$
Distilled water	10^9	5	40	1.6	33	56	7	$7.3\cdot10^{-6}$	$5.3\cdot10^{-11}$
Ordinary water	10^9	13	30	0.5	20	65	13	$2\cdot10^{-6}$	$2.3\cdot10^{-10}$

a value close in order of magnitude to that measured by G. P. Motulevich and I. L. Fabelinskii optically [4].

Since the density varies adiabatically in the sound wave, the temperature changes. The dielectric constant is a function of both pressure and temperature. We set up an experiment to determine the role of temperature variation. The basis for setting up the experiment were the following considerations. It follows from thermodynamics that

$$\left(\frac{\partial\varepsilon}{\partial p}\right)_S = \left(\frac{\partial\varepsilon}{\partial p}\right)_T + \frac{T\alpha}{C_p}\left(\frac{\partial\varepsilon}{\partial T}\right)_p, \quad (4)$$

where T is the absolute temperature, α the temperature coefficient of expansion, and C_p the specific heat.

If the second term of the right half of (4) is much smaller than the first one, the adiabatic change in ε is due to the temperature change. However, according to data available from the literature [3], the first term of the right half of (4) predominates, and the effect of temperature change is insignificant. However, all these data pertain to the propagation of light waves in the medium, i. e., when ε represents the square of the index of refraction of light waves. But if we use for water the equation obtained from statistical measurements, $\varepsilon \approx 88 - 0.35\,(T-273)$, we find that the second term of the right half of (4) is of the same order of magnitude as our value of $\frac{\partial\varepsilon}{\partial p}$, i. e., not at all small compared with the first term. In our experiments ε was perturbed by the sound field at a frequency of 5 mc, which must not be presumed to be large enough to disregard statistical data. The experiment, which was set up to determine the role of temperature variation, was based on the fact that the quantity α, entering into (4), vanishes for water at 4°. A portion of the effect due to the dependence of ε on temperature vanishes at that temperature. No change in the magnitude of the effect was observed in the experiment when the water was cooled to 4°. This indicates that at 5 mc the temperature change due to the adiabatic nature of the process does not play a noticeable role.

LITERATURE CITED

[1] L. L. Benshtein, Bull. Acad. Sci. USSR, Phys. Ser. 14, 2, 145 (1950).

[2] L. L. Benshtein, Doklady Acad. Nauk SSSR 75, 5, 635 (1950).

[3] Raman and Vencataraman, Proc. Roy. Soc. 171, 137 (1939).

[4] G. P. Motulevich and I. L. Fabelinskii, Bull. Acad. Sci. USSR, Phys. Ser. 14, 4 (1950).

Received February 6, 1955

Gor'kii Physical-Technical Research Institute of the Gor'kii State University

SOLUTION OF INVERSE PROBLEM OF GEOMETRIC ACOUSTICS

B. E. Kinber

The problem of two reflecting or two refracting surfaces, with which one specified field can be transformed in another specified field, is considered. A complete system of differential equations is obtained for the problem. The solution is carried out under the assumption that the geometric laws of acoustics (or optics) are valid.

For a known primary incident field, the secondary field reflected or refracted by bodies of known shape that are large compared with the wavelength, can be calculated with sufficient degree of accuracy using the laws of geometric acoustics with the exception of certain special cases. The inverse problem, i. e., determination of the configuration of reflecting or refracting bodies, that transforms a specified primary into a specified secondary field is of interest. Such a problem arises, for example, if it is necessary to produce a radiating system having a specified diffraction directivity characteristic. The primary field may be considered specified, if the radiator, i. e., horn, piston radiator, etc., is known. The secondary field is determined from the specified directivity characteristic. This is done by calculating the field in the aperture plane, using Fourier transforms or some other known method. Furthermore, using the eikonal equation and the law of conservation of energy in the field and the aperture (reflected or refracted), the secondary field is determined in the vicinity of the radiating system.

It can be shown that a single reflection or refraction is not enough to solve the problem of transforming the primary field into the secondary one. Thus, for example, if the secondary field is specified in the form of a plane wave of constant amplitude, and the primary field is specified in the form of a spherical wave of constant amplitude, this problem cannot be solved with the aid of a parabolic mirror. As is known, the amplitude of the plane wave resulting from this reflection is not constant. It will be shown below, that to transform the primary field into the secondary it is generally enough to have two reflections or two refractions.

Let us consider the difference between the statement of our problem and the usual statement of the problem in geometric optics. In our problem we seek the shapes of the reflecting or refracting bodies that would convert a single primary field, specified both in amplitude and in phase, into a single secondary field, specified in the same manner, i. e., in amplitude and in phase. To the contrary, in the ordinary statement of the problem of geometric optics one determines the reflecting or refracting systems that convert the object space into the image space, i. e., a set of diverging spherical waves into a set of converging spherical waves. Here, unlike in our problem, no requirements are imposed at all on the distribution of the amplitudes along the fronts of the converging and diverging spherical waves. This is why the parabolic mirror in the example cited above is not a solution to our problem under consideration but is a solution from the point of view of stating the problem in geometric optics. Let us furthermore indicate two other differences between the problems. In geometric optics, the specified fields are usually only spherical waves. In the problem analyzed here, both the primary and the secondary fields may have wave surfaces, differing from a sphere as required. In addition, in geometric optics one usually considers only reflecting or refracting systems having second-order surfaces. The surfaces of lenses and mirrors which are solutions of our problem will in the majority of cases be surfaces of a more complicated type.

We shall assume that both the primary and secondary fields are converted to a form suitable for the solution, i. e., they are specified in the form of a) the ray equations, b) the distribution of field amplitudes along any surface Q that intenects each ray once and only once.

This specification of the field is equivalent to the usual specification of the amplitude and phase of the field in each point of space, for knowing the field of the rays it is possible to plot the wave surfaces orthogonal to the rays, and the variation of the amplitudes of the field along each of the rays is determined from the law of conservation of energy flux along the beam of the rays. We shall consider hereinafter for the sake of simplicity the plane or the equivalent axially-symmetrical problem for media with constant indices of refraction, in which the rays are straight lines. Let us consider in sequence the solution for the case of reflections, i. e., using two mirrors, and for the case of refractions, i. e., using one lens.

Case of Reflection

Let us write down the equations for a system of rays, corresponding to the fields under consideration, as a function of the angle between the rays and the OX axis. In exactly the same manner, we shall write the value of the amplitude at the point of intersection between the ray and the surface Q as a function of this angle.

In accordance with the above assumptions, we write

$$y = a_1(\varphi)\,x + b_1(\varphi), \qquad A_1 = A_1(\varphi); \tag{1}$$

$$y = a_2(\theta)\,x + b_2(\theta), \qquad A_2 = A_2(\theta), \tag{2}$$

where φ is the angle between the ray of the primary field and the OX axis, θ is the angle between the ray of the secondary field and the OX axis, and $A_1(\varphi)$, $A_2(\theta)$ are the amplitudes of the primary and secondary fields on the surfaces Q_1 and Q_2.

Let us determine the connection between the rays of the primary and secondary fields, using the law of conservation of the energy flux in the beam of rays before and after reflection. We shall consider the reflection to be total, i. e., we shall assume the reflection coefficient to be unity.

We then have for the plane case

$$\int_{\varphi_1}^{\varphi} A_1^2(\varphi)\,\rho_1(\varphi)\,d\varphi = \int_{\theta_1}^{\theta} A_2^2(\theta)\,\rho_2(\theta)\,d\theta \qquad \begin{matrix}\varphi_1 \leqslant \varphi \leqslant \varphi_2 \\ \theta_1 \leqslant \theta \leqslant \theta_2,\end{matrix} \tag{3}$$

where $\rho_1(\varphi)$, $\rho_2(\theta)$ are the radii of curvature of the wave surfaces for the primary and secondary fields at the points of intersection of the rays with the surfaces Q_1 and Q_2.

Analogously, we have for the axially-symmetrical case

$$\int_{\varphi_1}^{\varphi} A_1^2(\varphi)\,\rho_1^2(\varphi)\sin\varphi\,d\varphi = \int_{\theta_1}^{\theta} A_2^2(\theta)\,\rho_2^2(\theta)\sin\theta\,d\theta. \tag{3a}$$

From Eqs. (3) and (3a) we can determine the connection between the angles φ and θ:

$$\theta = \theta(\varphi). \tag{4}$$

It follows from (4) that to solve the problem it is necessary to construct surfaces that reflect the primary-field rays in such a way as to transform the reflected ray of the primary field, making an angle φ, into a ray of the secondary field, making an angle θ. We shall further seek the coordinates of the two unknown mirror surfaces (X_1, Y_1) and (X_2, Y_2) as functions of the angle φ, considered as a parameter, i. e., we shall determine the coordinates of the points of the first and second mirrors, converting a ray making an angle φ into a ray making an angle $\theta(\varphi)$.

It follows from this (Fig. 1) that the point of the first mirror reflecting a ray of the primary field, satisfies the equation of this ray

$$Y_1(\varphi) = a_1(\varphi) X_1(\varphi) + b_1(\varphi) \tag{5}$$

and analogously for the second mirror [using (4)]

$$Y_2[\theta(\varphi)] = a_2[\theta(\varphi)]\, X_2[\theta(\varphi)] + b_2[\theta(\varphi)], \tag{6}$$

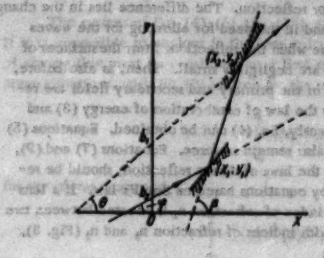

Fig. 1.

After the first reflection the ray should pass through the point (X_2, Y_2) and consequently

$$\frac{dY_1}{dX_1} = \tan\frac{\varphi + \beta}{2}, \tag{7}$$

where

$$\beta = \text{arc tan}\,\frac{Y_2 - Y_1}{X_2 - X_1}. \tag{8}$$

Since the ray, upon the second reflection, should make an angle θ, we have

$$\frac{dY_2}{dX_2} = \tan\frac{\beta + \theta}{2}. \tag{9}$$

The systems of Eqs. (3), (5), (7), and (9) solves our problem. This can be seen by rewriting these equations in the canonical form:

$$Y_1 = f_1(\varphi,\ X_1), \tag{5a}$$

$$Y_2 = f_2(\varphi,\ X_2), \tag{6a}$$

$$\frac{dY_1}{d\varphi} = \frac{dX_1}{d\varphi} g_1(\varphi, X_1, X_2, Y_1, Y_2), \tag{7a}$$

$$\frac{dY_2}{d\varphi} = \frac{dX_2}{d\varphi} g_2(\varphi, X_1, X_2, Y_1, Y_2). \tag{8a}$$

By way of initial conditions for the system of equations we can choose any two points lying on two rays, corresponding to each other in accordance with Eq. (4). The need for two reflections to solve the problem is not evident at first glance. It would appear that the transformation of a ray making an angle φ into a ray making an angle θ could be made with the aid of a single reflection at the point of intersection of the rays. One can readily see, however, that in this case the surface of the mirror cannot be made smooth, for Eqs. (7) and (9) are in general not compatible with Eqs. (5) and (6).

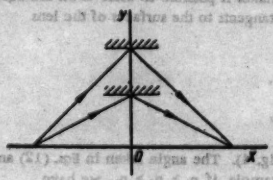

Fig. 2.

Let us consider the simplest example, illustrating this situation. Let us specify the primary and secondary fields in the form of spherical waves of constant amplitude, traveling from two points located symmetrically with respect to the O axis. It then follows from (3) that

$$\theta = -\varphi,$$

and Eqs. (7) and (9) are satisfied if the elements of the mirror are parallel to the OX axis (Fig. 2). On the other hand, the points of intersection satisfy the equation $x = 0$, which is incompatible with the first condition.

Let us remark that a physically-realizable solution should satisfy the following supplementary conditions: a) the surfaces of the mirrors must not cast shadows on each other; b) the surfaces of the mirrors must not intersect the caustics of the primary, secondary, or intermediate fields.

Case of Refraction

Unlike the preceding case, where two reflections require two mirrors, in the case of refraction all that is necessary is but a single lens. The necessary two refractions are carried out by the two surfaces of the lens. The solution of the refraction problem differs but little from that for reflection. The difference lies in the change in the law of transformation of the rays on the surfaces of the lens and in the need for allowing for the waves reflected from the surfaces of the lens. Let us first consider the case when the reflections from the surfaces of the lens are negligibly small. Then, as also before, the rays of the primary and secondary fields are related by the law of conservation of energy (3) and consequently, Eq. (4) can be obtained. Equations (5) and (6) also remain in force. Equations (7) and (9), obeying the laws of direct reflection, should be replaced by equations based on Snell's law. If a lens with an index of refraction n_2 is located between two media with indices of refraction n_1 and n_3 (Fig. 3), we have

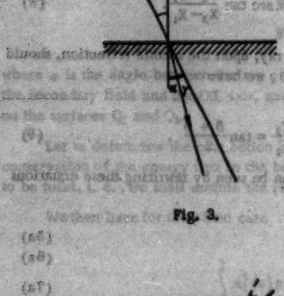

Fig. 3.

$$\frac{\sin(\gamma+\alpha)}{\sin\alpha} = N, \tag{10}$$

where N is the ratio of the index of refraction of the lens dense medium to that of the denser one ($N > 1$), α is the angle between the normal to the surface and the ray in the denser medium, and γ is the angle between the ray in the outer medium and the ray inside the lens, i. e.,

$$\gamma_1 = \beta - \varphi, \tag{11a}$$

$$\gamma_2 = \theta - \beta. \tag{11b}$$

Determining α from (10) we get

$$\tan\alpha = \frac{\sin\gamma}{N+\cos\gamma},$$

which makes it possible to write down the equations for the tangents to the surfaces of the lens

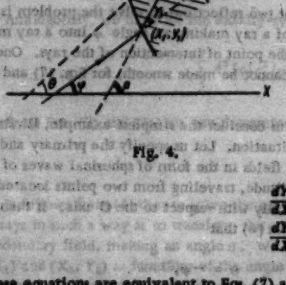

Fig. 4.

$$\frac{dY_1}{dX_1} = -\cot\left[\frac{\beta}{\varphi} - \alpha_1\right], \tag{12}$$

$$\frac{dY_2}{dX_2} = -\cot\left[\frac{\beta}{\theta} - \alpha_2\right], \tag{13}$$

These equations are equivalent to Eqs. (7) and (9) for reflection (Fig. 4). The angle taken in Eqs. (12) and (13) corresponds to the ray located in the denser medium. Thus, for example, if $n_3 > n_2 > n_1$, we have

$$\frac{dY_1}{dX_1} = -\cot(\beta - \alpha_1); \quad \frac{dY_2}{dX_2} = -\cot(\theta - \alpha_1).$$

Angles α and γ should have the same sign, with

$$|\gamma + \alpha| \leq \frac{\pi}{2},$$
$$|\cot \alpha| \geqslant \sqrt{N^2 - 1},$$

i. e., angles α and γ are bounded if the values of the indices of refraction are specified.

The system of Eqs. (4), (5), (6), (12), and (13) makes it possible to determine the shape of the lens surface. If it is impossible to neglect in the lens calculation the waves reflected from its surface, Eq. (3) for the balance of energy flux must be considered as a first approximation. The lens calculation must be carried out by successive approximations, with Eq. (3) written for the second and higher-order approximations in the following form

$$\int_{\varphi_0}^{\varphi} A_1^2(\varphi) \rho_1(\varphi) P_1(\varphi)\, d\varphi = \int_{\theta_0}^{\theta} A_2^2(\theta) \rho_2(\theta)\, d\theta \qquad (4a)$$

for the plane case, and

$$\int_{\varphi_0}^{\varphi} A_1^2(\varphi) \rho_1^2(\varphi) P_1(\varphi) \sin\varphi\, d\varphi = \int_{\theta_0}^{\theta} A_2^2(\theta) \rho_2^2(\theta) \sin\theta\, d\theta$$

for the axially-symmetrical case, where $P_1(\varphi)$ is the summary transmission coefficient for the ray φ, taking into account the losses during refraction by the first and second surfaces of the lens.

The solutions presented above are applicable also to optical problems. They can be easily generalized to the case when the media outside the lens have a variable index of refraction, or for the case of waveguide lenses or lenses made of anisotropic material. Let us also remark that the problem posed can also be solved using a larger number of refractions or reflections, but this is meaningful only in those cases, when additional conditions are specified, for example, concerning the polarization of the field vector.

Received July 3, 1954 Moscow

RADIATION OF SOUND FROM VIBRATING FACES OF AN ARBITRARY WEDGE

Part II

G. D. Maliuzhinets

Using the exact solution obtained in the first part of this investigation for the sound pressure produced by the vibrations of the faces of the wedge, it is shown that the presence of the edge of the wedge does not affect at all the radiated sound power, which is determined by the laws of geometric acoustics exactly. The edge effect reduces only to a reactive (elastic or inertial) correction to the radiation impedance.

6.* Effect of Edge of Wedge on the Radiated Sound Power

It will be shown below that the presence of the edge will not affect at all the radiated power. To explain the statement, let us cite the following example. Let an infinite plate vibrate with an amplitude that is everywhere the same. Then the power radiated will not change if we bend the vibrating plate along a straight line at any angle, retaining the same normal-velocity amplitude as before. This will give rise only to a reactive correction to the radiation impedance, which can have either an inertial or an elastic character.

Let us turn to calculate the sound power radiated by the vibrating faces into the region $-\Phi < \varphi < \Phi$. We shall assume here that the amplitudes of the velocities v_1 and v_2 are complex. Were there no diffraction phenomena near the edge of the wedge, the total radiation would be due only to the plane waves, radiated by each face in a normal direction. The amplitudes of the sound pressures, caused by these waves, are:

on the first face $p_1 = \rho c v_1$,
on the second face $p_2 = \rho c v_2$.

The power per unit length of the wedge would be determined from the following equation

$$W_0(r_1) = \frac{1}{2}\int_0^{r_1} (v_1^* p_1 + v_2^* p_2)\, dr = \frac{\rho c}{2}(|v_1|^2 + |v_2|^2) r_1.$$

The total power $W_0(\infty)$ is naturally infinite.

To calculate the power with allowances for the edge effect, it is necessary to replace p_1 and p_2 in the integral by the true sound pressures $p(r, \Phi)$ and $p(r, -\Phi)$, determined by Eq. (30):

$$p(r, \varphi) = \frac{\rho c}{2\pi i}\int_\gamma e^{-ikr\cos(\varphi - z)} [v_1 \eta_\Phi(z + \Phi) + v_2 \eta_\Phi(z - \Phi)]\, dz.$$

However, in this case the integral

$$W(r_1) = \frac{1}{2}\int_0^{r_1} [v_1^* p(r, \Phi) + v_2^* p(r, -\Phi)]\, dr$$

* The numbering of the sections, equations, and figures is continued from part I of the author's article published in the preceding issue of the journal.

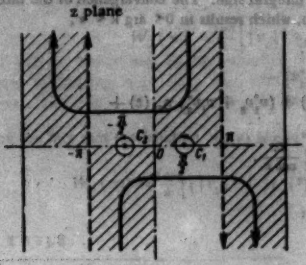

Fig. 12.

will have a real and imaginary part. The real part is equal to the average (in time) of the radiated power. On the other hand, the imaginary part determines the reactive component of the radiation impedance.

The simplest way is to integrate from zero to infinity. But this cannot be done directly, for the expression $W(r_1)$ should contain a term that becomes infinite as r_1 approaches infinity. However, if we separate only the edge effect, the difference under consideration becomes $W_1(r_1) = W(r_1) - W_0(r_1)$, and it is possible to go to the limit $r_1 = \infty$. Let us thus consider the additional (complex) power, caused by the edge effect:

$$W_1(\infty) = \frac{1}{2}\int_0^\infty \left\{ v_1^* \left[p(r, \Phi) - \rho c v_1 \right] + \right. \tag{49}$$

$$\left. + v_2^* \left[p(r, -\Phi) - \rho c v_2 \right] \right\} dr.$$

From the solution (30), changing the variable of integration, we get

$$p(r, \Phi) = \frac{\rho c}{2\pi i}\int_\gamma e^{-ikr\cos z} \left[v_1 \eta_\Phi(z + 2\Phi) + v_2 \eta_\Phi(z) \right] dz$$

and analogously

$$p(r, -\Phi) = \frac{\rho c}{2\pi i}\int_\gamma e^{-ikr\cos z} \left[v_1 \eta_\Phi(z) + v_2 \eta_\Phi(z - 2\Phi) \right] dz.$$

Expression (49) can therefore be rewritten as:

$$W_1(\infty) = \frac{\rho c}{2}\int_0^\infty \left\{ \frac{1}{2\pi i}\int_\gamma e^{-ikr\cos z} \left[|v_1|^2 \eta_\Phi(z + 2\Phi) + (v_1^* v_2 + v_1 v_2^*)\eta_\Phi(z) + \right. \right.$$

$$\left. \left. + |v_2|^2 \eta_\Phi(z - 2\Phi) \right] dz - |v_1|^2 - |v_2|^2 \right\} dr.$$

To simplify the calculations let us first assume that $\Phi > \frac{\pi}{4}$; being analytic, the result will be true also in the general case. Under this assumption the expression located in the square brackets under the integral sign is regular in the strip $|\operatorname{Re} z| \leq \pi$ everywhere, with the exception of simple poles at the points $\pm \pi/2$, with residues $|v_1|^2$ and $|v_2|^2$.

If we deform the integration contour γ, joining the upper and lower loops in such a way that two straight-line integration paths γ_1 and γ_2 are formed (Fig. 12), the above residues will cancel out the terms $-|v_1|^2$ and $-|v_2|^2$ in the braces. We then obtain

$$W_1(\infty) = \frac{\rho c}{4\pi i}\int_0^\infty dr \int_{\gamma_1 + \gamma_2} e^{-ikr\cos z} \left[|v_1|^2 \eta_\Phi(z + 2\Phi) + (v_1^* v_2 + v_1 v_2^*)\eta_\Phi(z) + \right.$$

$$\left. + |v_2|^2 \eta_\Phi(z - 2\Phi) \right] dz.$$

It is now possible to integrate with respect to r under the integral sign. The convergence of the integral required for this purpose is insured by the principle of extinction, which results in $0 < \arg k < \pi$.

Performing the integration, we obtain

$$W_1(\infty) = -\frac{\rho c}{4\pi k}\int\limits_{\gamma_1+\gamma_2}\left[|v_1|^2\eta_\Phi(z+2\Phi)+(v_1^*v_2+v_1v_2^*)\eta_\Phi(z)+\right.$$
$$\left.+|v_2|^2\eta_\Phi(z-2\Phi)\right]\frac{dz}{\cos z},$$

The last integral reduces to the residues at the poles $\pm\frac{\pi}{2}$:

$$W_1(\infty) = \frac{\rho c}{4\pi k}\int\limits_{C_1+C_2}\left[|v_1|^2\eta_\Phi(z+2\Phi)+(v_1^*v_2+v_1v_2^*)\eta_\Phi(z)+\right.$$
$$\left.+|v_2|^2\eta_\Phi(z-2\Phi)\right]\frac{dz}{\cos z} =$$
$$= \frac{\rho c}{4\pi k}\int\limits_C\left\{|v_1|^2\left[\eta_\Phi(z+2\Phi-\tfrac{\pi}{2})-\eta_\Phi\left(z+2\Phi+\tfrac{\pi}{2}\right)\right]+(v_1^*v_2+v_1v_2^*)\left[\eta_\Phi\left(z-\tfrac{\pi}{2}\right)-\right.\right.$$
$$\left.\left.-\eta_\Phi\left(z+\tfrac{\pi}{2}\right)\right]+|v_2|^2\left[\eta_\Phi\left(z-2\Phi-\tfrac{\pi}{2}\right)-\eta_\Phi\left(z-2\Phi+\tfrac{\pi}{2}\right)\right]\right\}\frac{dz}{\sin z},$$

where C is the closed contour surrounding the origin. Using the identity *

$$\eta_\Phi\left(z+\tfrac{\pi}{2}\right)+\eta_\Phi\left(z-\tfrac{\pi}{2}\right) = -\frac{\pi}{4\Phi}\tan\frac{\pi z}{4\Phi}.$$

Then

$$\eta_\Phi\left(z\pm 2\Phi+\tfrac{\pi}{2}\right)+\eta_\Phi\left(z\pm 2\Phi-\tfrac{\pi}{2}\right) = \frac{\pi}{4\Phi}\cot\frac{\pi z}{4\Phi}.$$

Therefore

$$W_1(\infty) = \frac{\rho c}{2\pi k}\int\limits_C\left\{|v_1|^2\eta_\Phi\left(z+2\Phi-\tfrac{\pi}{2}\right)-(v_1^*v_2+v_1v_2^*)\eta_\Phi\left(z+\tfrac{\pi}{2}\right)-\right.$$
$$-|v_2|^2\eta_\Phi\left(z-2\Phi+\tfrac{\pi}{2}\right)-(|v_1|^2-|v_2|^2)\frac{\pi}{8\Phi}\cot\frac{\pi z}{4\Phi}+$$
$$\left.+\frac{\pi}{8\Phi}(v_1^*v_2+v_1v_2^*)\tan\frac{\pi z}{4\Phi}\right\}\frac{dz}{\sin z}.$$

The expression in the square brackets under the integral sign is regular at the point $z = 0$. The residues for the terms containing $\cot\frac{\pi z}{\Phi}$ and $\tan\frac{\pi z}{\Phi}$ are zero. We therefore have

* See appendix.

$$W_1(\infty) = \frac{i\rho c}{k}\left[|v_1|^2\eta_\Phi\left(2\Phi-\frac{\pi}{2}\right) + |v_2|^2\eta_\Phi\left(\frac{\pi}{2}-2\Phi\right) - \left(v_1^* v_2 + v_1 v_2^*\right)\eta_\Phi\left(\frac{\pi}{2}\right)\right]$$

or using the fact that the function $\eta_\Phi(z)$ is odd*:

$$W_1(\infty) = \frac{i\rho c}{k}\left[\left(|v_1|^2 + |v_2|^2\right)\eta_\Phi\left(2\Phi-\frac{\pi}{2}\right) - \left(v_1^* v_2 + v_1 v_2^*\right)\eta_\Phi\left(\frac{\pi}{2}\right)\right]. \qquad (50)$$

TABLE

2Φ, degrees	$2\eta_\Phi\left(\frac{\pi}{2}\right)$	$2\eta_\Phi\left(2\Phi-\frac{\pi}{2}\right)$
0	$-\infty$	—
15	−42.8284	7.3095
18	−9.9443	5.5055
22,5	—	3.8284
30	−5.0000	2.3095
45	−2.8284	1.0000
90	−1.0000	0.0000
180	−0.3183	−0.3183
270	−0.1547	−0.3846
360	−0.0909	−0.4092

In the special case when $\Phi = \frac{\pi}{2}$

$$W_1(\infty) = \frac{i\rho c}{k}\left[|v_1|^2 + |v_2|^2 - \left(v_1^* v_2 + v_1 v_2^*\right)\eta_{\frac{\pi}{2}}\left(\frac{\pi}{2}\right)\right] = \frac{i\rho c}{k}|v_1 - v_2|^2\,\eta_{\frac{\pi}{2}}\left(\frac{\pi}{2}\right). \qquad (51)$$

If we also have $v_1 = v_2$, then $W_1(\infty) = 0$.

Another special case, $v_1 = v_2 = v$, leads to

$$W_1(\infty) = \frac{2i\rho c|v|^2}{k}\left[\eta_\Phi\left(2\Phi-\frac{\pi}{2}\right) - \eta_\Phi\left(\frac{\pi}{2}\right)\right] = \frac{i\rho c|v|^2}{k}\times\int_0^\infty\left(\tanh\frac{w\pi}{2}\coth w\Phi - 1\right)dw. \qquad (52)$$

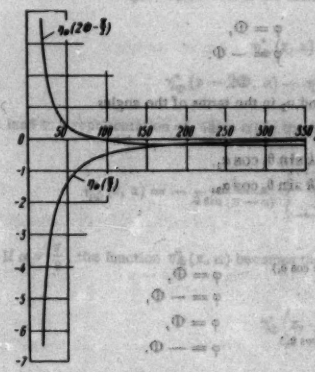

Fig. 13.

The function $\eta_\Phi(z)$* is real for a real argument. Consequently, the quantity $W_1(\infty)$ is pure imaginary. The diffraction effects thus do not affect the average active power, radiated by the wedge, which at sufficiently large values of r_1 is given by

$$W_0(r_1) = \frac{\rho c}{2}\left(|v_1|^2 + |v_2|^2\right)r_1.$$

The values of the $\eta_\Phi\left(\frac{\pi}{2}\right)$ and $\eta_\Phi\left(2\Phi-\frac{\pi}{2}\right)$, calculated with an accuracy to within four significant figures, are given in the table. With the aid of this table it is possible to calculate the reactive correction to the radiation impedance, due to the presence of the edge of the wedge, on the basis of Eqs. (50), (51), and (52). Plots of the function are shown in Fig. 13.

7. Generalization to the Case of Non-Uniform Velocity Distribution on the Faces

In Sections 1 and 2 we obtained an exact solution of the problem for the sound pressure in the wedge-

* See appendix of first part of the article.

shaped region $-\Phi < \varphi < \Phi$, if the specified amplitudes of the normal velocities v_1 and v_2 on the faces of the wedge are constant over each face.

Using an exactly analogous method it is possible to obtain a solution for the case when these amplitudes vary exponentially over the faces, i. e., when instead of the constant values v_1 and v_2, the values specified on the faces are $v_1 e^{-i(m_1 r + n_1 z)}$ and $v_2 e^{-i(m_2 r + n_2 z)}$, where z is the coordinate along the edge of the wedge, and m_1, m_2, n_1, and n_2 are arbitrary real or complex constants.

The boundary conditions for the sound pressure now become

$$-\frac{1}{ikpcr}\frac{\partial p}{\partial \varphi} = v_1 e^{-i(m_1 r + n_1 z)} \quad \text{at} \quad \varphi = \Phi,$$
$$\frac{1}{ikpcr}\frac{\partial p}{\partial \varphi} = v_2 e^{-i(m_2 r + n_2 z)} \quad \text{at} \quad \varphi = -\Phi. \tag{53}$$

If $m_1 = m_2 = n_1 = n_2 = 0$, the boundary conditions transform into those of Section 1. As previously, a solution to the problem, satisfying these conditions, satisfying the equation $\Delta p + k^2 p = 0$, and satisfying the extinction principle can be represented as a sum of solutions, corresponding to a specified vibration on only one face, with the other face remaining stationary:

$$p = p_1 + p_2,$$

where p_1 satisfies the following boundary conditions:

$$-\frac{1}{ikpcr}\frac{\partial p_1}{\partial \varphi} = \begin{cases} v_1 e^{-i(m_1 r + n_1 z)} & \varphi = \Phi, \\ 0 & \varphi = -\Phi \end{cases}$$

and p_2 satisfies the conditions

$$\frac{1}{ikpc}\frac{\partial p_2}{\partial \varphi} = \begin{cases} 0 & \varphi = \Phi, \\ v_2 e^{-i(m_2 r + n_2 z)} & \varphi = -\Phi. \end{cases}$$

It will prove convenient to express the constants m_1, n_1, m_2, and n_2 in the terms of the angles

$$n_1 = k\cos\theta_1, \qquad m_1 = k\sin\theta_1\cos\alpha_1,$$
$$n_2 = k\cos\theta_2, \qquad m_2 = k\sin\theta_2\cos\alpha_2, \tag{54}$$

so that the boundary conditions for p_1 and p_2 become

$$-\frac{1}{ikpcr}\frac{\partial p_1}{\partial \varphi} = \begin{cases} v_1 e^{-ik(r\sin\theta_1\cos\alpha_1 + z\cos\theta_1)} & \varphi = \Phi, \\ 0 & \varphi = -\Phi, \end{cases}$$
$$\frac{1}{ikpcr}\frac{\partial p_2}{\partial \varphi} = \begin{cases} 0 & \varphi = \Phi, \\ v_2 e^{-ik(r\sin\theta_2\cos\alpha_2 + z\cos\theta_2)} & \varphi = -\Phi. \end{cases}$$

If we introduce, in lieu of the sound pressures p_1 and p_2, new functions S_1 and S_2, such that

$$p_1 = \frac{pcv_1}{\sin\theta_1} S_1 e^{-ikz\cos\theta_1}, \qquad p_2 = \frac{pcv_2}{\sin\theta_2} S_2 e^{-ikr\cos\theta_2},$$

then we obtain for S_1 and S_2 which satisfy the equations

$$\Delta S_1 + (k \sin \theta_1)^2 S_1 = 0, \qquad \Delta S_2 + (k \sin \theta_2)^2 S_2 = 0,$$

the following boundary conditions

$$-\frac{1}{i(k \sin \theta_1) r} \frac{\partial S_1}{\partial \varphi} = \begin{cases} e^{-i (k \sin \theta_1) r \cos \varepsilon}, & \varphi = \Phi, \\ 0 & \varphi = -\Phi, \end{cases}$$

$$\frac{1}{i(k \sin \theta_2) r} \frac{\partial S_2}{\partial \varphi} = \begin{cases} 0 & \varphi = \Phi, \\ e^{-i (k \sin \theta_2) r \cos \varepsilon}, & \varphi = -\Phi. \end{cases}$$

We thus reduced the three-dimensional problems involving the fields produced by vibrations of only the upper or only the lower face, to two-dimensional problems, independent of the coordinate z along the edge of the wedge. But now the problem involving S_1 and S_2 contains instead of the wave number k the quantities $(k \sin \theta_1)$ and $(k \sin \theta_2)$.

Solutions for S_1 and S_2, in the form of Sommerfeld integrals

$$S_1(r, \varphi) = \frac{1}{2\pi i} \int_\gamma e^{-i (k \sin \theta_1) r \cos (\varphi - \varepsilon)} \eta^*_\Phi (\varepsilon + \Phi, \alpha_1)\, d\varepsilon,$$

$$S_2(r, -\varphi) = \frac{1}{2\pi i} \int_\gamma e^{-i (k \sin \theta_2) r \cos (\varphi - \varepsilon)} \eta^*_\Phi (\varepsilon + \Phi, \alpha_2)\, d\varepsilon \qquad (55)$$

are obtained in exactly the same manner as in Sections 1 and 2.

For the function $\eta^*_\Phi(z, \alpha)$ we obtain the following functional equations

$$\eta^*_\Phi(z, \alpha) + \eta^*_\Phi(-z, \alpha) = 0,$$

$$\eta^*_\Phi(z - 2\Phi, \alpha) - \eta^*_\Phi(z + 2\Phi, \alpha) = \frac{1}{\cos z - \cos \alpha},$$

which lead to a representation of $\eta^*_\Phi(z, \alpha)$ in the form of an integral

$$\eta^*_\Phi(z, \alpha) = -\frac{1}{4 \sin (\pi - \alpha)} \left\{ \int_{-\infty - i\omega}^{-\pi + i\omega} + \int_{\pi - i\omega}^{\pi + i\omega} \right\} \frac{\sin w (\pi - \alpha)\, e^{-i w z}}{\sin w\pi \cdot \sin 2w\Phi}\, dw. \qquad (56)$$

If $\alpha = \frac{\pi}{2}$, the function $\eta^*_\Phi(z, \alpha)$ becomes the previously studied function $\eta_\Phi(z)$:

$$\eta^*_\Phi\left(z, \frac{\pi}{2}\right) = \eta_\Phi(z).$$

Using the integral (56) one can readily verify that $\eta^*_\Phi(z, \alpha)$ satisfies also the functional relationship

$$\eta^*_\Phi(z - \pi, \alpha) - \eta^*_\Phi(z + \pi, \alpha) = \frac{\pi}{2\Phi \sin (\pi - \alpha)} \frac{\sin \frac{\pi}{2\Phi}(\pi - \alpha)}{\cos \frac{\pi z}{2\Phi} + \cos \frac{\pi}{2\Phi}(\pi - \alpha)}.$$

For several particular values of Φ and α, the integral (56) can be taken in a finite form; for example, for $2\Phi = \pi$ (wedge developed into a plane) we have

$$\frac{\eta_m}{2}(z, \alpha) = \frac{1}{2\pi(\cos z + \cos\alpha)}\left(z - \frac{(\pi - \alpha)\sin z}{\sin\alpha}\right).$$

The complete solution concerning the sound field radiated by the faces of the wedge with a velocity-amplitude distribution as given by (53) and (54) is given by the following equation

$$p(r, \varphi, z) = \frac{\rho c v_1}{\sin\theta_1} e^{-ikz\cos\theta_1} S_1(r, \varphi) + \frac{\rho c v_2}{\sin\theta_2} e^{-ikz\cos\theta_2} S_2(r, \varphi), \tag{57}$$

where S_1 and S_2 are given by (55) and (56).

The resultant solution can be investigated in a manner similar to that used for the simpler case in Sections 3, 4, 5, and 6. Let us remark that since the Solution (57) is suitable for any exponential velocity distribution, it is easy to obtain, using superposition and the Fourier integral, a solution for any velocity distribution on the faces of the wedge. A similar result can naturally be obtained by an entirely different method, using the Sommerfeld solution for the diffraction of a spherical wave by an ideal rigid wedge as a Green's function.

APPENDIX

The following theorem was used in Section 2 to obtain the functional equations that must be satisfied by the function of the angular distribution of the amplitudes in the Sommerfeld integral.

Theorem

If an analytic function $S(z)$ is regular for $|\operatorname{Im} z| \geq a$, then to satisfy the identity ($r > 0$)

$$R(r) = \int_\gamma e^{-ikr\cos z} S(z)\, dz \equiv 0 \quad (\gamma = \gamma_1 + \gamma_2)$$

(Fig. 14) it is necessary and sufficient that the function $S(z)$ be even, i. e., $S(z) = S(-z)$.

Proof

Assume that $S(z)$ is an arbitrary analytic function, regular at $|\operatorname{Im} z| \geq a$. It is possible to represent this function uniquely as a sum of an even component $f_1(z)$ and an odd component $f_2(z)$. In fact,

$$S(z) = \frac{1}{2}[S(z) + S(-z)] + \frac{1}{2}[S(z) - S(-z)] = f_1(z) + f_2(z).$$

The proof reduces to proving that the condition $f_2(z) \equiv 0$ is necessary and sufficient for the identity $R(r) \equiv 0$ to be satisfied.

Let us break down the integral $R(r)$ into two components corresponding to f_1 and f_2

$$R(r) = R_1(r) + R_2(r).$$

The first integral

$$R_1(r) = \int_\gamma e^{-ikr\cos z} f_1(z)\, dz$$

vanishes identically. To prove this, let us replace the integration variable z by $-z$. Then, using the symmetry of the contour γ and the fact that $f_1(z)$ is even, we get

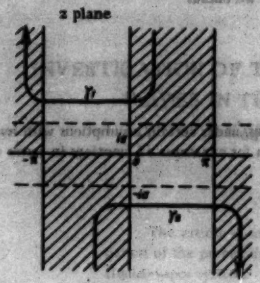

Fig. 14.

$$R_1(r) = -\int_{\gamma} e^{-ikr\cos(-z)} f_1(-z)\,dz =$$

$$= -\int_{\gamma} e^{-ikr\cos z} f_1(z)\,dz = -R_2(r),$$

from which $R_2(r) \equiv 0$.

For the identity $R(r) \equiv 0$ to hold, it is therefore necessary and sufficient to have

$$R_2(r) = \int_{\gamma} e^{-ikr\cos z} f_2(z)\,dz \equiv 0.$$

Breaking up in turn this integral into two terms corresponding to the two loops γ_1 and γ_2 of the contour γ, and seeing that $\int_{\gamma_1} = -\int_{\gamma_2}$ by virtue of the function $f_2(z)$ being odd, we can rewrite the latter identity as:

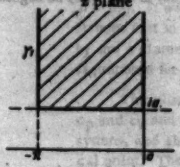

Fig. 15.

$$R_2(r) = 2\int_{\gamma_1} e^{-ikr\cos z} f_2(z)\,dz \equiv 0.$$

Assuming $r > 0$, let us introduce a change in variables, putting $\cos z = w$ and $z = \arccos w$. We then obtain

$$R_2(r) = 2\int_{\gamma_1} \frac{e^{-ikrw} f_2(\arccos w)}{\sqrt{1-w^2}}\,dw \equiv 0.$$

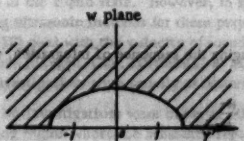

Fig. 16.

The two corresponding contours of integration γ_1 and γ' are shown in Figs. 15 and 16.

The cross-hatched parts of the planes correspond to each other. The function f_2 is regular in these areas.

Multiplying both parts of the equation by $e^{ikr\nu}$, where ν is any number such that $\operatorname{Im}\nu > \sinh a$, and integrating within the limits from $c > 0$ to infinity, we get

$$0 = 2\int_c^{\infty} dr \int_{\gamma'} e^{ikr(\nu-w)} \frac{f_2(\arccos w)}{\sqrt{1-w^2}}\,dw = \frac{2}{ik}\int_{\gamma'} \frac{e^{ikc(\nu-w)} f_2(\arccos w)}{(w-\nu)\sqrt{1-w^2}}\,dw.$$

We can now let c approach zero in such manner, that

$$\int_{\gamma'} \frac{f_2(\arccos w)}{\sqrt{1-w^2}} \frac{dw}{w-\nu} = 0.$$

By virtue of the sufficiently rapid decrease of the integrand with increasing w in the upper half-plane, it is possible to supplement the contour γ' in the upper half-plane by a semi-circle of infinitely large radius.

The integral then reduces to a residue at the point $w = \nu$, and we obtain

$$\frac{f_3(\arccos \nu)}{\sqrt{1-\nu^2}} = 0.$$

Consequently, $f_3(p) \equiv 0$ and the theorem is fully proven.

Let us remark incidentally that it is possible to prove in passing, under certain assumptions with respect to the form of the functions $\varphi(\nu)$, the following uniqueness theorem for expansion of functions in terms of Bessel functions of various real orders.

If $\int_0^\infty J_\nu(kr)\,\varphi(\nu)\,d\nu = 0$, then $\varphi(\nu) \equiv 0$ identically.

To prove this, let us consider

$$R_3(r) = 2\int_{\gamma_1} e^{-ikr\cos z} f_3(z)\,dz.$$

All that we require from the analytic function $f_3(z)$ (not necessarily odd) is that $f_3(z)$ be regular at $\operatorname{Im} z > 0$, and that it vanish sufficiently fast at $|\operatorname{Re} z| \to \infty$.

Then the integral

$$\frac{1}{\sqrt{2\pi}}\int_{\frac{\pi}{2}-i\infty}^{\frac{\pi}{2}+i\infty} f_3(z)\,e^{-i\nu z}\,dz = \begin{cases} F(\nu) & \nu > 0, \\ 0 & \nu < 0, \end{cases}$$

exists, and the function $f_3(z)$ can consequently be represented in terms of the Fourier integral

$$f_3(z) = \frac{1}{\sqrt{2\pi}}\int_0^\infty F(\nu)\,e^{i\nu z}\,d\nu.$$

Substituting this expression into the integral $R_3(z)$, and interchanging the sequence of integration, we get

$$R_3(r) = -\sqrt{\frac{2}{\pi}}\int_0^\infty J_\nu(kr)\,F(\nu)\,e^{-\frac{i\nu\pi}{2}}\,d\nu.$$

By virtue of the above argument, we have $f_3(z) = 0$ at $R_3(r) = 0$, but then we also have $F(\nu) \equiv 0$. This leads to the above theorem. The limitations imposed on the class of functions $\varphi(\nu) = F(\nu)e^{\exp\left[-i\frac{\nu\pi}{2}\right]}$ follow from the limitations imposed on $f_3(z)$.

Received March 1, 1955

Acoustics Institute of the Academy of Sciences USSR, Moscow

INVESTIGATION OF THE PROPAGATION OF ULTRASONIC WAVES IN THE CRITICAL REGION OF A LIQUID-VAPOR SYSTEM

V. F. Nozdrev

The article describes several experimental features of an investigation of the propagation of ultrasonic waves in the critical region of a liquid-vapor system.

Experimental material is cited on the velocity of ultrasound and on the adiabatic compressibility of organic substances both in the critical region along the saturation line, as well as in superheated vapors at $\rho = \rho_{cr}$. It was established experimentally for all the investigated substances that in the critical region a diameter exists for the sound velocity and a diameter exists for the wave impedance. An indirect method is proposed for determining the velocity of sound at the critical point.

The ultrasonic data were used to calculate the specific heats c_p and c_v and their ratios c_p/c_v in the critical region of a liquid-vapor system, and also to determine directly the specific heat c_v at the critical point. The results obtained are evaluated from the thermodynamic point of view.

Investigation of the critical region of a substance is of undisputed importance to the development of a theory of the liquid state. However, in spite of the great urgency of this problem, very few investigations employing ultrasonic methods for these purposes have been reported up to recently. Only few known investigations [5, 6, 13] deal with the velocity of sound in the critical region of low-atomic substances with low critical temperatures (oxygen, CO_2, ethylene). In all these investigations, the critical region was studied only for the gas. The investigations were usually performed with one state parameter (T or p) constant.

No investigations were made at all on the propagation and absorption of ultrasonic waves in the very interesting region where the substance separates into two phases (measurements along the saturation line). It is the purpose of our work to fill this gap. We investigated the propagation of ultrasonic waves in many substances both in the region where two phases exist, and also in the single-phase region (steam) near the critical point. The objects of the investigation were organic substances (saturated and aromatic hydrocarbons, alcohols, and acetates), which are of great interest not only scientifically, but also from the technical point of view. All these substances have relatively high critical temperatures, requiring complicated methods and techniques. The present-day level of the knowledge of the critical state requires refinement of the concept of "critical region."

The critical state of matter was discovered by Mendeleev, Andrews, and Van der Waals and can be characterized as the state of a substance, corresponding to definite values of pressure p_{cr}, volume V_{cr}, and temperature T_{cr}, which are its individual characteristics [1, 2, 3]. Later on, as the knowledge of critical state unfolded, a new concept, that of the critical region, arose. Let us remark first of all that the concept of the critical region is equivalent to the concept of "vicinity of the critical point," frequently encountered in the literature. Quantitatively the critical region can be determined as the region for which the following equation of state is valid

$$p = Atv - \frac{Bv^3}{3} + f(t), \qquad (1)$$

where $t = T - T_{cr}$, $v = V - V_{cr}$, and A and B are constants. This equation can be readily obtained by expanding $\left(\frac{\partial p}{\partial V}\right)_{T_{cr}}$ in a series of powers of t and v, retaining the first terms of the expansion, and taking into account the fact that at the critical point we have

$$\left(\frac{\partial p}{\partial V}\right)_{T_{cr}} = 0; \quad \left(\frac{\partial p}{\partial V^2}\right)_{T_{cr}} = 0. \tag{2}$$

Condition (2) does indeed make it possible to obtain in first approximation the relatively simple equation of state (1), which correctly characterizes the fundamental properties of the critical region. For example, for the case when saturated vapor and liquid coexist in equilibrium in the vicinity of the critical point, we can obtain from Eq. (1):

$$V_l - V_{cr} = -\sqrt{\frac{3A}{B}(T_{cr} - T)},$$

$$V_{sv} - V_{cr} = \sqrt{\frac{3A}{B}(T_{cr} - T)}, \tag{3}$$

where $V_l - V_{cr}$ and $V_{sv} - V_{cr}$ are proportional to the square roots of $T_{cr} - T$ and where A and B are constants. In this manner the phase-equilibrium curve in the (T,v) plane has a simple maximum, i. e., the values of T and v are parabolically related (Kalyete-Matias law).

The example cited above shows how rational and necessary it is to introduce the concept of critical region into the investigation of the critical state. From the above definition one cannot establish precisely the boundaries of the critical region, for these boundaries are of somewhat arbitrary character. The farther away we go from the critical point, the less closely will the equation be satisfied, but the medium remains continuous, and consequently, so do the values of the parameters that characterize this medium. Some investigators attempt to estimate the width of the critical region in degrees centigrade as a whole for all liquids. This is definitely a wrong approach to the solution of the problem. Every liquid will have its own width of the critical region in °C. For mercury, for example, this value may be on the order of tens of degrees, while for hydrogen it may be only fractions of a degree.

However, if one does nevertheless estimate the width of the critical region in terms of the temperature, it would be correct to make the comparison not in degrees, but in terms of the relative temperature (θ). Liquids obeying the laws of relative states, will have approximately equal widths of the relative-temperature interval, characterizing the critical region. Taking into account the above interpretation of the arbitrariness of the critical-region boundaries, the latter statement must be understood only in that meaning, that equal relative temperatures near the critical point will correspond to an equal accuracy of Eq. (1).

1. Certain Methodical Problems Involved in Investigation of the Critical Temperature.

The correct choice of the method of investigation is of decisive significance in the study of the critical region.

In our case one can investigate the propagation of ultrasonic waves in the critical region by one of two methods: electromechanical (Pierce interferometer) and optical.* Assuming hereinafter that it is possible to construct a universal autoclave, permitting the use of the three methods with a single instrument, we started our investigation using the optical method, which by now has been well tested by us in the investigation of the propagation of ultrasound in liquids and gases over a wide range of temperatures and pressures. The Pierce interferometer method was used many times by other authors for this purpose [5, 6, 13].

* Recently we have also been employing successfully in our laboratory a pulse method for the study of the critical region of a liquid-vapor system.

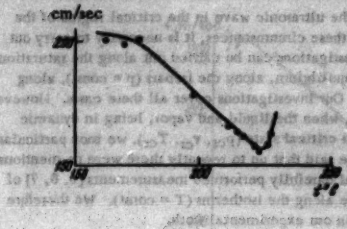

Fig. 1.

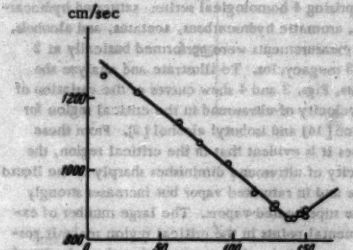

Fig. 2.

It has been erroneously assumed up to recently that the strong opalescence at the critical region would not permit the diffraction of light by the ultrasonic lattice to be observed in this case by optical methods. Our very first experiments refuted this assumption. Observing with a viewing tube the critical region of many organic liquids penetrated by ultrasonic beams, we obtained a bright diffraction pattern against the background of scattered light. True, when the system passed through states near the critical one, a strong blurring of the diffraction line was observed, and with it large fluctuations of the liquid and steam and of the diffraction lines, thus making the early measurements difficult and increasing considerably the experimental error. A thorough investigation of the behavior of the substance in the critical region, penetrated by an ultrasonic beam, made it possible to establish two very important laws, which were subsequently taken into account and led to an improvement of the procedure. It was established that the blurring of the diffraction lines varied with time. It is always possible to obtain sharp diffraction lines for the same values of p and T. Using instantaneous photography it is possible to photograph without particular complications the diffraction spectra at the instant that the diffraction lines become sharp. The above phenomenon, together with the sharp reduction observed by us in the blurring of the diffraction line with diminishing ultrasonic-beam intensity, has made it possible to increase the accuracy with which the velocity of ultrasound is measured to 1-2%. An even higher accuracy can be reached (on the order of 0.5%) in practice, if the investigation is carried out under the minimum possible ultrasonic-vibration intensity possible for the given liquid. In the study of the velocity of ultrasound (as in the study of other parameters in the critical region), it is very important that the critical conditions be observed as rigorously as the experimental conditions permit.

We carried out our preliminary experiments with disturbances to the critical conditions, i. e., by filling the autoclave with either more or less liquid than necessary to produce the critical state. Figure 1 shows the dependence of the velocity of ultrasound on the temperature in saturated methy-acetate vapor when the critical conditions are not satisfied. The curve was obtained with liquid filling 24.5% of the total volume. Here the liquid vaporizes completely at t = 226°C, i. e., 7.5°C below the critical temperature of methyl acetate. This example shows that the less liquid is put into the autoclave, the faster does the velocity of the ultrasound pass through the minimum, beginning to rise in superheated vapors.

Since the minimum velocity of the ultrasound occurs at the temperature when the liquid disappears in the autoclave, its numerical value can always be readily determined graphically. We later on carried out experiments of this kind systematically to study the propagation of ultrasonic waves in superheated vapors near the saturation line [4]. We also experimented with filling the autoclave with considerably more liquid than required to obtain the critical state. Figure 2 shows the velocity of ultrasound in the liquid phase of ethyl alcohol with liquid filling approximately 95% of the autoclave. Let us remark that in this case the velocity of ultrasound passes through its minimum at higher temperatures and pressures, than if the entire volume were to be filled with liquid.

2. Velocity of Ultrasound in the Critical Region of the Liquid-Vapor System

To clarify completely the picture of the propagation of the ultrasonic wave in the critical region of the liquid-vapor system and to study all the phenomena related to these circumstances, it is necessary to carry out the experiment in several directions simultaneously. Such investigations can be carried out along the saturation line, when the liquid and the saturated vapor are in dynamic equilibrium, along the isobar (p = const), along the isotherms (T = const), and along the isochores (ρ = const). Our investigations cover all these cases. However, taking into account the particular significance of the first case, when the liquid and vapor, being in dynamic equilibrium, pass through several equilibrium states and reach a critical state (p_{cr}, v_{cr}, T_{cr}), we took particular great pains in the investigation of this version [4, 9]. It must be said that up to recently there were no mentions of investigations of this type in the literature,* although several carefully performed measurements [5, 6, 7] of the velocity of ultrasound in the critical region have been made along the isotherms (T = const). We therefore paid less attention to investigations at p = const and T = const in our experimental work.

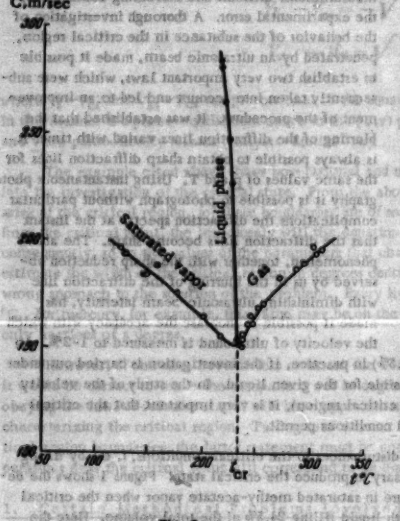

Fig. 3.

The velocity of ultrasound was measured in the critical region along the saturation lines for 15 liquids, comprising 4 homological series: saturated hydrocarbons, aromatic hydrocarbons, acetates, and alcohols. The measurements were performed basically at 2 and 3 megacycles. To illustrate and analyze the results, Figs. 3 and 4 show curves of the variation of the velocity of ultrasound in the critical region for hexane [14] and isobutyl alcohol [9]. From these figures it is evident that in the critical region, the velocity of ultrasound diminishes sharply in the liquid phase and in saturated vapor but increases strongly in the superheated vapors. The large number of experimental points in the critical region make it possible to conclude with assurance that the velocity of ultrasound does not become discontinuous in the critical region, but passes through a minimum. It must be noted that the visual observation of the diffraction pattern in the critical region also confirms convincingly the experimental results: the spectrum of diffraction by the ultrasonic lattice can be observed continuously as the substance passes through the critical state. That the velocity of sound should have a finite value in the critical state is readily seen also from purely thermodynamic considerations [10]. Actually, starting with the well-known thermodynamic relationships

$$\left(\frac{\partial p}{\partial v}\right)_S = \frac{c_p}{c_v}\left(\frac{\partial p}{\partial v}\right)_T, \tag{4}$$

$$c_p - c_v = -\frac{T\left(\frac{\partial p}{\partial T}\right)_v^2}{\left(\frac{\partial p}{\partial v}\right)_T}. \tag{5}$$

it is possible to obtain after simple transformations

* Report by W. Schneider was published in 1951. It is analyzed below.

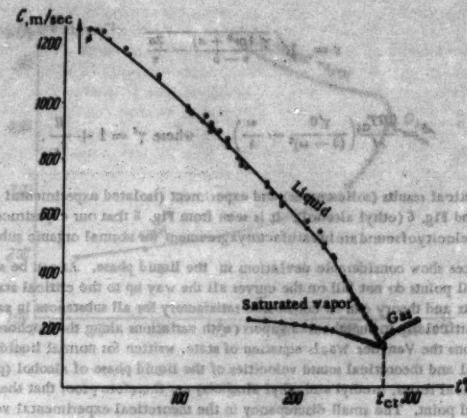

Fig. 4.

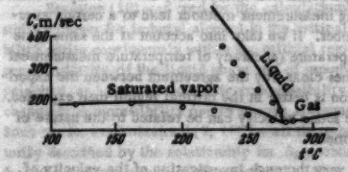

Fig. 5.

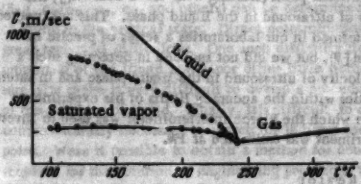

Fig. 6.

$$c^2 = \frac{M}{\rho^2}\frac{T}{c_v}\left(\frac{\partial p}{\partial T}\right)^2_v\left[1 + \frac{1}{\gamma - 1}\right]. \quad (6)$$

At the critical point we have $\gamma = \infty$, while $\left(\frac{\partial p}{\partial T}\right)_v$ and c_v remain finite, therefore

$$c^2_{cr} = \frac{MT_{cr}}{\rho^2_{cr} c_{v\,cr}}\left(\frac{\partial p}{\partial T}\right)^2_{v\,cr}. \quad (7)$$

Let us now proceed to compare the experimental data with the results that can be derived from the equation of state of the substance, allowing for the adiabatic process. Preliminary analysis of the equations of state that are most suitable for this purpose, and comparison of the sound velocities obtained from these equations with the experimental ones, have convinced us that the Van der·Waals equation of state is the most convenient for the study of our organic substances. We shall therefore compare below the experimental data with the equation for sound velocity obtained from this equation.

As is known, the velocity of sound will in this case be expressed in the following form:

$$c = \sqrt{\frac{\gamma'(pv^2 + a)}{v - b} - \frac{2a}{v}} \tag{8}$$

or in a transformed form

$$c^2 = \frac{9RT_{cr}}{M}\left(\frac{\gamma'\theta}{(3-\omega)^2} - \frac{\omega}{4}\right), \quad \text{where } \gamma' = 1 + \frac{R}{c_v}. \tag{9}$$

Comparison of the theoretical results (solid curves) and experiment (isolated experimental points) are given in Fig. 5 (propyl acetate) and Fig. 6 (ethyl alcohol). It is seen from Fig. 5 that our experimental results and the calculated values of the velocity of sound are in satisfactory agreement for normal organic substances.

Associated substances show considerable deviations in the liquid phase. As can be seen from Fig. 6, in this case the experimental points do not fall on the curves all the way up to the critical state. The correspondence between experiments and theory can be considered satisfactory for all substances in saturated vapors near the critical point, and particularly in superheated vapors (with variations along the isochore curve; $\rho = \rho_{cr}$). We used in our calculations the Van der Waals equation of state, written for normal liquids. The discrepancy between the experimental and theoretical sound velocities of the liquid phase of alcohol (particularly the lower members of the homological series, methyl and ethyl alcohols) are therefore proof that they remain associated all the way to the critical point. The small discrepancy in the theoretical experimental velocities of sound in the regions close to the critical point must be attributed for all substances also to the fact that in our calculations we took c_p/c_v = const, which, strictly speaking, cannot be done for the region near the critical point (see Section 4 of this article). We assume that these discrepancies will become even larger as the accuracy of the experiment is increased later on, for a more accurate experiment will undoubtedly lead to sharper minima in the values of the velocity of sound. Actually, all the existing measurement methods lead to a certain averaging of the sound velocity over the height of the working chamber. If we take into account at the same time the inadequate accuracy in measuring and maintaining the temperature (accuracy of temperature measurement is 0.1-0.01°C, instead of the required 0.001-0.0001°C) it becomes clear why the agreement between the experimental data and those obtained from the Van der Waals equation is better in the critical region then expected. It is understood that the shape and depth of the minimum of the sound velocity can be related to the nature of the substance also only if more accurate experiments are performed.

A recently published article [8] contains in our opinion a very thorough investigation of the velocity of ultrasound in the critical region of sulfur hexafluoride (t_{cr} = 45.55°C; p = 36 atmos), performed with a Pierce interferometer. The interferometer was placed in a thermostatic oven, in which the temperature was maintained with an accuracy to within 0.002°C. The investigation was performed at 600 kc. The results obtained for the liquid phase of saturated and superheated steam agree in principle with our own results. However, some substantial discrepancies do exist. It follows from [8] that near the critical point (starting with 0.6°C below t_{cr}) the velocity of ultrasound in saturated vapor exceeds the velocity of ultrasound in the liquid phase. This unexpected result cannot be explained by thermodynamics. We later performed in our laboratories a series of precise investigations of the velocity of ultrasound in the critical region [9], but we did not succeed in detecting such a phenomenon. We assume that this difference between the velocity of ultrasound in the liquid phase and in saturated steam, observed by Schneider for the same temperature, lies within the accuracy limits of his experiment. This assumption is confirmed by other investigations [5, 6], in which the Pierce interferometer was used to investigate the critical region of CO_2, and the accuracy of the experiment was estimated at 1%.

3. Adiabatic Compressibility in the Critical Region

As already mentioned above, several reports appeared in the recent literature on the investigation of various parameters of the critical state. We do not know, however, of any investigations in which a single method was used to investigate the compressibility of liquids and of their saturated or superheated vapors in the critical region. Our investigation fills this gap. Using the experimental results on velocity of sound in the critical

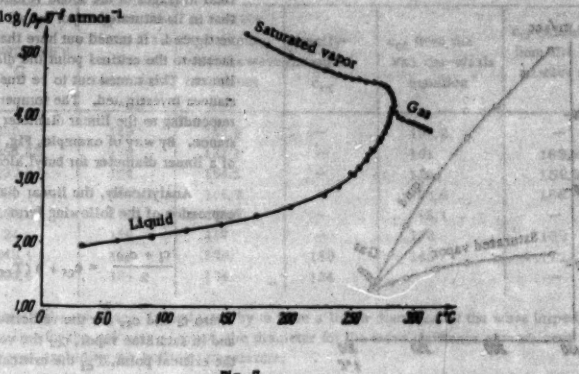

Fig. 7.

region and the tabular data on the density in the same region (we measured the density of superheated steam), we computed the coefficient of adiabatic compressibility both along the saturation lines, as well as beyond the cessation of the curve $p = f(T)$, when both phases become identical.

Equation (16) was used for the calculations. To analyze and illustrate the results, Fig. 7 shows compressibility curves for isobutyl alcohol in the critical region. These curves convince us that the adiabatic compressibility varies continuously within the critical region [9]. The same curves also show readily that the adiabatic compressibility of the liquid phase and of superheated steamincreases sharply as the critical temperature is approached, and that the adiabatic compressibility of saturated vapor, to the contrary, diminishes sharply. The change in compressibility occurs in such a manner that all these curves merge at the critical temperature. Such results were obtained [9, 14] for all the substances investigated in our laboratory. Our results are satisfactorily described by the relationship for β_{ad}, obtained from the Van der Waals equation of state with allowances for the adiabatic nature of the process [3, 14].

4. Concerning One Indirect Method of Determining the Velocity of Sound in the Critical State

Many thermodynamic and molecular-kinetic characteristics of the liquid and gas states of a substance (β_{ad}, c_p/c_v, c_p, c_v, and others) can be determined with great accuracy from experimental value of the velocity of sound in the critical state. Direct determination of sound velocity at the critical point involves, however, great technical difficulties. One such difficulty lies in obtaining the critical state itself, for near this state the properties of the liquid and vapor differ little from each other. Fluctuations in density, temperature, and pressure also make it very difficult to devise a procedure insuring the necessary accuracy and speed of measurement of the velocity of sound. Finally, itis difficult to obtain experimentally a stable critical state. It therefore becomes naturally necessary to search for indirect methods of determining the velocity of sound at the critical point. Were it possible to obtain a method for determining the velocity of sound, insuring at least the accuracy required for the solution of engineering problems, this in itself would be a great step forward in the solution of the problem. In searching for such a solution we tried the linear diameter method, used with success in its time by Matthias [3] to determine the density in the critical state.

The search was made in two directions.

1. The velocity of sound at the critical point was determined from the velocity of sound in liquid and its saturated vapor. Using our experimental curves for the velocity of sound in the liquid phase and in saturated

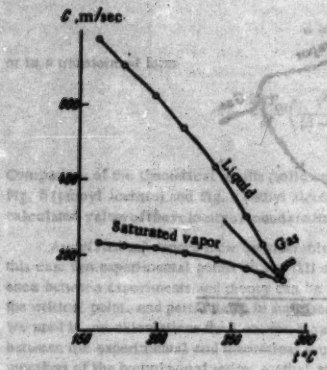

Fig. 8.

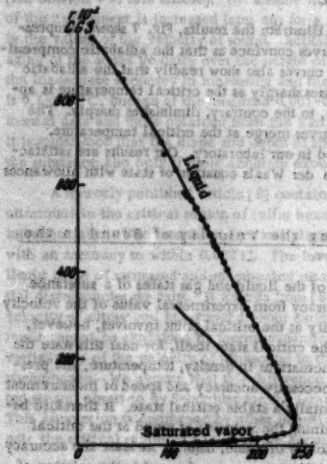

Fig. 9.

vapor, we plotted "diameters," obtained as arithmetical averages of the sound velocity in the liquid and that in its saturated vapor for all the substances investigated. It turned out here that in the region adjacent to the critical point the diameter actually is linear. This turned out to be true for all the substances investigated. The temperature range corresponding to the linear diameter varies with the substance. By way of example, Fig. 8 shows the presence of a linear diameter for butyl alcohol.

Analytically, the linear diameter is given by an expression of the following form

$$\frac{c_l + c_{sv}}{2} = c_{cr} + a(T_{cr} - T), \qquad (10)$$

where c_l and c_{sv} are the velocities of sound in liquid and in saturated vapor, c_{cr} the velocity of sound at the critical point, T_{cr} the critical temperature, T the temperature at which $(c_l + c_{sv})/2$ is determined, and a is the slope of the straight line $(c_l + c_{sv})/2$ relative to the abscissa axis.

The velocity of sound can be determined either from Eq. (10) or directly graphically. The calculated values of c_{cr} obtained in this manner are given in the table. Later we succeeded in measuring directly the velocity of ultrasound at the critical point in isobutyl alcohol (the temperature was determined with an accuracy to 0.1°C); there is good agreement between the velocity of sound at the critical point, obtained from the linear diameter, and from that measured directly (see table). We also tried the method of determining the velocity of sound at the critical point from wave impedance of the liquid and of its saturated vapor. As is known by wave impedance is meant the product of the density of the liquid (vapor) by the velocity of sound in this liquid (vapor)

$$r = \rho c. \qquad (11)$$

We used in our calculations the values of the sound velocity in liquid and in saturated vapor obtained from our experimental data, while the densities used were obtained from tables.

As can be seen from Fig. 9, the wave impedance diminishes with increasing temperature in liquid, but increases with increasing temperature in saturated vapor. The variation of r_l and r_{sv} is such that they become equal at the critical temperature. By way of an example, Fig. 9 shows the presence of a diameter for a wave impedance in ethyl alcohol. *

* The values of sound velocity in the liquid phase of ethyl alcohol near the critical point were taken from the work by K. Akhmetzyanov [15].

TABLE

Name of substance	Temperature t, °C	c_{cr} from the linear diameters of sound velocity	c_{cr} from the linear diameters of the wave resistances	directly-measured c_{cr}	c_{cr} from the Van der-Waals equation	c_{cr} calculated from the law of relative states
n-hexane	230	140	147.6	–	105.2	–
n-heptane	266.85	175	181.1	–	101	163.8
Methyl acetate	232.9	164	164.1	–	113	159.5
Ethyl acetate	250	146	146.7	–	98.6	166
Propyl acetate	232.2	125	108.2	–	96.1	–
Methyl alcohol	24	156	157	–	173	162
Ethyl alcohol	243.1	163	170	169	145	171
Isobutyl alcohol	283.4	134	134	134	–	–

It turned out that all the substances investigated by us have a linear diameter for the wave impedance. Unlike the linear diameter for the velocity of sound, the diameter for the wave resistance extends over a very wide temperature interval, including the boiling temperature.

The diameter for the wave impedance can be expressed in the following form

$$\frac{c_l \rho_l + c_{sv} \rho_{sv}}{2} = \rho_{cr} c_{cr} + b (T_{cr} - T). \tag{12}$$

The values of c_{cr} at the critical point were thus calculated both using Eq. (12), as well as directly graphically. The results of calculations are given in the table, which shows also the values of c_{cr} calculated from the diameter for the velocity of sound. The results are in satisfactory agreement. Analysis of the data given in the table shows that the values of c_{cr} obtained by the two methods are in closest agreement for those substances, for which there are more experimental values of sound velocity in the critical region (methyl acetate, ethyl acetate, methyl alcohol, isobutyl alcohol, etc.). To increase the accuracy of these two methods of determining c_{cr} in the critical state, it is thus necessary to have as many experimental values of the velocity as possible for the liquid phase and for the saturated vapor in the critical region.

There is no doubt that c_{cr} as determined from the diameter for the sound velocity should be somewhat more accurate, for in this case there is no need for experimental determination of the density ρ_{cr} at the critical point. It is of interest to compare the values of c_{cr}, obtained by using the straight-line diameter, with the values of c_{cr} obtained from the Van der Waals equation

$$c_{cr}^2 = \frac{9}{4} \frac{RT_{cr}}{M} (\gamma' - 1),$$

or

$$c_{cr}^2 = \frac{9}{4} \frac{R^2 T_{cr}}{M c_v}. \tag{13}$$

The equation as given by (13) yields a finite value for c_{cr} at the critical point, since the specific heat at constant volume c_v has a finite value in this case, and passes through a maximum at the critical point. According to the experimental data, the velocity of sound at the critical point passes through a minimum, which is in full agreement with (13).

The table gives the values of c_{cr} computed from Eq. (13). In this case the values of c_v were calculated using tabular thermodynamic data. The values of c_{cr} from Eq. (13) are not as close to the experimental ones.

This is not surprising: Eq. (13), as we already stated, was obtained from the Van der Waals equation. The capabilities of the method proposed for computing the velocity of sound at the critical point could be improved considerably were it possible to show that the velocity of sound obeys the law of relative states at the critical point [14]. It would be interesting to check, based on experimental data, whether the law of relative states is satisfied for the velocity of sound in the critical region. The table gives the results of such a verification, with c_{cr} as calculated from the well-known equation

$$\frac{c_1}{c_{cr_1}} = \frac{c_2}{c_{cr_2}} = \frac{c_3}{c_{cr_3}} = \text{const}. \tag{14}$$

The initial value of c_{cr}, needed for the computation was taken here directly from experiment; c_1, c_2, and c_3 were determined from the experimental sound-velocity curves for the critical region. According to the law of relative states for the velocities of sound in liquid and vapor phases [9, 14], it is possible to calculate c_{cr} from c_1, c_2 and c_3 either for the liquid or for the saturated vapor. Experiment, however, gives better agreement with the law of relative states for the velocity of sound in the liquid phase (14). We therefore calculated c_{cr} (see table) from the sound velocities for the liquid phase in the critical region.

The values of c_{cr} calculated from the linear diameter and from the law of relative states are in satisfactory agreement. The fact that the values of sound velocities at the critical point, obtained from the linear diameter, are in good agreement with the velocities of sound, directly obtained by experiment, indicates the existence of a very important regularity in the critical region. To calculate c_{cr} with greater accuracy it is necessary to employ the law of relative states within the individual homological series. This is particularly important when we deal with associated substances. The experimentally-established regularities in the critical region, namely the fact that the diameters for the sound velocity and for wave impedance are linear are undoubtedly of great scientific and practical value. However, until a theoretical derivation is obtained, the applicability of these laws will be relatively limited. We shall give here such a derivation for the diameter of the square of the wave impedance [14]. It is evident that to derive theoretically, for example, the diameters of the squares of the wave impedance, it is enough to show that the squares of the wave impedance of liquid and of its saturated vapor depend parabolically on the temperature. This is easy to do. We know from hydrodynamics that

$$c^2 = \frac{1}{\rho\beta_{ad}}. \tag{15}$$

By definition $\beta_{ad} = -\frac{1}{v}\left(\frac{\partial V}{\partial p}\right)_S$; let us introduce the value of β_{ad} into Eq. (15). Then

$$c^2 = -\frac{v}{\rho}\left(\frac{\partial p}{\partial v}\right)_S. \tag{16}$$

Since $\rho = \frac{M}{v}$, let us rewrite (16):

$$c^2 = -\frac{v^2}{M}\left(\frac{\partial p}{\partial v}\right)_S. \tag{17}$$

We know from thermodynamics that

$$\left(\frac{\partial p}{\partial V}\right)_S = \gamma\left(\frac{\partial p}{\partial V}\right)_T, \tag{18}$$

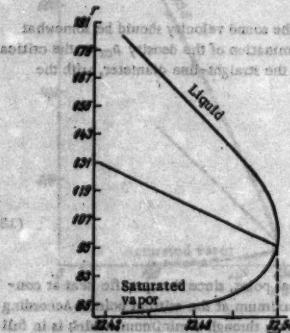

Fig. 10.

where

$$\gamma = \frac{c_p}{c_v}$$

Since in the region of the critical point

$$\left(\frac{\partial p}{\partial V}\right)_T = A(T - T_{cr}) + B(V - V_{cr})^3, \tag{19}$$

therefore, substituting (19) into (18), we get

$$\left(\frac{\partial p}{\partial V}\right)_S = \gamma [A(T - T_{cr}) + B(V - V_{cr})^3]. \tag{20}$$

Substitution of (20) into (17) yields

$$c^2 = \frac{-V^2}{M} \gamma [A(T - T_{cr}) + B(V - V_{cr})^3]. \tag{21}$$

If we consider, in accordance with Eq. (3), that for the critical region we have

$$V_l - V_{cr} = -\sqrt{\frac{3A}{B}(T_{cr} - T)}, \quad V_v - V_{cr} = \sqrt{\frac{3A}{B}(T_{cr} - T)},$$

where A and B are constants, we get

$$\left.\begin{aligned} c_l^2 &= -D\frac{V_l^2}{M}\gamma_l (T_{cr} - T) \\ c_{sv}^2 &= -C\frac{V_v^2}{M}\gamma_{sv}(T_{cr} - T) \end{aligned}\right\}, \tag{22}$$

where D and C are constants. Multiplying both halves of Eq. (22) by ρ^2, we get

$$\left.\begin{aligned} \rho_l^2 c_l^2 &= -DM\gamma_l (T_{cr} - T) \\ \rho_{sv}^2 c_{sv}^2 &= -CM\gamma_{sv}(T_{cr} - T) \end{aligned}\right\}, \tag{23}$$

or, since $r = \rho c$ we get

$$\left.\begin{aligned} r_l^2 &= -DM\gamma_l (T_{cr} - T) \\ r_{sv}^2 &= -CM\gamma_{sv}(T_{cr} - T) \end{aligned}\right\}, \tag{24}$$

where the right halves are positive, since the constants D and C are negative.

Thus, Eqs. (24) give a simple relationship between the velocity of sound, the density, the molecular weight, and the ratio c_p/c_v of the liquid phase and of saturated vapor in the critical region. If we put in first approximation $\gamma_l \cong$ const, $\gamma_{sv} \cong$ const, which is quite permissible up to states quite close to the critical point, Eqs. (24) will yield for liquids and for saturated vapors a relationship that is nearly parabolic, i. e., indeed in full agreement with the experiment. However, for the region closer to the critical point (0.5–1°), γ cannot be assumed

constant for the liquid and the saturated vapor, and therefore the question of deriving the linear diameter of the square of the wave impedance remains open for this rather narrow temperature range. It is important to note that direct computation of r_l^2 and r_{sv}^2 using Eqs. (24) makes it possible to obtain (see Fig. 10) a linear diameter also for the region where the value of γ of the liquid and of the saturated vapor varies considerably with temperature, i. e., in the very region that is adjacent to the critical point.

5. On the Question of Determining the Specific Heat of the Liquid-Vapor System

The existence of the theoretically-derived relationships (24) makes it possible to calculate many important parameters in the critical region. Thus, from the linear diameter for the wave impedance jointly with Eq. (1), or else from direct experimental determination of $(\partial p/\partial T)_v$ and $(\partial p/\partial v)_T$ we can calculate c_p, c_v, and c_p/c_v in the critical region with the required accuracy, and c_v directly at the critical point. For this purpose it is enough to employ the equations

$$c_v = \frac{T\left(\frac{\partial p}{\partial T}\right)_v^2}{r^2 + M\left(\frac{\partial p}{\partial v}\right)_T}; \quad \gamma = \frac{r^2}{M\left(\frac{\partial p}{\partial v}\right)_T}; \quad c_p = \gamma c_v, \tag{25}$$

which are readily derived from thermodynamics.

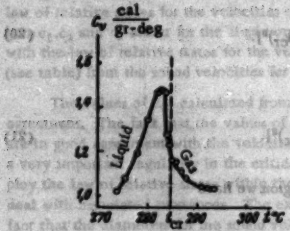

Fig. 11.

If $T = T_{cr}$ we get $\left(\frac{\partial p}{\partial v}\right)_T = 0$, and the first equation in (25) becomes

$$c_v = \frac{T\left(\frac{\partial p}{\partial T}\right)_{v\,cr}^2}{r_{cr}^2}. \tag{26}$$

Equation (26) makes it possible to calculate c_v directly at the critical point from experimental values of r_{cr} at the critical point.

We already dealt above with the method of determining r [see Eq. (12)]. At the present time we are using this method in our laboratory [9, 10]* to compute c_p, c_v, and c_p/c_v for many substances.

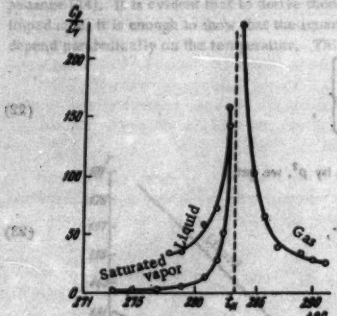

Fig. 12.

For the sake of illustration we show in Figs. 11 and 12 curves of c_v and c_p/c_v vs. temperature for isobutyl alcohol in the critical region [9, 14]. The results are in full qualitative agreement with the values of c_p measured directly in the critical region of a liquid mixture [11], showing that the phenomena occurring in the critical region of a liquid-vapor system and in the critical region of a mixture of two liquids have a common nature. Certain shifts of the maximum of c_v relative to the critical point, shown in Fig. 11, requires further study.

The specific heat in the critical region determined from the acoustic data are in good agreement also with the values of c_v and c_p/c_v obtained by another method [12].

* See also the diploma thesis by I. B. Rozhdestvenskii, Moscow State University, 1953.

LITERATURE CITED

[1] B. Golitsyn, J. Russ. Phys.-Chem. Soc. 69 (1889).

[2] M. Avenarius, Pogg. Ann. 151, 303 (1874).

[3] M. Vukolovich and I. Novikov, Equations of State (State Power Press, Moscow, 1948).

[4] V. Nozdrev, Doklady Akad. Nauk SSSR 85, 5 (1952).

[5] Herget, J. Chem. phys. 8, 537 (1940).

[6] B. Andersen, Am. Phys. Soc. 25, 6, 15 (1950).

[7] I. Neury, ICR. Acad. Sci. 234, 3, 303-309 (1952).

[8] N. Schneider, Can. J. Chem. 29, 3, 243-252 (1951).

[9] A. Povalishnikova, Dissertation, Moscow Regional Pedagogical Inst., 1953.

[10] L. Lependin, Dissertation, Moscow Regional Pedagogical Inst., 1953.

[11] V. Semenchenko and A. Skripov, Doklady Akad. Nauk SSSR 85, 6 (1952).

[12] V. Semenchenko, Bull. Moscow State Univ. 1948, 11.

[13] B. Shpakovskii, Doklady Akad. Nauk SSSR 3, 31 (1934).

[14] V. Nozdrev, Dissertation, Physics Faculty Moscow State Univ. 1950; Reports Moscow Regional Pedagogical Inst. 1952, 18.

[15] K. Akhmedzianov, Bull. Moscow State Univ. 1949, 6.

Received December 20, 1954

Moscow Regional Pedagogical Institute

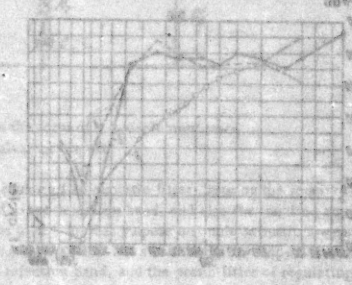

DEVICES TO PROTECT HEARING AGAINST HARMFUL EFFECTS OF NOISE

I. M. Polkovskii

Discussion of the causes of injury to hearing under industrial-noise conditions; the principal requirements that must be imposed on devices to protect against hearing injury are defined; equations are derived for the design of such devices, made either in the form of earplugs, or in the form of muffs fitting over the ear's helix.

Modern industrial enterprises are equipped with mechanisms and machines, which produce acoustic noise. These noises remain steady in time. In most cases, the noise is constant in time and is characterized by a relatively high intensity level and by components within a wide range of frequencies. The noise produces therefore a considerable disturbing and harmful effect on the human hearing and on the organism as a whole. In spite of individual successful attempts to attenuate noise at its source [1, 2, 3] — the noise intensity level is very high in many industrial enterprises. The creation of protective devices for individual use is therefore of considerable importance in the reduction of the damaging effect of noise on the human organism.

1. Causes of Injury to Hearing and Their Manifestations

The causes of injuries to hearing may be shock waves (for example, in blasting work) and acoustical noise.

Shock waves are always directional in character and are sensed as a purely mechanical effect or shock. The force of the shock against the eardrum depends on the rate of wave buildup. It has been established that injury to hearing occurs not as a result of high pressure, but as the result of the high velocity or rate of increase of pressure. Thus, caisson workers and divers experience considerably higher pressures than, for example, artillery gunners or demolition workers, but these pressures vary slowly and therefore do not cause injury to hearing. To reduce the shock caused by the action of the shock wave, it is necessary to bypass it to surfaces that are less sensitive than the eardrum. This can be done relatively simply, using, for example, an elastic rubber ear muff placed over the ear's helix.

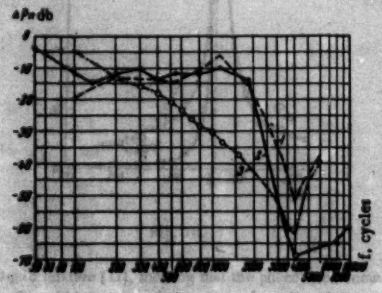

Fig. 1. Audiograms of persons who experienced hearing loss: 1) audiogram of textile worker, 2, 3) audiograms of artillery men.

The struggle against the injury produced by acoustic noise is more complicated, for the mechanism of the action of these noises on the human hearing apparatus is considerably more complicated. Examination of workers in "noisy" trades who exhibited hearing loss caused by damage to the inner ear established that regardless of the causes of the deafness (industrial noise, explosions, gunfire, etc.), the greatest damage to the hearing always occur at frequencies close to 4,000 cycles (Fig. 1). Investigations of

this phenomenon have made it possible to establish that even at very high noise levels protection against injury to hearing can be insured by suppressing the noise components starting with 1,000-1,200 cycles, in such a manner, that the attenuation is not less than 30-35 db in the range above 3,000 cycles. This means that one can use for protection against hearing injury low-pass acoustic filters with a bandwidth making it possible to insure a relatively high intelligibility of transmitted speech.

An important requirement on devices protecting against hearing injury is that they be convenient to use and that they remain stable in their characteristics under all meterological and climatic conditions. It should be noted that attempts undertaken in this direction abroad were not successful [4, 5, 6], for in all the types of devices known there for the protection against noise injury the required frequency characteristic of the attenuation introduced was produced by openings in the outer surfaces; when these openings became solid, the protective properties of these devices changed considerably.

Devices protecting against hearing injury can be made in the form of:

a) plugs inserted in the auditory canal,

b) elastic muffs fitting over the ear's helix, and

c) protective metallic diaphragms or high-speed valve devices.

The latter offer little advantage, for they lead to very cumbersome and complicated installation. We shall therefore consider hereinafter only the parameters of the first two types of devices.

2. Principal Equations for the Design of Devices of the Earplug Type

The characteristic feature of such systems is that one of their elements, namely the acoustic capacitance formed by the air volume between the eardrum and a section of the earplug, is always specified. In addition, a limiting frequency $f_c \approx 1{,}000$ cycles is also specified.

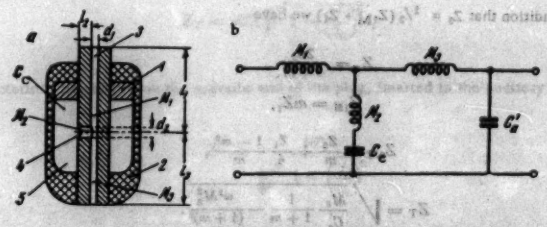

Fig. 2. Device of the earplug type, made in the form of a two-element low-pass filter. a) Sketch of construction, b) equivalent circuit.

The problem therefore reduces in principle to the choice of an acoustic filter, insuring the required rate of increase of attenuation when passing from the pass band to the rejection band, and also the required amount of attenuation in the rejection band. It is not advantageous to use for this purpose a simple acoustic low-pass filter, comprising a tube loaded by a certain volume of air, for this filter has a relatively low slope of the attenuation curve in the transition from the pass band to the rejection band, and the possibilities of regulating the characteristics of the system are limited because the only variable element in this case is the length of the tube.

The above shortcomings are eliminated to a considerable extent by using an earplug that comprises a two-element acoustic low-pass filter. A typical construction of such an earplug is shown in Fig. 2a. As can be seen from the figure, the earplug consists of a plastic core 1, pressed into rubber shell 2. A channel of round cross section 3 passes through the entire length of the core and connects the ear with the surrounding ear medium. The core has a transverse hole 4, which joins the longitudinal channel with the air chamber 5.

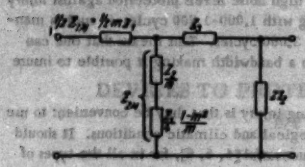

Fig. 3. Equivalent circuit of two-element acoustic low-pass filter, reduced to the canonical form.

The equivalent circuit of such a earplug is shown in Fig. 2b, where M_1 is the acoustic mass of the air in the longitudinal channel 3, up to the axis of the transverse opening 4; M_2 is the acoustic mass of the air in the transverse opening 4; M_3 is the acoustic mass of the air in the longitudinal channel 3 from the axis of the transverse opening 4 to the face of the earplug that is inserted into the ear; C_c is the acoustic compliance of the air volume of chamber 5; C'_a is the acoustic compliance of the air volume between the lower face of the earplug and the eardrum. Thus, the earplug shown in Fig. 2a represents a series connection of two L-pads, one of the m-type and the other of the constant-K type. Let us investigate the equivalent circuit of Fig. 2b, replacing it by the circuit of Fig. 3, where

$$Z_{1M} = j2\omega M_1, \tag{1}$$

$$Z_{2M} = j\left(\omega M_2 - \frac{1}{\omega C_a}\right), \tag{2}$$

$$Z_3 = \frac{1}{j2\omega C_a}, \tag{3}$$

$$Z_4 = j\omega M_3. \tag{4}$$

Under the condition that $Z_0 = {}^1/_2(Z_{1M} + Z_1)$ we have

$$Z_1 = \frac{2Z_3}{1+m}, \tag{5}$$

$$Z_{1M} = mZ_1, \tag{6}$$

$$Z_{2M} = \frac{Z_3}{m} + \frac{Z_1}{4}\frac{1-m^2}{m}, \tag{7}$$

$$Z_T = \sqrt{\frac{M_2}{C_a}\frac{1}{1+m} - \frac{\omega^2 M_2^2}{(1+m)^2}}. \tag{8}$$

From Eq. (8):

a) at $\omega = 0$, $|Z_T| = R_0$,

$$R_0 = \sqrt{\frac{M_2}{C_a}\frac{1}{1+m}}; \tag{9}$$

b) at $\omega = \omega_c$, $Z_T = 0$

$$\omega_c = \sqrt{\frac{1+m}{M_2 C'_a}}. \tag{10}$$

Let us determine the numerical value of R_0. We know that the acoustic mass of the tube, provided its dimensions are smaller than the minimum wavelength in the working range (λ_{min}), is

$$M_a = \rho \frac{l}{S}, \tag{11}$$

where ρ is the air density, l the length of the tube, and S the transverse area of the tube.

Under these conditions, the acoustic compliance of a volume V will be

$$C_a = \frac{V}{\rho c^2}, \tag{12}$$

where c is the velocity of sound in cm/sec.

From (9) and (10) we have, taking (11) and (12) into account

$$R_0 = \frac{\rho c^3}{2\pi f_c V}. \tag{13}$$

At $\rho = 1.2 \cdot 10^{-3}$ g/cm³, c = 34,400 cm/sec, f_c = 1,000 cycles, and V = 0.5* cm³, we have $R_0 \approx 460$.

Let us examine the conditions under which a filter of this type can be matched to the load impedance (i. e., to the impedance of the eardrum) and to the internal impedance of the generator (i. e., the impedance of open space).

Taking (13) into consideration, the characteristic impedance of the filter on the side of the outer face of the earplug is

$$Z_T = 460 \sqrt{1 - \left(\frac{f}{f_c}\right)^2}, \tag{14}$$

and the characteristic impedance on the opposite end of the plug, inserted in the auditory canal, is

$$Z = \frac{460}{\sqrt{1 - \left(\frac{f}{f_c}\right)^2}}. \tag{15}$$

According to experimental data [6], the frequency dependence of the impedance of the eardrum in the pass band of interest to us can be represented by the curve shown in Fig. 4. The same figure shows also the frequency dependence of the characteristic impedance of the filter, calculated from Eqs. (14) and (15). From a comparison of the two curves $|Z_1| = \varphi_1(f)$ and $|Z_d| = \varphi_2(f)$ it follows that in practice the impedance of the eardrum can be matched to characteristic impedance of the filter as seen looking at the outer face of the earplug only at a single frequency. With this, $|Z_1|$ and $|Z_d|$ are of almost the same order of magnitude over the entire pass band (with the exception of the very lowest frequencies). This means that no noticeable reduction in the transfer coefficient will be observed in the pass band of the filter.

It is seen from Fig. 4 that at $R_0 \approx 460$ the matching frequency is approximately the average frequency of the 200-1,000 cycle band, a band which is of decisive significance for the best intelligibility of speech when

* It has been established that when an earplug is inserted in the ear the air volume between the lower face of the plug and the eardrum is V ≈ 0.5 cm³.

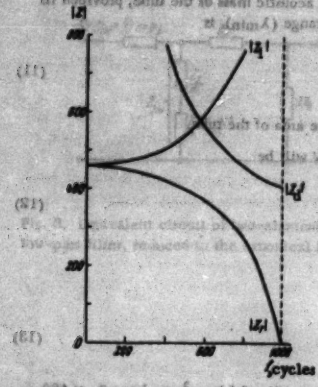

Fig. 4. Frequency dependence of the characteristic impedance of the acoustic filter and of the impedance of the eardrum.

ming devices to protect against hearing injury. Thus, and from this of view, it is advantageous to use $R_0 = 450$ as the basis for the calculations. The impedance of open air space is insignificant. Under our conditions therefore the generator will be working into a load impedance that is much higher than its intrinsic impedance. Let us find the basic relationships needed to determine the structural dimensions of the earplug.

From (5) and (6) we have

$$Z_{1M} = \frac{2m\,Z_0}{1+m}. \tag{16}$$

Substituting the values of Z_{1M} and Z_0 from (1) and (4) into (16), we get

$$M_1 = \frac{m}{1+m}\,M_0. \tag{17}$$

From (2), (3), (5), and (7) we have

$$M_2 = \frac{1-m^2}{1+m}\,\frac{M_0}{2m}, \tag{18}$$

$$C_E = \frac{2C_0}{m}. \tag{19}$$

The value of C_0 is given, and M_0 can be determined from (12) and (10):

$$M_0 = \frac{(1+m)\,\rho C^2}{\omega_0^2 V}. \tag{20}$$

Equations (17), (18), (19), and (20) make it possible to obtain all the equations needed for the structural calculations:

$$d_1 = 2.06\cdot 10^{-4}/_c \sqrt{\frac{l_2 V}{1+m}}\ \text{cm}, \tag{21}$$

$$l_1 = l_2\,\frac{m^2}{1+m}\ \text{cm}, \tag{22}$$

$$d_2 = 2.9\cdot 10^{-4}/_c \sqrt{\frac{m l_2 V}{1-m^2}}\ \text{cm}. \tag{23}$$

The value of the coefficient m necessary to produce the required rate of increase in attenuation, while passing from the pass band to the rejection band, can be determined from the equation

$$m = \sqrt{1-\left(\frac{f_0}{f_\infty}\right)^2}, \tag{24}$$

where f_∞ is the frequency of the maximum attenuation of the m-derived filter in the rejection band.

The quantities l_1 and l_2 must be specified on the basis of structural considerations, and must satisfy the conditions $l_1 \ll \lambda_{min}$ and $l_2 \ll \lambda_{min}$.

3. Design of Devices of the Earmuff Type, Fitting over the Ear's Helix

The simplest type of protective device of this form is the usual telephone earpiece, which with a known approximation can be considered as a L-type acoustic filter, similar in its properties to a low-pass filter (Fig. 5, Curve 1). This explains, in particular, why the predominant majority of telephone earmuffs made to fit over the ear's helix produce a negligible attenuation in the frequency region up to 800-1,000 cycles and insure a relatively low increase in attenuation when passing towards the higher frequencies; this was confirmed by many investigations of the properties of telephone earpieces. This is why not one of the known types of earmuffs provides sufficient protection against hearing injuries. As was already remarked, to produce the required frequency characteristic in a protective device against hearing injury, the device must comprise at least a two-element acoustic low-pass filter. This can be done, for example, in the device shown in Fig. 6a, consisting of a metal cup 1 with holes 2. The cup is rigidly fastened to a plastic insert 5, which has sounding openings 6, and which is located in an elastic rubber earmuff 4. The equivalent circuit of such a device is shown in Fig. 6b, where p_1 is the sound pressure on the outer surface of the device, p_2 the sound pressure directly acting on the ear owing to the fact that the earpiece does not fit tightly, M_{h_1} the acoustic mass of holes 2 in the outer surface of the device, M_{h_2} the acoustic mass of holes 6 in the plastic insert, C'_c the acoustic compliance of the air included between the outer cover and the earpiece, C'_{em} the equivalent acoustic compliance of the device, determined by the elasticity of its attachment to the head, M'_{em} the equivalent acoustic mass of the device, M_l the acoustic mass of the leakage due to the gaps and the imperfect fit between the device and the ears, and C'_a the acoustic compliance formed by the air volume at the ear is covered by the protective device.

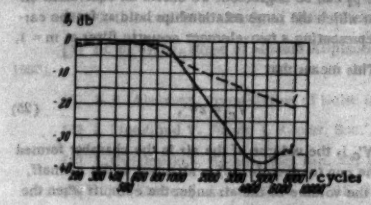

Fig. 5. Frequency characteristics of attenuation: 1) typical telephone earpiece, 2) protective device.

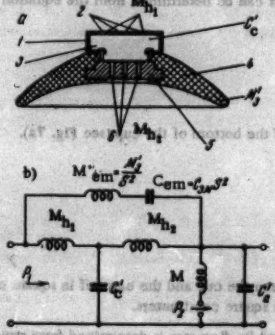

Fig. 6. Device of the earmuff type, fitting over the ear's helix, with holes in the outer surface: a) construction sketch, b) equivalent circuit.

Neglecting the effect of pressure p_2, acoustic compliance C_{em}, and of the leakage, and also neglecting the vibrations of the device as an integral unit (M_{h_1} and $M_{h_2} \ll M'_{em}$) we obtain an equivalent circuit which satisfies all the equations that are applicable to the earplug, which represents a two-element acoustic filter with m = 1.

However, another construction of a protective against hearing injury, suggested by us in 1952, is also possible. This is an earmuff, fitting over the ear's helix. A sketch of such a device is shown in Fig. 7a. As can be seen from the figure, the device consists of an elastic earmuff 1, having a plastic insert 2. A screw with a spiral spring 3 is used to attach flexibly a metal cup 4 to the earpiece. This device is a two-element acoustic low-pass filter, in which the acoustic mass of the first element is produced not by a large number of openings in the outer surfaces, but by some part of the mass of the cup 4. The equivalent circuit of such a device is shown in Fig. 7b, where p'_1 is the equivalent sound pressure acting on the outer surface of the device, M_{em} is the equivalent acoustic mass of the earmuff (including the mass of the plastic insert), M_{cup} the equivalent acoustic mass of a certain element (for example, a metal cup or membrane), C_c the acoustic compliance of the air chamber formed when the cup (membrane) is fastened to the earpiece, C_{cup} the equivalent acoustic compliance of the attachment of the metallic cup (membrane) to the earpiece, M'_l the acoustic mass of the leakage due to imperfect fit between the cup (membrane) and the earplug. The remaining symbols

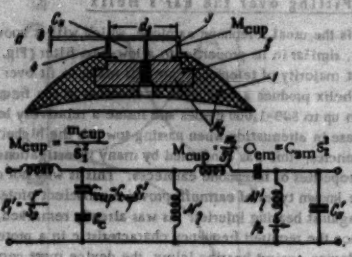

Fig. 7. Device of the earmuff type, fitting over the ear's helix, having no holes in the outer surface: a) construction sketch, b) equivalent circuit.

have already been defined in connection with Fig. 6b. If the compliance of the attachment is chosen to make $C_{cup} \gg C_{cc}$, then, considering that $j\omega M_1 \gg 1/j\omega C_{em}$ for practically all frequencies except the lowest ones, and considering that the leakages M_1' and M_1'' and also the effect of pressure p_2 can be neglected, we obtain an equivalent circuit, for which the same relationships hold as for the earplug, representing a two-element acoustic filter at m = 1.

This means that

$$V_c' = 2V', \tag{25}$$

where V_c' is the volume of the air in the chamber formed when the cup (or membrane) is attached to the earmuff, and V' the volume of the air under the earmuff when the latter coven the ear.

In our case we can assume $V' \approx 6$ cm^3 (this is the volume, in particular, derived for the chamber of an artificial ear by averaging a large number of statistical measurements).

If the cup is constructed in the form of a cylinder, its height can be determined from the equation

$$h = \frac{4V'}{\pi d_1^2} + \delta, \tag{26}$$

where d_1 is the internal diameter of the cup, and δ the thickness of the bottom of the cup (see Fig. 7a).

The mass of the cup is

$$M_{cup} = M_{em} \frac{S_1^2}{2S_2^2}, \tag{27}$$

where m_{em} is the mass of the earmuff, S_1 is the contact area between the cup and the earmuff in square centimeters, and S_2 the contact area between the earmuff and the ear in square centimeters.

Since the height of the cup can be determined from (26), and its diameter is determined from structural considerations with allowances for the type of earpiece selected, the density of the material required is obtained from (27):

$$\rho_3 = \frac{M_{em}}{V_{cup}} \frac{S_1^2}{2S_2^2}, \tag{28}$$

where V_{cup} is the volume of the cup material in cubic centimeters.

The frequency characteristic of the attenuation provided with the aid of such a device is shown in Fig. 5 (Curve 2).

Of the types of protective devices made in the form of earplugs and earmuffs fitting over the ear's helix, described above, the devices having holes in the outer surfaces have the substantial shortcoming, that they do not provide the stability required of protective devices. At the present time our industry is capable of producing

devices of this type for widespread use. The use of devices of this type will to a considerable extent, relieve workers in many trades of the unpleasant sensations produced by noise, and will also eliminate occupational loss of hearing. In addition, the use of devices for protection against hearing injury will yield certain economic gains by increasing labor productivity.

LITERATURE CITED

[1] G. L. Naviazhskii, Study of Noise (State Medical Press, 1948).

[2] Iu. S. Bykov, Noise of Modern Airplanes and Methods for Its Reduction (State Defense Press, Moscow, 1953).

[3] S. P. Alekseev, Investigation of Noise in the City of Moscow (Acad. Sci. USSR Press, 1950).

[4] L. Riuedi and V. Furret, J. Acoust. Soc. Am. 18, 2, 409-412 (1946).

[5] I. Cwialowski, J. Acoust. Soc. Am. 23, 1, 36-40 (1951).

[6] C. D. Critter, J. Acoust. Soc. Am. 18, 2, 413-417 (1946).

Received March 17, 1956 Moscow

ON THE DESIGN OF A RIBBON MICROPHONE

A. V. Rimskii-Korsakov

Analysis of the possibility of obtaining the most suitable dimensions of the moving element of a pressure-gradient ribbon microphone for a specified volume, for specified magnet characteristics, and for a specified frequency distortion. Design equations are obtained for the area and thickness of the ribbon and for the values of the maximum microphone sensitivity. Additional relationships are considered for the microphone used as a pressure receiver; sensitivity equations and the value of the active acoustic resistance in contact with the moving system of the microphone are given for this case.

Calculation of the voltage delivered by a ribbon microphone, or pressure-gradient receiver, to a matched load, with allowances for the electric braking of the ribbon by the current in the electric circuit of the microphone, and under the assumption that the impedance of this circuit is purely resistive leads to the well-known equation [1]

$$u = \frac{10^{-8} nBl'S \sin\left(\frac{\omega d}{2c_0}\cos\theta\right)}{\sqrt{\omega^2 m^2\left(1-\frac{\omega_0^2}{\omega^2}\right)^2 + \left(\frac{10^{-9}\rho c S}{2R_1}\right)^2}}\, p, \qquad (1)$$

where u is the voltage applied to the external load $R_a = n^2 R_1$, B the flux density in the microphone gap, l' the active length of the ribbon, $S = bl'$ the area of the ribbon, b the width of the ribbon (practically the distance between the pole pieces), ω the frequency of the sound, d the maximum path difference of the sound wave to the forward and rear side of the ribbon, c_0 the velocity of sound, θ the angle of incidence of the wave (measured from the direction of vibration of the ribbon), p the sound pressure of the incident wave, R_1 the internal resistance of the microphone (which we assume to equal the resistance of the ribbon), m the mass of the ribbon added to the air mass that vibrates with it, ω_0 the resonant frequency of the moving system in air, and n the turns ratio of the transformer matching the load R_a with the internal resistance R_1.

The active length of the ribbon is smaller than its total length, since the ribbon is corrugated. We shall assume the actual length of the ribbon to be

$$l = \kappa l', \qquad (2)$$

where κ is the "corrugation coefficient," showing by how many times the actual length l is greater than l'. The value of this coefficient is chosen from purely structural considerations to insure a dependable ribbon installation with a minimum natural frequency (minimum tension).

Using (2), we can find the mass of the ribbon

$$m_r = \rho_r b \varkappa l^2 \tau, \tag{3}$$

where τ is the thickness of the ribbon, ρ_r is the density of the ribbon material, and the electric resistance of the ribbon is

$$R_l = \frac{\delta \varkappa l^2}{b\tau}, \tag{4}$$

where δ is the specific resistivity of the ribbon material.

The mass of the air vibrating with the ribbon is estimated approximately by using L. Ia. Gutin's equation for a small pendulum, the area of which is assumed to equal the area of the ribbon:

$$m_R \simeq \frac{8}{3} \rho_0 a^3.$$

Here a is the radius of the equivalent piston, i. e., $a = \sqrt{\frac{bl^2}{\pi}}$; consequently, we finally get

$$m_R \simeq \frac{8}{3} \rho_0 \left(\frac{bl^2}{\pi}\right)^{3/2}, \tag{5}$$

where ρ_0 is the density of air.

The mass of the entire vibrating system is obtained by adding (3) and (5):

$$m = m_R + m_r. \tag{6}$$

The wave path difference d is determined basically by the perimeter of the pole piece. Denoting the latter by P, we can write

$$d = \nu P, \tag{7}$$

where ν is a coefficient depending on the configuration of the pole shoe and amounting to approximately 0.5.

Using the relationships introduced, we can rewrite (1) as:

$$E = \frac{u}{p} = \frac{10^{-4} \nu P B l^2 b \sqrt{R_a}}{2c_0 \left[\rho_r b l^2 \varkappa \tau + \frac{8}{3} \rho_0 \left(\frac{bl^2}{\pi}\right)^{3/2}\right] \sqrt{\frac{\delta \varkappa l^2}{b\tau}}} K_l K_h. \tag{8}$$

We made use here of Expressions (4), (6), (7), and also of $n = \sqrt{\frac{R_a}{R_l}}$ and $S^2 = bl^2$. In addition, the equation contains separately grouped frequency-dependent factors

$$K_l = \frac{1}{\sqrt{\left(\frac{R'}{\omega m}\right)^2 + \left(1 - \frac{\omega_0^2}{\omega^2}\right)^2}}, \tag{9}$$

$$K_h = \frac{\sin\left(\frac{\omega d}{2c_0} \cos\theta\right)}{\frac{\omega d}{2c_0}}. \tag{10}$$

The quantity K_l determines the frequency distortion in the low-frequency region, when the sound frequency is comparable with or smaller than the natural frequency ω_0, and K_h determines the same for high frequencies, when the wavelength is comparable with the path difference d. For the sake of brevity we designate by R' the active mechanical resistance, which is the equivalent of the braking effect of the electric circuit

$$R' = \frac{10^{-9}(Bl')^2}{2R_1}. \tag{11}$$

Using the Braude criterion to obtain the optimum correction of the frequency characteristic, we find that the following relationship must hold for the low frequencies

$$\frac{R'}{m} = \omega_0\sqrt{2}, \tag{12}$$

We then obtain

$$K_l = \frac{1}{\sqrt{1+\frac{\omega_0^4}{\omega^4}}}. \tag{13}$$

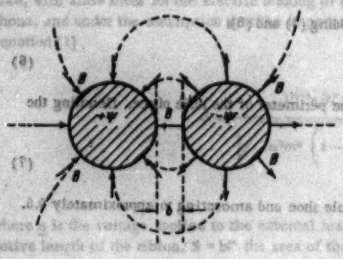

Expression (13) makes it possible to select the natural frequency ω_0 from the specified frequency distortion K_l at the lower limit of the frequency range, $\omega = \omega_l$. Analogously, one can specify the value K_h (and consequently also P), using the permissible value of K_h at the upper boundary of the frequency range, $\omega = \omega_h$, by substituting these values in (10).

However, this is not enough for engineering design. It is necessary to determine also in some manner the most suitable dimensions of the ribbon for a specified volume of magnet. For this purpose it is necessary to consider expression (8) in the middle-frequency region, where K_l and K_h assume values nearly equal to unity.

$$E_{mf} = \frac{10^{-4}\sqrt{P}l^2b\sqrt{R_0}B}{2c_0\left[\rho_l\frac{bl'\varkappa\tau}{4} + \frac{8}{3}\rho_0\left(\frac{bl'}{\pi}\right)^{3/4}\right]\sqrt{\frac{\delta\omega l'}{b\tau}}}. \tag{14}$$

We must first of all find the dependence between the flux density B on the dimensions of the gap, pole pieces, and magnet. For this purpose it would be necessary to solve the complicated problem of determining the magnetic field near the pole pieces. We shall introduce the simplifying assumption that the side surfaces of the pole pieces, between which the ribbon is contained, are right-circular-cylinder surfaces (see figure), and that the flux lines are perpendicular to the surfaces. On the line joining the centers of the pole pieces cross sections, between the pole pieces, i. e., in the place where the ribbon is located, the flux density will be approximately

$$B = \frac{2\Phi}{b},$$

where $+\Phi$ and $-\Phi$ are the magnetic potentials of the pole-piece surfaces.

Our assumptions, evidently, presuppose the following relationship

$$\frac{\partial \Psi}{\partial N} = \pm B,$$

where N is the outward normal to the pole-piece surface.

Let us now calculate the energy of the external magnetic field, produced around the pole pieces, assuming that it has a cylindrical divergence over the entire length of the pole piece (disregarding the distortion at the edges of the pole pieces). For this purpose let us integrate the quantity $\frac{1}{8\pi}\Phi\frac{\partial \Phi}{\partial N}$ over the side surface of the pole piece $S_s = Pl'$.

$$\varepsilon = \frac{1}{8\pi}\int_{(S_s)} \Psi \frac{\partial \Psi}{\partial N}\, dS = \frac{B^2 b}{8\pi} Pl'. \tag{15}$$

Let us calculate the additional energy in the external field of the magnets, corresponding to the leakage field, by multiplying the resultant values of ϵ by a factor of α so that the total energy of the external field will be

$$\varepsilon_0 = \alpha\varepsilon = \alpha B^2 P \frac{bl'}{8\pi}. \tag{16}$$

The total flux produced by the magnet will be

$$\Phi = BPl' \sqrt{\alpha}.$$

If the transverse section of the magnet is S_M, then the flux density produced by the magnet will be

$$B_M = \frac{\Phi}{S_M} = B\frac{Pl'}{S_M}\sqrt{\alpha} = \beta\sqrt{\alpha}B, \tag{17}$$

where

$$\beta = \frac{Pl'}{S_M}.$$

For further computations it is necessary to know the B-H curve for the magnet material used. The energy produced by the magnet in the external field (16) can also be expressed with the aid of the B-H curve:

$$\varepsilon_0 = \frac{B_M H_M}{8\pi} V = \frac{B^2 bPl'\alpha}{8\pi}, \tag{18}$$

where V is the volume of the magnet, which is given. We obtain a system of two equations

$$H_M = f(B_M), \quad H_M = \frac{bPl'}{\beta^2 V} B_M. \tag{19}$$

If the magnetization curve $H_M = f(B_M)$ is specified graphically, further calculation can be done only by trial and error, which is very inconvenient. We shall therefore represent part of this relationship in the form of

a parabola, restricting ourselves to the section from $H_M = 0$; $B_M = B_r$ (residual flux) to a value H_{M_1}, corresponding to the maximum energy delivered by the magnet. For alnico one can assume that the maximum value of the energy developed by the magnet occurs at $B_{M_1} = 2B_r/3$. If we denote the maximum value of the magnet energy per unit volume by e_M, we obtain for the range of interest to us

$$H_M = f(B_M) = 54\frac{\pi\mu_M B_M}{B_r^2}\left(1 - \frac{B_M}{B_r}\right). \tag{20}$$

Replacing the first equation in (19) by (20), we get

$$B_M = B_r(1 - \gamma bl'). \tag{21}$$

Here we have designated

$$\gamma = \frac{PB_r^2}{54\beta^{3/2}\sqrt{\pi\mu_M}}.$$

Inserting (21) in (17), we find B, which we substitute into (14) to obtain after slight transformations

$$E_{mf} = \frac{\nu P\sqrt{R_a}B_r(1-\gamma z^2)z\cdot 10^{-8}}{2c_0\sqrt{\alpha x^2}\beta\rho\sqrt{\delta}\left(y+\mu\frac{z}{y}\right)}. \tag{22}$$

Here we designated $y = \sqrt{\tau}$, $x = \sqrt{bl'}$, $\mu = \frac{8\rho_0}{3\pi^{1/2}\alpha\beta}$.

Equation (22) indicates that E_{mf} has a minimum with respect to the two variables x and y under the following conditions:

$$x = \frac{1}{\sqrt{3\gamma}}, \quad y = \sqrt{\mu x}. \tag{23}$$

Here we obtain that

$$\frac{(1-\gamma z^2)z}{y+\mu\frac{z}{y}} = \frac{4}{10\sqrt{\mu\sqrt{3\gamma}}}. \tag{24}$$

Using (24), we obtain from (22)

$$E_{mf\ max} = 6{,}94\cdot 10^{-9}\frac{\nu}{\alpha\sqrt{\alpha\beta}}\sqrt[4]{\frac{R_a}{\rho_r\rho_0\delta_0^2}}\sqrt{c_M\sqrt{B_r^3P^3}}. \tag{25}$$

With this, we must select

$$\tau = y^2 = \frac{8\rho_0}{3\pi^{1/2}\alpha\beta}\sqrt{bl'}, \tag{26}$$

$$bl' = x^2 = \frac{54\pi\mu_M\gamma\beta^3}{5\rho B_r^2}, \tag{27}$$

$$B_m = B_r(1 - \gamma x^2) = \frac{4}{5} B_r. \tag{28}$$

Equation (25) shows the character of the dependence of the sensitivity of the pressure-gradient ribbon microphone on the volume, on the specific energy of the magnet, and on the residual flux density, i. e., on the quality and quantity of the magnetic material, on the perimeter of the pole pieces, and also on the ribbon material (ρ_l, δ). The coefficients ν, κ, and α derived by us, the exact value of which cannot naturally be determined ahead of time, are also separated in the final result in a convenient form, showing what errors can occur if these are not accurately determined. Finally Eqs. (26), (27), and (28) make it possible to select rationally the structural dimensions of the ribbon and the transverse cross section of the magnet in such a way as to obtain maximum sensitivity for a specified magnet value. The coefficient α must be determined from Eqs. (11), (12), and (13). Substituting the value of R_l from (4) into (11), expressing τ and bl' in terms of $\underline{y}$ and $\underline{x}$ and using Eq. (23), and finally inserting the resulting value of R' into (12) we get

$$\frac{R'}{m} = \frac{10^{-3} B^2}{4 \delta x^2 \rho_m}. \tag{29}$$

Equation (29) shows that when the dimensions bl' and τ are optimal, the flux density in the microphone gap depends only on the properties of the ribbon material, on the nature of the corrugation, and on the natural frequency of the ribbon. Since the latter is determined from the frequency characteristic (K_l is specified), we get

$$B = \sqrt{2^{7/2} 10^9 \delta x^3 \rho_l \omega_0}, \tag{30}$$

where, according to (13)

$$\omega_0 = \omega \sqrt[4]{\frac{1 - K_l^2}{K_l^2}}.$$

Using (30), (28), and (17), we obtain β:

$$\beta = \frac{B_m}{B \sqrt{\alpha}} = \frac{4 B_m}{5 \sqrt{2^{5/2} 10^9 \alpha \delta x^3 \rho_l \omega_l} \sqrt[4]{\frac{1 - K_l^2}{K_l^2}}}. \tag{31}$$

If we specify $K_l = K_h = 0.5$, $f_l = 30$ cycles, $f_h = 10{,}000$ cycles, $R_M = 600$, $\kappa = 0.7$, $\alpha = 2$, and $\nu = 0.5$, then for a magnet 50 cm³ in volume and with characteristics corresponding to the alnico material, namely $B_r = 7 \cdot 10^3$ and $e_M = 7 \cdot 10^6$ erg/cm³, we obtain $R_M = 5600$, $B = 4700$, $\beta = 1.19$, $P = 4$ cm, $\gamma = 0.138$ cm⁻², $bl' = 1.45$ cm², $\tau = 1.83$ microns (aluminum ribbon), $E_{mf} = 0.127$ mv/bar (into a 600 ohm load).

Some opinions can be predicted concerning the nondirectional microphone. In the design of a pressure-receiver ribbon microphone, Eq. (1) must be changed, for in this case the force acting on the moving system of the microphone is independent of the path difference $\omega d/2c_0$. A suitable change yields

$$E_1 = \frac{10^{-8} n B l' \nu b \sqrt{R_a} K_1(\omega)}{2 \omega_0 \left[\rho_l b l' \varkappa \tau + \frac{8}{3} \rho_0 \left(\frac{b l'}{\pi} \right)^{3/2} \right] \sqrt{\frac{\delta \varkappa l'}{b \tau}}}, \tag{32}$$

where

$$K_1(\omega) = \frac{\frac{\omega}{\omega_0}}{\sqrt{\left(\frac{\omega^2}{\omega_0^2} - 1\right)^2 + \frac{\omega^2}{\omega_0^2}\left(\frac{R'}{m\omega_0}\right)^2}}, \tag{33}$$

The other symbols remain as before. The quantity $K_1(\omega)$ determines the frequency distortion of the system. If we take into account the fact that K_1 has a maximum at $\omega = \omega_0$, one can choose ω_0 at the center of the frequency range so as to make $\omega_l \omega_h = \omega_0^2$, and specify the reduction in the value of K_1 at the boundaries of the frequency range

$$K_1(\omega_l) = K_1(\omega_h) = K_1(\omega_0) \cdot 10^{-\Delta/20}, \tag{34}$$

where Δ is the permissible frequency distortion in decibels at the frequencies ω_l and ω_h.

We then determine the following: the relative attenuation of the system

$$\zeta = \frac{R'}{m\omega_0} = 10^{-\Delta/20} \sqrt{\frac{\omega_l/\omega_h + \omega_h/\omega_l - 2}{1 - 10^{-\Delta/20}}} \tag{35}$$

and the maximum value of K_1:

$$K_1(\omega_0) = \frac{1}{\zeta}. \tag{36}$$

Relationships (35) and (36) show that the sensitivity of the microphone diminishes with the transmitted bandwidth. This is characteristic for apparatus intended for conversion, amplification, and transmission of oscillations.

The frequency-independent part of Expression (32) can be investigated in analogy with the quantity E_{mf} [see Eq. (14)]. As a result we obtain, taking into consideration the optimum relationship as defined by Eqs. (23) and (24),

$$E_1 = 6.94 \cdot 10^{-4} \frac{1}{\varkappa\zeta\sqrt{\alpha\beta}} \sqrt{\frac{R_a}{\rho_1 \rho_0 c_0^2}} \sqrt[4]{\frac{\varkappa_a V_a B_r^2}{P}}. \tag{37}$$

It is impossible to obtain the value of R' called for in (35) by electric braking. Taking (29) into consideration, it is easy to verify that the required flux density cannot be attained. One therefore introduces additional mechanical braking, attaching to one side of the ribbon an "infinite" acoustic line (see [1] concerning this). Here it is necessary to employ an acoustic transformer. Assuming (35) to be attained entirely by mechanical braking, we get

$$R' = R_M = \zeta m \omega_0 = \rho_0 c_0 b l' n_a^2,$$

where R_M is the resistance of the acoustic system, attached to the ribbon. Allowing for (23), we get

$$n_a^2 = \frac{8\omega_0 \zeta \sqrt{bl'}}{3c_0 \pi^{3/2}}. \tag{38}$$

In this calculation, the quantity β remains indeterminate, but from (37) we see that it is desirable to have it as small as possible. However, decreasing β increases α. To find a relationship between the quantities it is necessary to refine the procedure used to calculate the magnetic system. P can be chosen by specifying that the system comprising the pole pieces and the ribbon must be large compared with the wavelength at high frequencies, to avoid additional frequency distortion.

LITERATURE CITED

[1] V. V. Furduev, Electroacoustics (State Tech. Press, Moscow, 1948).

Received February 9, 1954

Acoustics Institute, Academy of Sciences USSR, Moscow

TEMPERATURE DEPENDENCE OF ELECTROSTRICTION AND ELASTIC PROPERTIES OF CERAMIC BARIUM TITANATE

N. A. Roi

An electromechanical thickness gauge was used to determine, in the temperature range from 15 to 150°C, the Young's modulus and the electrostriction coefficients relating the deformation of ceramic barium titanate to the electric field intensity. The results were analyzed on the basis of the molecular model of the ceramic. Relationships were obtained between the electrostriction coefficients that relate the deformation with the field, the deformation with the polarization, the mechanical stress with the field, and the mechanical stress with the polarization. Conclusions were drawn concerning the temperature dependence of these coefficients.

1. The barium titanate ceramic [1], having high polarizability and considerable electrostriction, stands out from among other ferroelectrics for having in addition to high mechanical strength, moisture resistance, good property stability over a wide range of temperatures suitable for practical applications, and for having a distinguishing property peculiar to this ceramic, namely adaptability for the manufacture of electromechanical converters of any shape.

Thanks to these features, barium titanate ceramics are finding an every increasing use in the solution of many hydroacoustic and other problems, requiring the use of electromechanical converters [2-6].

Many problems concerning the properties of the ceramics as well as the properties of barium titanate monocrystals have by now already been treated in the literature to a greater or lesser extent. But there are still many problems, dealing principally with the electromechanical properties of these ceramics, which either have not yet been studied, or require further clarification, to obtain a better knowledge of the properties of the ceramic, which in turn will permit a more successful utilization of the distinguishing features of barium titanate ceramics in their applications.

It is therefore the task of this investigation to study experimentally the temperature dependence of the electrostriction and elastic properties of the ceramic.

An understanding of the molecular processes occurring in barium titanate in the phase-transition region near 120°C makes it possible to assume that the electrostriction properties of the ceramic will change considerably in this region. In face, since the spontaneous polarization is accompanied by a great deformation of the cells [7], one can expect in the vicinity of 120°, where the dielectric constant reaches exceedingly large values, a small extemal field to cause a large polar moment which would accordingly be accompanied by a large electrostriction deformation of the ceramic [8].

2. To investigate experimentally the electrostriction properties of the ceramic and of its temperature dependence, it was necessary to produce apparatus with which to measure the amplitudes of mechanical vibrations on the order of 10^{-9} and 10^{-8} cm at a temperature reaching 150°.

Such apparatus was produced in the form of a pulse electromechanical gauge, representing a version of a delay line. The pulse electromechanical gauge makes it possible to determine the vibration amplitudes of the investigated specimen by comparing it with the known amplitudes of quartz oscillations.

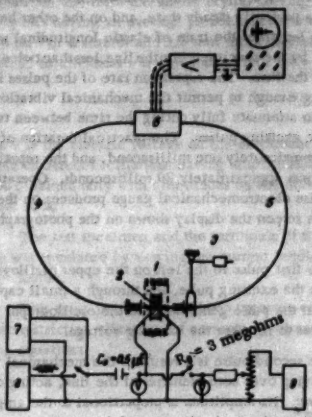

Fig. 1. Principal diagram of electromechanical gauge: 1) electric oven, 2) specimen, 3) lever system, 4) Section I, 5) Section II, 6) piezoelectric receiver.

The gauge is constructed as follows (Fig. 1).

The delay line consists of two identical sections of steel wire 1.3 mm in diameter and approximately 9 m long, wound in a helix so that one section is a continuation of the other. The diameter of the helix is 65-70 cm. The turns of the helix fit in slots of four supporting bars of "penoplast," located at equal distances about the circumference of the helix and secured vertically to a supporting plate.

Where the helix is discontinuous, the terminals of the sections are soldered to a piezoelectric receiver consisting of two round ceramic rods 2 mm in diameter and 3 mm long, the end faces of which are soldered as shown in Fig. 2. The ceramic was soldered to the metal, as is customary in soldering other temperature-resisting dielectric to metals, after first producing a silver coating by firing a special paste on the dielectric surface to be soldered.

The same method was used to solder to the other two ends of the sections insulating quartz end pieces, having spherical surfaces between which the tested specimen was clamped. The clamping pressure could be adjusted and maintained constant for any size gap ranging from 0 to 50 mm between the variable ends of the line. This was accomplished by the lever system shown in Fig. 1.

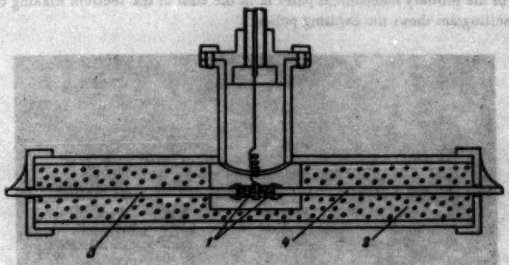

Fig. 2. Piezoelectric receiver of gauge: 1) ceramic piezoelectric elements, 2) "penoplast," 3) Section I, 4) Section II.

Applied to the specimen electrodes were voltage pulse trains of sinusoidal voltages, obtained from the output of a pulse generator, consisting of a sinusoidal generator, pulse transmitter, and power amplifier.

Under the influence of the electric voltage, the specimen carries out mechanical vibrations, which are radiated into the ends of the line section in contact with the specimen, are propagated in opposition to each other along the sections, and meet at the receiver, where the mechanical vibrations are transformed into an alternating voltage, which is amplified and applied to the vertical plates of an oscillograph. The duration of

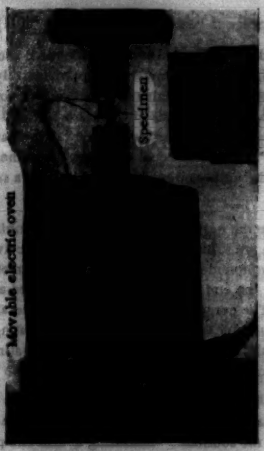

Fig. 3. Operating position of the tested specimen.

the electric pulses exciting the specimen is chosen, on one hand, to enable the mechanical vibrations of the specimen to reach a perfectly steady state, and on the other hand, to make the length of the train of elastic longitudinal waves, launched by the specimen into the line, less than twice the length of the line. The repetition rate of the pulses is made long enough to permit the mechanical vibrations in the line to attenuate fully during the time between two successive exciting pulses. The practical duration of pulses t_p was approximately one millisecond, and the repetition period t_r was approximately 20 milliseconds. Operation of the pulse electromechanical gauge produces on the oscillograph screen the display shown on the photograph (Fig. 4).

The first pulse to the left on the upper oscillogram represents the exciting pulse, fed through a small capacitance from the pulse generator into the oscillograph. This pulse serves to monitor the exciting voltage.

The second pulse is a result of the mechanical vibrations, arriving over both branches of the line, acting on the receiver. Its amplitude is proportional to the amplitude of the mechanical vibrations of the specimen, and we shall therefore call this the measuring pulse.

The distance between the forward fronts of the exciting and measuring pulses corresponds to the time delay t_d of the line, approximately 1.8 milliseconds.

The measuring pulse is followed, at intervals equal to twice the delay time, by pulses representing successive reflections of the primary mechanical pulse from the ends of the sections making contact with the specimen. The lower oscillogram shows the exciting pulses.

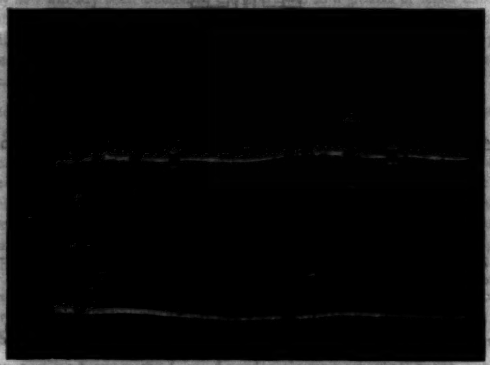

Fig. 4. Oscillogram taken during operation of gauge: 1) exciting pulse, 2) measurement pulse, 3) reflected pulses.

The measurement process consists of comparing the amplitudes of the measuring pulses, obtained from the specimen and from the quartz crystal serving as an amplitude standard. We had at our disposal four X section crystals having an average piezoelectric modulus d_{11} of $6.4 \cdot 10^{-8}$ CGSE. The crystals were in the form of discs 8 mm in diameter and 1.8 mm thick or parallelopipeds measuring 2.5 × 2.5 × 1 mm³. Their vibration amplitude in thickness was calculated from the equation

$$A = d_{11} V,$$

where V is the electric voltage on the electrodes of the plates in CGSE units. The gauge sensitivity made it possible to detect oscillations having amplitudes on the order of 10^{-10} cm, although stable, reproducible results can be obtained only with amplitudes on the order of 10^{-9} cm. At these amplitudes, the measurement accuracy reaches 10%.

The test specimen and the terminals of the gauge were placed in an electric oven, the temperature of which was regulated by varying the current feeding the oven. The specimen temperature was monitored with a thermocouple.

This setup made it possible to measure conveniently, at frequencies on the order of 10^6, the amplitudes of electrostriction vibrations of ceramic specimens at various temperatures. These measurements and the following equations

$$u_{zz} = \lambda_{33} E_z^2,$$

$$u_{xx} = u_{yy} = \lambda_{31} E_z^2$$

made it possible to calculate the electrostriction coefficients λ_{33} and λ_{31}. The following circumstances became clear as a result:

a) The coefficients λ_{33} and λ_{31} are independent of the field intensity within the employed range of intensities (up to 200 v/cm) at all values of temperature in the range of at least from 20 to 150°C.

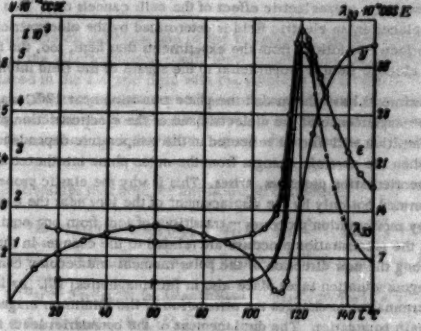

Fig. 5. Temperature dependence of the dielectric constant, of Young's modulus, and of the electrostriction coefficient for deformations along the field.

b) The following relationship

$$\lambda_{33} = 2{,}7\,|\lambda_{31}|,$$

holds for temperatures in the above range approximately, indicating that the electrostriction change in dimensions is accompanied by an increase in volume.

c) At room temperature $\lambda_{33} = 3{,}5 \cdot 10^{-6}$ CGSE.

d) The coefficients λ_{33} and λ_{31} exhibit considerable temperature dependence. The value of λ_{33} is approximately ten times greater near 120°C than at room temperature (Fig. 5).

e) The temperature dependence of the electrostriction coefficients, as well as the temperature dependence of the dielectric constant (Fig. 5) are subject to hysteresis [9].

The hypothesis predicted above concerning the possible existence of a change in electrostriction coefficients in the phase-transition near 120° is thus experimentally confirmed. Experiment shows also that the temperature dependence of the electrostriction coefficients is essentially a replica of the temperature dependence of the dielectric constant (Fig. 5). This fact can be explained qualitatively by the fact that the same molecular mechanism determines both the dielectric constant in the electrostriction coefficients, as well as the polar moment and the electrostriction deformation occurring when the ceramic is placed in an electric field. In fact, at temperatures above 120°C, when the ceramic is in the cubic phase, the electric field brings the ions of titanium and of oxygen closer together, thereby causing the formation of a polar moment and the deformation of the cells. The cells become apparently deformed in the same manner as in spontaneous polarization – the cells become elongated along the polar moment and compressed in the transverse directions.

As the temperature decreases, the energy of the thermal vibrations of the ions diminishes. As a result the same value of electric field intensity produces a greater polar moment and a suitably greater electrostriction cell deformation.

In the phase-transition region, the molecular processes occurring when the ceramic is placed in the electric field become more complicated, and the connection between polarization and electrostriction deformation of the ceramic becomes therefore less obvious. Electrostriction and piezoelectric cell deformation take place in this region along with reorientation of the polar tetragonal cells. However, the piezoelectric deformation does not affect the macroscopic dimensions of the ceramic, since the tetragonal cells are arranged at random in the ceramic, and as a result the piezoelectric effect of the cells cancels out. This is why the macroscopic deformation of a ceramic placed in an electric field is determined by the electrostriction deformation of the cell and by reorientation effects. It follows from the experiments that here, too, the macroscopic deformation of a ceramic placed in an electric field is proportional to the square of the field intensity.

4. The above experiments have shown that the phase transition near 120°C is associated with a substantial anomaly of the temperature dependence of the dielectric and of the electrostriction properties of the ceramic. One can expect that the transition will also be reflected in the temperature dependence of the elastic properties of the ceramic. In fact, when the ceramic changes from the cubic phase into the tetragonal one, a new molecular mechanism, consisting of reorientation processes, arises. This is why the elastic properties of a ceramic in the tetragonal phase are determined not only by the displacement of the ions near the equilibrium position, as in the cubic phase, but also by reorientation processes – transitions of ions from one equilibrium position to another. Thanks to electrostriction, the reorientation processes are related to the changes in the shapes of the elementary cells. The cells stretch along the new direction of the polar moment and become compressed in the perpendicular directions. An analogous situation takes place also in ferromagnetics [10]. As is known, applying external mechanical stresses to a ferromagnetic changes the orientation of the minimum magnetization axes; this causes a displacement of the domain boundaries. The displacement of the boundaries leads to a further change in the dimensions of the specimen, due to magnetostriction deformation, caused by the redistribution of the spontaneous magnetization vectors in the specimen. For this reason, the Young's modulus becomes considerably smaller than in the absence of displacement of domain boundaries, occurring, for example, when the specimen is magnetized to saturation. This effect was called the ΔE effect and was observed as early as in 1902. Bearing in mind the

analogy between the processes occurring in our material and in ferromagnetics, one can expect that the Young's modulus of our material will diminish upon transition into the ferroelectric phase. To see how the Young's modulus of the ceramic changes as a function of the temperature, we used the electromechanical gauge to measure the resonant frequency of the longitudinal vibrations of thin ceramic bars. As is known, in this case the resonant frequency is given by the equation

$$f = \frac{1}{2l}\sqrt{\frac{Y}{\rho}},$$

where l is the length of the bar, ρ the density of the material, and Y Young's modulus.

Inasmuch as l and ρ change little with temperature, one can assume that the change in resonant frequency is due in its entirety to the temperature variation of the Young's modulus.

In these experiments we used ceramic bars measuring on the order of 21 × 3.8 × 2 mm³. The electrodes were coated on the face measuring 21 × 3.8 mm². As in the preceding experiments, the electrostriction vibrations of the unpolarized ceramic were investigated.

After measuring the resonant frequencies of these bars at different temperatures and making suitable calculations, it became evident that the Young's modulus varies quite strongly with temperature (Fig. 5). It is seen in the figure that the Young's modulus for the cubic phase is approximately 1.4 times greater than the value for the tetragonal phase.

What attracts attention is the minimum of the Young's modulus near 110°. This temperature corresponds to the lower temperature boundary of the region of phase transition. At this temperature, almost all the microcrystals of the ceramic are in the tetragonal phase. However, the tetragonal ratio of the cells is quite close to unity at this temperature; therefore, on one hand, the reorientation effect of each cell is small here, and on the other hand, the number of reorientations is large. The fact that the Young's modulus has a minimum in this region of temperatures is evidence that the second circumstance predominates over the first, and therefore the net reorientation effect increases as the temperature rises to the phase-transition region. An analogous minimum of the Young's modulus occurs before the Curie point in ferromagnetics.

The decrease in the modulus as the temperature diminishes to 0°C is apparently due to the impending phase transition near 0°C. External action produces in this region not only cell deformation and a change in the domain structure, but also a transition of several portions of the lattice from the tetragonal to the orthorhombic phase and vice versa.

Having obtained information on the value and on the temperature dependence of the dielectric constant, of the Young's modulus, and of the electrostriction coefficients, which relate the deformation of the free specimen (i. e., when $\sigma_{ik} = 0$) placed in the electric field with the square of the intensity of this field, it is possible to determine the magnitude and the temperature dependence of the parameters that relate the deformation with the square of the polarization, and also the coefficients that relate the electrostriction mechanical stresses occurring in a clamped specimen (i. e., when $u_{ik} = 0$) with the square of the electric field intensity or with the square of the polarization.

We shall start with relationships that hold for any isotropic dielectric:

$$-\sigma_{xx} = c_{11}u_{xx} + c_{12}(u_{yy} + u_{zz}) + q_{11}P_x^2 + q_{12}(P_y^2 + P_z^2),$$
$$-\sigma_{yy} = c_{11}u_{yy} + c_{12}(u_{xx} + u_{zz}) + q_{11}P_y^2 + q_{12}(P_x^2 + P_z^2),$$
$$-\sigma_{zz} = c_{11}u_{zz} + c_{12}(u_{xx} + u_{yy}) + q_{11}P_z^2 + q_{12}(P_x^2 + P_y^2),$$
$$-\sigma_{xy} = c_{44}u_{xy} + q_{44}P_xP_y,$$
$$-\sigma_{xz} = c_{44}u_{xz} + q_{44}P_xP_z,$$
$$-\sigma_{yz} = c_{44}u_{yz} + q_{44}P_yP_z.$$

From these relationships one can find that when $E_x = E_y = 0$ and $E_z \neq 0$, we have a free specimen

$$u_{zz} = \lambda_{31} E_z^2, \qquad u_{zz} = \vartheta_{31} P_z^2,$$

$$u_{yy} = \lambda_{31} E_z^2, \qquad u_{yy} = \vartheta_{31} P_z^2,$$

$$u_{zz} = \lambda_{33} E_z^2, \qquad u_{zz} = \vartheta_{33} P_z^2,$$

and for a clamped specimen

$$-\sigma_{zz} = \gamma_{31} E_z^2, \qquad -\sigma_{zz} = q_{13} P_z^2,$$

$$-\sigma_{yy} = \gamma_{31} E_z^2, \qquad -\sigma_{yy} = q_{13} P_z^2,$$

$$-\sigma_{zz} = \gamma_{33} E_z^2, \qquad -\sigma_{zz} = q_{11} P_z^2.$$

Using the well-known relationship between c_{11}, c_{12}, Υ, and σ, where σ is the Poisson coefficient, and taking furthermore into consideration that $\epsilon \gg 1$, the parameters ϑ_{1k}, γ_{1k}, and q_{1k} can be expressed in terms of ϵ, λ_{1k}, Υ, and σ in the following manner

$$\vartheta_{31} = \frac{\lambda_{31}}{\epsilon^2} 16\pi^2, \qquad \vartheta_{33} = \frac{\lambda_{33}}{\epsilon^2} 16\pi^2,$$

$$\gamma_{31} = q_{13} \frac{\epsilon^2}{16\pi^2}, \qquad \gamma_{33} = q_{11} \frac{\epsilon^2}{16\pi^2},$$

$$q_{13} = -\frac{\sigma\lambda_{33} + \lambda_{31}}{(1+\sigma)(1-2\sigma)} \frac{16\pi^2 Y}{\epsilon^2}, \qquad q_{11} = -\frac{(1-\sigma)\lambda_{33} + 2\sigma\lambda_{31}}{(1-\sigma)(1-2\sigma)} \frac{16\pi^2 Y}{\epsilon^2}.$$

Worthy of attention from among these parameters are q_{11} and q_{13}. Let us rewrite them in the following form, using the fact that $\lambda_{33} = -2.7\lambda_{31}$:

$$q_{11} = -\frac{1 - 1.75\sigma}{1 - \sigma - 2\sigma^2} 16\pi^2 \frac{\lambda_{33}}{\epsilon^2} Y,$$

$$q_{13} = -\frac{\sigma - 0.37}{1 - \sigma - 2\sigma^2} 16\pi^2 \frac{\lambda_{33}}{\epsilon^2} Y.$$

From this it is clear that q_{11} and q_{13} depend on σ and on the combination $\frac{\lambda_{33}}{\epsilon^2} Y$. Based on our measurements, one can see that the combination $\frac{\lambda_{33}}{\epsilon^2} Y$ is independent of the temperature, at least in the range from 20 to 150°C.

Thus, the character of the temperature dependence of q_{11} and q_{13} depends on the character of the temperature dependence of σ. One can show, however, that the parameter q_{11} depends on σ rather weakly. As σ varies from 0 to 0.35 (with $\sigma = 0.28$ at room temperature), q_{11} changes only by 4%.

The character of the temperature dependence of the remaining parameters can be readily obtained from the relationships given above.

LITERATURE CITED

[1] B. M. Vul and I. M. Gol'dman, Doklady Akad. Nauk SSSR 46, 154 (1945).

[2] A. V. Rzhanov, Progr. Phys. Sci. (USSR) 38, 451 (1949).

[3] G. Bradfield, Supplimento novo cimento 7, 182 (1950).

[4] W. Mason, Piezoelectric Cystals and Their Use in Ultrasonics (Foreign Lit. Press, 1952) (Russian translation).

[5] O. Mattiat, J. Acoust. Soc. Am. 25, 291 (1953).

[6] L. Camp, J. Acoust. Soc. Am. 25, 297 (1953).

[7] H. D. Megaw, Proc. Phys. Soc. 58, 133 (1946).

[8] N. A.Roi, Doklady Akad. Nauk SSSR 73, 937 (1950).

[9] N. A.Roi, Doklady Akad. Nauk SSSR 81, 545 (1951).

[10] S. Vonsovskii and Ia. Shur, Ferromagnetism (State Tech. Press, 1948).

Received January 31, 1955

Acoustics Institute, Academy of Sciences USSR, Moscow

EQUIVALENT CIRCUITS OF ELEMENTS OF VIBRATING SYSTEMS WITH DISTRIBUTED CONSTANTS

I. G. Rusakov

Discussion of a method for representing a mechanical system with distributed constants in the form of equivalent circuits, suitable for a frequency range that includes several resonant frequencies.

The representation of elements of vibrating systems with distributed parameters (for example, such as rods, membranes, tubes, etc.) in the form of equivalent circuits is usually valid in a certain limited frequency range, within which the element with the distributed constants can be replaced within a certain approximation, by an equivalent element with a lumped constant. Proposed below is a method for treating such elements in which they are better represented in the form of equivalent circuits, suitable for use over a wide frequency range that includes several resonant frequencies of the elements.

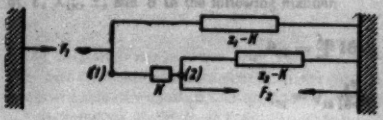

Fig. 1.

Let us consider an arbitrary linear mechanical converter, denoting by z_1 and z_2 its input and output no-load impedances and by K the coupling constant or the transfer impedance. The equation of a four-terminal network in the form of impedances is readily transformed to the form

$$F_1 = F_2 + (z_1 - K)\,v_1 + (z_2 - K)\,v_2,\quad K(v_1 - v_2) = F_2 + (z_2 - K)\,v_2.$$

From this, the equivalent circuit shown in Fig. 1 becomes evident. For a longitudinally-vibrating rod the impedances are given by the following equations

$$Z_1 = Z_2 = \frac{SE}{jc}\cot kl;\quad K = \frac{SE}{jc}\frac{1}{\sin kl},$$

where S is the cross-sectional area of the rod, E Young's modulus, c the velocity of propagation of the longitudinal waves in the rod, $k = \omega/c$, and l is the length of the rod.

Let us find

$$z_1 - K = z_2 - K = \frac{jSE}{c}\tan\frac{kl}{2}.$$

On the basis of the form of the impedances obtained, we can consider K to be a flexible impedance $\frac{1}{j\omega C}$, whereby

$$C = C_0\frac{\sin kl}{kl},$$

where C_0 is the static compliance of the rod.

In exactly the same manner, considering $(z_1 - K)$ and $(z_2 - K)$ to be inertia impedances $j\omega\frac{m}{2}$, we get an expression for the mass $\frac{m}{2}$:

$$\frac{m}{2} = \frac{m_0}{2}\frac{\tan\left(\frac{kl}{2}\right)}{(kl/2)},$$

where $m_0 = \rho lS$ is the total mass of the rod.

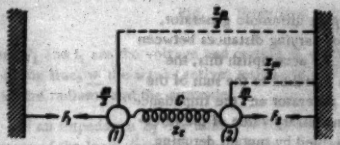

Fig. 2.

The equivalent circuit is shown in Fig. 2. Naturally, representing K in the form of a compliance and $(z - K)$ in the form of a mass is quite arbitrary, for as the frequency changes the signs of these impedances change, and the "masses" themselves become "compliances" and vice versa, but except for this reservation, the equivalent diagram of Fig. 2 will be formally correct for all frequencies, with the exception, perhaps, of the resonant frequencies themselves, when the impedances vanish or become infinite.

The circuit of Fig. 2 applies also to an acoustic waveguide — a tube with a rigid wall of small cross section, in which plane sound waves propagate. Here the mass m_0 and the compliance C_0 are

$$m_0 = \frac{\rho V}{S^2} \text{ and } C_0 = \frac{\rho c^2}{V},$$

where V is the total volume of the waveguide, and c and S are, as before, the velocity of sound and the cross-sectional area.

At low frequencies $kl \ll 1$, the frequency-dependent compliance C and mass m of the waveguide or of the rod should be replaced by their static values. The mass of the rod or of the waveguide is split equally between the input and the output sections. If the rod or waveguide are part of a more complicated vibrating system, the forces F_1 and F_2 can be replaced by reactions of the impedances connected to cross sections 1 and 2.

The method shown here for analyzing and drawing an equivalent circuit for a rod and tube can be readily extended to other similar elements of vibrating systems.

Received January 10, 1955

All-Union Scientific Research Institute of Physical-Technical and Radio-Engineering Measurements, Moscow

PRODUCTION OF ULTRASONIC RADIATION OF CONSTANT INTENSITY WHEN SOUNDING IN A VESSEL WITH AN UNTUNED BOTTOM

I. V. Skards

Analysis of the problem of producing an ultrasonic generator, producing radiation of constant intensity for varying distances between the radiator and the bottom of the vessel. To accomplish this, the impedance of the ultrasonic generator was matched to the sum of the internal impedance of the high frequency generator and the impedance caused by the losses of the radiator. The necessary value of the internal impedance of the generator can be obtained by mutual detuning of the resonant circuit of the output tube (primary tuned circuit) and of the resonant circuit of the quartz radiator (secondary tuned circuit). It was established experimentally that it is possible to stabilize the ultrasonic intensity within 4%.

When objects placed in ampoules which border on the contact-making medium are exposed to ultrasonic radiation, it is difficult to measure the ultrasonic intensity in the ampoule. Yet a necessary condition for obtaining repeatable results is that the intensity be constant. The presence of reflections of part of the sound energy from the bottom of the ampoule and the formation of a field of standing waves may cause small changes in distance to result in noticeable changes in intensity inside the ampoule. On the other hand, it is difficult to measure accurately the distance between the radiator and the ampoule, for to eliminate cavitation in the contact-making medium it is essential to change the hydrostatic pressure, for which purpose the contact-making medium is hermetically sealed.

The above circumstances have led us to construct an ultrasonic generator such that the ultrasonic intensity remains constant when the distance between the bottom of the vessel and the radiator is changed. It was necessary for this purpose to match the impedance of the ultrasonic generator with the sum of the internal impedance of the high frequency generator and the impedance caused by the losses of the radiator. The radiator used in the experiments was a flat quartz plate. The sounded material was placed in a flat-bottom glass ampoule. To obtain good cooling of the object, a thin-walled ampoule was used.

1. Matching the Impedance of the Ultrasonic Generator with the Sum of the Internal Impedance of the High-Frequency Current Generator and the Impedance Due to the Losses in the Suspension of the Quartz and in the Transformer Oil

Figure 1 shows the equivalent circuit of the entire path, starting with the high-frequency generator and ending with the sounded vessel. Here R_1 and X are the resistance and the reactance of the internal impedance of the generator, R_0 and X_0 the resistance and the reactance of the radiator mounting, Z_1 the (complex) impedance of the element between the quartz and the sounded vessel, and $\underline{w}$ and X_2 the resistance and reactance of the sounded vessel.

For the electric line, representing the mechanical element between the quartz and the sounded vessel, the following relationships hold:

$$V_1 = V_2 \cosh \gamma_1 + I_2 w \sinh \gamma_1, \qquad I_1 = \frac{V_2}{w} \sinh \gamma_1 + I_2 \cosh \gamma_1, \tag{1}$$

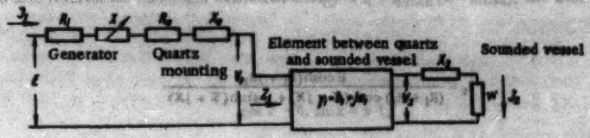

Fig. 1. Equivalent circuit of ultrasonic radiator.

where V_1 and I_1 are the voltage and current at the input of the line, V_2 and I_2 the voltage and current at the output of the line, w the wave (active) resistance, and $\gamma_1 = b_1 + ja_1$ the propagation constant for the element between the radiator and the ampoule.

If an impedance $Z_2 = w \tanh \gamma_2$ is connected to the output of the line, where $\gamma_2 = b_2 + ja_2$ is the propagation constant of the load circuit, the total input impedance can be expressed as follows:

$$Z_1 = w \frac{\sinh 2(b_1 + b_2) + j \sin 2(a_1 + a_2)}{\cosh 2(b_1 + b_2) + j \cos 2(a_1 + a_2)}.$$

Let us assume that $a_1 + a_2 = \frac{\pi}{2}(2k + 1)$, then $\cos 2(a_1 + a_2) = -1$, $\sin 2(a_1 + a_2) = 0$, and $z_1 = w \coth(b_1 + b_2)$.

If we assume that $a_1 + a_2 = \pi k$, then $\cos 2(a_1 + a_2) = +1$, $\sin 2(a_1 + a_2) = 0$, and $z_1 = w \tanh(b_1 + b_2)$.

In both these cases the impedance Z_1 is a pure resistance. The reactance X_0 can be compensated by varying the reactance X. We then obtain in the circuit with current I_1 a pure resistance

$$R = R_1 + R_0 + Z_1.$$

Here we have

$$R_{max} = R_1 + R_0 + w \coth(b_1 + b_2), \quad R_{min} = R_1 + R_0 + w \tanh(a_1 + a_2).$$

When the ampoule is displaced, only a_1 changes noticeably, changing with it $a_1 + a_2$; the remaining quantities can be assumed invariant.

Let us put for brevity

$$a_1 + a_2 = x, \quad b_1 + b_2 = y.$$

When x_0 is compensated for, x is invariant, and the distance between the ampoule and radiator is varied, the impedance in the primary circuit becomes

$$z = R_1 + R_0 + w \tanh(Y + jX). \qquad (2)$$

The current in the primary circuit is

$$I_1 = \frac{E}{R_1 + R_0 + w \tanh(Y + jX)}.$$

The currents in the primary and secondary circuits are related by

$$I_2 = I_1 \frac{\cosh (b_2 + ja_2)}{\cosh (Y + jX)}.$$

Then

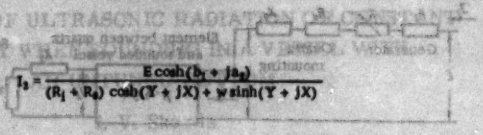

$$I_2 = \frac{E \cosh (b_2 + ja_2)}{(R_1 + R_0) \cosh (Y + jX) + w \sinh (Y + jX)}$$

or

$$I_2 = \frac{E \cosh (b_2 + ja_2)}{[(R_1 + R_0) \cosh Y + w \sinh Y] \cos X + j [(R_1 + R_0) \sinh Y + w \cosh Y] \sin X} \tag{3}$$

The numerator of the right half of the last expression is independent of the coordinates of the ampoule, and consequently, remains invariant when the ampoule position is changed. I_2 varies therefore only with the denominator.

Let us introduce the auxiliary variables

$$\xi = [(R_1 + R_0) \cosh y + w \sinh y] \cos x, \quad \eta = [(R_1 + R_0) \sinh y + w \cosh y] \sin x. \tag{4}$$

Equations (4) are those of an ellipse (in parametric form), with the semi-axes given by the expressions in the square brackets.

If $R_1 + R_0 = w$, then the expressions in the square brackets become equal, and the ellipse becomes a circle. The absolute value of I_2 is then constant, and the output power delivered to resistance w is independent of x or y. To accomplish this it is necessary to choose an equivalent generator such that the sum of its internal resistance R_1 and the mounting resistance R_0 equals the load resistance w:

$$R_1 + R_0 = w.$$

Let us determine the voltage V_2 across the load.

The no-load voltage is

$$E = (R_1 + R_0) I_1 + V_1. \tag{5}$$

At no-load $I_2 = 0$, and we obtain from (1)

$$V_1 = V_2 \cosh \gamma_1, \quad I_1 = \frac{V_2}{w} \sinh \gamma_1.$$

Substituting these values into Eq. (5) and taking into account that $R_1 + R_0 = w$, we get

$$E = \left[\frac{R_1 + R_0}{w} \sinh \gamma_1 + \cosh \gamma_1 \right] V_2 = e^{\gamma_1} V_2 = V_2 \exp [b_1 + ja_1].$$

From this it is evident that $|V_2|$ varies uniformly as Ee^{-b_1}; changing a_1 changes only the phase of V_2, without changing its absolute value. For any load impedance the current through this impedance is independent of a_1. Therefore, the power delivered to the ampoule becomes independent of the distance between the ampoule and the radiator not only when loaded by a pure resistance w, but when loaded by an impedance connected in series with the reactance X_2.

If $R_1 + R_0 \neq w$, the absolute value of V_2 varies with $x = a_1 + a_2$. To attain equality it is necessary to change the value of the internal resistance R_1 of the generator.

Let us consider two cases.

1. The load receives the maximum amount of energy at $I_1 = I_{1\min}$ ($R = R_{max}$), and with this $x = a_1 + a_2 = \frac{\pi}{2}(2k+1)$.

Then

$$\cos x = 0, \quad \sin x = \pm 1,$$

The absolute value of the denominator of (3), which equals

$$(R_1 + R_0)\sinh y + w\cosh y,$$

corresponds to the minor semi-axis of the ellipse (4)

$$(R_1 + R_0)\sinh y + w\cosh y < (R_1 + R_0)\cosh y + w\sinh y.$$

From this it follows that

$$R_1 + R_0 > w.$$

To satisfy the condition $R_1 + R_0 = w$ it is necessary to reduce R_1.

2. The load receives a maximum amount of energy at $I_1 = I_{1\max}$ ($R = R_{min}$), and with this $x = a_1 + a_2 = \pi k$, $\cos x = \pm 1$, $\sin x = 0$; the minor semi-axis of the ellipse (4) corresponds to the following value of the denominator (3):

$$(R + R_0)\cosh y + w\sinh y.$$

Then

$$(R_1 + R_0)\cosh y + w\sinh y < (R_1 + R_0)\sinh y + w\cosh y$$

and

$$R_1 + R_0 < w.$$

In this case R_1 must be increased.

2. Determination of the Parameters of the Line, Equivalent to the Mechanical Element Between the Quartz and the Vessel

To determine the parameters of the equivalent line, the following experiments were performed:

1. The internal impedance of the high-frequency generator was measured. For this purpose the operation of the generator with various loads, consisting of a pure resistance and capacitor, with which the inductance of the generator was compensated, was investigated.

2. The generator was connected to the ultrasonic radiator, irradiating an empty flat-bottomed vessel. The maximum and minimum currents in the tuned circuit, observed upon displacing the flat-bottomed vessel, were noted.

3. The ultrasonic radiator irradiated a flat-bottomed vessel, filled with water, the maximum and minimum currents in the tuned circuit were noted as the vessel was displaced.

4. The ultrasonic radiator was operated with cotton located in place of the vessel; the cotton absorbed the sound energy.

Since the parameters of the line were calculated on the basis of measurements of small current differences, the current in the radiated circuit had to be measured with great precision. In all cases the current was measured with the incandescent bulbs, the light intensity of which was measured photometrically. This method of current measurement gives more accurate results than using a thermocouple instrument, for insignificant changes in current flowing through the incandescent lamps cause considerable changes in their illumination intensity.

The impedances measured by the above method amount to:

$z_I = w \tanh b_1 + R_0$ and $z_{II} = \frac{w}{\tanh b_1} + R_0$ for an empty vessel;

$z_{III} = v \tanh(b_1 + b_2) + R_0$ and $z_{IV} = \frac{v}{\tanh(b_1 + b_2)} + R_0$ for a filled vessel; and

$z_V = w + R_0$ for cotton.

The following relationships were obtained for the parameters

$$R_0 = \frac{z_I z_{II} - \frac{b}{V}}{z_I - z_{II} - 2z_V} = \frac{z_{III} z_{IV} - z_V^2}{z_{III} + z_{IV} - 2z_V},$$

$$w = z_V - R_0, \quad \tanh b_1 = \frac{z_I - R_0}{w}, \quad \tanh(b_1 + b_2) = \frac{z_{III} - R_0}{w},$$

and for a_2:

$$w \operatorname{Re}(\tanh \gamma_2) = w \frac{\tanh 2b_2}{\cosh 2b_2 + \cos 2a_2} = w.$$

From this it follows that

$$\cos 2a_2 = \sinh 2b_2 - \cosh 2b_2 = -e^{-2b_2},$$

giving the absolute value of a_2.

For example, at $b_2 = 0.4$, we have

$$\cos 2a_2 = -0.4493, \quad 2a_2 = \pm[180° - 63.3°] = 116.7°, \quad a_2 = \pm 58.35°.$$

The value of X_2 is obtained from the expressions

$$X_2 = w \frac{\sin 2a_2}{\cosh 2b_2 + \cos 2a_2}, \quad X_2 = \pm w \frac{0.8934}{1.3374 - 0.4493}, \quad X_2 = \pm w \frac{0.8934}{0.8881} \approx \pm w.$$

3. Measurement of the Ultrasonic Intensity

We used three methods to determine the ultrasonic intensity in the ampoule.

1. A method in which the change in the optical transparency of bacterial suspension upon sounding is used.

2. A method in which the intensity is characterized by the difference in the steady-state temperature in the ampoule and the temperature of the cooler. The temperature in the ampoule was determined with a thermal resistance in the form of a thin wire spiral. Measuring the temperature in the ampoule before and after sounding, the difference between the temperatures in the ampoules and in the cooler was plotted vs. the square of the current in the quartz circuit. The system was calibrated in absolute intensities with the aid of an auxiliary wire

spiral, placed in the ampoule and heated with direct current. Comparing the amounts by which the temperature in the ampoule is higher when sounded with the heater than without the heater, it is possible to determine the absolute intensities, corresponding to certain values of current in the quartz circuit.

3. A method in which the intensity was determined from the rate at which the temperature rose in the ampoule.

The first of the above methods gives a relative characterization of the intensity under various sounding conditions, while the other two give directly the absolute ultrasonic intensity. Investigating the ultrasonic intensity changes in the ampoule with the above methods and assuming the waveguide to be linear, we checked the suitability of the above matching theory.

4. Verification of the Matching Theory

Equation (3) makes it possible to calculate $|I_2|$. Let us denote the value of I_1 min [at $x = \frac{\pi}{2}(2k+1)$] corresponding to I_2 by $I_{2\min}$, and the value of I_1 max [at $x = \pi k$] corresponding to I_2 by $I_{2\max}$.

We then have

$$\frac{I_{2\max}}{I_{2\min}} = \frac{(R_1 + R_0)\sinh y + \nu \cosh y}{(R_1 + R_0)\cosh y + \nu \sinh y}. \quad (6)$$

It follows from the measurement results that $b_1 \approx 0.4$, $b_2 \approx 0.4$, and $y \approx 0.8$. Since $\tanh 0.8 \approx {}^3/_5$, we have in this case

$$\frac{I_{2\max}}{I_{2\min}} = \frac{2(R_1 + R_0) + 3w}{3(R_1 + R_0) + 2w}; \quad (7)$$

$$\frac{R_1 + R_0}{w} = \frac{3I_{2\max} - 2I_{2\min}}{3I_{2\max} - 2I_{2\min}}.$$

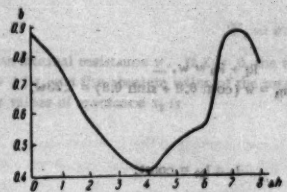

Fig. 2. Dependence of ultrasonic intensity on the displacement of the ampoule relative to the radiator, when the ratio $\frac{R_1 + R_0}{w}$ is very large or very small.

Let us compare the calculated and experimental power in the load as functions of the distance between the ampoule and radiator at different ratios of the resistances $R_1 + R_0$ and w.

1. If the ratio $\frac{R_1 + R_0}{w}$ is very large or very small, the calculated ratio of $I_{2\max}$ to $I_{2\min}$ is close to 1.5, and the ratio of the maximum to minimum energy obtained is approximately 2.25. This agrees with the experimental results represented in Fig. 2. The abscissa of the plot shows the change Δh of the distance h between the ampoule and radiator in centimeters. The ordinate axis shows the ultrasonic intensity B in relative units. The sounding took place with constant current in the radiator circuit.

2. The dependence of the energy in the ampoule on the distance between the ampoule and radiator was checked with an internal generator resistance $R_1 = 650$ ohms, $R_0 = 250$ ohms, $w = 600$ ohms. At these resistance values we have $R_1 + R_0 = 900$ ohms $\approx 1.5w$.

The measurements yielded the following values of the parameters

$$b_1 \approx 0.4 \text{ and } b_2 \approx 0.4.$$

Then

$$y = b_1 + b_2 = 0.8,$$

$$\cosh y = 1.337, \sinh y = 0.888.$$

It follows from Eq. (4) that the extreme values of the denominator of Eq. (3) are

$$\xi_0 = (R_1 + R_0)\cosh 0.8 + w\sinh 0.8 = 2.89w \text{ (corresponding to } I_{2\min}\text{)},$$
$$\eta_0 = (R_1 + R_0)\sinh 0.8 + w\cosh 0.8 = 2.67w \text{ (corresponding to } I_{2\max}\text{)}. \quad (8)$$

Consequently

$$I_{2\max} = 1.1 I_{2\min}.$$

A 10% change in I_2 changes the load energy by 20%, in agreement with the results of the experiments shown in Fig. 3. The axes of the graph indicate the same quantities as Fig. 2.

3. It was established experimentally that the energy arriving at the ampoule is independent of the distance between the radiator and ampoule when the resistances are fully matched:

$$R_1 = 325 \text{ ohm}, R_0 = 250 \text{ ohm}, w = 600 \text{ ohm}.$$

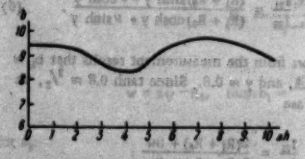

Fig. 3. Dependence of ultrasonic intensity on the displacement of the ampoule with respect to the radiator at $\frac{R_1 + R_0}{w} = 1.5$.

Then

$$R_1 + R_0 \approx w,$$
$$\xi_1 = \eta_1 = w(\cosh 0.8 + \sinh 0.8) = 2.23w,$$

With this

$$I_1 = I_{2\max} = \text{const}.$$

The experimental results are shown in Fig. 4, where the symbols are the same as in the two preceding figures. It is evident from the plot that as the distance between radiator and ampoule is varied, the maximum difference between the energies arriving at the ampoule does not exceed 4%.

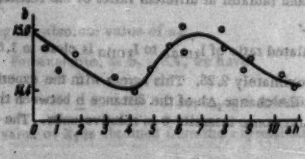

Fig. 4. Dependence of ultrasonic intensity on the ampoule displacement relative to the radiator for complete matching: $R_1 + R_0 \approx w$.

4. Let us compare the case of full matching of the resistances with the case corresponding to Expression (8).

The current ratio in the load is:

$$\frac{I_{2\max}}{I_2} = \frac{2.89}{2.23} = 1.25, \quad \frac{I_{2\max}}{I_1} = \frac{2.67}{2.23} = 1.20.$$

The power ratio in the load is

$$\left(\frac{I_{2\max}}{I_2}\right)^2 = 1.56, \left(\frac{I_{2\max}}{I_1}\right)^2 = 1.43.$$

The above numbers show that if the resistances are fully matched, the power delivered to the load increases by 56% compared to the previous minimum value, and by 43% compared with the previous maximum power value. This also is in agreement with the experimental results.

5. Transmission of Ultrasonic Waves Through the Bottom of the Vessel

The transmission factor D through the bottom of the ampoule can be determined from the known relationship

$$D = \frac{4\left(\frac{\rho_2 \vartheta_2}{\rho_1 \vartheta_1}\right)^2}{4\left(\frac{\rho_2 \vartheta_2}{\rho_1 \vartheta_1}\right)^2 \cos^2 \frac{2\pi d}{l_2} + \left[\left(\frac{\rho_2 \vartheta_2}{\rho_1 \vartheta_1}\right)^2 + 1\right]^2 \sin^2 \frac{2\pi d}{l_2}},$$

where d is the thickness of the ampoule bottom, l_2 the length of the ultrasonic wave in the ampoule material, ϑ_2 the velocity of sound propagation in the ampoule material, ϑ_1 the velocity of sound propagation in the contact-making medium, ρ_2 the density of the ampoule material, ρ_1 the density of the contact-making medium. If a glass ampoule with a bottom of thickness d = 0.3 mm is placed in water, the sound transmission coefficient calculated from this relationship is D = 0.7. Changing the thickness of the ampoule bottom by 10% changes the ultrasonic-intensity transmission through the ampoule by 3%.

Let us again return to the equivalent circuit of Fig. 1. From the point of view of the change in ultrasonic intensity, changing the thickness of the ampoule bottom is equivalent to changing the reactance X_2. If the input is matched, $R_1 + R_0 = w$, the load sees a source with an emf:

$$V_2 = e^{-0.4-j\alpha_1} E = e^{-j\alpha_1} 0.670E$$

and an internal resistance w. If $X_2 = 0$, the total impedance of the circuit is 2w; if $|x_2| = w$, the total impedance is $2w \pm jw$, and the absolute value of the total impedance is $\sqrt{2^2 + 1}\, w = \sqrt{5}\, w$. The current ratio in the load at these values of reactance x_2 is

$$\frac{I_{\text{н}(X_2=0)}}{I_{\text{н}(X_2=w)}} = \frac{\sqrt{5}}{2} \approx 1.12.$$

The ratio of the power delivered to the load is:

$$\frac{P_{(X_2=0)}}{P_{(X_2=w)}} = \frac{5}{4} = 1.25.$$

The power delivered to the load at $X_2 = 0$ is 25% greater than that delivered at $X_2 = w$.

6. Determination of Optimum Detuning of the Output Circuits of the High-Frequency Generator

Figure 5 shows the diagram of the generator tuned circuits. Circuit I is connected to the output tube of the generator, and Circuit II contains the radiator having a resistance r and a capacitance C_2. In the diagram, L_1, C_1, and ρ are the inductance, capacitance, and equivalent resistance of the first circuit, respectively, I is the total current flowing through the first circuit, i and L_2 are the current and inductance in the second circuit, and M is the mutual inductance.

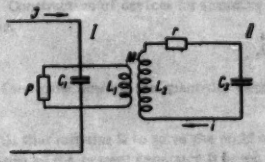

Fig. 5. Equivalent diagram of output circuits of ultrasonic generator.

Let us show that the internal resistance of the generator can be changed by merely varying the detuning between Circuits I and II. Let us consider Circuits I and II under working conditions. Replacing the output tube by an equivalent current generator with a short-circuit current I and shunting conductance ρ, and introducing r_2 (resistance of the second circuit) and C_2 (stray capacitance), we obtain the equivalent generator circuits shown in Fig. 6.

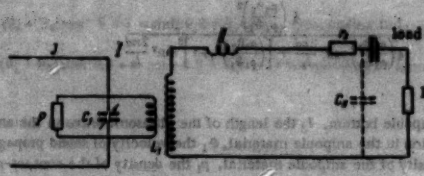

Fig. 6. Diagram of output circuits of ultrasonic generator.

The reactance of the first circuit is

$$X_1 = \omega L_1 - \frac{1}{\omega C_1}.$$

The reactance of the second circuit (see Fig. 6) is

$$X_0 + \xi = \omega L_2 - \frac{1}{\omega C_2}.$$

The reactance of the second circuit is represented in the form of two quantities: the initial reactance X_0 and a supplementary reactance ξ, which varies approximately from +200 to −200 ohms, depending on the position of the ampoule. Denoting the average of capacitance C_2 by C_{20}, we obtain $X_0 = \omega L_2 - \frac{1}{\omega C_{20}}$.

The current I is given by the equation

$$I = -\frac{i}{\omega M}(rL_1\omega - j\omega C_1 X_1)\left\{r + \frac{rM^2\omega^2}{\rho^2\omega^2 L_1^2 + \omega^2 C_1^2 X_1^2} + \right.$$

$$\left. + j\left[\xi + X_0 - M^2\omega^2 \frac{\rho^2\omega L_1 - \omega^2 C_1 X_1}{\rho^2\omega^2 L_1^2 + \omega^2 C_1^2 X_1^2}\right]\right\}. \qquad (9)$$

The change in the absolute value of the current I in the second circuit as a function of the ampoule position is determined by the change in the absolute value of the quantity contained in the last bracket. For Relationship (2) to remain in force, the square bracket should contain only ξ, i. e., we should have

$$M\omega^2 = X_0 \frac{\rho^2\omega^2 L_1^2 + \omega^2 C_1^2 X_1^2}{\rho^2\omega L_1 + \omega^2 C_1^2 X_1}. \qquad (10)$$

This means that

$$X_0 = \frac{\omega^2 M^2}{\omega L_1}\left[1 + \frac{\omega C_1 X_1^2}{\rho^2\omega^2 L_1^2 + \omega^2 C_1^2 X_1^2}\right]. \qquad (11)$$

TABLE 1

X_1, kohm	$\rho^2\omega^2L_1^2+\omega^2C_1^2X_1^2$	X_2, kohm	$\rho S^2=\frac{M^2}{\rho^2L_1^2+C_1^2X_1^2}$, kohm	$R=\frac{C_2+C_3}{C_2}\times$ $\times(\rho S^2+r_2)$	X_2, kohm	R_2, kohm
−0.253	$3.4\cdot10^{-3}+100\cdot10^{-3}=$ $=103.4\cdot10^{-3}$	−0.042	0.0144	+0.443	−0.03	0.443
−0.125	$3.4\cdot10^{-3}+24.6\cdot10^{-3}=$ $=28.0\cdot10^{-3}$	−0.094	0.0533	+0.794	−0.08	0.803
−0.049	$3.4\cdot10^{-3}+3.7\cdot10^{-3}=$ $=7.1\cdot10^{-3}$	−0.156	0.210	2.104	0.16	2.1
0.076	$3.4\cdot10^{-3}+0.09\cdot10^{-3}=$ $=3.49\cdot10^{-3}$	+0.076			+0.07	

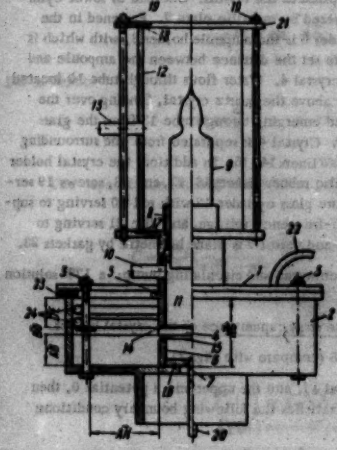

Fig. 7. Construction of devices for sounding the ampoule.

If this condition is satisfied, then

$$|i| = I\frac{S}{r+\rho S^2}, \tag{12}$$

where

$$S = \frac{\omega M}{\sqrt{\rho^2\omega^2L_1^2+\omega^2C_1^2X_1^2}} \tag{13}$$

As can be seen from (12), if I, r, and ρ remain constant, the value of |i| is determined by S. If the impedances are matched, the internal resistance of the current generator is small. It is therefore necessary to ascertain for what values of the mutual inductance M will the internal impedance of the generator be a minimum for optimum values of C_1 and L_2, if L_1, C_2, r, and ρ are given.

An answer to this question is given by Eq. (12). As can be seen, the value of i is affected by M and C_1 only through S, regardless of whether it is M or C that changes. With this it is necessary that Eq. (13) be satisfied. Thus, as long as Eq. (12) remains in force, a change in M cannot by itself change the internal impedance. In principle it is possible to work with any fixed value of M, varying S with the aid of C_1. For this to be possible, it is necessary to satisfy the inequality

$$M > S\rho L. \tag{14}$$

If we know now all the quantities except L_2, the value of X_2 from (11) will determine the optimum value of L_2.

All that remains is to solve the problem of determining the optimum value of S. The minimum internal impedance of the current generator is given by (12) if $S \to 0$, but then we also have $|i| \to 0$. The maximum value of |i| for given values of I, r, and ρ is obtained for the following value of S:

$$S = \sqrt{\frac{r}{\rho}}.$$

It is seen from the above that the internal impedance of the generator can be varied by detuning the output circuit; for example (Fig. 6), if $\rho = 73 \cdot 10^{-3}$ mS, $\omega L_1 = 0{,}8$ kohm, and $r_1 = 0{,}034$ kohm, we have

$$\frac{\omega^2 M}{\omega L} = 0{,}02 \text{ kohm}, \quad \frac{C_1 + C_2}{C_1} = 9,$$

$$\frac{1}{\omega C_1} \gg R.$$

Table 1 gives a comparison of the calculated and experimental values of these quantities.

For the current generator to have low internal impedance it is necessary to reduce the stray capacitance C_2.

7. Reduction of the Stray Capacitance of the Crystal Holder

a) Construction of a device used to sound the ampoule (Fig. 7).

Using a metal disc 1, a special porcelain part 2, and screws 3, the quartz crystal 4 is mounted between cylinders 5 and 6, through which the high frequency voltage is applied to the crystal. One end of lower cylinder 6 is covered by metallic plate 7. Fastened in the upper cylinder 5 is the ampoule holder 8, with which it is possible to set the distance between the ampoule and the quartz crystal 4. Water flows through tube 10 located in space 11 above the quartz crystal, flowing over the ampoule and emerging through tube 13 from the glass cylinder 12. Crystal 4 is separated from the surrounding space by lead linen 14, 15. In addition, the crystal holder comprises also rubber gaskets 16, 17, and 18, screws 19 serving to secure glass cylinder 12 with rod 20 serving to supply the high-frequency voltage, and disc 21 serving to attach the glass cylinder. The oil is cooled by tubular cooler 24, and vessel 2 is made hermetic by gaskets 23.

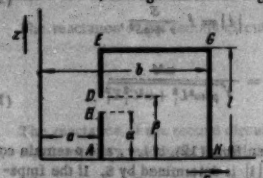

Fig. 8. Simplified diagram of crystal holder.

The device is connected to a closed cooling system with thermostat and circulating pump; a 17% solution of alcohol in water is used as a coolant.

b) Effect of varying certain crystal holder dimensions on the stray capacitance of the crystal holder.

A simplified diagram of the crystal holder is shown in Fig. 8 (compare with Fig. 7).

If we assume that the lower part of the holder has a potential +1, and the upper one a potential 0, then the potential U between the holder, the metal disc, and the bolts satisfies the following boundary conditions:

$$U = 1 \text{ on } AB, \text{ i. e., } r = a, \quad 0 \leqslant z \leqslant \alpha,$$
$$U = 0 \text{ on } DE, \text{ " } r = a, \quad \beta \leqslant z \leqslant l,$$
$$U = 0 \text{ on } EG, \text{ " } a \leqslant r \leqslant b, \quad z = l,$$
$$U = 0 \text{ on } GK, \text{ " } r = b, \quad 0 \leqslant z \leqslant l.$$

The potential between B and D depends primarily on the quartz. To simplify the calculations, we assume that the potential varies linearly, i. e.,

$$U = \frac{\beta - z}{\beta - \alpha} \text{ on } BD, \text{ i. e., if } r = a, \ \alpha \leqslant z \leqslant \beta.$$

TABLE 2

l, cm	a, cm	b, cm	s, cm	s − a, cm	C, μμf
6.65	3.0	8.0	2.79	0.64	6.17
5.00	3.0	8.0	2.79	0.64	6.35
6.00	2.25	6.11	2.79	0.64	5.25
6.00	2.25	7.64	2.79	0.64	4.90
6.00	2.25	9.16	2.79	0.64	4.69
6.65	2.25	6.06	2.79	0.64	5.30
6.65	2.25	7.50	2.79	0.64	5.00
6.65	2.25	8.50	2.79	0.64	4.85

Neglecting the capacitances caused by the rear sides of the bolts and of the cooling tubes, one can assume that points A and K lie on the same flux line, i. e.,

$$\frac{\partial U}{\partial z} = 0 \text{ on } AK, \text{ i. e., if } \quad 0 \leqslant r \leqslant b, \; z = 0.$$

Let us denote

$$\alpha' = \frac{2a}{\pi l}, \quad b' = \frac{2b}{\pi l}, \quad \alpha' = \frac{2a}{\pi l}, \quad \beta' = \frac{2\beta}{\pi l}.$$

The capacitance (in cm) of the lower part of the holder is determined from the following expression:

$$C = \frac{\varepsilon \varepsilon_0}{2} \left\{ \frac{4}{\pi(\beta' - \alpha')} \sum_{n=0}^{\infty} \frac{\cos(2n+1)\alpha' - \cos(2n+1)\beta'}{(2n+1)^3} \sin(2n+1) z_0 \times \right.$$
$$\left. \times \frac{T_0(b') B_1(\alpha') + B_0(b') T(\alpha')}{T_0(b') B_0(\alpha') - B_0(b') T_0(\alpha')} \right\}. \tag{15}$$

Here

$$T_0(X) = J_0(iX), \qquad B_0(X) = iH_0^{(1)}(iX),$$
$$T_1(X) = -iJ_1(iX), \qquad B_1(X) = -H_1^{(1)}(iX),$$

for oil $\varepsilon_0 = 2.2$.

Table 2 shows the calculated values of the capacitance for various values of l, a, and b.

It follows from the results that small changes in the values of l and b do not influence the capacitance greatly.

LITERATURE CITED

[1] L. Bergmann, Der Ultraschall und seine Anwendung Wissenschaft und Technik (1954).

Received March 21, 1955

Institute of Microbiology, Academy of Sciences of the Latvian SSR, Riga.

SECONDARY FIELD IN STEREOPHONIC TWIN-CHANNEL TRANSMISSION AND CERTAIN FIXED POSITIONS OF THE SOURCE OF SOUND IN THE PRIMARY FIELD

P. G. Tager

The article reports on a theoretical investigation devoted to the study of the two most important parameters of the secondary sound field, affecting the stereophonic effect: the differences in energy levels perceived by the listener from both loudspeakers, and the differences in the perception times of the signals from these loudspeakers. The effect of various factors in twin-channel electro-acoustic system on the stereophonic effect was investigated; it was shown that the sound engineer can always produce a good stereophonic effect in the secondary sound field by skillfully employing several of these factors during the recording and re-recording.

In binaural perception in open air, the listener receives in the acoustic field two signals from each source of sound. The difference in perception time of these two signals – received by the right and left ear, respectively – is always less than a millisecond, and the difference in perception levels, even if the source of sound is merely 3 m from the listener, is already less than 1 decibel. If an electroacoustic consisting of n channels connects the primary and secondary sound fields, the listener in the secondary sound field (disregarding the reverberations in both rooms) receives $2n$ signals from each source of sound in the primary sound field. The listener first perceives two binaural signals from one of the loudspeakers, both signals being shifted from each other by a maximum of several tenths of a millisecond and differ in level from each other by a maximum of several tenths of a decibel. The listener will then receive after some time (ranging in practice from 0 to several tenths of a millisecond), and not at all simultaneously, the remaining $(2n-2)$-paired interconnected sound signals; the differences between these signals and the first pair of the binaural signals may differ in practice from zero to tens of decibels, depending on the distance between the source of sound and the microphones and the distances between the microphones, furthermore on the position of the listener with respect to the loudspeakers and on the distances between the speakers. Such a system of multi-channel sound transmission is customarily called stereophonic. Thus, the perception conditions in stereophonic transmission differ radically from direct binaural perception of one or several (moving or stationary) sources of sound in the primary acoustic field.

Let one sound source A and two microphones M_1 and M_2 be located in the primary sound field (Fig. 1). N_1 and N_2 denote here the directions for which the directivity of the microphones makes their sensitivity a maximum. We shall also assume that the maximum energy density of the directional sound source A is in the N_A direction. Let us introduce the symbols

$$m = m_2 - m_1; \quad \mu = m_2 / m_1. \tag{1}$$

Loudspeakers P_1 and P_2 are located in the secondary sound field (Fig. 2) and produce a maximum sound-energy density in the directions D_1 and D_2. Each loudspeaker is connected to the corresponding microphone by an individual channel. Let us investigate the sound field at any point S having coordinates x and y.

Let us study the two parameters of the secondary sound field. First, we shall investigate the ratio of the sound energies of each pair of binaural signals, perceived by the listener S from loudspeakers P_1 and P_2, respectively (neglecting the distances between the listener's ears). Second, we investigate the time difference at

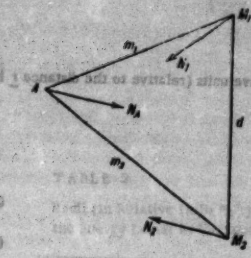

Fig. 1. Sound source A and microphones M_1 and M_2 in the primary sound field.

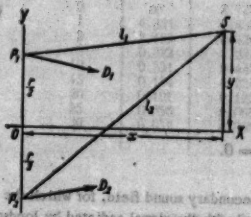

Fig. 2. Listener S and loudspeakers P_1 and P_2 in the secondary sound field.

which the listener perceives each pair of binaural signals, arriving from loudspeakers P_1 and P_2, respectively, under the same conditions. Let us begin with the first task.

Denoting by Δ the ratio of the sound energies received by the listener S from both loudspeakers P_1 and P_2, i. e.,

$$\Delta = \frac{\epsilon_1}{\epsilon_2}, \tag{2}$$

where ϵ_1 and ϵ_2 are the sound energies received by the listener S from each of the loudspeakers P_1 and P_2. If this ratio is expressed in decibels, evidently the difference in energy levels perceived by the listener from loudspeakers P_1 and P_2, respectively, will be $\delta = 10\log\Delta$.

Omitting intermediate calculations, we can write Expression (2) in the following form

$$\beta^2\mu^2\frac{l_2^2}{l_1^2} = \Delta, \tag{3}$$

where

$$\beta^2 = \frac{\varkappa_1\gamma_1\varkappa'_P\varkappa'_M k_1^2\varkappa'_A}{\varkappa_2\gamma_2\varkappa''_P\varkappa''_M k_2^2\varkappa''_A}. \tag{4}$$

Let us call the dimensionless quantity $\beta\mu$ the twin-channel stereophonic-transmission factor. All the coefficients in the right half of Eq. (4) may be functions of frequency. The factor β^2 (or β) can assume any value, provided it is positive, or may be equal to zero. In the case when the sound source A has no directivity ($\varkappa'_A = \varkappa''_A = 1$), the microphones M_1 and M_2 are also nondirectional ($k_1 = k_2 = 1$), both microphones are structurally identical ($\varkappa'_M = \varkappa''_M$), and if furthermore both communication channels between the primary and secondary sound fields have the same gain coefficients ($\gamma_1 = \gamma_2$), loudspeakers P_1 and P_2 are structurally identical ($\varkappa'_P = \varkappa''_P$) and are nondirectional ($\varkappa_1 = \varkappa_2 = 1$), we have

$$\beta = 1. \tag{5}$$

Transforming Eq. (3) we get

$$x^2 + \left(y - \frac{\Delta + \beta^2\mu^2}{\Delta - \beta^2\mu^2}\cdot\frac{r}{2}\right)^2 - \frac{\beta^2\mu^2\Delta}{(\Delta - \beta^2\mu^2)^2}r^2 = 0. \tag{6}$$

Equation (6) represents the geometric locus of the points in the secondary sound field, at which the ratio of the sound energies, received by listener S, have a specified value Δ. This is an equation of a family of nonintersecting circles, the centers of which are located on the ordinate axis at distances from the origin

$$y_0 = \frac{\Delta + \beta^2\mu^2}{\Delta - \beta^2\mu^2}\cdot\frac{r}{2}. \tag{7}$$

The radii of these circles are

$$R_0 = \left| \frac{\beta\mu}{\Delta - \beta^2\mu^2} \sqrt{\Delta}\, r \right|. \tag{8}$$

To make the results more general, it is advisable to employ relative units (relative to the distance r between loudspeakers). In that case Expressions (6), (7), and (8) become

$$\left(\frac{x}{r}\right)^2 + \left(\frac{y}{r} - \frac{y_0}{r}\right)^2 = \left(\frac{R_0}{r}\right)^2, \tag{9}$$

$$\frac{y_0}{r} = \frac{\Delta + \beta^2\mu^2}{2(\Delta - \beta^2\mu^2)}, \tag{10}$$

$$\frac{R_0}{r} = \left| \frac{\beta\mu\sqrt{\Delta}}{\Delta - \beta^2\mu^2} \right|. \tag{11}$$

Let us proceed now to calculate the effect of the time difference at which listener S receives sound signals from loudspeakers P_1 and P_2, respectively. It is clear from Figs. 1 and 2 that the delay time is

$$t = \frac{m + l_2 - l_1}{c}, \tag{12}$$

where $c = {}^1/_3$ m/millisecond is the velocity of sound.

Upon transformation, Eq. (12) can be written as

$$x^2 - \frac{r^2 - (ct - m)^2}{(ct - m)^2}\, y^2 + \frac{r^2 - (ct - m)^2}{4} = 0. \tag{13}$$

Equation (13) represents the geometric locus of the points in the secondary sound field, for which the signal radiated by loudspeaker P_2 is delayed by a specified time t compared with the signal radiated by loudspeaker P_1. The time delay t ranges from $(m - r)/c$ to $(m + r)/c$.

In this case Eq. (13) is the equation of a family of nonintersecting hyperbolas. It is more convenient to write down Eq. (13) so as to use relative units, namely

TABLE 1

Ordinates (in Relative Units y_0/r) of the Centers of the Circles that Represent Equal-Difference Curves for the Energy Levels in the Secondary Sound Field

Energy-level difference δ, db	Twin-channel stereophonic-transmission factor βμ					
	1	1.2	1.5	2	3	5
0	∞	−2.773	−1.300	−0.833	−0.625	−0.542
1	4.362	−7.451	−1.770	−0.959	−0.662	−0.553
2	2.210	10.438	−2.883	−1.156	−0.714	−0.568
5	0.962	1.336	2.966	−4.275	−1.042	−0.645
10	0.611	0.668	0.790	1.167	9.500	−1.167
15	0.533	0.548	0.577	0.645	0.898	4.275
20	0.510	0.515	0.523	0.542	0.599	0.833
25	0.503	0.505	0.507	0.513	0.529	0.586
30	0.501	0.501	0.502	0.504	0.509	0.526

$$\left(\frac{x}{r}\right)^2 - \frac{1-\tau^2}{\tau^2}\left(\frac{y}{r}\right)^2 + \frac{1-\tau^2}{4} = 0, \tag{14}$$

where

$$\tau = \frac{ct-m}{p}. \tag{15}$$

TABLE 2

Radii (in Relative Units R_0/r) of Circles Representing Equal-Difference Curves For the Energy Levels in the Secondary Sound Field

Energy-level difference δ_{+1}, db	Twin-channel stereophonic-transmission factor $\beta\mu$					
	1	1.2	1.5	2	3	5
0	∞	2.727	1.200	0.667	0.375	0.208
1	4.334	7.435	1.698	0.819	0.435	0.236
2	2.152	10.426	2.839	1.042	0.509	0.269
5	0.822	1.239	2.924	4.246	0.914	0.407
10	0.351	0.443	0.612	1.054	9.487	1.054
15	0.184	0.224	0.87	0.407	0.746	4.245
20	0.101	0.122	0.153	0.208	0.330	0.667
25	0.056	0.068	0.085	0.114	0.174	0.305
30	0.032	0.038	0.048	0.064	0.096	0.162

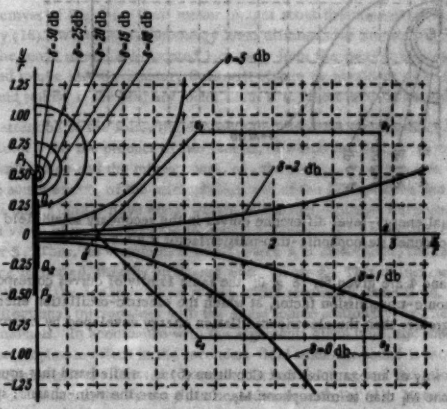

Fig. 3. Equal sound-level difference curves in the secondary sound field for a twin-channel stereophonic-transmission factor $\beta\mu = 1.2$.

We shall call the dimensionless quantity τ the delay factor; its possible numerical values range from -1 to $+1$. Let us note that it follows from (15) and (12) that $\tau = \frac{l_2 - l_1}{r}$.

Let us analyze our results briefly. Tables 1 and 2 give the numerical values of the ratios $\frac{Y_0}{r}$ and $\frac{R_0}{r}$, calculated from Eqs. (10) and (11). Figures 3 and 4 are graphic interpretations of some of the results given in Tables 1 and 2. As before, P_1 and P_2 denote the loudspeakers.

Inasmuch as stereophonic sound transmission is of great significance in motion pictures, Figs. 3 and 4 show also a conventional screen Q_1Q_2, as well as a wide screen P_1P_2. If we assume for a wide screen angular dimensions of 20 × 40° (from the seats with the best view), we get $P_1P_2 = 1.74\ Q_1Q_2$. In Figs. 3 and 4 loudspeakers P_1 and P_2 are located exactly on the vertical boundaries of the wide screen. The boundaries of the seats in the motion picture theater are denoted by $ac_1c_2c_3$. Here we assume $Oe = Q_1Q_2/5 = P_1P_2/2.87$ and $e_1e_2 = 0.6\ Oe$. The boundaries ac_1 and ac_2 of the seats are so chosen in Figs. 3 and 4 to make any portion of the wide screen visible at an angle not exceeding 45° (the insignificant number of seats that are close to the screen near the point a should be discarded.

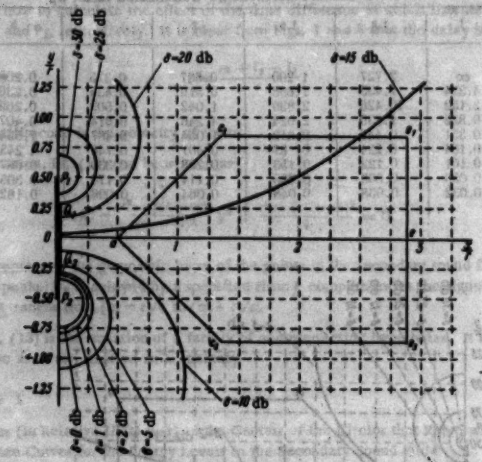

Fig. 4. Equal energy-level difference curves in the secondary sound field for a twin-channel stereophonic-transmission factor $B\mu = 5$.

The curves on Figs. 3 and 4 are given for $\delta \geq 0$; the same family of curves corresponds to those values of the twin-channel stereophonic-transmission factor, at which the electric-oscillation energy developed by the microphone M_1 is equal to greater than the electric-oscillation energy developed by microphone M_2, i. e., when $B\mu \geq 1$.

Let us first assume, by way of an example, that Condition (5) is satisfied and that sound source A in Fig. 1 is 5 times closer to microphone M_1 than to microphone M_2. In this case the twin-channel stereophonic-transmisstion factor is $B\mu = 5$ and the curves on Fig. 4 give the energy distribution in the secondary sound field. We see first of all that in all seats of the theater the sound energy coming from loudspeaker P_1 is considerably greater than the sound energy coming from loudspeaker P_2. This difference in energy level may range from 11 to 19 decibels, over the seat location, depending on the seat position. Based on Jordan's experimental investigations

[1], one can assume approximately that if the energy-level difference is 30 db, the apparent sound source in the secondary field is localized at the louder loudspeaker; if the energy-level difference is decreased, the apparent sound source is displaced in an approximately linear manner to an intermediate position between the loudspeakers. Thus, all the listeners located within the seating zone, will localize the apparent sound source in the right half OP_1 of the screen, but at somewhat different positions, depending on the position of the seats in the theater.

If the sound source A in Fig. 1 moves and occupies a position that is symmetrical with respect to microphones M_1 and M_2, the twin-channel stereophonic-transmission factor, taking (5) into account, will be $\beta\mu = 1$. In this case the energy distribution in the secondary sound field will correspond to the curves determined by the second columns to the left in Tables 1 and 2; for listeners located exactly on the symmetry axis ae, the energy-level difference is zero. It is clear that these listeners will localize the apparent sound source at the center O of the screen, as indeed is necessary. The listeners located in the zone ac_1e_1e, depending on their position, will receive the sound energy from loudspeaker P_1 at a level of 0-3 db higher than from loudspeaker P_2; these listeners will localize the apparent sound source very near the center O of the screen, but nevertheless in its right half OP_1.

For intermediate positions of sound source A in the primary sound field, corresponding to intermediate values of $\beta\mu$, the energy distribution will be that given by Tables 1 and 2, and particularly by the curves of Figs. 3 and 4. It is clear from these data that as the numerical value of the twin-channel stereophonic-transmission factor is decreased, the apparent sound source shifts gradually to the left for listeners located within the viewing zone, as indeed is necessary.

It becomes quite evident from the above that to obtain stereophonic effect in the secondary sound field in the case of twin-channel transmission with the aid of loudspeakers (eliminating separation), it is necessary to move the microphones in the primary sound field. In fact, assume that the microphones M_1 and M_2 in the primary sound field (Fig. 1) are placed 0.2 m apart. If sound source A occupies any position, but not less than 1 m from the nearest microphone, the twin-channel stereophonic-transmission factor may assume only the values determined from the following inequality

$$1{,}2 \geqslant \beta\mu \geqslant 0{,}833. \qquad (16)$$

In this case the curves of Fig. 3 (or their mirror images about the abscissa) correspond to the limiting value of this inequality (16). We see that the energy level difference in the seating zone does not exceed approximately 4.5 db (when the sound source A is located 1 m away from the nearest microphone). In practice, therefore, the apparent sound source in the secondary field will always be localized near the center of the screen for any position of the sound source in the primary sound field, i. e., there will be no stereophonic effect.

Let us now turn attention to the following exceedingly important circumstance. The twin-channel stereophonic-transmission factor $\mu\beta$ is the product of two factors, of which the first, μ, is from (1) the ratio of the distances between the sound source and the microphones, and the second, β, depends in accordance with (4) on the directivities of the sound source, of the microphones, and of the loudspeakers and on the gain in the sound channels. Inasmuch as both β and μ have equal weight in the twin-channel stereophonic-transmission factor, then, using some fixed value of μ, it is possible to obtain a stereophonic effect in the secondary sound field by varying only the factor β. Thus, for example, if sound source A is directional, the ratio K'_λ/K''_λ of Eq. (4) will vary as the sound source is rotated, thereby producing a change in β. This in turn, will be accompanied by a change in the localization of the apparent sound source in the secondary sound field. Such an effect can be obtained by rotating directional microphones with the sound source stationary, or else by varying the gain coefficients in the sound channels. In accordance with the arguments given here, the sound engineer can therefore always obtain a good stereophonic effect in the secondary field when the sound is recorded or re-recorded by cleverly changing simultaneously the distances between the sound source and the microphones as well as one or several coefficients contained in the factor β, in accordance with Eq. (4). Naturally, each portion of the primary sound field requires a suitable preliminary calculation.

Table 3 gives the numerical values of the coefficients $\frac{1-\tau^2}{\tau^2}$ and $\frac{1-\tau^2}{4}$ in Eq. (14) for the hyperbolas. It is seen from Fig. 5 that the delay factor for the entire seating zone ranges from $-0{,}5$ to $+0{,}5$. De-Boer

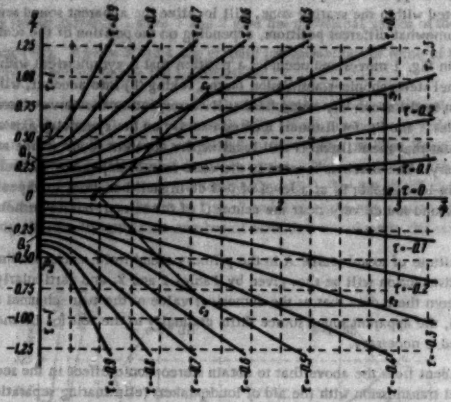

Fig. 5. Curves of equal values of delay factor in the secondary sound field.

TABLE 3

Coefficients $\frac{1-\tau^2}{\tau^2}$ and $\frac{1-\tau^2}{4}$ in Eq. (14) for the Hyperbolas, Which Serve as Curves of Equal Values of the Delay Factor τ in the Secondary Sound Field

Delay factor, τ	Coefficients $\frac{1-\tau^2}{\tau^2}$	$\frac{1-\tau^2}{4}$
0	∞	0.250
±0.1	99.000	0.248
±0.2	24.000	0.240
±0.3	10.111	0.228
±0.4	5.250	0.210
±0.5	3.000	0.188
±0.6	1.778	0.160
±0.7	1.041	0.128
±0.8	0.562	0.090
±0.9	0.235	0.048
±1.0	0.000	0.000

found on the basis of his experimental investigations that the localization of the apparent sound source in the secondary field is equally affected by a five-fold delay time $\underline{t}$ (in milliseconds) as by an energy level difference δ (in decibels); here both factors affect the localization in an additive manner [2]. If, for example, we assume m_1 = = 2 m, m_2 = 10 m, r = 10 m, and take (15) into account, the delay time for the entire seating zone will range from 9 to 39 milliseconds. The delay time will contribute to a reinforcement of the stereophonic effect in the secondary sound field, but it contributes much less to the production of the stereophonic effect than the difference in energy levels. Thus, to improve the stereophonic-transmission effect of one moving sound source it is necessary to strive to obtain a higher ratio of the twin-channel stereophonic-transmission factors, calculated for the extreme positions of the sound source. Analogously, to improve the stereophonic-transmission effect of several stationary sound sources, it is also necessary to obtain a higher ratio of twin-channel stereophonic-transmission factors, calculated for the two sound sources that are furthest apart.

The graphs of Figs. 3 and 4 are plotted in relative units. This means, that from the point of view of the difference in energy levels as received by the listener from the two loudspeakers the stereophonic effect, which is most sensitive to this energy difference, will be the same in all geometrically-similar theater halls, from the very smallest to the very largest.

The curves of Figs. 3-5 pass approximately along the seating zone; therefore the listenem both nearest and farthest to the screen will localize the movement of the apparent sound source approximately between the

same points on the screen; however, the angular displacement of the apparent sound source will be greater for listeners sitting closer to the screen than for those seating further away. For this reason, the stereophonic effect will be worse in the seating zone that is furthest from the screen than for that portion of the zone located closer to the screen.

Although the above method of studying the secondary sound field should be further extended to include any position of one or several sound sources in the primary sound field and to include a multi-channel system of interconnecting the primary and secondary sound fields, nevertheless the above investigation makes it possible to establish the basic laws of stereophonic transmission.

LITERATURE CITED

[1] V. L. Jordan, "A system for stereophonic reproduction," Acustica 4, 1, 38-38 (1954).

[2] R. Vermeulen, "Stereophonic reproduction," Audio 38, 4, April, 21 and 57 (1954).

Received March 19, 1955

All-Union Scientific-Research Motion-Picture Photography Institute, Moscow

CHRONICLE

CONFERENCE ON ELECTROACOUSTICS

Kiev, July 1-5, 1955

A conference on electroacoustics, organized by the Commission on Acoustics, was held in Kiev from the first through the fifth of July 1955. This conference was organized by the Commission on Acoustics, by the Acoustics Institute of the USSR Academy of Sciences, and by the Kiev Order of Lenin Polytechnic Institute.

Participating in this conference were up to 200 scientific and engineering workers in the field of electroacoustics, sound motion pictures, sound recording and other fields of science related to acoustics from Kiev, Moscow, Leningrad, Riga, and other cities.

Brief Summaries of the Papers Delivered at the Conference

A. G. Al'mukhamedov. Pulse Method of Measuring Irregularities in the Movement of the Sound Track (Kiev Polytechnic Institute).

Short pulses are recorded on a magnetic tape and are then reproduced with a delay equal to the time required for the track to cover the distance between the gaps of the recording and reproducing heads. Fluctuations in the delay time, which are proportional to the fluctuations in the speed of the track, are measured with the aid of an electronic oscilloscope.

M. S. Antsyferov. Electrodynamic Vibrometers for the Audio Range (Geophysics Institute, USSR Academy of Sciences).

Vibrometers were developed for frequency ranges up to 200 cycles and up to 5000 cycles. The basic structural distinguishing feature is the use of a housing serving as magnetic yoke made of Armco steel with an internal permanent magnet (core) made of "Magnico" alloy. With an output impedance of 200-300 ohms, the velocity sensitivity of the instruments are 1 and 0.1 v/cm/sec, respectively. The instruments weigh 6 and 1 kg, respectively.

B. G. Belkin. New Generator for Acoustic Measurements (Scientific Research Motion Picture Photography Institute).

To obtain a noise signal having a constant spectral density within a certain frequency band, "white" noise was recorded on a photographic sound film. By varying the speed of the sound film, the recorded band can be smoothly transposed over the entire range of interest.

L. M. Brekhovskikh. Present-Day Status of the Theory of Propagation of Sound Waves (Acoustics Institute, USSR Academy of Sciences).

A survey of the more significant advances in the theory of propagation of sound waves during the past 10-15 years, and a formulation of the principal problems that need to be considered in the immediate future.

A. F. Veklenko. Audibility of Intermodulation Distortion (Scientific Research Motion Picture Photography Institute).

Investigation of the effect of the height of the lowest tone, the height of the highest tone, and of the absolute value of the distortion level on the absolute and differential discrimination threshold.

G. S. Veksler. Certain Problems in Present-Day Techniques of Magnetic Recording (Kiev Polytechnic Institute).

By refining the procedure for selecting the optimum magnetic parameters of the sound track, the author considers it advantageous to estimate the quality of the magnetic-dielectric tapes from their magnetic indices, and not from their electroacoustic indices, as is done at the present time. An instrument was developed to determine rapidly the magnetic parameters of tapes, wires, and powders.

N. F. Vollemer. Instrumental Spectral Analysis (Kiev Polytechnic Institute).

Bringing out the fine points of the distinction between the mathematical determination of the spectral-analysis process and the possibility of its approximate realization in actual measuring instruments, the optimum types and parameters of analyzers are determined. Spectrometers covering the infrasonic, sonic, and ultrasonic bands have been constructed on the basis of this investigation.

V. M. Vol'f. Concerning Nonlinear Conversions of Oscillations of Complex Waveform (Kiev Polytechnic Institute).

An analytic investigation was made of the nonlinearity products obtained at the output of quadratic and cubic nonlinear systems in response to periodically-repeated input pulses of triangular, sawtooth, rectangular, exponential, and bell-shaped form.

E. M. Gardash'ian and A. N. Kacherovich. Automatic Recording Instrument for Measuring Several Acoustic Parameters of Rooms (Scientific Research Motion Picture Photography Institute).

The instrument consists of a logarithmic amplifier and high-speed level recorder producing an inked record. The speed of the paper is 10 mm/sec, the dynamic range is 60 db, the speed of recording up to 300 db/sec. The instrument is provided with a system of octave filters for the 100-200, 200-400, 300-600, 600-1200, and 2400-4800 cycle bands. Prolonged tests of the instrument under operating conditions have confirmed that it is suitable for the investigation of acoustic properties of rooms.

S. G. Genhman and E. L. Feinberg. Instrument to Measure the Correlation Coefficient of Stationary Noises (Acoustics Institute, USSR Academy of Sciences, and P. N. Lebedev Physics Institute of the USSR Academy of Sciences).

The instrument is based on measuring the average output current, proportional to the probable coincidence (or noncoincidence) of the signs of the instantaneous values of two noises, the correlation of which is being determined. The operating theory of the instruments yields a connection between the correlation coefficient and the measured average value of the output current for noises having normal distribution, and also for certain other cases. The instrument can be used to detect weak signals when the noise level exceeds the signal, and also to measure small signal ratios (or small noise ratios).

M. I. Kamovskii. Frequency Characteristic of Certain Distributed Systems of Coherent Radiators (Kiev Polytechnic Institute).

If coherently-operating radiators are placed at distances comparable with the wavelength, the radiation impedance of the radiator in the group may differ substantially from the radiation resistance of a single radiator. This circumstance makes it possible to increase the low frequency output using radiators of small sizes to equip rooms or open spaces with distributed systems. The active component is calculated for various groups of radiators.

M. V. Laufer. Investigation of Methods for Measuring Irregularities in the Motion of Sound Tracks (Kiev Polytechnic Institute).

Considering that existing integral and spectral methods do not make it possible to investigate in detail speed fluctuations inherent in sound-recording apparatus, the author proposes the use of the phase-detector method for this purpose. Here a signal of specified frequency is recorded by the elements that are displaced along the path of the track. Upon limitation, the amplified signals are applied to the input of the phase detector; the amplitude of the output signal is proportional here to the irregularity coefficient, and the frequency is proportional to the frequency of speed fluctuation.

R. G. Ofengenden. Magnetic Recording of Pulses (Institute of Physics, Ukraine SSR Academy of Sciences).

Investigation of the time characteristics of reproducing heads of two types, making it possible to determine the resolution of a system using contact-making and contactless recording of magnetic pulses.

A. V. Rimskii-Korsakov. Investigation of Audibility of Nonlinear Distortion in the Transmission of Music and Speech over an Electroacoustic Channel (Leningrad Electrotechnic Communication Institute).

Considering that speech and music can be looked upon as a random fluctuating process, the probability that the intensity of the distortion products in the critical range of hearing would be greater than the threshold intensity is determined, taking into account the fact that the audibility threshold is determined by the masking caused by the fundamental (undistorted) signal, and also by the noise interference at the hearing location.

S. M. Rytov. Acoustic Properties of Finely-Laminated Medium (P. N. Lebedev Physics Institute, USSR Academy of Sciences).

A medium consisting of alternating layers of two isotropic solids, thin compared with the propagated wavelength, can be considered on the average to be a homogeneous but anisotropic substance with an anisotropy, corresponding to a crystal of hexagonal symmetry. Expressions are obtained for the effective constants of such a "crystal" as a function of the constants of both substances and of the thickness of the layers. Five sound propagation velocities are calculated as functions of the same parameters, three for the shear waves and two for the compression waves.

B. D. Tartakovskii. Public Adress Systems in Open Spaces Using Distributed Loudspeaker Systems (Experience in Installing Public Address Systems in the All-Union Agricultural Fair) (Acoustics Institute, USSR Academy of Sciences).

A distributed system using specially-developed DGR-25 loudspeakers, suspended at a height of 3.5 to 8 m and 20 to 32 meters apart, was used. The deviation in the sound field along the avenues did not exceed 4 db. No echoes were heard from either speakers in the same string, or from speakers in neighboring strings. The loudspeakers were combined structurally with the lamps. The loudspeakers were fed by underground cables. Tests of the system confirmed on one hand the theoretical calculations, and demonstrated on the other hand, the high quality of distributed sound-reproduction systems.

I. E. El'piner. On the Mechanism of the Biological Action of Ultrasonic Waves. (Institute of Biological Physics, USSR, Academy of Sciences).

Ultrasonic waves, by causing instantaneous breakdown of vegetable and animal cells, contribute to the separation of biologically-active substances, such as ferments, vitamins, hormones, etc. In some cases, ferments believed absent from certain cells were detected. The increased yield of vitamins extracted from sounded cells is evidence of the effect of ultrasonic waves on intracellular biologically-active molecular complexes. This circumstance makes the use of ultrasonics exceedingly promising for the study of various aspects of the living action of cells.

A resolution adopted at the end of the conference reflected the principal problems discussed after the presentation of the papers.

SECOND INTERNATIONAL ACOUSTICAL CONGRESS

The second international congress on acoustics will be held on June 17 through 24, 1956.

The first international congress was held in Delft, Holland, in June 1953. It was attended by more than 300 scientific and engineering workers in acoustics from 22 countries. The congress was devoted to problems in electroacoustics, including sound recording, radio-broadcasting apparatus, methods of acoustical measurements, audiometry, and hearing apparatus, and ultrasonic and musical acoustics. 84 papers, including 7 survey articles,

were read at the sessions. The surveys listed the results of the developments in the various branches of acoustics, and formulated new pending problems.

The second Acoustic congress will be devoted to physical and biological acoustics. Particular attention will be paid to the problems of the interrelationship between branches of acoustics, as well as to practical applications.

International acoustic congresses are organized once every three years by the International Acoustic Commission, which is one of the specialized UNESCO commissions. Invited to organize the second congress was the American Acoustical Society, which offered to hold the Congress jointly with the regular convention of the Society. The congress will be held in Cambridge, which is an important acoustical center in the USA.

SURVEY OF METHODS FOR EVALUATING AND MEASURING THE DIFFUSENESS OF A SOUND FIELD

V. V. Furduev

The problem of methods for the quantitative evaluation and measurement of the diffuseness of a sound field in closed rooms (in particular, in radio-broadcasting and recording studios) is not a new one; in the acoustics literature of the last five years we find a large number of papers (both theoretical and experimental) devoted to the determination and measurement of various quantities which quantitatively characterize the degree of sound-field diffuseness. The attempts at a quantitative evaluation of diffuseness are dictated, as we see it, by the following concepts. In the first place the formulas of classic reverberation theory are based, as we know, upon the assumption of the complete diffuseness of the sound field in a closed room; therefore the evaluation of the degree of diffuseness must yield the criteria which determine the usefulness of these formulas that are widely used in engineering practice. In the second place, it has been established by purely experimental means that the application of sound scattering structures (and, generally speaking, any more or less considerable violation of proper geometric shapes) leads to an appreciable improvement in the acoustic properties of a room for the same (or for an insignificantly changed) reverberation time. Since such measures are directed toward raising the degree of diffuseness of the sound field, the thought arises that the acoustic quality of a room must be determined not only by the reverberation time but also by a new characteristic quantity which is associated with the degree of diffuseness of the field. The proposed survey of papers which have been published up to this time has as its purpose the preparation for a proper judgment concerning the entire complex of problems which are associated with the determination and measurement of diffuseness, and the charting of paths for the further investigation of these problems.

Statistics of Intrinsic Vibrations

Certain concepts which lead to a quantitative evaluation of field diffuseness in a closed volume were advanced by R. Bolt [1] on the basis of investigating the statistical characteristics of the intrinsic frequency spectrum of that volume and the intensity of the exciting factors in it. The original thought consists of the fact that in volumes having a correct geometric shape (spheres, cubes, parallelepipeds etc.) a so-called degeneration of the spectrum is observed; certain various types of intrinsic vibrations coincide in frequency. Under these conditions the spectrum density of the intrinsic frequencies diminishes, and definite directions of the wave

vector became noticeably predominant. As a criterion which characterizes the decrease of diffuseness as a consequence of degeneration, Bolt proposed the quantity

$$\Psi = \frac{\frac{1}{N}\sum(\delta f)^2}{\left(\frac{1}{N}\sum\delta f\right)^2} = \frac{N}{(\Delta f)^2}\sum(\delta f)^2, \qquad (1)$$

where δf is the interval between adjacent intrinsic frequencies in the band $\Delta f = \sum\delta f$, N is the number of intrinsic frequencies in this band. It can easily be seen that in the case of an equidistant spectrum, $\delta f = \frac{\Delta f}{N}$ and $\psi = 1$; of coune, this case is of no interest in architectural acoustics. If the intervals δf are encountered with a probability which is proportional to $e^{-\frac{\delta f}{\overline{\delta f}}}$, where $\overline{\delta f}$ is the mean value of the interval δf, then (as can easily be calculated) $\psi = 2$; this value corresponds to a statistically random distribution of intrinsic frequencies. When degeneration of one or another multiple frequency is present, the intervals increase and ψ increases also; thus the degree to which the parameter ψ approaches the value 2 can serve as a measure of diffuseness.

However along with the quantity ψ it is necessary to introduce still another parameter which characterizes the statistics of the excitations that give rise to the various intrinsic vibrations. In experiments with a closed volume a source of sinusoidal waves excited forced vibrations in a number of resonators so that the amplitudes of these vibrations depended upon the degree to which the resonators were detuned with respect to the excitation frequency. The distribution of the amplitudes is associated with the sharpness of the corresponding resonant characteristics; in other words, it is associated with the attenuation of the resonators. But under one or another set of special excitation conditions certain resonators may not be excited at all. If this is the case (here again we are dealing with the case of degeneration), and if in addition the attenuation is not so great that the excitation of resonators which are greatly detuned proves comparable with the excitation of resonators which are only slightly detuned, then the field forfeits its diffuse character. In order to take this side of the process into account Bolt introduces a second statistical parameter:

$$\Phi = \frac{\frac{1}{N}\sum a^2}{\left(\frac{1}{N}\sum a\right)^2}, \qquad (2)$$

where a is a quantity which determines the amplitude of the forced vibrations of the resonators (the total number of resonators is equal to N). The excitation parameter Φ (as well as the interval parameter ψ) increases when degeneration is present (i.e., when the diffuseness of the field is violated in some manner). Computation shows that for volumes which have a completely improper shape (when the energy distribution of the resonators is Gaussian) it must be true that $\Phi = \frac{\pi}{2} = 1.57$. The degree to which Φ approaches this value can be viewed as a measure of the diffuseness of the field.

Some interesting experimental results are given in a recently published paper by M. Schröder [2]; these results provide a clear answer to the problem of how the geometric symmetry of the resonating volume must be violated to make the values of the parameters ψ and Φ correspond to the case of volumes which have a completely improper shape. The experiments were carried out on simulators: electromagnetic oscillations were investigated in hollow metallic resonators, and this made it possible to guarantee a high resolving power for the analysis. It can be shown that a resonator with a volume V and a surface S has a figure-of-merit $Q \approx \frac{V}{Sd}$, where d is the thickness of the layer through which the electromagnetic energy penetrates; for centimeter waves which are selected according to the concepts governing the simplification of the experimental

procedure, $d \approx 10^{-4}$ cm and the figure-of-merit is several tens of thousands. This makes it possible to reliably separate the resonant frequencies from one another and to determine the parameters ψ and ϕ with a small error. Schröder's measurements yielded an unexpected result. It proved true that degenerations which increased the interval parameter ψ were completely eliminated by a very insignificant violation of geometric symmetry. For example, for a cube 20cm on a side, $\psi = 28$, but if one of the sides if decreased by 1mm, then ψ is lowered to 2.4, i.e., the distribution of the intervals approximated a purely random distribution. An investigation of the excitation statistics showed, for example, that a case which is known to be degenerative - the excitation of a rectangular resonator in the middle of one of its boundaries (here only one-fourth of all of the intrinsic vibrations are excited) - became a normal case of the diffuse mixing of all the possible intrinsic vibrations if a body with a volume of the order of a cube whose side equalled a wavelength was introduced into the interior of the resonator (irrespective of the volume of the resonator, of its shape and of the disposition of the disturbing body). Schröder's results made it possible to come to the definite conclusion that, as far as room acoustics is concerned, the statistical parameters used by Bolt are not of practical interest. The inescapable deviations from a proper geometric shape and the inescapable presence of disturbing bodies of dimensions which are comparable to a wavelength in the rooms must necessarily lead to the complete diffuseness of the field when this diffuseness is evaluated on the basis of Bolt's criteria. Complete diffuseness is determined by the following condition when it is examined in this special sense: a source which emits a sinusoidal tone and which is located at any place in the room excites a very large number of resonators in such a manner that the distribution of their intrinsic frequencies and absorbed energies is random.

Frequency Irregularity

As far back as 1935, E. Wente [3] thought to examine a closed room as an acoustical transmission channel with a definite frequency responce. Let a loudspeaker be located at some point in the room, and let that loudspeaker emit a constant power in the form of a sinusoidal tone with a slowly varying frequency; a logarithmic automatic recording pen which is coupled to an oscillator records the level of the sound pressure received by a microphone placed at another point in the room. When different pairs of points are selected for the location of the loudspeaker and the microphone, the details of the experimentally obtained characteristic will, of course, be different. However such statistical parameters as the average height of the peaks, the average interval between peaks (or the points of intersection with the median-level line) may not depend upon the selection of one or another pair of points.

The measurements performed by Wente showed, in particular, that in a certain band of frequencies

$$J = \Sigma P_{max} - \Sigma P_{min} = \bar{h}n, \tag{3}$$

where P_{max} and P_{min} are the maximum and minimum pressure levels in decibles, $\bar{h}$ is the average height of the peaks, n is their number in the band Δf, the nonuniformity of the transmission depends upon the average absorption coefficient in that band and decreases with an increase in their coefficient.

In discussing the results of the measurements obtained by Wente, R. Bolt and R. Roop [4] found it useful to refer the transmission nonuniformity to a unit frequency interval, since this nonuniformity was the more substantial, the narrower the frequency band in which it was measured. In fact, for a given nonuniformity the average height of the peaks, as can be seen from Formula (3), increases with a decrease in n (i.e., it increases to the degree that the band Δf narrows). The quantity

$$F = \frac{1}{\Delta f}(\Sigma P_{max} - \Sigma P_{min}) = \frac{\bar{h}n}{\Delta f} = \frac{\bar{h}}{\overline{\delta f}}, \tag{4}$$

where $\overline{\delta f} = \frac{\Delta f}{n}$ is the mean value of the interval between the peaks of the transmission frequency characteristic, has been given the name of frequency irregularity.

The theoretical and experimental investigation of frequency irregularity which was undertaken by Bolt and Roop led them to the conclusion that this quantity must depend not only upon the absorption but also the shape of the room. The latter dependence is such that in rooms which have an improper shape the frequency irregularity is less than in rectangular rooms of comparable volume. From this the conclusion was drawn that the frequency irregularity F is related to the degree of diffuseness of the field: the smaller the value of F, the greater the diffuseness of the sound field in the room. In evaluating this conclusion two facts should be kept in mind. In the first place, in making their theoretical analysis of frequency irregularity, Bolt and Roop assumed that the average interval δf between the peaks of the characteristics coincided with the average interval between the intrinsic frequencies of the room. In the second place, the experimental determination of F was performed in rooms having a comparatively small volume (less than 75 m^3); under these conditions the above-indicated decrease in the frequency irregularity of a room having an improper shape (V = 45 m^3) was detected only in the frequency range below 1000 cps. In the region of higher frequencies the shape of the room did not have a noticeable effect upon the magnitude of the frequency irregularity. It must be assumed that Bolt and Roop either did not notice the limited significance of their results or did not consider this limitation to be essential from a practical point of view.

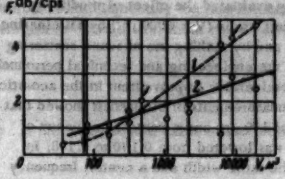

Fig. 1. Frequency irregularity in rooms having various volumes (the arrows indicate the points which refer to the acoustically defective rooms):

1) For a center frequency of 1650 cps.
2) for a center frequency of 375 cps.

Their proposed criterion of diffuseness was sympathetically received in engineering and technological circles. Using as a basis their successful experience in improving the acoustic qualities of radio-broadcasting studios by making use of semicylindrical scattering structures, W. Furrer and A. Lauber [5] undertook the measurement of frequency irregularity in rooms of various volumes (chiefly in radio-broadcasting studios); the volumes of the rooms investigated by them were within the limits of from 37 to 20,000 m^3 (the latter figure refers to a large Baroque-style church). The measurements were performed in two frequency bands (whose width is not indicated) having central frequencies of 375 and 1650 cps. The results of the measurements prompted the authors to propose another quantity in the capacity of a diffuseness characteristic; this quantity, although it is associated with frequency irregularity, is not identical to it. The fact is that the values of frequency irregularity which were measured by Furrer and Lauber as a function of room volume (Fig. 1) did not permit them to distinguish acoustically defective rooms from adequate ones on the basis of this index; the differences between defective and adequate rooms could not be analyzed in terms of the difference between the values of frequency irregularity. Starting from the idea that a large number of low peaks is an indication of "good" diffuseness, whereas a small number of high peaks, on the contrary, indicates the violation of field diffuseness, Furrer and Lauber selected the quantity

$$D = \frac{F}{n}, \qquad (5)$$

as the characteristic quantity; this is the quantity they proposed to call the diffuseness, although according to the reasoning of the authors this quantity decreases with an increase in the degree of diffuseness. It is evident that the quantity D is in essence a quantity which measures the average height of the peaks; in fact, comparing Formulas (4) and (5), we have

$$D = \frac{\bar{h}}{n\delta f} = \frac{\bar{h}}{\Delta f},$$

i.e., for a given frequency band width D is directly proportional to $\bar{h}$. Plotting the curves for the values of D in the bands with central frequencies of 375 and 1650 cps as a function of the volume of the investigated rooms (Fig. 2), Furrer and Lauber found that acoustically defective rooms differ from normal rooms in that their values of D are higher (i.e., their degree of diffuseness is less).

On the basis of the results of their investigations Furrer and Lauber came to the conclusion that the quantity D is a "new and evidently useful practical criterion of the homogeneity of a sound field and, by the same token, of the acoustical quality of a room". Such a conclusion led to the development of special (automatic) equipment for measuring the frequency irregularity [6, 7]. Making use of this equipment, Furrer and Lauber [6] quantitatively evaluated the effect of modifying the structure of a large concert studio (V = 5000 m³) by eliminating the smooth parallel surfaces and by making use of sound-scattering elements. In the opinion of the engineering and technical personnel this modification led to a considerable improvement in the acoustic quality of the studio. The measurements of diffuseness showed that in the band having a width of 100 cps and a central frequency of 425 cps the magnitude of D was lowered from 0.170 to 0.108; in addition, in a band having the same width and a central frequency of 1650 cps the value of D (which was close to 0.09) remained practically constant. The authors considered that this result was irrefutable proof of the concept that the quantity D is sensitive precisely to the shape of the room.

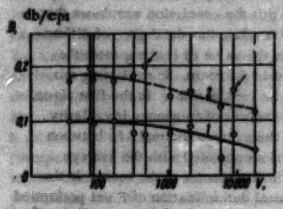

Fig. 2. Diffuseness of the field in rooms having various volumes:
1) For a center frequency of 1650 cps.
2) for a center frequency of 375 cps.

For the purposes of completing the list we shall note still another modification of frequency irregularity. By using simulators to investigate the effectiveness of scattering structures of various shapes, T. Sommerville and F. Ward [8] evaluated the effect of scattering according to its effect upon the quantity

$$L = l - l_0 \qquad (6)$$

where l is the total length of the transmission frequency characteristic in a certain frequency band, and l_0 is the distance between the boundary frequencies of this band as measured along the axis of abscissas. It is not difficult to see that this quantity, which has been called linear irregularity, is directly proportional to the transmission nonuniformity as measured according to Wente; the proportionality coefficient depends upon the scale of both axes of the frequency characteristic on which the values of l and l_0 are measured.

The value of the frequency irregularity as a criterion for the acoustic quality of rooms was placed in doubt in the paper by A. Nickson and R. Muncey [9] from a somewhat unexpected point of view.

Referring to the fact that music and sound consist not of sinusoidal but rather of frequency-modulated oscillations, Nickson and Muncey undertook to make a comparison of the frequency irregularity as measured according to a sinusoidal tone and according to a frequency-modulated tone in the frequency band extending from 800 to 1000 cps. The modulation depth was ± 3% for a modulation frequency of 6 cps. Notwithstanding the small modulation depth, the authors detected that this modulation depth led to a lowering of the frequency irregularity by approximately a factor of 3 in comparison to that measured with a sinusoidal tone. Of course, we should not be surprised at this; one needs only to note that the quantity measured in this manner has no meaning if it is called frequency irregularity, since it is precisely irregularity which is eliminated by modulation.

The problem of frequency irregularity and other characteristic quantities which are associated with it is theoretically examined by M. Schröder [10]. Schröder is completely correct when he notes that the computations of Bolt and Roop which are based upon the proposition that the intrinsic frequency spectrum of the room is not too dense are only valid when the following limiting condition obtains: the interval between intrinsic frequencies must be comparable to the width of the resonant curves for individual resonators which are excited by a sinusoidal tone source. However if this interval is small in comparison to the width of the resonant curves, then a sufficiently large number of the resonant maximums overlap one another. Under these conditions the intervals between the peaks of the transmission frequency characteristic are determined not by the distribution of intrinsic frequencies but by the width of the resonant curves (or, by the average attenuation of the resonators which is the same thing). The computation of the average interval between peaks which was carried out by Schröder showed that on the basis of the above assumption the interval $\overline{\delta f}$ (as we should expect on the basis of purely physical concepts)

is inversely proportional to the mean reverberation time T in the examined frequency band:

$$\overline{\delta f} = \frac{7}{T}. \tag{7}$$

As far as the average height $\bar{h}$ of the peaks is concerned, this quantity is a constant provided that the number of simultaneously excited resonators is sufficiently large in order to assure that the distribution of the energies associated with them can be assumed normal:

$$w(p^2) = \frac{1}{\overline{p^2}} e^{-\frac{p^2}{\overline{p^2}}} \tag{8}$$

($\overline{p^2}$ is the mean-square value of the pressure). In fact, introducing the quantity

$$z = \ln \frac{p^2}{\overline{p^2}}$$

which measures (in nepers) the pressure level with respect to the mean pressure, we write

$$p^2 = \overline{p^2} e^z.$$

Differentiating with respect to z, we have

$$\frac{d(p^2)}{dz} = \overline{p^2} e^z. \tag{9}$$

Multiplying Equations (8) and (9) we find

$$w(p^2)\, d(p^2) = e^{z - e^z}\, dz = w(z)dz. \tag{10}$$

The distribution function for the random variable z therefore is of the form:

$$w(z) = e^{z - e^z}. \tag{11}$$

As is proven in probability theory, the dispersion of this distribution is

$$\overline{z^2} - \overline{z}^2 = \frac{\pi^2}{6};$$

and the mean-square deviation is equal to

$$\sigma = \sqrt{\overline{z^2} - \overline{z}^2} = \frac{\pi}{\sqrt{6}} = 1{,}28 \text{ nepers} = 11 \text{ db}$$

The average height of the peaks, of course, does not coincide with the mean-square deviation, since certain minimums of the characteristic may lie above and certain maximums, on the contrary, may lie below the line representing the mean level. However both quantities depend upon one and the same distribution; the average height of the peaks is, in the same manner as σ, constant, and according to the computations of Schröder we find the value

$$\bar{h} \approx 10 \text{ db}$$

for it.

It must be noted that the original assumptions upon which the computations which lead to Formulas (7) and (10) were based are valid for the frequency region which Schröder defines by the inequality

$$f > 4 \cdot 10^3 \sqrt{\frac{T}{V}},$$

where V is the volume of the room in cubic meters, T is the reverberation time in seconds. Condition (11) is satisfied if no more than ten intrinsic frequencies whose spectrum is not degenerate can fit within the limits of the width occupied by the resonant curve.

Substituting the values of (7) and (10) into Formulas (4) and (5), we come to the conclusion that the frequency irregularity

$$F = \frac{10}{7} T = 1.43T \text{ db/cps} \qquad (12)$$

is directly proportional to the reverberation time. The simple physical meaning of this result is that the frequency irregularity which is measured, as can be seen from Formula (4), by the average slope of the frequency characteristic between its maximums and minimums increases with a decrease in the average attenuation (i.e., it increases with an increase in the reverberation time). As far as the diffuseness computed by the method of Furrer and Lauber is concerned, it is a function solely of the band width of the investigated frequencies:

$$D = \frac{10}{\Delta f} \text{ db/cps} \qquad (13)$$

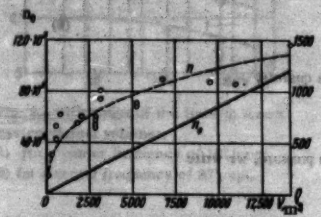

Fig. 3. Number of intrinsic frequencies (n_0) and the number of peaks (n) of the transmission frequency characteristic in rooms of various volumes (in the band 70-4000 cps).

The theoretical results obtained by Schröder were thoroughly verified by the measurements obtained by G. Kuttruff and R. Thiele [11]. They investigated 17 rooms with volumes ranging from 62 to 14,000 m³ (included in these were two radio-broadcasting studios with a variable reverberation). The frequency of the sinusoidal tone varied sufficiently slowly so that the acoustic regime could be assumed stationary (as Bolt and Roop showed, the condition $\frac{df}{dt} < \frac{17.5}{T^2}$ must be satisfied in order for this to be true).

The distance between the loudspeaker and the microphone exceeded the so-called "reverberation radius" $R = 0.1\sqrt{\frac{V}{\pi T}}$ by several times. First it was established that there was no direct relationship between the number of intrinsic frequencies $n_0 = f(V)$ and the number of peaks $n = \varphi(V)$ in the characteristic (Fig. 3.), as is also assumed by Schröder's theory. The results obtained by Kuttruff and Thiele which are given below refer to the frequency band extending from 70 to 4,000 cps; their accuracy is within ± 10%.

$$\frac{n}{T} = 584, \qquad (14)$$

$$\overline{\delta f} = \frac{6.73}{T}, \qquad (15)$$

$$\overline{h} = 9.81 \text{ db} \qquad (16)$$

On the basis of this data we obtain the following value for the frequency irregularity:

$$F = \frac{\overline{h}}{\overline{\delta f}} = 1.45T \pm 15\% \qquad (17)$$

Figure 4 shows the results of determining the frequency irregularity in the auditoriums investigated by Kuttruff and Thiele; the small circles indicate the values of F/T as averaged over the frequency range of 70 to 4,000 cps. As a comparison with Formulas (7), (10) and (12) shows, these values coincide very well with the results of the Schröder theory. As far as the diffuseness is concerned, the value

$$D = \frac{9.81}{\Delta f} \qquad (18)$$

is satisfactorily verified by the results given above for the measurements obtained by Furrer and Lauber in the band $\Delta f = 100$ cps with a central frequency of 1650 cps: $D \approx 0.09$.

Thus it has been clarified that the measurement of the frequency irregularity and other quantities associated with it does not produce any new information concerning the quality of a room, as compared to the information obtained from a knowledge of the reverberation time. This conclusion is only justified, of course, provided that the theoretical assumptions of Schröder are correct. If one did not suspect that the measurements of Furrer and Lauber in the region of comparatively low frequencies (400-500 cps) contained a systematic error, then one could only assume that Condition (11) must be replaced by a more rigorous condition.

In conclusion it is necessary to make two remarks which touch upon the relationship between the frequency irregularity (and of the quantities derived from it) and the diffuseness of the field. In the first place, when it is asserted that the quantities F and D must decrease with an increase in the diffuseness of the field, the problem of the limiting transition to outdoor arises. In this transition F and D must go to zero (if the frequency response of the measured tract is perfect), although the field in unbounded space is in no sense diffuse. This contradiction is eliminated if we take into account the fact that the quantities F and D are statistical parameters that completely lose their meaning when there is no aggregate of a large number of individual resonators having the definite properties of a statistical ensemble. In the second place, it is impossible to find a sufficiently clear physical characteristic to describe that sound-field state which is characterized by the term "diffuseness" in the various papers devoted to frequency irregularity. Furrer and Lauber make use of this term on an equal level with the term "homogeneity" and even note [6] that this term is more appropriate. However, if we accept the meaning of the homogeneity of a field in the direct sense of the word, i.e., as the constancy of the sound energy density over the entire volume of the room (of course, at a sufficient distance from the sound source), then it seems to us that the measurement of the transmission frequency characteristics does not yield any information concerning this inhomogeneity. The concepts advanced by Bolt and Roop [4] are of a very fragmentary nature; their ideas reduce to the following. The square of the sound pressure at a certain point in the field is the squared sum of the pressures associated with the excitation of very many resonators:

Fig. 4. Frequency irregularity in rooms having various volumes.

$$p^2 = \left(\sum_i p_i\right)^2 = \sum_i p_i^2 + \sum_i \sum_{k \neq i} p_i p_k .$$

In averaging with respect to frequency over a more or less wide frequency band (this is what is done in determining frequency irregularity) the second term may become sufficiently small in comparison to the first term; this means that the addition of the resonator vibrations is "on the average" an energy addition (i.e., these vibrations are "incoherent"). Evidently it is this condition which must characterize the particular field diffuseness which Bolt and Roop had in mind; of course, this condition is in no way equivalent to the condition which is evaluated by means of the statistical parameters of the intervals ψ and of the excitations Φ, although this latter condition is considered fulfilled when we are speaking of diffuseness in the sense indicated here. It must be noted that this diffuseness is not the same as that which is assumed in the classical reverberation theory, since this theory may not necessarily make use of quantities which are averaged over the frequency range.

Directional Diffuseness

If the diffuseness criteria examined above are directly associated with the wave theory of a sound field in a closed room, then the criteria proposed by R. Thiele [12] and the metering procedure developed by him are based upon the concepts of geometric acoustics; these concepts evidently enjoy preference in the case of large rooms (such rooms are precisely those of greater interest from the practical point of view). The purpose of measurements performed by Thiele was the investigation of the sound energy distribution in the various

directions along which the sound approached the receiver. For these measurements the sound source was a "ball" loudspeaker (13 conical loudspeakers in a hemispherically shaped container). The measurements were performed for a wa"ing tone with a frequency of 2 ± 1 kc and a modulation frequency of 12 cps. An electrodynamic microphone placed at the focus of a parabolic mirror with a diameter of 1.2m was used in the capacity of a sound receiver. The directivity pattern of the receiver was such that when the source was moved through an angular displacement of 8° with respect to the axis of the receiver, the sensitivity (under the conditions of unbounded space) decreased by a factor of two. In measuring the energy which was received from various directions the angle of elevation α of the receiver axis was given several fixed values, whereas the azimuthal angle φ was continuously varied from 0 to 360°. In investigating the reflections from the ceiling the angle of elevation α was continuously varied, and the azimuthal angle φ corresponded to a direction toward the sound source. The results of the measurements were plotted upon polar diagrams; the directions from which relatively large amounts of sound energy were received showed up in the form of "teeth" on the distribution curves. Two examples of polar diagrams of this kind are shown in Fig. 5. On the basis of representing a diffuse field as a field in which the sound energy is received more or less uniformly from all directions (this corresponds to the smooth circles on the polar diagrams), Thiele established a quantative measure of diffuseness on the basis of the following concepts.

Let $A(\alpha, \varphi)$ be a quantity which determines the energy flux in the direction having the angular coordinates α and φ; the average value of this quantity in the examined solid angle θ will be

$$M = \frac{1}{\theta} \int_{\alpha_0}^{\pi/2} \int_{0}^{2\pi} A(\alpha, \varphi) \cos\alpha \, d\alpha \, d\varphi,$$

where

$$\theta = 2\pi \int_{\alpha_0}^{\pi/2} \cos\alpha \, d\alpha = 2\pi (1 - \sin\alpha_0);$$

here α_0 is the smallest angle of elevation which is used during the measurements. The average absolute deviation of A from M is

$$\Delta M = \frac{1}{\theta} \int_{\alpha_0}^{\pi/2} \int_{0}^{2\pi} |A(\alpha, \varphi) - M| \cos\alpha \, d\alpha \, d\varphi.$$

Let us assume that $m = \frac{\Delta M}{M}$ and let us agree to define the value of m which is measured under the conditions of unbounded space by m_0. Then the degree of diffuseness of the field can be determined by the quantity

$$d = 1 - \frac{m}{m_0} \qquad (19)$$

which becomes zero under outdoor conditions ($m = m_0$) and becomes equal to unity in an ideal reverberant room ($\Delta M = 0$ and $m = 0$). Thiele calls the quantity d the directional diffuseness, thus underlining the special meaning which is incorporated in the concept of diffuseness. It is necessary to note that although the measurement of $A(\alpha, \varphi)$ is performed with comparative ease, it is nevertheless true that the computation of d by numerical integration (this is necesary in order to determine M and ΔM) is extremely difficult. This fact complicates the practical utilization of the criterion proposed by Thiele.

The values computed by Thiele for the directional diffuses at various points in the auditoriums investigated by him are of specific interest. Thus, for example, in the Duisberg Theatre Hall ($V = 5000\ m^3$, $T = 1.1\ sec$*)

* Here and henceforth we shall cite the values of reverberation time for a frequency of 1000 cps.

values of $\underline{d}$ ranging from 0.31 (the middle of the second balcony) to 0.48 (the middle of the orchestra) were determined. In the Hamburg Opera Theatre Hall ($V = 6000\ m^3$, $T = 1.4$ sec) smaller values were obtained (0.13 in the 9th row of the balcony and 0.17 in the 18th row of the orchestra). The highest value of $d = 0.66$ was obtained from measurements in the central portion of a church ($V = 8500\ m^3$, $T = 5.4$ sec). However, in

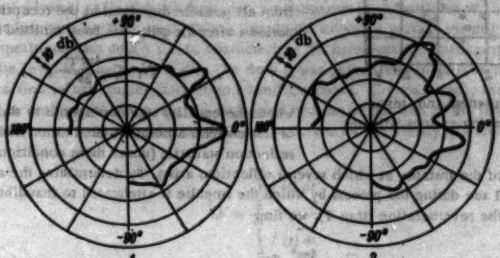

Fig. 5. Polar characteristics which determine the dependence of energy flux upon the angle of elevation of the receiver.
Diagram 1 corresponds to a sound source placed on the stage of the opera theatre in Hamburg, diagram 2 corresponds to a sound source placed in the orchestra pit; the spot at which the measurements were taken was the 18th row of the orchestra.

this case the directional diffuseness is far from the limiting value. By taking into account the directivity pattern of the sound receiver which was used, Thiele computed the values which would be obtained if it were assumed that all directions were completely uniform with the exception of the direction from which direct sound was received (i.e., under the conditions which are presupposed by reverberation theory). The result of this computation proved unsatisfactory: in all cases values of $d > 0.9$ were obtained. This proves that the generally accepted reverberation theory is based upon an idealized case which is far from the actual conditions. Although Thiele does not provide data regarding the effects of the sound-scattering structures upon the directional diffuseness, he nevertheless postulates that precisely such an effect determines the attainable improvement in the subjectively evaluated acoustic quality of auditoriums and studios (in particular, of musical auditoriums). The quality which has come to be called "fullness of sound" must, in the opinion of Thiele, be directly associated with relatively high values of directional diffuseness. In evaluating directional diffuseness as one of the possible criteria of the acoustical quality of auditoriums, it is first necessary to clarify within what limits this quantity can vary for a given volume and a given reverberation time.

In survey by E. Meyer [13] we found several sets of data regarding the mean values of directional diffuseness and reverberation time (Fig. 6) in rooms having various volumes (predominantly in radio-broadcasting studios). In rooms having volumes up to 5,000 m^3 the values of $\underline{d}$ (averaged for a number of points) lie in the range of from 0.4 to 0.6; in very large auditoriums (10,000 m^3 and greater) the directional diffuseness is considerably lower (to 0.1 and lower) notwithstanding the increase in the reverberation time. This conclusion is verified by the measurements performed by T. Arni [14]: in a comparatively small ($V = 1800\ m^3$) concert hall in Helsinki values of $\underline{d}$ were found which ranged from 0.33 to 0.49; in a large hall in Turku ($V = 10,000\ m^3$) the directional diffuseness was 0.18-0.25, although the surfaces of the walls were made to be strongly scattering in an attempt to increase the diffuseness. Here we should recall the insufficient fullness of sound noted in tests which were made of the acoustical qualities of the "Festival Hall" in London ($V = 22,000\ m^3$). It is possible that this defect was associated with the low directional diffuseness, although the designers [15] assumed that this defect was caused by insufficient reverberation (1.5 sec at 500 cps).

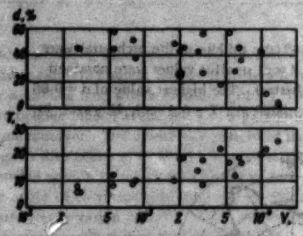

Fig. 6. Directional diffuseness and reverberation time in rooms having various volumes.

The decrease in the directional diffuseness of auditoriums having a large volume can be explained by the fact that relatively high values of diffuseness are only possible when the sound signal experiences a sufficiently large number of reflections per unit time. A statistical analysis of the reflections of a pulse in rectangular rooms [16] shows that the number of reflections which are received from all possible directions at the reception point during a period t after the pulse has been emitted is

$$N_t < \frac{4\pi c^3 t^3}{3V},$$

where the equality sign corresponds to the case of more or less uniform absorption distribution and to nondegenerate reflection statistics (under these conditions there are no nonrandom coincidences of the instants at which several reflections arise). By determining the average value $\bar{n}$ of the pulses received in 1 sec during the process by which the impulse is attenuated to inaudibility (this time can be assumed equal to the reverberation time T), we find

$$\bar{n} < \frac{4\pi c^3}{3V} T^3, \qquad (20)$$

where c is the velocity of sound.

If, as was assumed, the directional diffuseness is an increasing function of $\bar{n}$, then it must decrease with increasing volume in spite of the fact that the reverberation time increases (provided that T does not exceed the optimum values). In fact, the optimum reverberation time increases no more rapidly than $\sqrt[3]{V}$ in any case; therefore n decreases approximately in inverse proportion to the linear dimensions of the auditorium. As far as the problem concerning the possibility of varying the directional diffuseness without varying the reverberation time is concerned, it is possible to provide data which has been obtained by investigating a model of a rectangular room (2 × 1 × 1 m³) by means of an ultrasonic signal with a frequency of approximately 25 kc [13]. For smooth walls a value of d = 0.69 was found; by modifying these walls with scattering gratings the directional diffuseness was raised to 0.75 for the same reverberation time. A redistribution of the same amount of sound-absorbent material made it possible to vary the directional diffuseness over a range of from 0.26 to 0.46. These figures prove the possibility of examining the directional diffuseness as a quantity which does not depend upon reverberation time over known limits. On the basis of theoretical reasoning, such a possibility is associated with the undoubted effect of the shape of the room and the bounding surfaces of the room upon the number of reflections which arrive at the reception point in the initial echo period during which the reflected signals still have a sufficiently high level. It can be definitely supposed that the guarantee of a high directional diffuseness is desirable in reverberation chambers designed for measuring the absorption coefficients of acoustic materials under conditions where all possible angles of incidence have an equal probability. Diffuseness measurements made according to the Thiele method in such chambers are of undoubted interest. However, in making such measurements it is practical to make use of a microphone which, instead of a large reflector, has some other reception unit which does not increase the diffuseness due to additional reflections from the receiver (for example, a microphone with a set of tubes having various lengths). As far as the utilization of the Thiele criterion for evaluating the acoustic quality of auditoriums is concerned, at the present time there is not yet sufficient experimental data on the existence of a definite correlation between the values of the directional diffuseness and the subjective evaluations of the conditions governing speech and music perception in closed rooms. In the following section we shall show that the possibility of a single valued correlation of such a nature is at least doubtful.

Diffuseness and Definition (Clarity)

In discussing the conditions which determine the acoustic quality of auditoriums, many authors have, independently of one another, expressed the thought that it is necessary to distinguish between two qualitatively different parts in the composite reverberation sound. The first of these parts, which provides useful amplification to the sound without adversely affecting its definition, encompasses the repetitions of the fundamental signal which arrive at the listener's ear with small delays that do not exceed a certain magnitude t_0; the second portion, which contains repetitions with delays $t > t_0$, characterizes the reverberation "background" which impedes perception when the level is excessively high. The time t_0 was determined in various ways by different researchers; in the literature we find values ranging from 30 to 60 milli-seconds. Comparatively recently R. Thiele [12], having again returned to the problem of separating the useful and non-useful portions of the reverberation sound, proposed the following quantity in the capacity of a quantitative criterion for the clarity of sound which is heard in a closed room:

$$D = \frac{\int_0^{t_0} I(t)\,dt}{\int_0^{\infty} I(t)\,dt}; \qquad (21)$$

this quantity provides the ratio of the useful portion of the echo energy to the over-all amount of that energy. On the basis of the results obtained in the paper by G. Haas [17] on the effect of a single echo upon speech perception *, Thiele selected a value t_0 = 50 milliseconds, since the echo which arrived at the limits of this interval was not noticeable (when it arrived from any arbitrary direction) even when its level was 6-8db higher than the level of the primary (leading) signal. The measurements of definition were performed by Thiele at many points in radio-broadcasting studios and in theatres by means of a circuit which integrated the energy

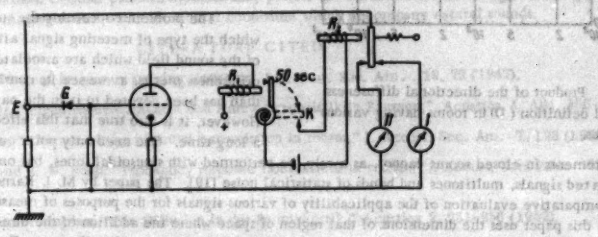

Fig. 7. Circuit for measuring definition (clarity)

of the signal received by the microphone; this integration was first performed for the time interval encompassing the period from 0 to 50 milliseconds, and then for the interval encompassing the period from 50 milliseconds till the instant at which the signal disappeared. The circuit of the metering unit is depicted in Fig. 7. The plate current of the tube restrains the armature of the relay R_1 which is under spring tension. When the first pulse appears at the input E of the circuit the grid of the tube receives a negative cutoff potential through the rectifier G; the armature of the relay R_1 is freed and the contacts K close in 50 milliseconds. Then the relay R_2 operates and transfers the input voltage from the thermal instrument I to an identical instrument II. The time required for the relay R_2 to trip is of the order of 1 millisecond. The sound from a spark discharge having a duration of approximately 0.1 milliseconds served as the metering signal; therefore the spectrum of the signal was very wide. A nondirectional condenser microphone with a pass band of up to 15 kc was used in the capacity of a receiver. Without dwelling in detail upon the results of these interesting measurements,

* It should be noted that the results obtained by Haas to a certain extent repeat the conclusions drawn in the paper by A. B. Rabinovich [18] which was published 11 years earlier.

we shall only note that they verified the relationship between good speech intelligibility and high values of definition. However in certain individual cases it was noted that the sound of music was not fully satisfactory for large values of D. We cannot fail to underline the fact that the requirements of high definition and high directional diffuseness are to a considerable degree mutually contradictory. In fact, the number of delayed signal repetitions which are received by the listener in the course of the first 50 milliseconds of the echo period is not so great that the useful portion of the echo could be considered diffuse. Relatively high values of directional diffuseness can be guaranteed solely at the expense of the non-useful portion of the echo if the levels of the reflected signals in this portion of the echo are sufficiently great. However under these conditions the non-useful portion of the echo can easily become harmful; it is unquestionably harmful for the perception of speech (it considerably lowers the intelligibility of speech), and this is well known from many years of experience. In the perception of music the conditions may be different [18]; however even in this case an increase in diffuseness at the expense of definition can only be considered allowable to a limited extent (and at that only for certain limited types of musical programs).

Here it is appropriate to note the idea of E. Meyer [13] to the effect that a useful criterion of the acoustic quality of auditoriums (provided the optimum reverberation condition obtains) might be found in obtaining the product of the diffuseness and the definition. Meyer gives values of this product as found in auditoriums having various volumes (Fig. 8), and comes to the conclusion that these values "characterize the investigated rooms in a manner which is not too bad". However it is very difficult to perceive a sufficient basis for such a conslusion: the values of (D · d) given by Meyer for rooms having volumes ranging from 6000 to 13,000 m³ vary irregularly over very wide limits (from 0.05 to 0.3), and it must also be noted that all of the investigated auditoriums have a "good acoustical reputation".

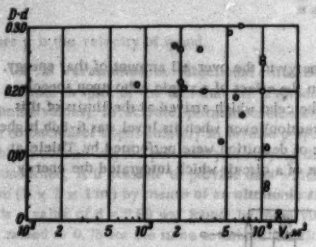

Fig. 8. Product of the directional diffuseness (d) and definition (D) in rooms having various volumes.

The Part Played by the Metering Signal

The problem concerning the substantial degree to which the type of metering signal affects those properties of the sound field which are associated with the degree of diffuseness merits, as we see it, considerably more attention than has been devoted to it in the papers examined above. However, it is also true that this effect has been known for a long time. One need only point out the fact that acoustic measurements in closed rooms cannot, as a rule, be performed with sinusoidal tones, but only with frequency-modulated signals, multitones and bands of statistical noise [19]. The paper by M. I. Karnovskii [20] is devoted to a comparative evaluation of the applicability of various signals for the purposes of measurements in closed rooms; this paper uses the dimensions of that region of space where the addition of the direct and reflected signals deviates from the law of energy summation due to the presence of interference effects as the criterion of comparison. It is evident that the size of this region is the smaller, the faster the autocorrelation function of the signal decreases with an increase in delay. For a signal spectrum of equal width and for a frequency band which has the same center-frequency value the best metering signal (as we might expect) proves to be a band of white noise; the dimensions of the interference region are in this case minimal. It is not difficult to see that this criterion is directly associated with the evaluation of the degree of sound-field diffuseness; it is sufficient to be reminded of the fact that the diffuseness of the field, as it is derived on the basis of classic reverberation theory, is associated precisely with the condition of the energy addition of the direct signal and all of its delayed repetitions at any point in a closed room. Let an acoustical signal of any arbitrary type be radiated by a non-directional source into a medium which extends without limit. At any two points which are equidistant from the source the signals are identical and their coefficient of mutual correlation is equal to unity. Such a field is in no sense diffuse. When such a signal produces a sound in a closed room the conditions are completely different. When the distance between two points equidistant from the sound source is small, the mutual correlation between the signals received at these points will be considerable; however it must

diminish with an increase of this distance as long as the metering signal is a random process. The rapidity with which the correlation disappears is determined not only by the acoustical properties of the room but also to a very considerable degree by the statistical structure of the signal. It is also understandable that the directivity of the sound source must produce a known effect upon the space interval in which the mutual correlation exists.

As far back as 1951, S. G. Gershman [21] advanced the idea that a sound field in a room is the more diffuse, the smaller the correlation interval. The quantitative characteristic of diffuseness can be determined as a certain appropriately selected function of this interval; the selection of such a function can be, of course, varied and requires additional investigation. Without prejudging the problem involved in finding the most rational determination of this function and in selecting the metering procedure, let us note that the criterion of diffuseness which is assumed here can be measured for actual sounds (speech and music), and that in each individual case it will depend upon the statistical properties of these sounds. Such a dependence seems necessary to us in principle; it is impossible to speak of the diffuseness of a field in a closed room without a direct indication of the type signal for which the degree of diffuseness is being determined. It is evident that for periodic (in particular, for sinusoidal) signals no room can guarantee the diffuseness which is assumed on the basis of the statistical reverberation theory, since the signals which are received at any two points in the room will always be coherent and therefore will not obey the law of energy summation.

In the further development of the problem involved in the methods of evaluating and measuring the diffuseness of a sound field it would be impossible not to take into account the dependence (which is essential in principle) of the rationally selected diffuseness criteria upon the statistical structure of the sound signal which is used for the measurements. The practical meaning of this dependence is verified to a sufficient degree by the universally known fact that the subjective evaluation of the acoustic quality of auditoriums and studios under the conditions which accompany various types of sounds (speech, musical compositions of one or another style) proves, as a rule, to be extremely varied. One can confidently assert that the correlation methods of measuring the diffuseness of a field are the best methods for taking into account the structure of the signal, and therefore in comparison to other possible methods they possess the incontestable advantage that they make it possible to perform measurements under the actual conditions which accompany natural sounds.

LITERATURE CITED

[1] R. H. Bolt, "Normal frequency spacing statistics," J. Acoust. Soc. Am. 19, 79 (1947).

[2] M. Schröder, "Eigenfrequenzstatistik und Anregungsstatistik in Räumen," Acustica 4, AB1, 456-468 (1954).

[3] E. C. Wente, "Characteristics of sound transmission in rooms," J. Acoust. Soc. Am. 7, 123 (1935).

[4] R. H. Bolt and R. W. Roop, "Frequency response fluctuations in rooms," J. Acoust. Soc. Am. 22, 280-289 (1950).

[5] W. Furrer and A. Lauber, "Die Diffusion in der Raumakustik," Acustica 2, 251-256 (1952).

[6] W. Furrer and A. Lauber, "Die raumakustiche Diffusität in Schallaufnahme- und Radiostudios," Acustica 4, 29-33 (1954).

[7] P. V. Brüel, "Automatic recording of frequency irregularity in rooms," Acustica 4, 21-25 (1954).

[8] T. Somerville and F. L. Ward, "Investigation of sound diffusion in rooms by means of a model," Acustica 1, 40-48 (1951).

[9] A. F. B. Nickson and R. W. Muncey, "Frequency irregularity in rooms," Acustica 5, 44-46 (1955).

[10] M. Schröder, "Die statistichen Parameter der Frequenzkurven von grossen Räumen," Acustica 4, AB2, 594-600 (1954).

[11] H. Kuttruff and R. Thiele, "Uber die Frequenzabhängigkeit des Schalldrucks in Räumen," Acustica 4, AB2, 614-617 (1954).

[12] R. Thiele, "Richtungsverteilung und Zeitfolge der Schallrückwürfe in Räumen," Acustica, 3, AB2, 291-302 (1953).

[13] E. Meyer, "Definition and diffusion in rooms," J. Acoust. Soc. Am. 26, 630-636 (1954).

[14] P. Arni, "Sound diffusion in concert halls and the possibilities of its measurement," Proc. Eleventh session of Tech. Commiss. of CIR (1954).

[15] P. H. Parkin, W. A. Allen, H. J. Purkis and W. E. Scholes, "The acoustics of the Royal Festival Hall, London," J. Acoust. Soc. Am. 25, 246-259 (1953).

[16] R. H. Bolt, P. E. Doak and P. J. Westervelt, "Pulse statistics analysis in room acoustics," J. Acoust. Soc. Amer. 22, 328-340 (1950).

[17] H. Haas, "Uber den Einfluss eines Einfachechos auf die Hörsamkeit von Sprache," Acustica 1, 49-58 (1951).

[18] A. V. Rabinovich, "On the degree to which echo is noticeable and the effect of echo upon the intelligibility of speech," J. Tech. Phys. (USSR) 10, 605-616 (1940).

[19] L. Beranek, Acoustical Measurements (Foreign Lit. Press, Moscow, 1952) Chap. 12.

[20] M. I. Karnovskii, "A comparison of the applicability of white noise bands, a multitone and a wailing tone for acoustical measurements in rooms," Trans. Acoustics Commission Acad. Sci. USSR, 1955, No. 8, 160-167.

[21] S. G. Gershman, "The correlation coefficient as a criterion of acoustic quality in a closed room," J. Tech. Phys. (USSR) 21, 1492-1496 (1951).

Moscow Electrical-Engineering Communications Institute

Received May 24, 1955

THE MEASUREMENT OF SOUND ATTENUATION IN A SURFACE ISOTHERMAL LAYER OF WATER

A. N. Barkhatov

The paper shows that a method [1] described earlier for investigating the propagation of sound in a laminarily-inhomogeneous medium can be successfully utilized under laboratory conditions for investigating the attenuation of sound in a surface isothermal layer of water when a medium with a negative vertical sound velocity gradient is present below that layer. The experimentally measured values of attenuation are found to be in good agreement with the theoretically computed values.

The paper by L. M. Brekhovskikh [2] uses wave theory methods to solve the problem of the propagation of sound from a point nondirectional source in a laminarly-inhomogeneous medium, where the sound velocity depends upon the coordinate z in the following manner:

$$c = c_0 \quad \text{for} \quad 0 \leqslant z < H; \quad c = \frac{c_0}{\sqrt{1+2\eta(z-H)}} \quad \text{for} \quad H \leqslant z < \infty \qquad (1)$$

and remains constant in planes which are perpendicular to z. The boundary $z = 0$ is assumed to be completely reflective (this corresponds, for example, to the case when the half-space $z > 0$ is water, and $z < 0$ is air).

Since for those cases of sound propagation in a laminarly-inhomogeneous medium which are of practical interest the value of the quantity is $\eta z << 1$, the Law of Variation (1) can be reduced to the form

$$c(z) = c_0[1 - \eta(z-H)] \quad \text{for} \quad H \leqslant z < \infty, \qquad (2)$$

and when $H = 0$ it can be reduced to the particular case examined by Pekeris [3].

Thus in [2] the problem of the propa gation of sound in a surface homogeneous quasi-isothermal layer is solved for the case when this layer is located above a medium with a constant vertical sound velocity gradient.

This problem was examined in more detail by L. M. Brekhovskikh and I. D. Ivanov in [4]; this paper showed that when sound is propagated in a homogeneous layer a special kind of sound "attenuation" occurs which is associated with the sucking out of sound energy into the medium which has the sound velocity gradient. The magnitude of the sound attenuation is characterized by the parameter

$$s = 1.64 \frac{H}{c_0} (\xi / f^2)^{1/3},$$

where $\xi = \eta c_0$ and f is the frequency in cps. The value of the parameter $s = 0$ corresponds to the case of maximum attenuation (the Pekeris case).

In a paper by the author [1] a method is described for the laboratory investigation of law governing the attenuation of sound with respect to distance in a laminarly-inhomogeneous medium with a constant vertical temperature gradient; in practical terms this also means that the sound velocity gradient is constant. The results of the measurements satisfactorily agreed with the values of sound attenuation computed according to the Pekeris theory.

The method which we developed for the simulated investigation of the sound field in a laminarly-inhomogeneous medium was also used for the study of the sound attenuation in an aqueous medium in which the following vertical temperature distribution obtained:

$$t = t_0 \text{ for } 0 \leqslant z < H; \; t = t_0 [1 - a(z - H)] \text{ for } z \geqslant H, \tag{3}$$

and where the isothermal surfaces were horizontal.

A medium which has such a temperature distribution along its depth can, to a certain approximation, be assumed analogous to a medium in which the Velocity Variation Law (2) exists. The dependence of the velocity gradient upon the coordinate z when $z \leq H$ (this dependence obtains for a constant temperature gradient) is taken into account in the computations, as in the preceding paper, by averaging the velocity gradient with respect to the depth over which the measurements are taken.

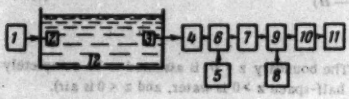

Figure 1. Block diagram of the Unit; 1) high-frequency pulse generator, 2) radiator, 3) sound pressure receiver, 4) amplifier for the received signals, 5) selector-pulse generator, 6) selector amplifier, 7) peak detector, 8) 10 kc carrier-frequency oscillator, 9) modulator, 10) minimum limiter, 11) logarithmic recording pen, 12) bath.

The experimental unit, which consists of a tub with thermal, mechanical and electroacoustical equipment, is described in [1]; it was used earlier in investigating the sound field in a region of geometric shadow. An oscillator formed pulses with a duration of approximately 40 microseconds which were "filled" with a carrier frequency of 530 kc; these pulses were converted into acoustical pulses by means of a radiator in the form of a round plate of polarized barium titanate with a diameter of 7mm. The sound was received by means of an acoustical probe which consisted of a barium titanate cube with dimensions of 2 x 2 x 2mm^3; the sound pressure reading was obtained in divisions of the scale-grid of the electronic oscilloscope screen.

Before performing measurements a constant vertical temperature gradient was established in the tub. The next task was to obtain a homogeneous (with respect to temperature) surface layer of water. The most effective method for this proved to be the utilization of a sharp lowering of the room temperature, combined with a wind created above the surface by ventilators.

Thus we were able to obtain an isothermal layer with a thickness of from 2 to 10 cm., A negative temperature gradient which differed little from the initial one was maintained below this layer. A crossarm was located above the tub, and this device made it possible to position the acoustical probe at various points in order to measure the sound pressure.

However, the method for investigating a sound field by measuring the acoustic pressure at various points suffers from the disadvantage that when the dimensions of the tub are large a considerable time is required for performing the acoustical measurements. The very results of the measurements obtained for the sound field when the point system is used may prove to be insufficiently accurate if the conditions under which the sound is propagated in the tub vary during the period over which the experiment is conducted. In addition, plotting a sound field according to measurements taken at various points requires the additional manipulation of the measured results.

Instead of investigating the sound field by points it is possible to make use of the method that involves the automatic recording ot the sound along the length of the bath. This method is described in more detail in the paper by V. Ia. Iashkov and the author [5]. The basis of this method is the utilization of a selector pulse generator for segregating the direct acoustic signal which arrives at the sound-pressure receiver. The block diagram of the unit is shown in Fig. 1.

The following signals, which are time-shifted with respect to one another, appear at the input of the amplifier 4 which receives the pulses: an electrical pulse which is induced by the high-frequency oscillator, a voltage from the direct acoustical pulse, and a voltage from the pulses obtained as a result of reflections from the bottom of the tub and from the walls etc. The unit is designed for segregating the direct acoustical pulse voltage from this sum of voltages. For this purpose the amplifier which receives the pulses must become operative at time intervals which are equal to the time required for the propagation of a pulse from the radiator to the acoustical probe, and must become cut off as soon as this pulse has passed. The time required for a pulse to be propagated from the radiator to the probe depends linearly upon the distance between them. The necessary cutoff time of the amplifier (as measured relative to the instant at which the pulse is produced by the oscillator) is automatically varied with the variation in the distance between radiator and probe by means of a linear resistance which is mounted along the length of the bath; when the probe is moved relative to the radiator a contact which is mounted upon the carriage containing the probe slides along the linear resistance. In order to segregate the required pulse from the signal received by the probe, a selector amplifier 6 is utilized; this amplifier is coupled to a pulse-selector oscillator 5. By selecting the instant at which the selector amplifier becomes operative, it is possible to segregate any pulse, including the first acoustical pulse. The pulse signal which is selected by the selector amplifier is fed to a peak detector 7 whose time constant is equal to 0.05 sec. The carriage with the acoustical probe is automatically moved along the bath at a constant rate by means of a motor having a reducer and pulley-block system. At the rate of probe motion which is utilized in the experiment (7.5 cm/sec) the voltage across the detector load is able to follow the amplitude variations in the received high-frequency pulse. The positive voltage which is obtained from the detector load is fed to a cathode follower. A voltage which is proportional to the amplitude of the selected high-frequency pulse appears across the load of the cathode follower. This voltage can be utilized for the automatic recording of the sound pressure on a linear scale (for example, by means of a loop oscillograph).

In order to obtain recordings of the sound in decibels we utilized a logarithmic level-recording pen of the Neiman type. For this purpose the measured voltage must be converted into an alternating voltage having a frequency which lies within the limits of the working frequencies of the recording pen and an amplitude which varies in proportion to the signal. Such a conversion can be accomplished by means of the modulator 9 which has a master oscillator 8 in the form of a symmetrical multivibrator operating at a carrier frequency of 10 kc. In order to eliminate the conversion nonlinearity which exists in the circuit for small signals, we introduce a minimum-limiter 10. The small-amplitude limiter does not pass a voltage of less than 3 volts. The output voltage appears at the input of the recording pen 11 and is recorded on a logarithmic scale.

A control check shows that the results obtained in measuring the sound field according to points and by means of the automatic recording pen coincide. Both methods were used in carrying out the work. Tests were made involving the measurement of sound attenuation in a quasi-isothermal surface layer below which a

constant negative vertical temperature gradient was simulated by the method described earlier. The experiment was performed under conditions that were such that it was possible to investigate the propagation of sound at various values of the parameter s; this was achieved by combining an appropriate thickness of a homogeneous layer with an appropriate magnitude of the velocity gradient. The frequency and duration of the emitted pulses did not vary during any of the tests. In addition, a study was made of the effect of the relative depths to which the sound radiator and receiver were immersed upon the sound attenuation (the relative immersion depths shall henceforth be respectively characterized by the numbers $m = \frac{h}{H}$ and $n = \frac{z}{H}$, where h and z are the immersion depths of the radiator and receiver respectively). This present paper examined the sound field formed by a source located in a homogeneous layer ($m < 1$). The field is also examined most fully with the boundaries of the homogeneous layer.

Many experiments in which the parameter s was varied within limits of from 0.4 to 3.0 made it possible to detect a number of regularities in the distribution of the sound field. In the region close to the radiator an interference pattern was observed which proved to be the wider, the greater the value of the parameter s. As the distance from the radiator increased, the succession of maximums and minimums was replaced by a monotonic decrease in the sound intensity. As an example, Fig. 2 shows two experimental curves which demonstrate the dependence of the sound attenuation on the dimensionless quantity qR for various values of the parameter q and for identical values of the quantities m and n. R is the distance from the radiator, and q is of the following form [4]:

$$q = k_0\left(\frac{3\eta}{k_0}\right)^{1/3}, \quad \text{where } k_0 = \frac{\omega}{c_0}.$$

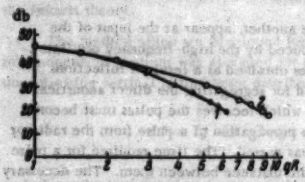

Fig. 2. Curves for the attenuation of sound for various values of the parameter $-s < 1$, $m = n = 0.25$: 1) H = 1cm, a = 0.4°/cm, s = 0.43, $q = 7.2^1/M$, 2) H = 2cm, a = 0.3°/cm, s = 0.85, $q = 7.2^1/M$.

From a comparison of the curves it is evident that the sound attenuation per unit of the quantity qR increases (other conditions being equal) when the parameter s decreases. This conclusion is in agreement with the theory [2, 4].

Figure 3 shows the experimental dependence of the sound attenuation upon the relative immersion depth of the receiver. From a comparison of the curves given in the figure it is evident that inside the isothermal layer the magnitude of the attenuation is the greater, the closer the sound receiver is shifted toward the surface of the water. This conclusion is also in agreement with the theory.

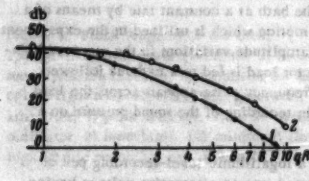

Fig. 3. A comparison between experimental and theoretical data: 1) H = 1 cm, m = n = 0.5, a = 0.5°/cm; s = 0.36, $q = 5.2^1/m$, 2) H = 2 cm, m = n = 0.25, a = 0.4°/cm, s = 0.68, $q = 4.7\ 1/M$.

A more accurate comparison of the experimental data on the attenuation of sound in a homogeneous layer with the theoretical values was performed for individual arbitrarily selected experiments. Figure 4 shows the theoretical curves of the sound attenuation (the curves are plotted on the basis of computations made by the thoretical division of the Acoustics Institute of the Acad. Sci. USSR) for two cases of sound propagation. The figure also shows the experimental points which, as can be seen from the figure, fit closely to the theoretical curves. Thus it can be assumed that the theory of sound propagation in the examined medium (this theory is expounded in [2, 4]) agrees well with the experimental values for small values of the parameter s ($s > 1$).

Figure 5 shows two experimental attenuation curves which were determined for $s > 1$. No accurate quantitative comparison of such curves with the theoretical curves was performed, but it is possible to compare the curves in Fig. 5

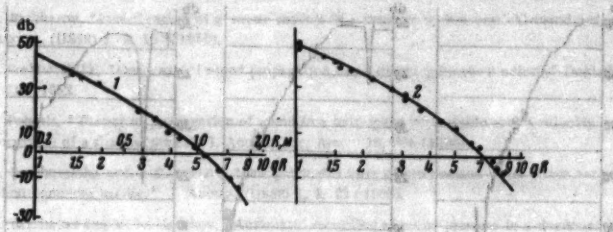

Fig. 4. Curves for the attenuation of sound at various levels s = 1.23, m = 0.2; 1 – n = 0.4, 2 – n = 0.8

with the theoretical curve 6 in Fig. 2 of [4]; this latter curve was plotted for s = 1 and can be used as a comparison, since the values of the quantities m and n are identical in the curves being compared: m = 0.2, n = 0.4. When s = 1, the average theoretical attenuation per unit qR in the interval from qR = 1 to qR = 10 is equal to 4.5 db. In the same range the experimental curves in Fig. 5 produce attenuation values of 4.7 and 3.2 db, respectively, for values of s which are equal to 1.2 and 3.0, respectively. A comparison of these values shows that for large values of s the experimentally obtained attenuation values are somewhat too large in comparison to the theoretical values.

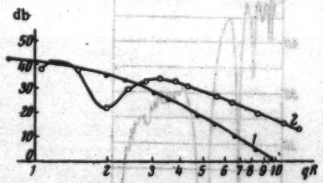

Fig. 5. Curves for the attenuation of sound for various values of the parameters s > 1, m = 0.2, n = 0.4: 1) H = = 5 cm, a = 0.3°/cm, s = 1.23, q = 3.9²/M, 2) H = = 9 cm, a = 0.4°/cm, s = 3.0, q = 4.5²/M.

The utilization of automatic pen recording made it possible to investigate the sound field in various horizontal planes (different values of n) for a constant position of the source (identical values of m) relatively quickly (and therefore for sound propaganation conditions which remained practically constant). Examples of recordings which were made in this manner are shown in Figs. 6 and 7. The distance from the radiator is read along the x axis, and the decibels are read from the y axis. Different curves (a, b, c) were obtained at various levels. The Neimanograms verified the conclusions we had obtained (using another method) concerning the dependence of the attenuation upon the depth to which the receiver is shifted inside of the isothermal layer (Fig. 6a, b). From Fig. 6 and especially from Fig. 7, in which the curves b and c are obtained at levels lying in an inhomogeneous medium it is evident that the deeper the sound receiver penetrates, the wider the region occupied by the interference extremums becomes. Thus in Fig. 6 the region occupied by the maximums and minimums extends over the following distances: in Fig. a to approximately 70 cm, in Fig. b to 100 cm and in Fig. c to 115 cm. In Fig. 7 this region extends 80, 180 and 200 centimeters, respectively, for curves a, b and c.

On the basis of the width of the interference region it is possible to make certain judgments concerning the applicability limits of geometric theory. As has been shown in [2], a criterion for the applicability of geometric acoustics when sound is propagated in a homogeneous layer is the requirement $R \ll s \frac{H^2}{\lambda}$.

For the propagation conditions under which the curves in Figs. 6 and 7 were plotted it must be true that R ≪ 120 cm.

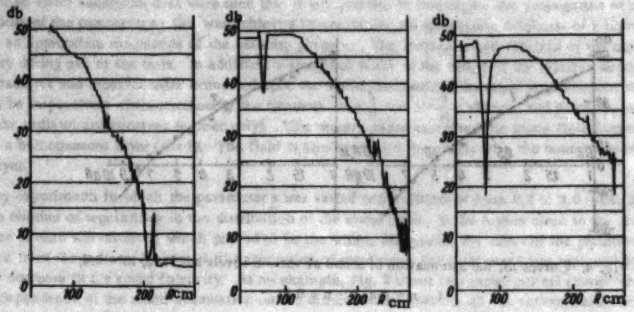

Fig. 6. Recordings of the attenuation of sound along the bath at various depths H = 4.5 cm, h = 2 cm, a = 0.53°/cm; s = 1.74: a) z = 1 cm, b) z = 3 cm, c) z = 5 cm.

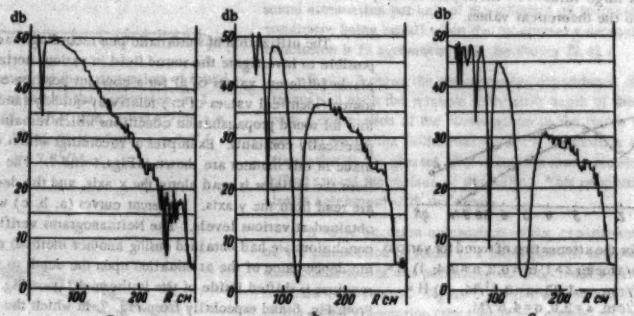

Fig. 7. Recordings of the attenuation of sound along the bath at various depths H = 4.5cm, h = 2 cm, a = 0.7°/cm, s = 1.80; a) z = 2 cm, b) z = 8 cm, c) z = 12 cm

On the basis of examining the data given above on the dimensions of the interference region it must be concluded that this condition is actually fulfilled within the limits of the homogeneous layer, but below the layer (in the inhomogeneous medium) the applicability limits of geometric theory are evidently extended.

I express my appreciation to I. L. Shmelev for his help in performing the experiment.

LITERATURE CITED

[1] A. N. Barkhatov, "Investigation of acoustic shadow in a medium with a vertical sound-velocity gradient," J. Acoust. (USSR) 1, 2, 121 (1955).

[2] L. M. Brekhovskikh, "One case of sound propagation in an inhomogeneous medium," Doklady Acad. Nauk SSSR 87, 715, 1952.

[3] C. L. Pekeris, "Theory of propagation of sound in a half-space of variable sound velocity under conditions of formation of a shadow zone," J. Acoust. Soc. Am. 18, 295 (1946).

[4] L. M. Brekhovskikh and I. D. Ivanov, "One particular form of attenuation when waves are propagated in laminarly-inhomogeneous media," J. Acoust. (USSR) 1, 1, 23 (1955).

[5] A. N. Barkhatov and V. Ia. Iashkov, "Automatic recording of sound pressure in a deadened basin," Sci. Records Gor'kii State University 27, 150 (1954).

Physico-Engineering Research Institute of the Gor'kii State University

Received March 25, 1955

THE INTENSITY OF HARMONIC AND MODULATION COMPONENTS WHEN WAVES OF COMPLEX SHAPE ARE NONLINEARLY DISTORTED

V. M. Vol'f

The paper gives a method for computing the intensity of modulation and harmonic components which are formed when waves of complex shapes are nonlinearly distorted. The intensity of the harmonic and modulation components is computed for the case of nonlinear distortion of triangular, sawtooth and rectangular waves. Relationships are obtained which show that when waves of a complex shape are nonlinearly distorted the intensity of the modulation components can considerably exceed the intensity of the harmonic components. On this basis certain facts of auditory theory are explained.

The perception of nonlinear distortion in complex sounds is chiefly associated with the appearance of modulation tones. The harmonics which are simultaneously formed play a secondary role in this case [1]. Up to this time the relationship between the intensities of the modulation and harmonic components has not been taken into account in examining the causes of this phenomenon. In addition, the computations which are performed in accordance with the method proposed below show that in the case of complex waves containing nonlinear distortion the intensity of the modulation tones can exceed the intensity of the harmonics by so much that this factor must be taken into account in order to clarify better certain experimental data on the auditory perception of nonlinear distortion. It is difficult to show the relationship between the modulation and harmonic components in general form for actual sound material (if not entirely impossible). Therefore we shall investigate the case when a nonlinear system of the form

$$i = a_1 u(t) + a_n u^n(t) \tag{1}$$

(where $n > 1$ is a whole number) is subjected to a periodic signal

$$u(t) = \sum_{k=1}^{p} C_k \sin(\omega k t + \varphi_k). \tag{2}$$

The fact that sound wave spectra [in contrast to Equation (2)] may contain components whose frequencies are not related in a harmonic manner does not change the essence of the case, since we shall examine the relationship between modulation and harmonic components from the energy point of view.

Raising each of the components in the right-hand side of Equation (2) to the n-th power and then adding them, we find the nonlinearity product of harmonic origin:

$$i_{hn} = a_n \sum_{k=1}^{p} C_k^n \sin^n(\omega k t + \varphi_k) - \sum_{k=1}^{p} I_{k0}. \tag{3}$$

where I_0 is the dc component which is formed when each of the components of Equation (2) is raised to the n-th power.

Then we obtain

$$i_{mn} = a_n \left[\sum_{k=1}^{p} C_k \sin(\omega k t + \varphi_k)\right]^n - a_n \sum_{k=1}^{p} C_k^n \sin^n(\omega k t + \varphi_k) - \left[I_{\Sigma 0} - \sum_{k=1}^{p} I_{k0}\right], \tag{4}$$

for the nonlinearity product of modulation origin (i_{mn}), where $I_{\Sigma 0}$ is the dc component which is obtained when the entire right-hand side of Equation (2) is raised to the n-th power.

Having performed our computations in accordance with Equations (3) and (4) and having then passed on to finding the intensity of the nonlinearity products of modulation P_{mn} and harmonic P_{hn} origin, we would thus have solved the problem which has been posed. However the computation of $\left[\sum_{k=1}^{p} C_k \sin(\omega k t + \varphi_k)\right]^n$ poses an extremely difficult operation when the number of components in the signal spectrum is large, even in the case when special methods of computation are utilized [2,3]. Meanwhile these difficulties in making the computations can be circumvented if the nonlinearity product of modulation origin is determined directly from the left-hand side of Equation (2) [i.e., if we do not resort to the expansion of u(t) into a harmonic series]. This device can be successfully utilized in those cases when the function u(t) can be fairly simply expressed analytically, when it satisfies the Dirichlet conditions and when its integration does not present any appreciable difficulties. In accordance with what we have said above, we write the intensity of the oscillations at the output of the nonlinear system:

$$P_{\Sigma n} = \frac{1}{T} a_n^2 \int_0^T u^{2n}(t)\, dt. \tag{5}$$

Subtracting the intensity of the dc component

$$P_{0n} = \left[\frac{1}{T} a_n \int_0^T u^n(t)\, dt\right]^2, \tag{6}$$

from Expression (5) we determine the intensity of the alternating components of the nonlinearity product:

$$P_{\sim n} = P'_{\Sigma n} - P_{0n}, \tag{7}$$

which represents the sum of the nonlinearity products of harmonic and modulation origin.

In accordance with Expression (3), the intensity of the nonlinearity product which is of harmonic origin (P_{hn}) can be represented in the form

$$P_{kn} = \frac{1}{2} a_n^2 z(n) \sum_{k=1}^{p} C_k^{2n}, \tag{8}$$

where z(n) is a certain function of the nonlinear-system characteristic. In particular, when n = 2, z(n) = 0.25, and when n = 3, z(n) = 0.625.

In Expressions (7) and (8) it is possible to determine the intensity of the nonlinearity product of modulation origin:

$$P_{mn} = P_{\sim n} - P_{kn} \tag{9}$$

On the basis of Expressions (5) - (9) the ratio between the intensity of the nonlinearity product of modulation origin and the intensity of the nonlinearity product of harmonic origin will be

$$q_n = \frac{P_{mn}}{P_{kn}} = \frac{\frac{1}{T}\int_0^T u^{2n}(t)\,dt - \left[\frac{1}{T}\int_0^T u^n(t)\,dt\right]^2 - \frac{1}{2} z(n) \sum_{k=1}^{p} C_k^{2n}}{\frac{1}{2} z(n) \sum_{k=1}^{p} C_k^{2n}}. \tag{10}$$

Evidently Equation (10) solves the problem posed above.

Below we examine the values of q_n for the case when nonlinear systems of the form

$$i = a_1 u(t) + a_2 u^2(t) \tag{11}$$

and

$$i = a_1 u(t) + a_3 u^3(t) \tag{12}$$

are subjected to periodic waves of triangular, sawtooth or rectangular shapes (Fig. 1, a, b, c). As can be seen from Fig. 2, where the corresponding spectra of these waves are shown, almost all of the energy in the triangular wave is concentrated at the first harmonic frequency. In the sawtooth wave the energy is distributed more uniformly over the spectrum. And finally, the energy is distributed still more uniformly over the spectrum in a rectangular wave for which the relative width of the pulses is small. In order to obtain a quantitative characteristic for the energy distribution over the frequency spectrum we introduce the coefficient L which provides a picture of the energy distribution of the input signal among the first harmonic and all of the other harmonics of the spectrum:

$$L = \frac{\sum_{k=1}^{p} C_k^2}{C_1^2}, \tag{13}$$

where C_1 is the amplitude of the first harmonic.

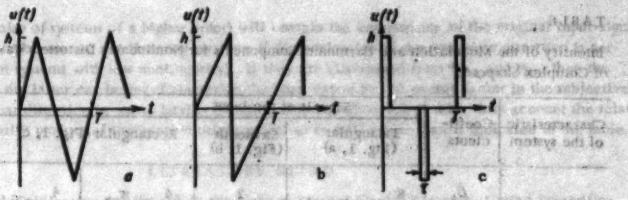

Fig. 1

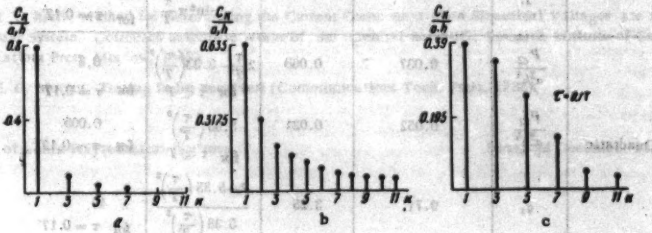

Fig. 2

Turning to an examination of the table in which the values of q_n (computed for the three examined waves) are given, we note first of all that the smallest value of the nonlinearity product of modulation origin occurred for the transmission of triangular pulses. In that case the intensity of the nonlinearity product of modulation origin is less than the intensity of the nonlinearity product of harmonic origin (see coefficients q_2 and q_3). The latter is quite natural, since approximately 98% of the entire energy in the wave (see the coefficient L) is relegated to the harmonic of the fundamental frequency in the spectrum of the triangular pulses. Of course, the intensity of the modulation components, which in this case are due to the interaction of the low-power components of the input spectrum, cannot be significant here.

The relative increase in the nonlinearity product of modulation origin occurs in accordance with the increase in the power of the higher harmonics of the input signal spectrum. This can easily be seen from an examination of sawtooth waves and of rectangular waves with pulses having a small relative width ($\tau \ll T$). For example, if $\tau = 0.1T$, then L = 2.6. Under these conditions the intensity of the nonlinearity product of modulation origin in a quadratic system is 40 times greater than the intensity of the nonlinearity product of harmonic origin. A corresponding value for the intensity of the nonlinearity product of modulation origin in a cubic system will under these conditions be 1200 times greater than the intensity of the harmonic components. For a small relative width of the rectangular pulses L increases and q_2 and q_3 prove to be still larger.

The data in the table contradicts the idea that there is a singlevalued quantitative relationship between the harmonics and the modulation tones in frequency-independent systems, and that because of this the coefficient of the harmonics (as measured on a pure tone) determines the value of the modulation tones which will occur when waves of a complex shape are transmitted [4]. In fact, as can be seen from the table, for one and the same nonlinear system the relationship between the intensity of the modulation and harmonic components depends heavily upon the nature of the input signal. Since the perception of nonlinear distortion is basically determined by modulation components, then in a case where the evaluation of the sound quality is applied to various sound material, it should not be surprising if the system with the smaller harmonic coefficient will

TABLE

Intensity of the Modulation and Harmonic Components for Nonlinearly Distorted Waves of Complex Shapes*

Characteristic of the system	Coefficients	Signals at the input			
		Triangular (Fig. 1, a)	Sawtooth (Fig. 1, b)	Rectangular (Fig. 1, c)	
Linear	$\frac{C_k}{a_1 h}$	$\frac{8}{\pi^2 k^2}$ $k = 2m+1$, $m = 0.1.2.3\ldots$	$\frac{2}{\pi k}$ $k = 1.2.3\ldots$	$\frac{4}{\pi k}\sin\pi\frac{\tau}{T}k$ $k = 2m+1$.	$\frac{4}{\pi k}\sin 0.1\pi k$ $m = 0.1.2.3\ldots$
	L	1.02	1.64	$0.79\frac{\pi\frac{\tau}{T}}{\sin^2\pi\frac{\tau}{T}}$	2.6 for $\tau = 0.1T$
Quadratic	$\frac{P_{\Omega}}{a_2^2 h^4}$	0.037	0.068	$2\frac{\tau}{T} - 5.33\left(\frac{\tau}{T}\right)^2$ for $\tau \ll T$	0,2 for $\tau = 0,1T$
	$\frac{P_{2\Omega}}{a_2^2 h^4}$	0.052	0.021	$5.33\left(\frac{\tau}{T}\right)^2$ for $\tau \ll T$	0.005 for $\tau = 0,1T$
	q_2	0.71	3.25	$\frac{2-5.33\left(\frac{\tau}{T}\right)^2}{5.33\left(\frac{\tau}{T}\right)^2}$ for $\tau \ll T$	40 for $\tau = 0.1T$
Cubic	$\frac{P_{\Omega}}{a_3^2 h^6}$	0.061	0.122	$2\frac{\tau}{T} - 17\left(\frac{\tau}{T}\right)^3$ for $\tau \ll T$	0.2 for $\tau = 0,1T$
	$\frac{P_{3\Omega}}{a_3^2 h^6}$	0.082	0.021	$17\left(\frac{\tau}{T}\right)^3$ for $\tau \ll T$	0.0001? for $\tau = 0,1T$
	q_3	0.75	5.8	$\frac{2.0-17\left(\frac{\tau}{T}\right)^4}{17\left(\frac{\tau}{T}\right)^3}$ for $\tau \ll T$	1200 for $\tau = 0,1T$

produce a greater deterioration of the sound quality due to nonlinear distortion than the system with a large harmonic coefficient. This once again confirms the fact that the harmonic coefficient is insufficient as a criterion in evaluating nonlinear distortion in sound transmission systems.

The fact that $q_3 > q_2$ when complex spectra are distorted is also worthy of attention. Therefore the relative value of the nonlinearity product of modulation origin in a cubic system is greater than that of a quadratic system. This must be taken into account in explaining the experimentally observed fact that nonlinear distortion of complex sound (speech, music etc.) is more sharply perceived by the auditory apparatus when this distortion is produced by a cubic system as compared to a quadratic system (provided their harmonic coefficients are equal). Besides the higher harmonics and modulation frequencies the nonlinearity product of

* For the notation see Fig. 1.

a cubic system (and also of systems of a higher order) will contain the components of the original input-signal frequency. These components are not linearity products if the evaluation of the nonlinear distortion is performed by the ear (for systems with low nonlinearity). If they are eliminated from P_{mn} and P_{hn}, then the relationship between the latter can better characterize the part played by the energy factor in the subjective evaluation of nonlinear distortion in waves having complex shapes. When this is taken into account the relative value of the nonlinearity product of modulation origin proves to be still larger than is indicated in the table.

LITERATURE CITED

[1] S. N. Rzhevkin, Hearing and Speech in the Light of Modern Physics Research, United Scientific-Technical Institute of the Peoples Commissariat of Post and Telegraph, 1936.

[2] V. A. Kotel'nikov, Scientific-Engineering Collection of the Leningrad Communications Institute, 14, 1936.

[3] I. V. Basik, Method for Determining the Current Component when Sinusoidal Voltages are Applied to a Nonlinear System. Collected Scientific Works of the Central Scientific Research Institute of Communications (Communications Press, Moscow, 1948).

[4] E. G. Momot, Testing Radio Receivers (Communications Tech. Press, 1936).

Kiev Order of Lenin Polytechnical Institute

Received December 13, 1954

ON THE MEASUREMENT OF THE CORRELATION COEFFICIENT

S. G. Gershman and E. L. Feinberg

A device is analyzed which is based upon the utilization of the relationship between the correlation coefficient of two noise signals and the probability that the signs of the instantaneous values of these noise signals will coincide. The output effect of the device is a measure of this probability. The electrical circuit contains the following units: a circuit for transforming the input voltages into pulses, an electronic relay at whose output coincident pulses are obtained, a circuit for averaging these pulses, and an indicator. The theory of the device is analyzed. The theoretical results are used for the purpose of calibration and for evaluating the errors of measurement. It is shown that the device can be utilized not only for measuring the correlation coefficient but also for certain other purposes, including various types of measurements in an acoustic field. Results are cited which are based upon the experimental utilization of the device.

In analyzing noise and in investigating the passage of noise signals through various conversion systems statistical methods have been more and more widely utilized in recent years; in particular, correlation functions have been utilized in order to describe the process. It can be asserted that in studying many problems a description which makes use of correlation functions is more adequate than a description which is based upon expansion into Fourier integral (or series) form. This applies first of all to very wide-band (in the spectral sense) processes which are encountered especially often in acoustics. Thus, for example, in architectural acoustics the correlation characteristics are evidently of essential importance in determining the acoustical properties of rooms [1]. The separation of two superimposed processes is often possible precisely because of a utilization of the difference in their correlation properties; this fact, in particular, explains the high degree to which statistical methods permeate the theory of signal reception in the absence of interference [2, 3], communications theory [4], and the theory of radar devices [5]. It is obvious that the correlation properties of sound play a very important part in understanding the operation of the auditory apparatus when studying such questions as speech intelligibility etc.

During the last ten years the Acoustics Institute of the Acad. Sci. USSR has conducted investigations of correlational relationships in sound fields, and it is natural that in doing so the necessity arose for an instrument which made it possible to measure correlation parameters directly. This paper is devoted to a description of such an instrument [6] and to several possible applications of it.

The problem involved in finding which particular correlation characteristic should serve as a measure of correlating two processes remains unanalyzed to this day. In noise theory and in communications theory the correlation coefficient R is usually considered an appropriate measure of the mutual relationship between two processes or the mutual relationship between the values of one quantity x which are taken at various instants in time $x(t)$, and $x(t + \tau)$. Of course, the correlation coefficient R is more appropriate as such a measure than the correlation function $\varphi = \overline{x(t)\,x(t+\tau)} = \overline{x^2}R$ (the line above the expression denotes averaging), since the correlation function φ is a measure not only of the degree to which processes are coupled, but is also a measure of their intensity $\overline{x^2}$; this interferes with the ability to recognize the degree to which the processes are coupled. In addition to this, it is known that the correlation coefficient is not an ideal measure of correlation, since for certain processes (for example, periodic ones) it may be equal to zero even when single-valued correlation is present.*

Often a better measure of the mutual correlation is the so-called correlation ratio ([7], p. 385). However, for ensembles which obey a normal distribution law and which have a normal correlation, as in all cases in which the regression is linear [7], the correlation ratio is equal to the correlation coefficient. Therefore, it is possible to assume that the utilization of the correlation coefficient in the capacity of a measure of mutual dependence is justified and practical precisely for stochastic processes which have a normal distribution of their instantaneous values and a normal correlation.

It is important to note that acoustic fields which are encountered in practice most often belong precisely to this class. It can be seen from the Liapunov theorem ([7], p. 275) that any process which is a composite of many independent processes obeys the normal law. This therefore must also apply to shock noise, to noise which arises due to vortical flow around bodies in water or air (since these types of noise are created by a multitude of different vortices which are developed individually and independently), for hydroacoustic noise which arises in the wake of a moving body as a consequence of the sound radiated by the multitude of air bubbles which perform vibrations whose phases are mutually independent, for cavitational noise, and in general for the majority of noises which are encountered in acoustics practice and which have sufficiently wide bands.

The noise produced by resonant sources may not satisfy this requirement; however this subject requires clarification. It is known [2] that a stochastic process which has a constant intensity that differs from zero solely in the frequency band ranging from $\omega_a = 2\pi f_a$ to $\omega_b = 2\pi f_b$ obeys the normal distribution law for instantaneous values and has a normal correlation (i.e., for such a process the probability $P(x)$ of a specified value of the stochastic quantity x and the probability $P(x, y)$ of combining two values $x(t)$ and $y = x(t + \tau)$ are equal to

$$P(x) = \frac{1}{2\sqrt{\pi I_0}}\, e^{-\frac{x^2}{4I_0}}, \quad I_0 = \overline{x^2}; \tag{1}$$

$$P(x, y) = \frac{1}{4\pi I_0 \sqrt{1-R^2}}\, e^{-\frac{x_1^2+x_2^2-2x_1x_2R}{2I_0\sqrt{1-R^2}}} \tag{2}$$

By basing the proof of this assertion upon a harmonic (Fourier) expansion of the quantity x as the function of time t, it is possible essentially to make use of phase averaging with respect to the various harmonics which are thus assumed to be mutually independent. From what has been said above it is evident that normal correlation and a normal distribution of the instantaneous values occur, in particular, for any process which is obtained by passing a stochastic process with normal correlation through any arbitrary narrow-band π - filter (thus the process has a time dependence which can approximate a sinusoidal function as closely as desired). The assertion that the distribution of instantaneous values and the correlation are normal in such an almost sinusoidal process clearly contradicts reality. However the contradiction is only an apparent one. The fact is that in making the proof still another important condition is imposed. Namely, the averaging during the derivation is performed

* Thus for example, for $X = \cos \omega t$ the autocorrelation coefficient is $R = \cos \omega\tau$, (i.e., the coefficient can acquire all values, even including null values, although in actual fact the values of x at any two instants of time are rigidly coupled).

over an infinitely large time interval, whereas the judgment concerning the distribution of values and the averaging in an actual process is performed during the observation time (i.e., during a certain finite time T). In other words, in order for Formulas (1) and (2) to be valid it is necessary that the averaging time be much greater than the correlation interval τ_0 (i.e., much greater than the time during which the correlation between instantaneous values of the investigated quantity is dissipated),

$$\overline{x(t)\,x(t+\tau_0)} \ll \overline{x_0(t)}.$$

Thus it must be true that

$$T \gg \tau_0 \approx \frac{1}{f_b - f_a}, \qquad (3)$$

where $f_b - f_a = \Delta f$ is the band width.

Therefore it is also true that a "monochromatic" signal, which in actual fact still has a certain finite spectral width, yields a normal distribution if the observation (or the actual averaging) is performed over a sufficiently long period. On the contrary, the requirement of phase independence is not fulfilled, for example, if the noise consists of the sequence of pulses having a rigorously determined shape, particularly if we are speaking of a sequence of rectangular pulses of the same amplitude (i.e., a "telegraph signal"). Therefore for two stochastic sequences of such processes the correlation coefficient may not necessarily coincide with the correlation ratio.

The method and instrument described below are first of all designed for measuring correlation coefficients for stochaster processes which have a normal distribution. In other cases it is necessary to know the type of process (in the statistical sense) in order to calibrate the instrument.

Let us now pass over to a description of the manner in which the instrument is arranged. If we observe the signs of the functions $x_1(t)$ and $x_2(t)$ (where $x_1(t) = x_1(t+\tau)$ or $x_2(t) = nx_1(t+\tau) + y(t)$, where n is a constant coefficient and $y(t)$ is some other function, then any one of four combinations is possible:

$$+,+;\quad -,-;\quad +,-;\quad -,+.$$

The possibility of each of these combinations, as will become evident below, depends upon the correlation coefficient. The instrument which is used is based upon measuring the probability of one (or two) of these combinations of signs.

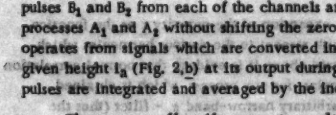

Fig. 1

In principle the circuit of the instrument (Fig. 1) is a two-channel amplifier with symmetrical limiting in each stage AL_1 and AL_2, and with a common output unit OU containing the indicator I. The processes under study are fed to the inputs of the channels after having been converted into electrical signals - for example, $A_1 = x_1(t)$ (Fig. 2,a) and $A_2 = x_1(t+\tau)$ (Fig. 2,c). A_1 and A_2 are converted into a sequence of rectangular pulses with a height V_0 (Figs. 2,b and 2,d) by means of the amplifier-limiters. The output pulses B_1 and B_2 from each of the channels are formed at the points of transition between the zero of the input processes A_1 and A_2 without shifting the zero lines. The over-all output unit of the electronic-relay type operates from signals which are converted into rectangular pulses, and likewise yields rectangular pulses of a given height i_a (Fig. 2,b) at its output during the time for which the signs coincide in both channels. These pulses are integrated and averaged by the indicator which contains an inertial element (T in Fig. 1).

The average effect (for current or voltage) at the output is equal to

$$i = \frac{i_a \sum_1^m \Delta t_m}{T}. \qquad (4)$$

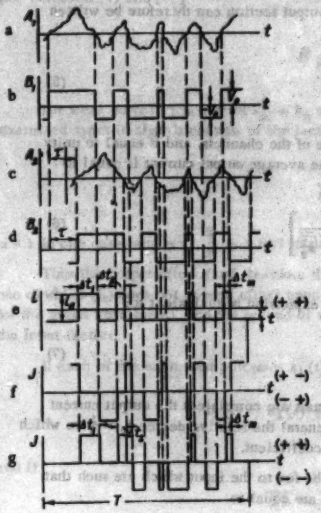

Fig. 2

Thus the durations of those time intervals during which the instantaneous values of A_1 and A_2 in both channels simultaneously have the required sign are selected and summed, for example (in order to be specific), a positive sign (in other variants a negative sign may be used, or opposite signs may be used).

The resultant duration $\frac{\Sigma \Delta t_m}{T}$ of the coincidence intervals (as normalized to the averaging time) is a measure of the probability of the selected combination of signs. It is this quantity which is directly measured by the instrument.

Instead of an electronic relay we also utilized a linear circuit for averaging the pulses formed by the channels. By depending upon the circuit which was used for effecting the transition from the conversion channels to the common load of the output unit, it was possible to distinguish between the coincidence (Fig. 2,g) or non-coincidence of signs (Fig. 2,f). In both cases it is possible to use pulses of either one or both polarities for the purposes of integration and averaging.

If a random variable voltage without a dc component is fed to the input of a channel, then the resultant duration of the time intervals during which the instantaneous values are positive will, on the average, comprise one-half of the observation time.

If one and the same signal is fed to both inputs, then the signs coincide in both channels; the pulses in the output section (Fig. 2,e) always take up an average of one-half of the observation time, and the average current at the output is equal to $\frac{1}{2}i_a$; here i_a is an amplitude which is specified solely by the parameters of the output unit and which is completely independent of the signal properties. Henceforth we shall assume that it is equal to unity: $i_a = 1$.

However if the signals at the inputs of both channels are completely independent, then the probability that positive signs coincide is equal to $(\frac{1}{2})^2 = \frac{1}{4}$ and the average current is equal to $\frac{1}{4}$.

It is evident that, depending upon the degree of correlation between signals, the average output current will vary from $\frac{1}{4}$ to $\frac{1}{2}$.

First of all let us examine what such an instrument will read when a stochastic sequence of positive and negative rectangular pulses of given height are originally fed to its inputs (i.e., A_1 and A_2 are of the form B_1 and B_2 at the inputs, and this form is therefore not altered when the signals pass through the amplifier and the limiter). Thus we shall assume that the current in each channel $x_1(t)$ and $x_2(t)$ is either equal to V_0 or to $-V_0$; here the resultant duration of all the positive pulses is equal to the resultant duration of the negative pulses, so that

$$\overline{x_1^2} = \overline{x_2^2} = \overline{V_0^2},$$

$$\overline{x_1(t)} = \overline{x_2(t)} = 0.$$

The current at the output exists only during those time intervals when the currents x_1 and x_2 in both channels are positive. The instantaneous value of the current in the output section can therefore be written in the form

$$i(t) = \frac{[x_1(t) + V_0][x_2(t) + V_0]}{4V_0^2}. \tag{5}$$

In actual fact, this quantity becomes zero if $x = -V_0$ in even one of the channels, and is equal to unity when the signals in both channels have a positive value. Therefore the average output current is equal to

$$\bar{i} = \frac{V_0^2 + \overline{x_1 x_2}}{4V_0^2} = \frac{1}{4}\left[1 + \frac{\overline{x_1 x_2}}{\sqrt{\overline{x_1^2}}\sqrt{\overline{x_2^2}}}\right]. \tag{6}$$

According to the definition of the correlation coefficient R this expression is equivalent to:

$$\bar{i} = \frac{1}{4}(1 + R). \tag{7}$$

Thus it is true that (depending upon the degree to which the signals are correlated) the output current varies from $i_0 = \frac{1}{4}$ (when R = 0) to $i = \frac{1}{2}$ (when R = 1). However in general the relative degree $i_0 = \frac{1}{4}$ to which the "background" is exceeded is simply equivalent to the correlation coefficient.

Let us pass on to an examination of our basic case. Let signals be fed to the input which are such that they obey a normal law (i.e., the probabilities of the values x_1 and x_2 are equal to

$$P(x_1) = \frac{1}{2\sqrt{\pi I_0}} e^{-\frac{x_1^2}{2I_0}}, \quad I_0 = \overline{x_1^2}. \tag{1'}$$

The probability of combining the values of x_1 and x_2 is given by Formula (2); for the sake of simplicity we shall assume that the intensities I_0 of the signals are identical.

Hence, integrating $P(x_1x_2)$ with respect to x_1 and x_2 within the limits from 0 to ∞, it is easy to find the total probability of both x_1 and x_2 being positive [7]:

$$w_{++} = \int_0^\infty \int_0^\infty P(x_1, x_2)\, dx_1 dx_2 = \frac{1}{4}\left(1 + \frac{2}{\pi} \arcsin R\right). \tag{8}$$

It can be easily seen that the probabilities of various sign combinations are correlated by the relationships $w_{++} = w_{--} = \frac{1}{2} - w_{+-} = \frac{1}{2} - w_{-+}$. It is evident that when $r_0 = 1$ this is the actual value of the average current at the output. Thus for normally correlated noise it is also true that the relative excess above the constant (uncorrelated) component $i_0 = \frac{1}{4}$ is a direct measure of the correlation coefficient.

Since under these conditions rectangular signals are fed to the relay inputs, it may be said that when there is nonlinear conversion in the amplifier-limiters the correlation coefficient will become equal to R_p*

* It can be shown that the correlation ratio P also changes after conversion and is again equal to the correlation coefficient (as it was for normal correlation before conversion) $P_p = R$. This is valid for any processes which are symmetrically distributed with respect to sign, namely, if $w_{++} + w_{--} = w_{+-} + w_{-+} = 1/2$. Such a result can be assumed to be a consequence of the fact that under the indicated conditions the regression remains rectilinear after conversion.

(see Formulas (7) and (8)):

$$R_p = \frac{2}{\pi} \arcsin R_n \tag{9}$$

For weak correlation $\arcsin R_n \approx R_n$ the difference between the readings of the instrument for the two examined types of signals consists of the fact that in the formula

$$\bar{i} = \frac{1}{4}(1 + \alpha R) \tag{10}$$

$\alpha = 1$ in one case, and $\alpha = \frac{2}{\pi} \approx 0.637$ in the other case.

Thus the output effect (and therefore the readings of the indicator as well, contain two components, one of which (i_0) does not depend either upon R or upon the intensity of the signals (and is a constant quantity for the given instrument), and the second of which $i_k = \frac{1}{4}\alpha R$ is completely determined by the correlation of the input factors.

If each of the examined processes $x_1(t)$ and $x_2(t)$ can be decomposed into a sum of two noise signals:

$$x_1(t) = u_1(t) + v_1(t), \quad x_2(t) = u_2(t) + v_2(t), \tag{11}$$

and if

$$\overline{u_1 v_1} = \overline{u_1 v_2} = \overline{u_2 v_1} = \overline{u_2 v_2} = 0, \tag{11a}$$

(i.e., if the noise signals which are summed in each channel are mutually independent), then the correlation coefficient is equal to

$$R_x = \frac{\overline{x_1 x_2}}{\sqrt{\overline{x_1^2}\,\overline{x_2^2}}} = \frac{\overline{u^2} R_u + \overline{v^2} R_v}{\overline{u^2} + \overline{v^2}}. \tag{12}$$

Here $R_u = \frac{\overline{u_1 u_2}}{\sqrt{\overline{u_1^2}\,\overline{u_2^2}}}$ $\quad R_v = \frac{\overline{v_1 v_2}}{\sqrt{\overline{v_1^2}\,\overline{v_2^2}}}$ are the autocorrelation coefficients of the processes $\underline{u}$ and $\underline{v}$ respectively. Substituting Equation (12) into Equation (8), we obtain the probability $\underline{w}$ as a function of the ratio between the intensities of the processes $\underline{u}$ and $\underline{v}$ and of their correlation coefficients:

$$w_{++} = \frac{1}{4}\left[1 + \frac{2}{\pi} \arcsin \frac{\overline{u^2} R_u + \overline{v^2} R_v}{\overline{u^2} + \overline{v^2}}\right]. \tag{13}$$

In the case when $R_u = 0$ and thus u_1 and u_2 are not correlated with one another (i.e., they are independent noises, such as the noises of the tubes in the instrument etc.), the correlation coefficient between x_1 and x_2 is equal to

$$R_x = \frac{\overline{v^2}}{\overline{v^2} + \overline{u^2}} R_v \tag{14}$$

and the relative excess above the constant component i_0 of the input effect of the device will be equal to

$$\frac{i_R}{i_0} = \frac{2}{\pi} \arcsin \frac{\overline{v^2}}{\overline{v^2} + \overline{u^2}} R_v. \tag{15}$$

If one of the processes [for example, v(t)] is a periodic function of time, then R_v is also a periodic function of τ; here the output current of the device also has a periodic component. This is sufficient in order for the instrument to be utilized in the capacity of a detector for periodic signals when interference is present. Of course it is impossible to assume that Formula (15) is valid if the distribution v(t) is not normal. However when $\overline{v^2} \ll \overline{u^2}$, and if the distribution $\underline{u}$ is normal, then the distribution $\underline{x}$ is also sufficiently close to normal and we shall again have [see below, Formula (18)]:

$$i \simeq \frac{1}{4}\left(1 + \frac{2}{\pi} \frac{\overline{v^2}}{\overline{u^2}} R_v\right). \tag{16}$$

The maximum relative excess of the correlation coefficient of the output effect (this maximum value occurs when $R_v = 1$) is equal to

$$i_{R\max} = \frac{2}{\pi} \frac{\overline{v^2}}{\overline{u^2}}. \tag{17}$$

However if the distributions P(v) and P(u) are not normal either for $\underline{v}$ or for $\underline{u}$, but $\overline{u^2} \gg \overline{v^2}$, then the following formula * is again valid (as can easily be proven):

$$w_{++} = \frac{1}{4}(1 + \alpha R), \text{ where } \alpha = 4P^2(0)\,\overline{u^2}. \tag{18}$$

* The total probability of operation for conditions under which the inequalities $u_1 > -v$ and $u_2 > -v$ are in effect is equal to

$$w_{++} = \int_{-\infty}^{+\infty} P(v)\,dv \int_{-v}^{\infty} P(u_1)\,du_1 \int_{-v}^{\infty} P(u_2)\,du_2.$$

Since by definition $\overline{u^2} \gg \overline{v^2}$ and P is an even function, it follows that

$$\int_{-v}^{\infty} P(u_1)\,du_1 = \int_{0}^{\infty} + \int_{0}^{v} = \frac{1}{2} + \int_{0}^{v} P(u_1)\,du_1 \simeq \frac{1}{2} + vP(0);$$

therefore

$$w_{++} = \frac{1}{4}[1 + 2vP(0)]^2,$$

whence we obtain Equation (18).

Thus if u obeys a normal law, then $P(0) = \frac{1}{\sqrt{2\pi}\bar{u}_2}$, $\alpha = \frac{2}{\pi}$; in other cases it is necessary to calibrate the instrument.

The sensitivity of the instrument (i.e., the possibility of measuring small variations in the correlation coefficient) is limited first of all by the stability of the average value of the constant component $i_0 = \frac{1}{2}$ in Formulas (7), (8), (10) or (18). Fluctuations in this quantity (which does not depend upon the intensity of the noise signals being studied) in turn (as we shall show) do not depend upon fluctuations in the intensity. They are associated solely with the finite observation time T and are determined by the mean frequency characteristic of the noise. These fluctuations can be roughly evaluated in the following manner. The number of positive pulses which are fed per unit time from each channel to the terminal relay is equal to one-half the number of passages through zero per unit time. But for an ideal band-pass filter the number of zeros in one second is equal to [see [2], Formulas (3) - (12)]

$$2\left[\frac{1}{3}\frac{f_b^3 - f_a^3}{f_b - f_a}\right]^{\frac{1}{2}}, \tag{19}$$

where f_a, f_b are respectively the lower and upper boundaries of the spectrum. Approximately, (with an accuracy of up to a coefficient of the order of unity), this number can be considered equal to $f_b + f_a$. Therefore the number of pulses per unit time in each channel will be of the same order of magnitude, and the number ν of pulses per unit time in the terminal unit is approximately twice as large as this number (as we can easily show), and is thus approximately equal to

$$\nu \simeq (f_b + f_a). \tag{20}$$

The number of pulses in the terminal unit during the averaging time T is νT, and the relative fluctuation of this number is $1/\sqrt{\nu T}$. The relative fluctuation of the constant component i_0 is of the same order of magnitude. If we assume that the indicator is able to distinguish between differences ΔR in the correlation coefficient R which are such that they produce a variation in the average current which is no less than its mean-square fluctuations, then for normal noise it must follow that [in accordance with Equations (8) and (20)]

$$\Delta \frac{2}{\pi} \arcsin R = \frac{2}{\pi}\frac{1}{\sqrt{1-R^2}}\Delta R \geqslant \frac{1}{\sqrt{(f_a + f_b)T}}, \tag{21}$$

i.e., the smallest variation which is still distinguishable is equal to

$$(\Delta R)_{\min} \simeq \sqrt{\frac{1-R^2}{(f_a + f_b)T}}. \tag{22}$$

The instrument, as we can see is especially sensitive to the appearance of a small disturbance in an almost complete correlation, when $(1 - R) \ll 1$. In general it is true that in the audiofrequency region (for example, when $f_a + f_b \sim 3000$ and when the averaging time is of the order of one second) the correlation coefficient can be measured with an accuracy of up to several percent provided that the conversion of the input voltages by the amplifier-limiter channels is ideally rectangular. Making use of both polarities (++ and −−) in order to form the coincidence pulses, it is possible to decrease the relative fluctuations at the output of the

of the instrument by $\sqrt{2}$ times by means of doubling the number of integrated pulses.

In a practical design of the instrument care should be taken to make the frequency-phase characteristics of the conversion channels identical and to maintain a constant zero line i.e., we must achieve amplification and symmetrical limiting without forming dc components at various levels; the complete identity of the gain coefficients is not required. In addition, we should strive to achieve electrical independence between channels. The causes of mutual coupling, which leads to parasitic correlation inside the instrument, may be due to coupling through common supply sources, as well as to inadequate screening. The requirements which are imposed upon the gain coefficient K (without taking the limiting into account) are of especial interest. For small values of K or for a weak input signal x_1^2 trapezoidal pulses of the same height will be obtained at the output of the conversion channel instead of rectangular pulses with a height V_0. It can be proven that in this more general case when the correlation is complete (the worst case) the ratio between the output current and the current which obtains when there is no correlation whatsoever is not equal to two but is equal to

$$\frac{i_{R=1}}{i_{R=0}} = 2\left[1 - \frac{V_0}{V\sqrt{2\pi K}\sqrt{x_1^2}}\right]. \qquad (23)$$

Having specified the accuracy requirements of the instrument, it is possible to determine the required value of the gain coefficient K from this formula. Thus, when $\sqrt{x^2} = 10^{-2}$ v, $V_0 = 1$ v a gain coefficient of $K \approx 5 \cdot 10^4$ is required in order to obtain an accuracy of 1% $\left(\frac{i_{R=1}}{i_{R=0}} = 2\,[1 - 0{,}01]\right)$. The value of V_0 is selected in such a way that the condition $V_0 > E$ is fulfilled, where E is the operating threshold for the output coincidence circuit.

Figure 3 shows the circuit of one of the correlometers which we have built and which is based upon the indicated principles. The types of tubes utilized are indicated in the figure. The over-all gain of each channel is equal to $3.5 \cdot 10^6$. In order to attain identical phase characteristics for each of the channels a phase correction ($R_{11}C_6C_9C_{13}$) is provided for. At the output of the circuit the tubes which select the coincidence of signs (− −) operate without negative bias. The positive pulses from the output of the channels do not appear in the output unit*.

The resultant output effect which obtains after integration is recorded by the Neiman level recorder (which uses a linear potentiometer) by means of an auxiliary oscillator which operates at 800 cps and a ring modulator. In addition, the output circuit contains pointer instruments with time constants of the order of 1 and 0.1 sec. The instrument usually operates for input voltages which lie in the range from 100 microvolts to 300 millivolts ($\sqrt{x^2(t)}_{min} = 10^{-4}$ v) in the frequency range of 80-100 cps. The external view of the instrument is shown in Fig. 4.

The correlometer described here was used for the solution of various problems. a) For obtaining the autocorrelation functions of various types of noise. The noise being studied was fed to the inputs of the instrument with a relative time shift τ. The shift was achieved either by an electrical delay line or by spacing the input microphone in the sound field. As an example, Fig. 5 compares the computed curves for the probability $w = \bar{1}$ and the autocorrelation coefficient R for a constant-intensity spectrum in the frequency range 400-800 cps (solid lines) with the experimental results obtained for the noise which is segregated from thermal noise by a band-pass filter which has the same frequency boundaries. Curve 1 yields a directly measured probability of $\bar{1} = i_{\Delta} w_{--}(\tau)$, and Curve 2 yields the correlation coefficient which is determined in accordance with Formula (8) in the following manner for normal correlation:

$$R(\tau) = \sin\left[\frac{\pi}{2}(4\bar{i} - 1)\right]. \qquad (24)$$

* In another circuit variant we made use of a bipolar output circuit which simultaneously used two sign coincidences: (++) and (− −).

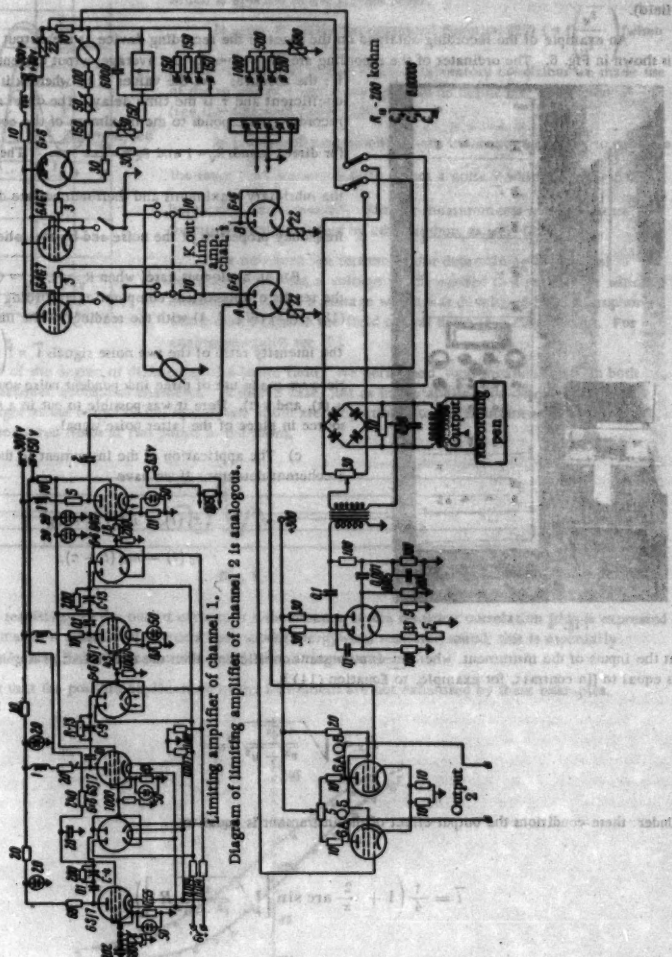
Limiting amplifier of channel 1.
Diagram of limiting amplifier of channel 2 is analogous.
K. out lim. ampl. chan. 1
Output recording pen
Output 2

The curves $R(\tau)$ which are obtained in this manner have already been given in [1]. b) The measurement of the mutual correlation between two noise signals each of which is the sum of two noise signals [see Formulas (11) and (11a)]. Such a case was encountered by us in architectural acoustics when we attempted to measure the correlation between the sound pressures at two points in a closed room (in the presence of a so-called diffuse field).

An example of the recording obtained on the sheet of the recording device at the output of the instrument is shown in Fig. 6. The ordinates of the recording are the values for the average output current of the instrument $\bar{i}$; the abscissas are the values of $k\tau$ where k is a proportionality coefficient and τ is the time delay. The chief maximum on the recording corresponds to the maximum of the correlation coefficient for direct sounds $R_v = 1$ and $R_x = \frac{\overline{v^2}}{\overline{v^2 + u^2}}$. The magnitude of the subsidiary maximums and their number are determined by the frequency properties of the noise and by the ratio $\frac{\overline{v^2}}{\overline{u^2}}$.

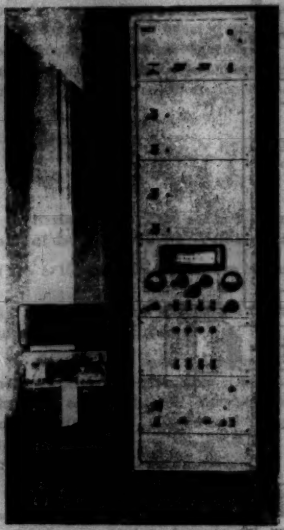

Fig. 4

For an analogous case, when $R_v = 1$, $R_u = 0$, we compared the results of theoretical computation according to Formulas (13) - (15) (Fig. 7, 1) with the readings of the instrument when the intensity ratio of the two noise signals $\bar{i} = f\left(\frac{\overline{v^2}}{\overline{u^2}}\right)$ was varied. Here we made use of three independent noise sources, $u_1(t)$, $u_2(t)$, and $v(t)$. Here it was possible to cut in a sinusoidal voltage source in place of the latter noise signal.

c) The application of the instrument in the capacity of a coherent detector. If we have

$$x_1(t) = u(t) + v(t),$$
$$x_2(t) = mv(t + \tau), \tag{25}$$

at the inputs of the instrument, where m is a constant coefficient, then the coefficient of mutual correlation is equal to [in contrast, for example, to Equation (14)]

$$R_x = \sqrt{\frac{\overline{v^2}}{\overline{v^2 + u^2}}}\, R_v. \tag{26}$$

Under these conditions the output effect of the instrument is equal to

$$\bar{i} = \frac{1}{4}\left(1 + \frac{2}{\pi} \arcsin\left[\sqrt{\frac{\overline{v^2}}{\overline{v^2 + u^2}}}\, R\right]\right) \tag{27}$$

and we are actually utilizing the instrument in the capacity of a coherent detector. In that case the signal $v(t)$ which is fed to one of the inputs against the background of the interference $u(t)$ is detected at the output

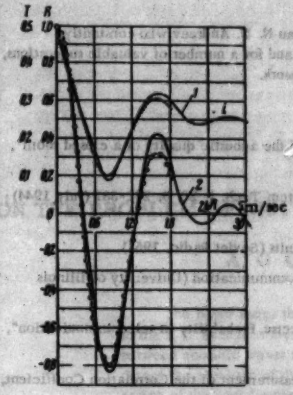

Fig. 5

of the instrument when τ is varied smoothly because of the mutual correlation with the voltage from the local source $x_g(t) = mv(t + \tau)$ which is applied to the second input.

In order to verify the computed Function (27) $i = f\left(\frac{\overline{v^2}}{\overline{u^2}}\right)$ [when $R_{xy} = 1$ –Curve 2 in Figure 7] under laboratory conditions we made use of the values of v which lay up to 20 db below the "interference" u (see the points on Curve 2, Fig. 7).

In individual experiments where it was not necessary to measure the ratio $\frac{\overline{v^2}}{\overline{u^2}}$ we wer able to detect a noise v which lay 40-45 db below the "interverence". Similar measurements for correlation functions were published by other authors as well [8, 9].

We also used the instrument for determining the mutual correlation between a voltage which was fed to a reproducer which emitted noise, and a voltage which was developed by a microphone which was placed in the field of that noise in a closed room. For analogous results see [9].

d) The evaluation of the degree of diffuseness of a sound field. We performed such measurements in both reverberant and deadened acoustical chambers. In such a case, just as in the application described in part (b), we have voltages at the output of the instrument which are proportional to the resultant sound pressures of the direct and scattered fields at two points in the room.

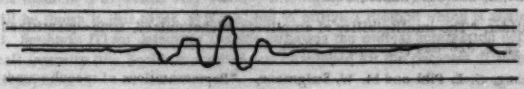

Fig. 6

The special sensitivity of the output current to a disturbance in the resultant correlation [this is expressed by Formula (22)] makes it possible to detect a very weak (energywise) scattered sound; this is especially important in investigating fields in deadened acoustic measuring chambers.

It is evident that the possible applications of the instrument are not exhausted by these examples.

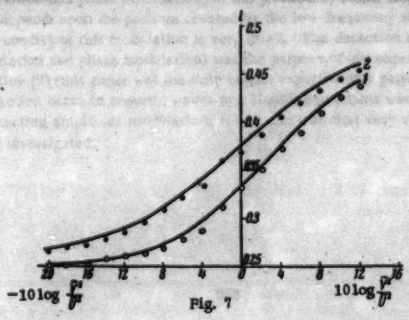

Fig. 7

In conclusion the authors express their appreciation to Academician N. N. Andreev who constantly showed great interest in this paper, to V. S. Grigor'ev for his great help and for a number of valuable suggestions, and to N. S. Antonov for his creative participation in the experimental work.

LITERATURE CITED

[1] S. G. Gershman, "The correlation coefficient as a criterion of the acoustic quality of a closed room", J. Tech. Phys. (USSR) 21, 11, 1492-1496 (1951).

[2] S. O. Rice, "Mathmatical analysis of random noise", Bell. System Tech. J. 23, 3, 282-332 (July, 1944); 24, 1, 41-156 (January, 1945).

[3] V. I. Bunimovich, Fluctuation Processes in Radio-Receiving Units (Soviet Radio, 1951).

[4] C. E. Shannon and W. Weaver, The Mathematical Theory of Communication (University of Illinois Press, 1949) pp. 3-89.

[5] Ph. M. Woodward and I. L. David, "Information theory and inverse Probability in telecommunication", Proc. IRE, 99, part III, 58, 37-44 (March, 1952).

[6] E. L. Feinberg and S. G. Gershman, Method for the Direct Measurement of the Correlation Coefficient, Patent Certification No. 4010, September 13, 1950.

[7] S. N. Bernshtein, Theory of Probability (State United Press, State Tech. Press, 1946).

[8] I. W. Lee, Cheatham and Wiesner, "Application of correlation analysis to the detection of periodic signals in noise", Proc. IRE 38, 10, 1165-1171 (1950).

[9] Kenneth W. Goff, "The application of correlation techniques to some acoustic measurments", J. Acoust. Soc. Amer. 27, 2, 236-246 (March, 1955).

[10] I. C. R. Licklider, "The intelligibility of amplitude-dichotomized, time-quantitized speech waves", J. Acoust. Soc. Amer. 22, 6, 820-824 (November, 1950).

[11] Sze-Hou Chang, G. E. Pihl and M. W. Essigmann, "Representations of speech sounds and some of their statistical properties", Proc. IRE, 39, 2, 147-153 (1951).

[2, 4, and 5] have been translated into Russian; see Theory of the Transmission of Electrical Signals in the Presence of Interference, Collected Translations (Foreign Lit. Press, 1953). Abridged Contents of [11] are contained in Problems of Modern Physics (Acoustics) (Foreign Lit. Press, 1952).

Acoustics Institute of the Acad. Sci. USSR, Moscow

Received June 28, 1955

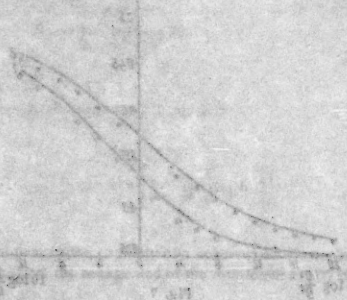

ON THE PROBLEM OF MUTUAL INTERACTION BETWEEN SOUNDWAVES

A. G. Gorelik and V. A. Zverev

The paper shows the possibility of utilizing a method which is analogous to the I. L. Bershtein method [1] for detecting and investigating the interaction between acoustic waves in liquids. This method makes it possible not only to detect the presence of the very small modulation which is caused by the interaction of the soundwaves, but also to determine the nature of this modulation (amplitude modulation, phase modulation). Control experiments are performed which verify the fact that the modulation is caused by interaction between acoustic waves.

For ordinary (not very large) intensities the interaction between acoustic waves which is caused by the nonlinearity of the medium is expressed very weakly, and highly sensitive equipment is required for its detection. As will be shown in this paper, it is possible to utilize a method which is analogous to the one developed by I. L. Bershtein [1] for detecting and investigating the mutual interaction between acoustic waves which have a small intensity (the Bershtein method was developed for the purposes of investigating small phase variations in radiophysics).

Let us examine (Fig. 1) a standing ultrasonic wave of frequency ω which is formed in a column of water between a quartz radiator A and receiver B. When the distance between them is equal to a whole number of halfwaves, resonance occurs in the column of water. Let a radiator C (a hydrophone) create an acoustic wave of frequency Ω (here $\Omega < \omega$), which is propagated in a direction perpendicular to AB. Due to the nonlinearity of the medium periodic (at a frequency Ω) variation of the parameters (density, temperature, absorption coefficient, etc.) of the water column AB takes place under these conditions; this in turn leads to modulation (both amplitude modulation and phase modulation) of the pressure upon the receiver B. The magnitude of this modulation naturally depends upon the pressure created by the low-frequency radiator C. As computation shows, under ordinary conditions this modulation is very small. The detection and investigation of this modulation (both amplitude modulation and phase modulation) was the purpose of our experiments. Let us note that in the paper by G. L. Mikhailov [2] (this paper was the only earlier experimental paper which we knew to be devoted to the nonlinear interaction between acoustic waves in a liquid) equipment was used which was only practical for the purposes of detecting amplitude modulation; it was also true that very viscous liquids (for example, glycerine) were being investigated.

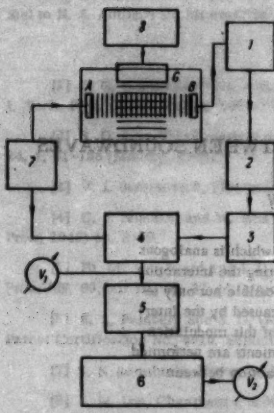

Fig. 1. Over-all block diagram of the unit: 1) High-frequency amplified, 2) attenuator, 3) phase-shifter, 4) balancing network, 5) detector, 6) low-frequency resonant amplifier, 7) standard signal generator, 8) audio-signal generator, V_1 is a VKS-7 voltmeter, V_2 is a vacuum-tube voltmeter.

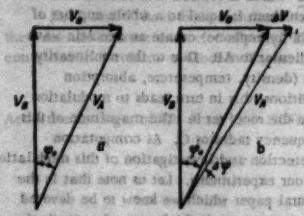

Fig. 2. Voltage diagram illustrating how the voltages are added at the input to the detector.

The idea of the method used by us here is clarified by means of the vector diagram shown in Fig. 2. The vector V_A depicts the electric voltage which is tapped directly from the radiating quartz, the vector V_B is the voltage obtained from the acoustic receiver through the amplifier and phase-shifter when the low-frequency radiator is cut out. These voltages are fed to the input of the balancing network. A difference voltage depicted by the vector V_0 is formed at the output of the latter (the block diagram of the electrical section of the unit is shown in the same Fig. 1). Now let phase and (or) amplitude modulation of the receiver pressure B (and therefore of the voltage V_B as well) appear as a consequence of cutting in the low-frequency radiator C. As a consequence of this the amplitude of V_0 will vary periodically. If we feed the wave V_0 to the input of the detector, then when modulation is present the output current of the latter will have a component of frequency Ω.

The method used here makes it possible not only to detect the presence of modulation (even very weak modulation) but also to determine its nature (amplitude modulation or phase modulation).

In order to distinguish between amplitude modulation and phase modulation it is possible to make use of the following method. If a small phase difference φ_0 is fixed between the voltages V_A and V_B and then if a minimum in V_0 is achieved by controlling the magnitude of V_B (this case is shown in Fig. 2,a), then the magnitude of V_0 will be very insensitive to a variation in the magnitude of V_B. However if the magnitudes of V_A and V_B are fixed so that a small difference exists between them and if a minimum in V_0 is achieved by varying the angle φ_0 (this will occur when $\varphi_0 = 0$) then the magnitude of V_0 will be very insensitive to a variation in φ_0. Thus by adjusting V_0 to a minimum by varying the amplitude of V_B we shall adjust the unit to receive phase modulation; adjusting V_0 to a minimum by varying the phase φ_0 we shall adjust the unit to receive amplitude modulation. In order for the sensitivity of the detector to be constant during such a process it is necessary to maintain the amplitude of V_0 constant.

Thus the circuit which we used makes it possible to analyze the type of modulation of the V_B -wave by increasing the depth of the existing amplitude modulation by an appropriate adjustment, or, using another adjustment, by changing the existing phase modulation into amplitude modulation.

The fluctuation sensitivity limit when measuring phase modulation by the method indicated here was evaluated by I. L. Bershtein [3].

Let the phase variation occur according to a sinusoidal law:

$$\Delta\varphi = \alpha \cos \Omega t \qquad (\alpha \text{ is constant})$$

Then the fluctuation limit is expressed in terms of the formula

$$\alpha_{min} = \frac{2}{bV_B}\sqrt{I_0 e \gamma \Delta F},$$

where I_0 is the dc component of the plate current I of the detector tube, γ is the depression coefficient averaged over a period, e is the charge on an electron, Δf is the pass band of the filter at the output of the detector,

$$b = \left(\frac{dI}{dV}\right)_{V=V_0}.$$

Let V_B = 10 v, b = $4 \cdot 10^{-3}$ amp/ v, $I_0 = 8 \cdot 10^{-3}$ amp, γ = 0.3, ΔF = 1 cps. In that case $\alpha_{min} = 4 \cdot 10^{-4}$ angular seconds.

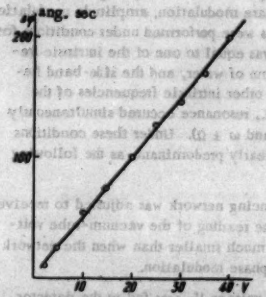

Fig. 3. Graph for the phase modulation (in angular seconds) as a function of the voltage which is applied to the low-frequency acoustic radiator.

In our experiments there was no necessity in striving to attain the fluctuation limit, since we obtained a value of α of the order of several tens of angular seconds or greater (Fig. 3).

We used identical quartz plates tuned to a frequency of 1.5 megacycles in the capacity of acoustical radiator and receiver. The voltage source which supplied the radiating quartz was a standard signal generator of the type GSS-6 which was also tuned to a frequency of 1.5 megacycles. The radiating quartz was connected in series with an inductance, and this made it possible to apply a voltage of 30v to it. The voltage obtained from the quartz receiver was amplified by a high-frequency resonant amplifier and was applied to one of the balancing network arms through a phase-shifter. A signal obtained directly from the GSS-6 signal generator was applied to the other arm of the balancing network. The balancing network was based upon two 6AC7 tubes that worked into a common plate load which consisted of a tuned circuit. The difference signal V_0 is developed across the tuned circuit and is then applied to the detector input. The current component with the frequency Ω is segregated at the output of the detector by an amplifier which is tuned to this frequency ($4 \cdot 10^3$ cps). Our amplifier had a pass band of 5-7 cps and a voltage gain of up to $2 \cdot 10^4$. The presence of the signal having the frequency Ω at the output of the amplifier was observed by means of the vacuum-tube voltmeter.

The calibration of the unit was performed in the following manner. When the low-frequency acoustic source was cut out a signal from the GSS-6 signal generator was applied to the radiating quartz; this signal was amplitude modulated to a known depth. Only the signal from the acoustic receiver was applied to the input. By controlling its magnitude by means of an attenuator, we achieved a situation where it received a value of V_0 which was the same as the difference signal which was obtained when measuring the modulation. Then we obtained the relationship between the readings of the voltmeter and the depth of amplitude modulation. To a sufficient degree of accuracy this function proved to be linear.

Let us now pass on to a description of the experiment which showed the presence of modulation that was caused by the interaction between a low-frequency wave and a high-frequency wave. An unmodulated wave is applied to the radiating quartz from the GSS-6 signal generator. The electrical voltages from both the radiator and the receiver (after passing through an amplifier) are fed to both arms of the balancing network. As long as the low-frequency radiator is off, the vacuum-tube voltmeter reads zero. When the low-frequency radiator is turned on, the pointer of the vacuum-tuve voltmeter deflects, and the deflection of the pointer of the vacuum-tube voltmeter is proportional to the voltage applied to the radiator. Figure 3

shows the resulting experimentally-obtained linear relationship between the magnitude of α (the amplitude of the periodic phase variation of the high-frequency sound) and the voltage applied to the low-frequency radiator. Let us note that at a voltage of 10v the low-frequency radiator used in our experiments (a radiator of the electrodynamic type) required a power of 0.1 watts.

A great deal of attention was devoted to proving that the observed effect - the reading of the vacuum-tube voltmeter-actually represented the result of the interaction between acoustic waves and not a subsidiary effect produced in the equipment.

In particular, the following experiments were performed.

1. The low-frequency sound beam was blocked. Under these conditions the voltmeter read zero. This proved that electrical induction effects played a negligible role.

2. The high-frequency sound beam was blocked. The voltmeter read zero when the high-frequency beam was blocked at any point. This proved that the equipment responded only to modulation and not to a weak signal of frequency Ω which might possibly fall upon the receiving quartz due to scattering effects.

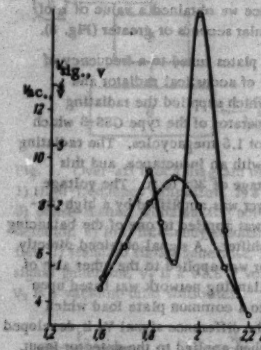

Fig. 4. Amplitude-modulation depth as a function of the frequency ω. The solid curve represents the readings of output instrument, the dash-dot line represents the variation of the voltage across the acoustic receiver. The left-hand ordinate scale represents the voltage across the acoustic receiver, the right-hand scale represents the voltage across the output vacuum-tube voltmeter.

Experiments were performed in analyzing the type of modulation obtained (phase modulation, amplitude modulation). A series of measurements were performed under conditions for which the frequency ω was equal to one of the intrinsic frequencies ω_n of the column of water, and the side-band frequencies $\omega \pm \Omega$ equalled other intrinsic frequencies of the water column $\omega_{n \pm 1}$ (i.e., resonance occured simultaneously at three frequencies: ω and $\omega \pm \Omega$). Under these conditions phase modulation was clearly predominant, as the following experiments showed:

1. When the balancing network was adjusted to receive amplitude modulation the reading of the vacuum-tube voltmeter at the output was much smaller than when the network was adjusted to receive phase modulation.

2. When only the voltage V_B was fed to the detector from the quartz receiver (without passing through the balancing network) the voltmeter read practically zero.

When the frequency ω varied (deviation from resonance) strong amplitude modulation appeared. The dependence of the depth of the amplitude modulation upon the frequency ω is shown in Fig. 4. The solid line depicts the readings of the output voltmeter. The dashed line shows the corresponding values of V_B (the resonant curve of the water column).

The observed phenomena can easily be explained if we assume that the chief role in our experiment is played by the periodic variation in the propagation velocity of the wave (and not in the absorption coefficient), due to the effect of the wave Ω and therefore by the periodic variations in the tuning of the water column AB. If this column is tuned to resonance, a small detuning effect varies only the phase of its oscillations (to a first approximation). However if the water column is not at resonance a small additional detuning effect produces a noticeable change in the amplitude of the vibrations as well.

LITERATURE CITED

[1] I. L. Bershtein, "San'lak's experiment with radiowaves," Doklady Akad. Nauk SSSR 75, 635 (1950).

[2] G. D. Malkhalov, "The interaction of ultrasonic waves in liquids," Doklady Akad. Nauk SSSR 89, 663 (1953).

[3] I. L. Bershtein, Dissertation, Institute of Radio-Engineering and Electronics of the Acad. Sci. USSR, 1955.

Gor'kii Physico-Engineering Research Institute of the
Gor'kii State University

Received May 4, 1955

THE APPLICATION OF A COMPOSITE PIEZOELECTRIC DIPOLE IN INVESTIGATING THE MECHANICAL PROPERTIES OF POLYMERS

I. G. Mikhailov and V. A. Solov'ev

The composite-dipole method in its usual form is impractical for investigating materials with high losses and low sound velocities (polymers). In order to solve this problem we propose to use specimens with a small cross-section (smaller than the cross-section of the piezo-crystal). The possibility of working with such specimens is proven in practice. Certain results are given which were obtained by this method. It is found, for example, that stretched specimens of vinyplast exhibit elastic anisotropy.

The method of investigating Young's modulus and the mechanical losses in solid bodies by means of a composite piezoelectric dipole has been utilized by many authors (see, for example, [1]). The most widely used variant of this method is the one in which the dipole is a piezoquartz rod of rectangular cross-section whose length is directed along the Y axis of the crystal, and whose thickness and width are directed along the X(electrical) and Z (optical) axes respectively. Under these conditions metallic electrodes are deposited upon the large boundary surfaces (those perpendicular to the X axis). The rod is supported by means of wire threads which are soldered to the electrodes at their centers (the nodal points of the displacements when vibrations occur). These same wire threads are utilized to supply an ac voltage to the electrodes. The electric field which is directed along the thickness of the rod (the X axis of the crystal) causes a tension-compression deformation to occur along the Y axis. A specimen of the investigated material in the form of a rod of equal cross-section is glued onto a cross-sectional cut of the original rod. In this usual variant of the method the length of the specimen is chosen in advance so that the resonant vibration frequencies of the quartz and of the specimen are approximately coincident (in practice, coincidence within limits of 5-10% is sufficient). The inconvenience of this preliminary adjustment is compensated by a number of substantial advantages. In the first place, when the length of the specimen is selected in this manner the nodal plane of the oscillations of the composite dipole almost coincides with the center of the quartz rod (i.e., there is no necessity of changing the support points). In the second place, since the resonant frequency of the dipole is close to the resonant frequency of the quartz, it is possible to obtain large vibration amplitudes. Finally, the computations are greatly simplified in such a case.

The magnitude of the displacement current through the quartz at a frequency ω which is close to the resonant frequencies of the quartz Ω and of the specimen Ω_0, is equal to

$$I = \left[i\omega C_0 + \frac{4(eb)^2}{l(m+m_1)(\omega-\Omega_0)+\pi(XS+X_1S_1)}\right]V, \qquad (1)$$

where V is the voltage; C_0 is the static capacitance between electrodes. The second term yields the current which is associated with the piezoelectric polarization of the quartz. Here e is the piezoelectric constant, b is the width of the electrodes, S and S_1 (these quantities are equal) are the cross-sectional areas of the quartz and the specimen, m and m_1 are their masses. The material of the rods is characterized by complex Young's moduli $E = E' + iE''$ and $E_1 = E_1' + iE_1''$ (the imaginary part characterizes the losses), by sound velocities c and c_1, and also by acoustic impedances $Z = \sqrt{\rho E} = \rho c + iX$ and $Z_1 = \rho_1 c_1 + iX_1$ (ρ and ρ_1 are densities). The resonant frequencies of the rods are equal to $\Omega = \pi \frac{\nu}{l}$ and $\Omega_1 = \pi \frac{\nu_1}{l_1}$, where l and l_1 are the lengths of the rods (we are only examining the first harmonics). The resonant frequency of the composite dipole is equal to

$$\Omega_0 = \frac{\Omega m + \Omega_1 m_1}{m + m_1}. \qquad (2)$$

The equivalent electrical circuit corresponding to Equation (1) consists of a series RLC circuit and a shunt Capacitance C_0, where

$$L = \frac{m + m_1}{8\,(eb)^2}, \quad R = \frac{\pi (XS + X_1S_1)}{4\,(eb)^2}, \quad C = \frac{1}{\Omega_0^2 L}. \tag{3}$$

In order to measure the parameters of the equivalent circuit of the dipole it is connected in series with a small resistance (in our unit the resistance was equal to 100 ohms) to an oscillator which can be smoothly tuned over a sufficiently wide range. Then the vacuum-tube voltmeter is used to measure the voltage across the dipole and the current through it at frequencies which correspond to the maximum and minimum admittances. These frequencies, which can be called (the nomenclature is not completely rigorous here) the resonant and antiresonant frequencies ω_r and ω_a, are measured by a heterodyne wavemeter. The computations are performed according to the formulas

$$\Omega_0 = \omega_r + (\omega_a - \omega_p)\frac{I_a}{I_a + I_p}, \quad R = \frac{V}{I_p - I_a}, \quad \Omega_0 C_0 = \frac{\sqrt{I_a I_p}}{V}, \tag{4}$$

$$C = C_0 \cdot \frac{2(\omega_a - \omega_p)}{\Omega_0} \cdot \frac{I_p - I_a}{I_p + I_a}, \quad L = \frac{1}{\Omega_0^2 C}.$$

From measurements which are taken with the unloaded quartz, its resonant frequency Ω and its losses X are determined. On the basis of Formula (3) we then determine Ω_0 and X_1 and compute c_1. The coefficient (eb) is found from the formula for L_1.

In addition to the indicated methods still other methods for measuring the parameters for the equivalent circuit are available, but they are more complex and are used less often.

The majority of work which is done according to the method described above is associated with metals and crystals (i.e., with metals which have a sufficiently high sound velocity and small losses). We made an attempt to apply this method to the investigation of the mechanical properties of high-polymers in the frequency range of from 10^6 to 10^8 cps, since for the time being there are no other methods which are useful in this frequency range*. However, its application with respect to polymers encounters a series of important difficulties. First of all, Formulas (4) are only applicable when the losses are not too large (i.e., when $(\omega_a - \omega_r) C_0 \ll \frac{1}{X}$ and when it is possible to assume that the quantity ωC_0 is constant within the limits of the resonant curve). If, as is the case with the majority of polymers, this condition is not fulfilled, then Formulas (4) yield a value for R which is too large. The nature and magnitude of the error in determining Ω_0 is difficult to evaluate, since the equation for the extremal frequencies proves to be of the fifth degree; in any case, Formula (4) cannot be utilized.

Thus the results of the paper by Rinehart [2] in which $I_r - I_a$ comprised several percent of $\sqrt{I_r I_a}$ are obviously in error. The same is true of the results obtained by Subrahmanyam [3], at least for polymethylmethacrylate at high temperatures (according to our measurements, the losses in polymethylmethacrylate are so large even at 50-60° C that Formulas (4) are no longer valid). Further, a source of error is the small sound velocity in polymers which in turn gives rise to a small wavelength in the specimen. When the cross-sectional dimensions of the specimen are comparable to a wavelength the resonant frequency is lowered due to the inertia of the vibrations along the thickness of the specimen.

---

* We know only four papers in which polymer-type substances were examined by means of a composite dipole. Two of them [2, 3] evidently contain errors, and in the two other papers [4, 5] certain special variants of the method were used which, in our opinion, are the less convenient and less accurate.

In [3] the correction for the cross-section should have comprised approximately 10 m/sec. (The authors of this paper erroneously assumed that the correction could be diminished if the system is operated on the third harmonic, i.e., if a longer specimen is used.) In many cases the wavelength is so small that the resonant frequency of the transverse vibrations proves to be close to the working frequency; then measurements are entirely impossible.

In order to eliminate these errors we attempted to use specimens with a cross-section S_1 which was less than the cross-section S of the quartz. Similar measurements have already been made [5], but this modified method requires thorough verification. An accurate theoretical solution of the problem involving the vibrations of rods having a finite width is impossible, and such a solution is replaced by an approximate unidimensional problem. For unequal cross-sections difficulty arises in formulating the boundary conditions at the quartz-specimen boundary. The condition requiring the equality of the displacements at each point must be replaced by the far from obvious condition requiring the equality of displacements which are averaged over the cross-section.

In formulating the conditions for the voltages, two postulates are possible.

1. If we assume that the end-face surfaces are not deformed but move as rigid pistons, then all of the resultant forces which act from both sides upon the boundary surface must be equal.

2. The opposite postulate which states that the stresses are only compensated at the points where the rods touch one another, requires that the average stresses at the boundary be equal. Here it is implicitly assumed that the free portion of the end-face surface of the rod is deformed in some way. To select one of these conditions and to solve the problem involved in whether or not a unidimensional approximation is applicable for the solution of this problem is only possible on the basis of experiment, since from a theoretical point of view both of these conditions are internally contradictory. From the first postulate we obtain Formulas (1), (2), (3) (with $S_1 \neq S$) and the second postulate leads to the same formulas but S_1 is replaced by S, and m and m_1 are replaced by $\rho_1 S$ and $\rho_1 S$.

The figure shows data obtained from measurements with specimens whose cross-sections were varied from 2.2 to 7.5 mm². The computations were performed according to Formulas (1), (2) and (3). Within the limits of the dispersion produced by measurements taken on identical specimens we obtain results which are fully in agreement. Thus, experiment verifies the first postulate. By means of this method we were able to investigate a number of materials with large losses and small sound velocities (of course, the condition of course, $X_1 < < \rho_1 c_1$ must hold for resonance). In performing these investigations we made a large number of measurements of the sound velocity c and the losses (which characterize the reactive portion of the specific acoustical impedance X) in industrial polymethylmethacrylate as functions of temperature. The curves are given in the figure. Let us note that the curve for c does not have the sharp bend which Subrahmanyam reported. In investigating vinyplast specimens by means of the method described above, we detected elastic anisotropy which was associated with the presence of "frozen" highly-elastic deformation. We investigated specimens which were cut out of vinyplast sheets in various directions before and after annealing. The unannealed sheets possessed a residual extension of 15-20% in length (in the direction of the calendering) and a corresponding compression in thickness; there was no deformation in the width. After annealing (2 hours at 120°C) the residual deformations disappeared and the sound velocity c was identical (1710 ± 10 m/sec) in all directions in the plane of the sheet. In unannealed sheets c ≈1700 m/sec along the width and 1760 m/sec along the length. In the direction of the sheet thickness c was somewhat less (approximately 1670 m/sec before annealing and 1680-1690 m/sec after annealing).

We also performed measurements of the sound velocity in a vinyplast specimen which was stretched by 75%, when hot and in specimens of polymethylmethacrylate and polystyrene which were stretched by 80-100%. In vinyplast we observed an increase of c in the direction of the extension (up to 1920 m/sec), and in polystyrene and polymethylmethacrylate the velocity of sound did not vary within the limits of the errors involved in the method (10 -20 m/sec). In all cases the deformation was completely reversible when the heating process was repeated. It can be assumed that the partial orientation of the molecular chains was the reason for the appearance of anisotropy during the stretching process. Under these conditions a number of intramolecular bonds arise which are oriented in the direction of the extension. If the forces of interaction between atoms are considerable greater

along the chain than between adjacent chains, then such an orientation must give rise to elastic anisotropy. Evidently in polystyrene and polymethylmethacrylate the rigidity of the bonds between chains is of the same order as the rigidity of the intramolecular bonds. We also measured the mechanical losses X simultaneously with the sound velocity. Within the limits of error (± 10%), X did not depend upon the amount of stretching. At 20°C and at 75 kc in vinyplast $X = 6.5 \cdot 10^{-3}$ g/sec.$^{-1}$cm^{-2}, and in polystyrene $X = 0.45 \cdot 10^{-3}$ g/sec.$^{-1}$ cm^{-2}.

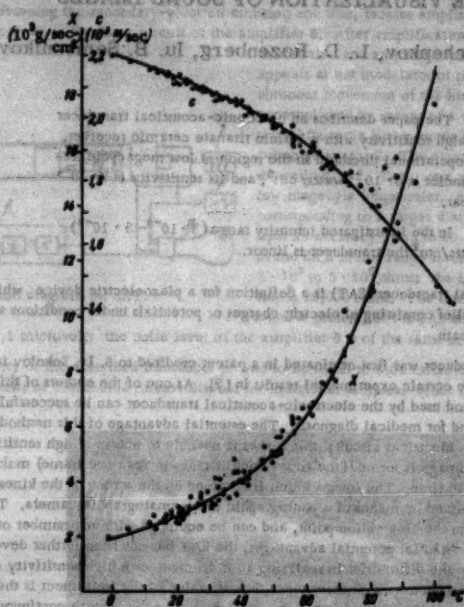

LITERATURE CITED

[1] Kedi, Piezoelectricity and its Practical Applications (Foreign Lit. Press, 1929).

[2] J. S. Rinehart, "Temperature dependence of Young's modulus and internal friction of lucite and karolith," J. Appl. Phys. 12, 811 (1941).

[3] S. V. Subrahmanyam, "Temperature dependence of ultrasonic velocity in plastics," J. Chem. Phys. 22, 1562 (1954).

[4] M. Kornfel'd, "Measurements of the shear modulus in solid and liquid bodies," J. Expt.-Theoret. Phys. (USSR) 13, 116, (1943).

[5] N. S. Ageeva, I. E. Zhukov, M. A. Isakovich, A. L. Sozedova and In. M. Sukharevskii, "An electro-mechanical Q-meter-a device for measuring the modulus of elasticity and the losses in materials at ultrasonic frequencies," J. Tech. Phys. (USSR) 22, 1029, (1952).

Leningrad Order of Lenin A. A. Zhdanov State University

Received March 11, 1955.

AN ELECTRONIC-ACOUSTICAL TRANSDUCER FOR THE VISUALIZATION OF SOUND IMAGES

P. K. Oshchepkov, L. D. Rozenberg, Iu. B. Semennikov

The paper describes an electronic-acoustical transducer of high sensitivity with a barium titanate ceramic receiver. Its operational threshold in the region of low megacycle frequencies is $3 \cdot 10^{-9}$ watts/cm^2, and its sensitivity is $2 \cdot 10^{-8}$ v/bar.

In the investigated intensity range ($3 \cdot 10^{-2}$–$3 \cdot 10^{-3}$) watts/cm^2 the transducer is linear.

The electronic-acoustical transducer (EAT) is a definition for a piezoelectric device which converts a sound pressure relief into a relief consisting of electric charges or potentials under conditions where the latter are scanned by an electron beam.

The idea for such a transducer was first originated in a patent credited to S. Ia. Sokolov in 1936 [1]. Later, in 1948, the same author gave certain experimental results in [2]. As one of the authors of this paper [3] indicated in a survey, the method used by the electronic-acoustical transducer can be successfully utilized both for ultrasonic defectoscopy and for medical diagnosis. The essential advantage of this method is the possibility of amplifying the signal in an electrical circuit; this makes it possible to obtain a high sensitivity. The very small time during which the image is formed (the time which it takes to scan one frame) makes it possible to observe processes which vary in time. The image which is obtained on the screen of the kinescope can be visually observed and can be fixed by means of a photographic or cinematographic camera. The kinescope can be placed at any distance from the observation point, and can be equipped with any number of repeaters. However, notwithstanding these substantial potential advantages, the EAT has not been further developed. This fact can evidently be explained by the difficulties in realizing an instrument with high sensitivity and a good viewing field. In addition, the essential factor which determines the use-value of the instrument is the ability to obtain a truly sealed-off electronic-acoustical transducer (i. e., one which does not require continuous evacuation).

Below we provide a description of an electronic-acoustical transducer which satisfies these basic requirements and derive its basic characteristics.

Barium titanate ceramic was used in the capacity of the piezoelectric transducer. This selection was determined by the ease with which plates of large dimensions could be obtained and by the lesser danger of damaging them when the temperature variations were large (this was true, notwithstanding the fact that the piezoconstant "g" which determines the operation of the transducer in a receiver regime is considerably smaller for barium titanate ceramic than, for example, for quartz.

One of the most substantial difficulties consisted of creating a vacuum-tight joint between the ceramic and the glass case of the EAT; in achieving this, it was necessary to take into account the difference in the linear expansion coefficients of the glass and the ceramic on the one hand, and the necessity of heating to 400°C when evacuating and aging the EAT on the other hand. In the process of solving this problem, we tested a variety of different combinations from which we finally selected a satisfactory one.

The schematic cross-section and the connection diagram for the EAT are shown in Fig. 1. The ceramic plate (target) 1 with a diameter of 120 mm is joined to the glass case 2 of the EAT by means of a vacuum-tight

joint 3. The external casing of the instrument 10 is grounded. The electron beam which is created by an electron gun 5 of the ordinary type knocks secondary electrons out of the inside surface of the target; these secondary electrons are collected by the collector which is connected to the input of amplifier 6 through the leads 4. The acoustic wave which is incident upon the external surface of the target, creates resonant vibrations along the thickness of the target, and this in turn, leads to the formation of charges of alternate sign on the inside surface of the target. The presence of this potential relief, which corresponds to the incident sound relief, changes the conditions governing the secondary-electron emission and thus, creates amplitude modulation of the collector current which flows in the input circuit of the amplifier 6. After amplification at the carrier frequency, demodulation and amplification at low frequency, the signal appears at the modulator of the kinescope 9. The synchronous movement of the kinescope and EAT beams is accomplished by means of a sawtooth voltage which is obtained from the line-sweep generator 7 and the frame-sweep generator 8. The external appearance of the EAT is shown in Fig. 2. Tests were performed in the region of low megacyle frequencies. A square frame 85 x 85 mm, corresponding to a target diameter of 120 mm, was scanned with an accuracy of up to 60 lines. The output impedance of the EAT in this range fluctuates within the range of from $3 \cdot 10^3$ to $5 \cdot 10^3$ ohms; the input impedance of the amplifier is 20,000 ohms. The intrinsic noise level (when no sound is present) of the EAT in the working frequency band is approximately 1 microvolt; the noise level of the amplifier 6 is of the same order of magnitude.

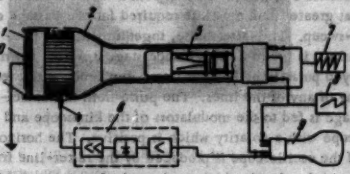

Fig. 1. Connection diagram for EAT.

The sensitivity of the described transducer proved to be equal to 0.02 microvolts/bar on the average, varying within the limits of 0.005-0.05 microvolts/bar for individual samples. Since the resultant noise level of the unit as a whole is approximately 1.5 microvolts, a 2 microvolt signal must be noticeable against the noise background.

Fig. 2. External view of the EAT.

Measurements of threshold signals showed that the system did in fact, react to a threshold sound pressure of 50-100 bar; this corresponds to a threshold intensity of $3 \cdot 10^{-9}$ watts/cm^2.

For the purposes of comparison, let us indicate that the sensitivity threshold of other methods is considerably higher. Thus (see [3, 4]), methods which make use of the thermal and chemical effects of ultrasonic waves require 0.1-5.0 watts/cm^2, the method of surface relief has a threshold of $3 \cdot 10^{-9}$ watts/cm^2. The data for the sensitivity of the shadow method are not available in direct form in the literature, but if we assume that it is possible to detect a relative variation of the order of 10^{-6} in the refractive index by means of this method, then this corresponds to an intensity of $3 \cdot 10^{-4}$ watts/cm^2. Thus, the described transducer has a threshold intensity which is 10^5 times greater than the most sensitive of the known visualization methods.

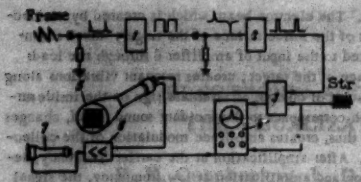

Fig. 3. Block diagram of the electronic stroboscope.

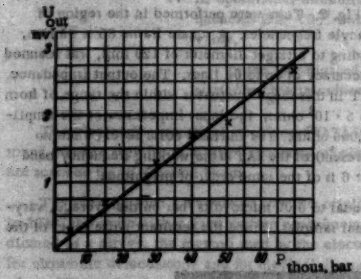

Fig. 4. Image of mirror reflection from a cyclinder.

In order to objectively evaluate the operation of the EAT we developed an electronic stroboscope * which made it possible to analyze the intensity distribution along any line and to measure the magnitude of the signal at an arbitrary point of the raster.

The circuit illustrating the principle of the stroboscope is shown in Fig. 3. The frame-sweep pulse is fed to a phantastron circuit 1 (after differentiation) which smoothly varies the time delay. The trailing edge of the delayed pulse (after it is differentiated) brings the Kipp-relay 2 into action; this relay produces a rectangular pulse with a duration which is somewhat greater than the time required for one passage of the line-sweep. The latter pulse, together with the line-sweep pulses, is fed to a coincidence stage 3, which permits the delayed pulse to be brought into coincidence with the beginning of any of the lines. The pulse from the coincidence stage is fed to the modulators of the kinescope and the oscilloscope with a polarity which is positive. The horizontal sweep of the oscilloscope is produced by the raster-line frequency, and the signals which produce the image are fed to the vertical deflection input. At the instant that the pulse which unblocks the electron beams appears, a picture which represents the distribution of the potential relief along one of the raster-lines appears upon the oscilloscope screen.

Figures 4 and 5 show the images which are obtained when the EAT is placed in the focal plane of an acoustic lens which produces an image of the object being irradiated by the sound waves. Figure 4 shows the appearance of mirror reflection from a cylinder, Figure 6, a shows mirror reflection from a sphere. The signal distribution obtained by the stroboscope

Fig. 6. Mirror reflection from a sphere; a) image, b) signal distribution along the central line.

*The inventor of this device was V. I. Fomin.

Fig. 6. Image of two apertures in a non-transparent screen.

Fig. 7. Amplitude characteristic of the system.

along a raster-line which passes through the center of the image is given in Fig. 5, b. Figure 6 shows the image (for sound waves which are transmitted through the object) of two apertures in a non-transparent screen which is focused upon the input surface of the EAT by an acoustic lens. Figure 7 shows the amplitude characteristic of the entire system; this characteristic shows that linearity is maintained over the entire investigated range up to sound pressures of 70,000 bar at the input.

The following scientists participated in the development, production and testing of the EAT: V. I. Rybalka, T. I. Didus', E. I. Buznikova, M. A Disus', M. G. Sirotiuk and V. I. Stepanov.

LITERATURE CITED

[1] S. Ia. Sokolov, Patent Certification No. 49426, August 31, 1936; American Patent Certification No. 2164185. July 8, 1937; English Patent Certification No. 477139, May 13, 1937.

[2] S. Ia. Sokolov, "The application of ultrasonics in physics and engineering," Factory Lab. 11, 1328-1335 (1948).

[3] L. D. Rozenberg, "Survey of methods for the visualization of ultrasonic fields," J. Acoust. 1, 2, 99-109 (1955).

[4] M. S. Ardenne, "Über ein Schallsichtverfahren mit electronenoptischen Bildwandler," Nachrich. tech Z. 5, 2, 49-51 (1955).

Acoustics Institute and A. A. Baikov Metallurgy Institute of the Acad. Sci. USSR

Received September 13, 1955.

THE DEPENDENCE OF THE COERCIVE FORCE AND THE PERMITTIVITY OF CERAMIC BARIUM TITANATE UPON MECHANICAL STRESSES

N. A. Roi

It is shown that by meam of the special application of mechanical stresses it is possible to substantially increase the coercive force of ceramic barium titanate. A study of the temperature variation of the permittivity of the ceramic in both the stressed and free states leads to the conclusion that the thermodynamic theory in its general form, without a consideration of the effects due to the variation of domain structure, is in contradiction with the experimental results.

As we know, mechanical stresses cause variations in the magnetic properties of ferromagnetics, and these variations are to a known degree similar to the variations which are caused by the effects of a magnetic field. On the other hand, it has been indicated many times that ferroelectrics, in particular, ceramic barium titanate, behave in a manner analogous to ferromagnetics in many respects. Therefore, it is of interest to trace the possible variations in the properties of the ceramic when mechanical stresses are applied to it, and to compare these properties with variations which are caused by the effects of an electric field. In solving this problem it was proven most convenient to create a set-up in which a cylindrical specimen was subjected to radial compression. For this purpose, slightly conical ceramic bars were pressed in a heated state (at 500°C) into steel cylinders which were ground to fit them. After cooling, the ceramic proved to be radially compressed, since the coefficient of expansion of the steel is greater than that of the ceramic. It is not possible to determine reliably the magnitude of the pressure which is produced under these conditions, since it is very probable that an irreversible deformation of the steel is produced during the pressing process, and an irreversible deformation of the ceramic is produced during the cooling process (this deformation of the ceramic is associated with the phase transition that occurs near 120°C). The residual stress is roughly of the order of several atmospheres. In our experiments we utilized ceramic bars 15 mm in diameter and 20 mm high, and steel cylinders with wall thicknesses of 1.5, 2 and 2.5 mm. The conical angle and the depth of the fit during the pressing process were identical for all specimens; therefore, the most strongly compressed specimens are the ones with cylinders having the thickest walls. The specimens were then cut along a direction perpendicular to their axes. As a result, we obtained ceramic discs 2 mm high which were enveloped by compressing rings. Electrodes were applied to the free end-faces of the discs, and the radius of the electrodes was approximately 1 mm less than the radius of the ceramic discs. The coercive force in a static regime was measured in the following manner for the resulting specimens. Specimens which were polarized in the ordinary manner were made to perform resonant radial vibrations by means of a small alternating field. Simultaneously, the specimens were subjected to a dc field which was opposite in sign to the field in which the specimens had been polarized. The depolarizing field intensity was increased sufficiently slowly so that the amplitude of the vibrations acquired a steady-state value at each value of field intensity. The depolarizing field intensity which corresponded to the disappearance of the vibrations was assumed to be equal in magnitude to the coercive force in a static regime.

The coercive force in the most intensely compressed specimens, as experiments showed, was equal to 5 kv/cm, and this value is twice as great as the coercive force of the free ceramic when it is polarized and tested under identical conditions.

Let us note that the coefficient of electromechanical coupling, as determined for radial vibrations by the following expression [1]

$$k^2 = \frac{\Delta f}{f_R}\left[R_1^2 - (1-\sigma^2)\right],$$

where $\sigma = 0.27$, $R_1 = 2.03$, $\Delta f = f_A - f_R$ (f_A is the antiresonant frequency, f_R is the resonant frequency), proved to be exactly the same for specimens with compressing rings, as it was for the free ceramic (17-20%). In addition, since at higher values of coercive force it is possible to apply a higher exciting voltage to the ceramic resonator without running the risk of depolarizing it, it may be expected that the utilization of such methods for increasing the coercive force of the ceramic when designing hydroacoustic radiators will make it possible to obtain a large specific acoustic power from them.

The large value of the coercive force in the compressed specimens is evidently due to the following. The depolarization process may proceed along two different paths due to the effects of the reverse field: the reorientation of polar tetragonal cells through an angle of 90°, or a reorientation through an angle of 180°. In the case of compressed ceramic, the 90° reorientations are impeded, however since they are associated with the radial expansion of the specimen. Therefore the depolarization in the case of compressed specimens will occur chiefly by the way of 180° reorientation. The impediment of one of the depolarization mechanisms is the cause of the increased coercive force of compressed ceramic.

In several compressed specimens which had not been subjected to polarization, we measured the permittivity ϵ_{comp} as a function of temperature. Then in order to determine the behavior of the permittivity of the same specimens in the free state (ϵ_{fr}) the pressure was removed by cutting the rings. In order to keep all the conditions under which ϵ was measured constant (with the exception of the pressure) the cut rings were not removed from the ceramic discs.*

In order to eliminate aftereffect, the specimens were heated to 300°C. After several days (such a period was necessary in order to allow the specimens to reach a normal state) measurements of the permittivity were performed. As a result of the measurements it was determined that at room temperature $\epsilon_{comp} < \epsilon_{fr}$, whereas the difference between stable values of ϵ_{comp} and ϵ_{fr} is 20% of ϵ_{fr}. The temperature dependence of ϵ_{comp} and ϵ_{fr} in the temperature range of from 85 to 135°C is shown in the figure. Here the displacement of the ϵ_{comp}-maximum by approximately 1° (with respect to the ϵ_{fr}-maximum) toward higher temperatures, the decrease in the temperature-hysteresis loop and the increase in the permittivity of the cubic phase all attract attention.

Radial compression is qualitatively equivalent to the axial extension of the specimen in terms of the effect it has upon the shape of the specimen and in terms of the nature of the molecular processes which it gives rise to. The difference is that extension of the specimen along the axis is accompanied by an increase in volume, and radial compression is accompanied by a decrease in volume. It is of interest to make a quantitative comparison between the variations in permittivity caused by radial compression of the specimen and by axial extension. For this purpose we performed the following experiments. By means of a hydraulic device which made it possible to produce a controllable radial compression upon disc-shaped specimens we investigated the behavior of the permittivity of ceramic at various pressures at room temperature. The magnitude of the pressure reached 1,000 atm.

These experiments clarified the fact that the decrease in permittivity which occurs after the pressure is applied can be described by the expression $\Delta\epsilon = \Delta\epsilon_\infty\left(1 - e^{-\frac{t}{\tau}}\right)$, where $\Delta\epsilon_\infty$ is the maximum permittivity variation which corresponds to a given value of pressure, τ is the relaxation time (which is approximately equal to 14-15 min), t is the time as measured from the instant at which the pressure is applied.

*It should be noted that the junction between the ceramic and the ring is so strong that it is easier to break the ceramic than to separate it from the ring.

The measurements of steady-state values of permittivity at various pressures showed that the permittivity decreases linearly when the pressure is increased. The proportionality coefficient (normalized to the magnitude of permittivity) proved to be the following under these conditions:

$$\frac{\partial \varepsilon_{33}}{\varepsilon_{33}\partial \sigma_{rad}} = -2.4 \cdot 10^{-10}\ \text{CGSE},$$

where σ_{rad} is the radial compression stress.

Let us convert this quantity to a tensile stress σ_{33} which creates an identical deformation along the axial direction of the specimen. Since the effect of σ_{rad} is equivalent to the effect of $\sigma_{11} = \sigma_{22}$ and is equal to them in magnitude, it follows that σ_{rad} will create the same deformation as σ_{33} provided that $\sigma_{rad} = \sigma_{11} = \sigma_{22}$ if $\sigma_{33} = -2\sigma\sigma_{11}$ (σ is the Poisson coefficient). Therefore,

$$\frac{\partial \varepsilon_{33}}{\varepsilon_{33}\partial \sigma_{33}} = -\frac{1}{2\sigma}\frac{\partial \varepsilon_{33}}{\varepsilon_{33}\partial \sigma_{rad}} = 4.4 \cdot 10^{-10}\text{CGSE}$$

The direct measurement of permittivity in the tensile direction of the specimen (this is accomplished by means of a lever device) yielded results on the basis of which we were able to determine that

$$\frac{\partial \varepsilon_{33}}{\varepsilon_{33}\partial \sigma_{33}} = 3.8 \cdot 10^{-10}\ \text{CGSE}.$$

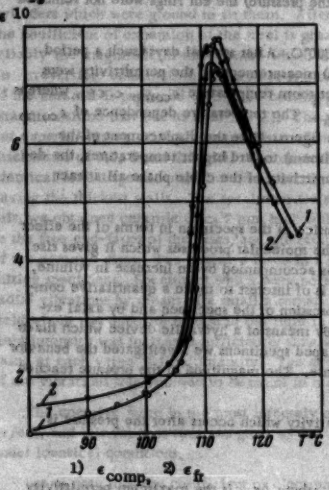

1) ϵ_{comp}, 2) ϵ_{fr}

This result agrees with the results obtained for radial compression to an accuracy of up to 15%. Thus radial compression is, to a first approximation, equivalent to the extension of the specimen along its axis as far as the effect upon the permittivity is concerned. By taking into account the difference between the change in volume which occurs during extension and during radial compression, we would only obtain a negligibly small correction, since the relative variation in the permittivity which occurs for all-sided compression is equal to 10^{-10} CGSE [2].

From a molecular point of view we can give the following interpretation to the observed dependence of the permittivity upon the mechanical stress when the ceramic is heated to various temperatures. When the ceramic is in the cubic phase the increase in the permittivity, as measured along the axis of a radially compressed specimen, is evidently due to the nonlinearity of the bonds between the titanate and oxygen ions. The bonds are weakened when the distance between those titanate and oxygen ions which lie along straight lines that make small angles with the axis of the specimen increases. The dc field (in contrast to the effect of stretching) decreases the distance between the titanate and oxygen ions, and as a result, the cells form polar moments. As we know, the permittivity decreases under these conditions, and this is proof that the rigidity of the bonds between the titanate and the oxygen ions increases. The compression of the specimen along its axis must evidently lead to the same results. When the ceramic makes a transition into the ferroelectric phase, the effect of an increase in the distance between the titanate and oxygen ions is masked by the fact that radial compression has the additional effect

of creating a domain texture; such a texture causes the polar moments of the domains to align themselves predominantly along the axis of the specimen. Therefore, the measured permittivity is basically determined by the permittivity along the polar axis of a cell, and this value, as we know, is approximately 10 times smaller than the permittivity in the perpendicular direction.

It is also possible that the mechanical stress, in impeding the variation of the domain structure, decreases the reorientational, dipole portion of the permittivity of the ceramic. Thus, macroscopically radial compression (or the eqivalent tensile extension of a specimen along its axis) causes variations in the permittivity which differ in sign, depending upon which phase obtains for the ceramic.

This result is of substantial significance with regard to the thermodynamic theory of ceramics. The thermodynamic theory determines the derivatives of the permittivity with respect to the mechanical stress in the form of electrostrictional coefficients. In this theory, the electrostrictional coefficients of the ceramic do not change sign when the ceramic makes the transition from a non-ferroelectric phase into a ferroelectric phase. Thus, the thermodynamic theory in its usual form (which does not take into account the effects produced by a variation in the domain structure) leads to a contradiction of the experimental results in the case examined here.

LITERATURE CITED

[1] W. P. Mason, "Barium-titanate ceramic as an electromechanical transducer," Phys. Rev. 74, 9, 1134 (1948).

[2] B. M. Vul, L. F. Vereshchagin, "The dependence of the permittivity of barium titanate upon pressure," Doklady Akad. Nauk SSSR 48, 9, 662 (1945).

Acoustics Institute of the Academy of Sciences USSR, Moscow

Received January 31, 1955

METHOD FOR MEASURING THE MECHANICAL PARAMETERS OF RUBBER AT SONIC AND ULTRASONIC FREQUENCIES

V. V. Tiutekin

A method is described for determining the mechanical parameters of rubber over a continuous range of frequencies; this method makes it possible to measure the modulus of elasticity and the loss coefficient for shear deformations in the frequency range of from 4 to 50 kc.

Theory of the Method

In this paper a method described in [1] is modified in such a way as to make it possible to measure the elastic shear parameters of rubber over a continuous range of frequencies without the necessity of such a complex mechanical device as the pulse pipe. For this purpose we utilized an acoustically long line which consisted of a duraluminum pipe at one end of which a radiator that emitted acoustical pulses was fastened (trains of longitudinal waves) (Fig. 1). During its rest intervals, the radiator operates in the capacity of a receiver for the pulses which are reflected from the opposite end of the pipe. The rubber test specimen (which is shaped in the form of a ring that surrounds the pipe) is glued onto the external surface of the pipe at its free end. The longitudinal waves which are excited in the wall of the pipe by the radiator are converted into shear waves in the rubber specimen and are propagated along its thickness. The portion of the tube which is encompassed by the rubber specimen is examined as a load upon an acoustically long line, and the impedance of this load is measured in order to determine the unknown quantities μ_0 and η. In turn the impedance is determined on the basis of measuring the complex coefficient of reflection $\overline{\beta} = |\beta| e^{-i\varphi}$ from the load.

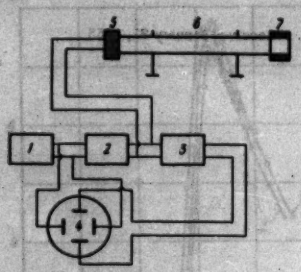

Fig. 1. Over-all diagram of the unit: 1) Oscillator, 2) Pulse source, 3) Phase-shifter, 4) Oscilloscope, 5) Radiator, 6) Acoustically long line, 7) Test specimen.

The modulus of the reflection coefficient is expressed by the formula $|\beta| = \frac{a_1}{a_2}$, where a_1 is the amplitude of a pulse which is reflected from the load, a_2 is the amplitude of a pulse reflected from the free end of the line when it is unloaded (i. e., when the specimen is removed from the surface of the pipe). The phase of the reflection coefficient is computed according to the formula

$$\varphi = \varphi_1 - \varphi_2 + \pi - 2kl, \qquad (1)$$

where $k = \frac{\omega}{c}$; φ_1 and φ_2 are respectively the reflection phases of the same pulses; l is the length of the portion of the pipe to which the rubber is glued; ω is the angular frequency; c is the velocity of longitudinal sound waves in the wall of the pipe. The latter term of expression (1) takes into account the additional doubled phase lag over the length l which arises when the specimen is placed farther away.

The addition of the quantity π to the resultant phase is due to the fact that phase inversion occurs when a pulse is reflected from the free end of the line.

The load impedance $Z_L = \rho c (R_L + iX_L)$ is expressed in terms of the complex coefficient of reflection β in the following manner [1]:

$$R = \frac{1-|\beta|^2}{1+|\beta|^2-2|\beta|\cos\varphi}, \quad X = \frac{2|\beta|\sin\varphi}{1+|\beta|^2-2|\beta|\cos\varphi}.$$

Here ρc is the wave impedance of the line. From the load impedance Z_L it is possible to determine the mechanical impedance of the specimen per unit surface ($Z_0 = R_0 + iX_0$) by means of the nomogram which is given in [1]. In this nomogram the values of $R = kl\,R_L$ and $X = kl\,X_L$ are plotted along the coordinate axes, and the auxiliary quantities L_1 and η_1 are determined according to the curvilinear grids (these auxiliary quantities are used to compute the values of R_0 and X_0):

$$R_0 = \rho\omega d'\eta_1\left(\frac{L_1}{kl}\right)^2, \quad X_0 = \rho\omega d'\left[\left(\frac{L_1}{kl}\right)^2 - 1\right]. \qquad (2)$$

Here ρ is the density of the pipe material, and the quantity d' is determined in terms of the thickness d of the pipe wall and the outer radius R of the pipe:

$$d' = d\left(1 - \frac{d}{2R}\right).$$

Let us note that in contrast to [1] the impedance of the specimen can be determined not only for an individual frequency (the resonant frequency of the rod) but also over a very wide and continuous frequency range. The determination of the complex shear modulus $\mu = \mu_0(1 - i\eta)$ according to the known value of the impedance of the specimen $Z_0 = R_0 + iX_0$ is described in [2].

EXPERIMENTAL RESULTS

In the process of developing the method being described here we performed measurements of the mechanical parameters of several types of rubber over the frequency range of from 4 to 50 kc at a temperature of $t = 20°C$. It can be shown that the sensitivity of the method depends upon the quantity $Z_0/\rho\omega d$: the greater this quantity, the greater the impedance of the pipesector to which the rubber specimen is glued differs from the impedance of the same pipe segment with the specimen removed ($Z_{tp} = -i\rho c \tan kl$). Thus in order to obtain a high sensitivity it is necessary to have the following:

1) a small thickness of the pipe wall;

2) a small density for the pipe material (therefore, duraluminum was chosen in the capacity of this material);

3) values of Z_0 which are as large as possible; this is achieved for specimen thicknesses of

$$l_0 \approx 0.25\lambda_0, \qquad (3)$$

where λ_0 is the wavelength of a shear wave in the rubber.

Experiment shows that for one and the same specimen it is possible to achieve sufficient sensitivity only within the limits of approximately one octave; therefore, in order to perform measurements over a wide range

of frequencies it is necessary to use several specimens of varying thickness.

The lower frequency boundary f_{lo} of the frequency range over which the measurements are made is determined from the condition which requires that the thickness of the specimen must be several times less than the radius of the pipe (the condition for which the shear wave in the rubber specimen may be assumed to be plane) and must at the same time satisfy Condition (3). In addition, the lower frequency boundary is determined by the length of the pipe. In order to guarantee that the pulse be sufficiently monochromatic it must contain at least several waves; this determines the minimum spatial length of the pulse. The length of the pipe must be more than one-half of the pulse length in order for the reflected pulse not to be superimposed upon the direct one. The upper boundary frequency of the working range, f_{hi}, is limited by the transverse resonance of the pipe which occurs for $2\pi R = \lambda = c/f_p$ [3]. Since f_{hi} must be less than f_{res}, it follows that $f_{hi} < c/2\pi R$.

On the basis of the selected values of f_{lo} and f_{hi}, and with the aim of obtaining maximum sensitivity, we selected optimum dimensions for the pipes. In doing so, we used different dimensions for them in two different

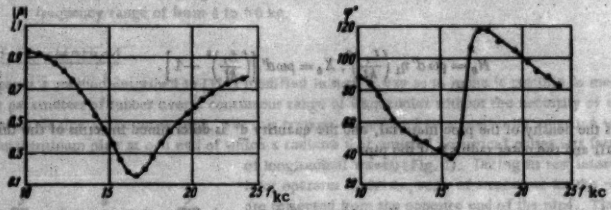

Fig. 2. Modulus of the reflection coefficient $|\beta|$ and the phase φ of the reflection as a function of frequency for the rubber specimen.

frequency ranges. In the range from 4 to 15 kc, we used pipes 5 mm long with an outer diameter of 40 mm and a wall thickness of 2 mm; in the range of from 10 to 50 kc we utilized pipes that were 2-3.5 m long, with an outer diameter of 28 mm and wall thicknesses of 1 and 2.5 mm. A metal plate 2 mm thick is pressed into one end of the pipe, and then the end-surface of the pipe is ground down. The radiator is tightly pressed to this end-face so that its radiating surface makes a tight contact (this radiator is a packet of Rochelle-Salt plates). The radiator is contained in a plexiglas shell which is screwed onto the end of the pipe and is pressed against the end-face of the pipe by means of a piston-and-spring device. Bearing screws are used to fasten the pipe into two rings which are supported by metallic stands. The reflection of pulses from the bearing screws is almost completely negligible since the ends of the screws which touch the pipe are sharply pointed. The circuit of the unit is depicted in Fig. 1. The electrical section of it is completely identical to the system described in [1].

In order to verify the possibility of making use of this method in a practical manner we measured the frequency characteristics of μ_θ and η for various types of rubber. In order to eliminate random experimental errors we applied a graphical smoothing process to the measured and computed quantities. As an example, in Fig. 2, the points represent the measured characteristics and the curves represent the smoothed characteristics for the modulus of the reflection coefficient $|\beta|$ and for the reflection phase φ as a function of frequency for one rubber specimen. In the same manner we also smoothed all of the intermediate quantities which were computed from the nomograms. The values which we obtained for μ_θ and η in conventional units for various frequencies are given in Fig. 3. Here the figure also shows the values of μ_θ and η which were obtained by the pulse-pipe method [1] and by the electromechanical Q-meter method [2]. The difference in the values obtained by the various methods does not exceed the measurement error of each method. It is evident from the graphs in Fig. 3 that μ_θ and η increase with frequency. This is in accordance with the theory of the relaxation processes which accompany periodic shear stresses in rubber (see, for example, [4] and [5]).

Along with the frequency dependence of μ_θ and η we measured the temperature dependence of these

quantities for various types of rubber. In order to measure the temperature dependence of the mechanical parameters of rubber, the end of the pipe upon which the specimen was glued was placed in a thermostat. In order to measure the phase and amplitude of the reflection we utilized the method involving a comparison with a second (standard) pipe which was subjected to exactly the same temperature conditions. The length of the standard pipe was less than the length of the pipe which carried the rubber test specimen, and this difference in length was equal to the length l of the specimen. The phase was computed according to the formula $\varphi = \varphi_1 - \varphi_2 + \pi$. The measurements were performed in the temperature range of from +5°C to +20°C, although in principle it is possible to perform measurements over a wider range.

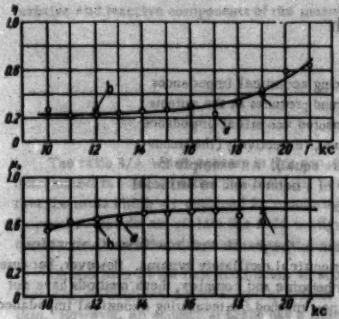

Fig. 3. Shear modulus μ_θ and loss coefficient η (in conventional units) as a function of frequency; a) specified method, b) pulse-pipe method, c) Q-meter method.

Along with the measurements of $\mu_\theta(t°)$ and $\eta(t°)$ by means of the specified method, we measured the same dependence at the same frequency by the electromechanical Q-meter method. As experiment showed, the results obtained by the two different methods are in good agreement. The nature of the dependence of μ_θ and η upon temperature also agrees well with the conclusions which are derived on the basis of relaxation theory.

The merits of the described method for measuring the mechanical parameters of rubber are: 1) the possibility of measuring these parameters over a wide (approximately 3.5 octaves) and continuous frequency range; 2) the comparative simplicity of the mechanical section of the unit and the simplicity of the measurements themselves; 3) the possibility of measuring specimens which have a large area; 4) the possibilities of making measurements over a wide temperature range.

The shortcomings of the method are the difficult-to-control effect of the glue layer upon the measured quantity, as well as the complex and cumbersome computations which must be made; these computations lower the accuracy of determining μ_θ and η on the basis of the measured values of $|\beta|$ and φ and thus, lead to a considerable dispersal in the final results. This dispersal attains 10-12%. However, the measured results obtained by the above method, and the good agreement of these results with results obtained by other methods show that this particular method of measuring the mechanical parameters of rubber is fully valid for practical purposes.

In conclusion the author expresses his deep appreciation to Iu. M. Sukharevskii and N. S. Ageeva for their help in performing this work, and to I. A. Viktorov, V. I. Kashina and I. S. Kislenko for their aid in performing the measurements.

LITERATURE CITED

[1] N. S. Ageeva, "Measurement of the elastic parameters of materials by the pulse-pipe method," J. Acoust. (USSR) 1, 2, 110 (1955).

[2] N. S. Ageeva, I. P. Zhukov, M. A. Isakovich, A. L. Sosedova and Iu. M. Sukharevskii, "The electromechanical Q-Meter – a device for measuring the modulus of elasticity and the losses in materials by means of ultrasonic waves," J. Tech. Phys. (USSR) 22, 6, 1029 (1952).

[3] Rayleigh, Theory of Sound, Vol. I (State Tech. and Theor. Lit. Press, 1955). (Russian Translation)

[4] A. P. Aleksandrov and Iu. S. Lazurkin, "Study of polymers," J. Tech. Phys. (USSR) 9, 14, 1249 (1939).

[5] T. Alfrey, The Mechanical Properties of High-Polymers (Foreign Lit. Press, 1953).

Acoustics Institute of the Academy of Sciences USSR, Moscow

Received April 20, 1955.

METHOD FOR MEASURING ACOUSTICAL IMPEDANCE ON THE BASIS OF MEASURING THE GEOMETRIC DIFFERENCE BETWEEN SOUND PRESSURES

V. N. Fedorovich

The paper describes a method for measuring acoustical impedances on the basis of measuring the difference in sound pressures at the outputs of two acoustical fourpoles loaded by the measured acoustical impedance and by an infinitely large acoustical impedance, respectively (the acoustical pressures at the inputs of the fourpoles are equal). An example is given of measuring the acoustical impedance of a natural and an artificial ear by means of the described unit.

The measurement of acoustical impedances is just as important in the practice of experimental acoustics as is the measurement of electrical impedances in investigating electrical oscillatory systems. However, because the existing methods of measuring acoustical impedances are cumbersome and complex, these methods have not received wide application. Therefore, all attempts to develop a new method for measuring acoustical impedance are of definite interest to acoustical metrology.

This paper is devoted to an examination of a new method for measuring acoustical impedance, a method which in many cases, may prove more convenient than any proposed up to this time.

General Theory of the Method

The method of measuring acoustical impedances which is examined below, belongs, according to Beranek's terminology, to the group of methods classified as "measurements at the surface of an object" (the term "object" is assumed to mean an acoustical material or an element in an oscillatory system, whose impedance is to be measured) and consists of the separate measurement of pressure and velocity. In this method the determination of the velocity is performed by means of measuring the geometric difference between the pressures acting at the outputs of two identical acoustical fourpoles (see below, Fig. 1) of which one (1) has a load in the form of an acoustical impedance z_x of the measured object, and the other (2) has a load in the form of a sufficiently rigid wall ($z = \infty$) when the acoustic pressures at the inputs of both fourpoles are identical in both phase and modulus.

If A and B are the parameters of the acoustical fourpoles, z_x is the measured acoustical impedance, p_1 is the pressure at the inputs of both fourpoles, p_2 is the pressure at the output of fourpole 2 (at the surface of the measured object), p'_2 is the pressure at the output of fourpole 1 (at the surface of the infinitely rigid wall), v_2 is the velocity at the output of fourpole 1 (the velocity of the measured object), then it is possible to write the following relationships:

$$p_1 = Ap_2 + Bv_2, \quad p_1 = Ap'_2. \tag{1}$$

On the basis of these relationships we have

$$Ap'_2 = Ap_2 + Bv_2 \text{ and } v_2 = \frac{A}{B}(p'_2 - p_2). \tag{2}$$

Equation (2) shows that by measuring the geometric difference between the pressures p'_2 and p_2 and then multiplying this difference by the known ratio between the parameters of the fourpoles, A/B, it is possible to determine the velocity at the output of fourpole 1 (this velocity simultaneously represents the unknown input velocity of the measured object).

Since this method makes it possible to measure velocity, it is possible to create a method for measuring the acoustical impedance. For this purpose it is necessary to measure the pressure at the surface of the object and the phase difference between the pressure and the velocity (in addition to the velocity itself). Then the resistive and reactive components of the measured acoustical impedance (z_x) are determined from the equation

$$z_x = \frac{p_2}{v_2} = \frac{B}{A} \times \frac{p_2}{p'_2 - p_2}. \tag{3}$$

The ratio B/A which appears in this equation is a constant of the metering unit and can be, as shown below, determined in advance either theoretically or experimentally. In pursuing this line of reasoning, it is assumed that the units which are designed for measuring the acoustic pressure have an infinitely large acoustical input impedance and do not violate the field configuration. In addition, it is assumed that both acoustical fourpoles are identical, and that the sound wave at the surface of the object is a plane wave.

On the basis of the first assumption an acoustical probe should be preferable for measuring pressures, since metering microphones have relatively greater dimensions and therefore, substantially distort the field configuration. However, an acoustical probe has a finite input impedance, and therefore, it is necessary to complete the relationships given above by adding a correction for the shunting effect produced by the input impedance of the probe.

In that case, Relationship (1) acquires the following form:

$$p_1 = Ap_2 + Bv_2, \quad p'_1 = Ap'_2 + Bv'_2, \tag{4}$$

where v'_2 is the velocity at the output of fourpole 1. Defining the input impedances of the probes which are used to measure the pressures p_2 and p'_2 by z_{px}, it is possible to write

$$p_1 = Ap_2 + Bv_2 = p_2\left(A + B\frac{z_x + z}{z_{px} z_x}\right) \text{ and } p'_1 = Ap'_2 + Bv'_2 = p'_2\left(A + \frac{B}{z_{px}}\right), \tag{5}$$

whence

$$Ap_2 + \frac{B}{z_x}p_2 + \frac{B}{z_{px}}p_2 = Ap'_2 + \frac{B}{z_{px}}p'_2$$

or

$$p_2\left(A + \frac{B}{z_{px}}\right) + p_2\frac{B}{z_x} = p'_2\left(A + \frac{B}{z_{px}}\right)$$

and

$$z_x = \frac{B}{A + \frac{B}{z_{px}}} \cdot \frac{p_2}{p'_2 - p_2}. \tag{6}$$

From this it follows that the input impedance of the probe (provided the probes are identical) does not introduce any errors into the measured result.

It is only necessary to take into account the shunting effect of z_{pr} in determining the constant of the instrument; this constant will be of the form

$$\left(\frac{B}{A+\frac{B}{z_{pr}}}\right).$$

The probes which measure the acoustic pressures are electroacoustical devices which, in addition to their acoustical sections, also contain an electrical section. This fact can be utilized in order to eliminate the necessity of observing the requirements with regard to identical acoustical fourpoles 1 and 2 and equal acoustical input impedances for the probes, since these requirements are difficult to realize in practice.

In order to prove this assumption let us turn to the expressions

$$p_1 = A_1 p_x + B_1 v_x, \qquad p'_1 = A_2 p'_x + B_2 v'_x \tag{7}$$

and let us assume that all of the coefficients are different; let us also take into account the additional equations

$$e_2 = \frac{1}{A_4} p_2, \qquad v_2 = \frac{p_2}{z_{pr}}, \qquad e'_2 = \frac{1}{A_3} p'_2 \tag{8}$$

and

$$v'_2 = \frac{p'_2}{z'_{pr}}, \tag{9}$$

where e'_2 and e_2 are the voltages developed across the probes at the pressures p'_2 and p_2, and where $1/A_3$ and $1/A_4$ are the complex sensitivities of the probes.

$$\frac{1}{z_{pr}} + \frac{1}{z_x} = \frac{z_x + z_{pr}}{z_x \cdot z_{pr}},$$

where z_{pr} and z'_{pr} are the input impedances of the probes, z_x is the measured impedance, v'_2 and v_2 are the velocities at the outputs of fourpoles 1 and 2.

On the basis of (7) we have the following relationship:

$$A_1\left[A_2 + B_2\left(\frac{1}{z_{pr}} + \frac{1}{z_x}\right)\right] e_2 = A_2\left(A_1 + \frac{B_1}{z_{pr}}\right) e'_2$$

or

$$A_1\left(A_1+\frac{B_1}{z_{pc}}\right)e_2+\frac{A_1\cdot B_1}{z_x}e_2=A_2\left(A_2+\frac{B_2}{z_{pc}}\right)e'_2. \tag{10}$$

By controlling the complex sensitivities ($1/A_1$ and $1/A_2$) of the probes it is possible to achieve a situation where the following equation is fulfilled:

$$A_1\left(A_1+\frac{B_1}{z_{pc}}\right)=A_2\left(A_2+\frac{B_2}{z_{pc}}\right), \tag{11}$$

In that case

$$A_1\left(A_1+\frac{B_1}{z_{pc}}\right)\cdot(e'_2-e_2)=\frac{A_1\cdot B_1}{z_x}e_2 \tag{12}$$

and

$$z_x=\frac{B_1}{A_1+\frac{B_1}{z_{pc}}}\cdot\frac{e_2}{e'_2-e_2}. \tag{13}$$

It follows from Equation (13) that in order to determine the impedance of the object it is necessary to measure the voltage e_2 which is developed across the probe that measures the pressure p_2 at the surface of the object, the geometric difference between the voltages e_2 and e'_2 which are developed across the two probes [one of these probes measures the pressure p_2 at the surface of the object, and the other measures the pressure p'_2 at the surface of the sufficiently rigid wall (at the output of fourpole 2)], and the phase difference between voltage e_2 and the voltage difference (e'_2-e_2). In addition, it is first necessary to determine the constant of the instrument in accordance with the expression

$$\frac{B_1}{A_1+\frac{B_1}{z_{pc}}}.$$

As was shown in the description of the experimental portion of the work, Condition (11) can be fulfilled in a comparatively easy manner by an appropriate selection of the electrical parameters in the probe circuits. The criterion for the observation of Condition (11) may consist of a zero value for the geometric voltage difference (e'_2-e_2) over the entire range of the measured frequencies when the loads at both ends of the fourpoles (1) and (2) are equal (for example, absolutely rigid walls).

(standard) impedance z_{pc} is connected to the output of fourpole (1) instead of the unknown impedance; then the quantities e_2 and (e'_2-e_2) are measured and the constant of the instrument

$$\frac{B_1}{A_1+\frac{B_1}{z_{pc}}}=z_{pc}\frac{e'_2-e_2}{e_2} \tag{14}$$

is computed in accordance with Equation (13).

An adjustable acoustical impedance (such as the one described in [1]) can be used in the capacity of the standard. The characteristics of this impedance are computed with sufficient accuracy according to its dimensions, and if the temperature dependence of the impedance is not taken into account these characteristics remain constant with the passage of time.

A Description of the Metering Unit

Figure 1 depicts the block diagram of the metering unit which was developed in accordance with the theory discussed above. As can be seen from the figure, the acoustic fourpoles 1 and 2 are constructed in the form of segments which are equal in length (a and b) and which are a part of the same pipe c. In order to assure a certain suppression of resonances, these sections of the pipe (excluding the places at which the probe tubes k and l are located) are filled with thin metallic rods d. Between the indicated sectors soundwaves from a radiator are introduced into the internal cavity of the pipe c through a thin tube e which is inserted through an aperture f in the center of the side-wall of the pipe c. A sound pressure p_1 is developed in the volume h, and this

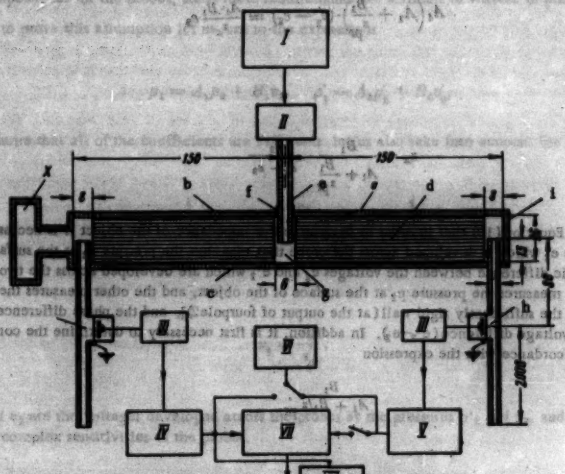

Fig. 1. Block diagram of the unit designed for measuring acoustical impedance: I) audio-oscillator, II) sound source, III) input stage, IV) amplifier which produces phase inversion, V) amplifier, VI) phase compensation, VII) summing stage with adjustable gain, VIII) 180° phase-shifter, IX) vacuum-tube voltmeter, X) phasemeter.

pressure is the input pressure for both of the fourpoles 1 and 2. The sector a which represents fourpole 1 is closed at its output by a sufficiently rigid wall i. The probe k serves for measuring the acoustic pressure p'_2. The oscillatory system x whose acoustic impedance is to be measured is connected to the output of Section b. The acoustic pressure p_2 upon the input of this system is measured by means of the probe l.

For the purpose of measuring the geometric difference between the sound pressures ($p'_2 - p_2$) the circuit is provided with a network that finds the difference between the voltages developed across the probes. In order to fulfill Equation (11) the electrical circuit of the unit contains a selection of capacitors which makes it possible to compensate the phase difference between the probe voltages; it is also provided with a gain adjustor in the amplifier circuit for probe k, and this adjusting circuit equalizes the absolute magnitudes of these voltages. The absolute magnitudes of the voltages were measured by a vacuum-tube voltmeter, and the phase differences between the voltages ($e'_2 - e_2$) and e_2 were measured by means of a phasemeter.

Calibration of the Unit and the Metering Procedure for Determining the Acoustical Impedance

In order to determine the constant of the instrument we utilized an impedance of the metallic type (which had an inside diameter of 4 mm and was 9 mm long) as a standard impedance. The modulus and phase of this impedance were determined by computation according to the following formulas:

$$|z_{st}| = \frac{\rho c}{S}\sqrt{1 + 3\frac{a}{k} + \frac{a^2}{k^2}}, \tag{15}$$

$$\varphi_{st} = \arctan\frac{\frac{a}{k}}{1 + \frac{a}{k}}, \tag{16}$$

where the attenuation coefficient was $\left(\alpha = \frac{2{,}8\cdot 10^{-4}\sqrt{f}}{r}\right)$, $k = \frac{\omega}{c}$, r and $\underline{r}$ was the radius of the pipe.

The calibration procedure consisted of measuring the modulus and phase of the ratio

$$\left(\frac{e'_2 - e_2}{e_2}\right)_{cal} = |K|e^{j\psi} \tag{17}$$

when the standard impedance was connected to the unit; the constant of the unit was determined [in accordance with Expression (14)] in the following manner:

$$\frac{B_1}{A_1 + B_1/z_{pc}} = |z_{st}|\,|K|e^{j(\psi+\varphi_{st})}. \tag{18}$$

During the measurements the unknown acoustical impedance was connected to the output of fourpole 2. At all frequencies at which the measurements were made the required acoustic pressure was established at the input of the acoustic impedance, and the moduli of the voltages e_2 and ($e'_2 - e_2$) were measured as well as the phase difference φ_x between them. Further computations of the measured acoustical impedances were performed on the basis of the formula

$$z_x = \frac{|e_2|}{|e'_2 - e_2|}|z_{st}|\,|K|e^{j(\psi+\varphi_{st}+\varphi_x)} \tag{19}$$

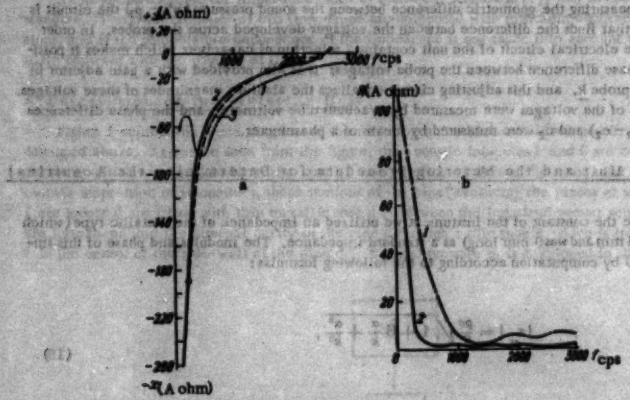

Fig. 2. Acoustical impedance of an artificial and a natural ear, as measured through a telephone earpiece with a large aperture: a) reactive, b) resistive component of the impedance: 1) natural ear (median curve for 10 people), 2) artificial ear, 3) computed curve.

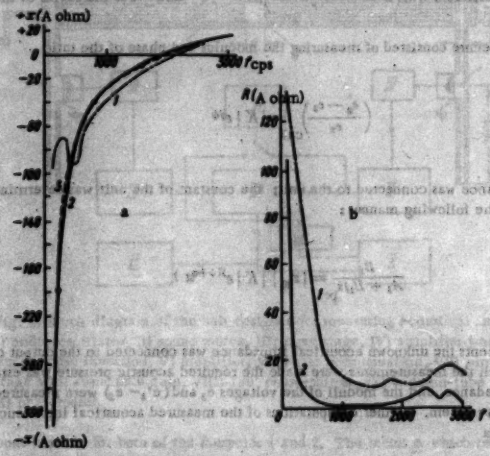

Fig. 3. Acoustical impedance of an artificial and a natural ear, as measured through a telephone earpiece with small apertures: a) reactive, b) resistive component of the impedance: 1) natural ear (median curve for 10 people), 2) artificial ear, 3) computed curve.

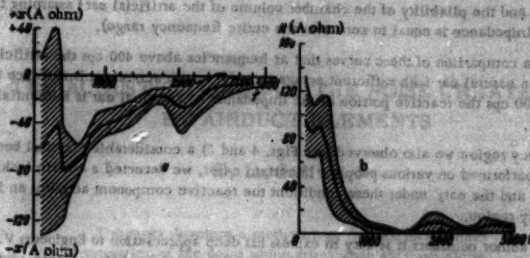

Fig. 4. Curves depicting the dispersal of the magnitudes of the acoustical impedance of the natural ear as determined for 10 people and as measured through a telephone earpiece with small apertures:
a) reactive, b) resistive component.

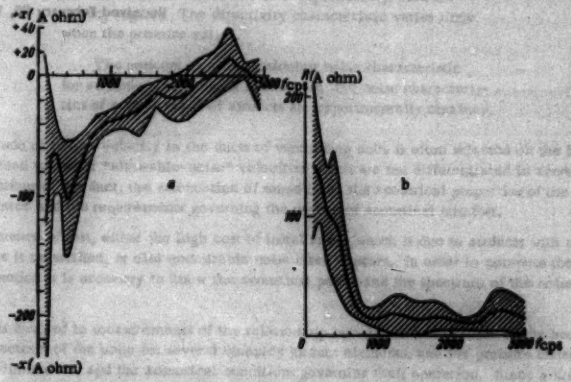

Fig. 5. Curves for the dispersal of the magnitudes of acoustical impedance for a natural ear as measured for 10 people through a telephone earpiece with a large aperture:
a) reactive, b) resistive component.

Measurements of the Acoustical Impedances of a Natural and an Artificial Ear

As an example, we provided results which were obtained by performing acoustical impedance measurements upon a natural and an artificial ear by the method described above. In making these measurements the telephone earpiece which was pressed to the natural ear or to the artificial ear was connected to the described metering unit. The sound pressure was maintained constant and equal to 10 bar at all frequencies. Measurements were made of the acoustical impedances by means of two telephone earpieces which had apertures with different dimensions. Figures 2 and 3 show the results of these measurements. On the same figures, the dashed curves correspond to the computed acoustical impedance of a system consisting of the coupled mass at the aperture of

the telephone earpiece and the pliability of the chamber volume of the artificial ear (assuming that the resistive component of the impedance is equal to zero over the entire frequency range).

It is evident from a comparison of these curves that at frequencies above 400 cps the artificial ear reproduces the properties of a natural ear with sufficient accuracy as far as the acoustical impedance is concerned. At frequencies below 400 cps the reactive portion of the impedance of a natural ear is substantially less than that of an artificial ear.

In the low-frequency region we also observed (see Figs. 4 and 5) a considerable dispersal between the results of measurements performed on various people. In certain cases, we detected a certain leakage between the telephone earpiece and the ear; under these conditions the reactive component acquires an inertial character in the low-frequency region.

In conclusion, the author considers it is duty to express his deep appreciation to Engineers V. L. Boltsov and L. M. Litvak for their participation in the work described in this paper and for their valuable advice.

LITERATURE CITED

[1] F. Willard, Meeker, H. Frank and Slaymaker, "A wide range adjustable acoustic impedance," J. Acoust. Soc. Amer. 16).3, 178-182(1945).

Leningrad

Received February 25, 1955

THE ACOUSTIC POWER OF THE NOISE CREATED BY AIRDUCT ELEMENTS

E. Ia. Iudin

The paper develops a methodology for an experimental investigation of the noise which arises when air flows along channels (in airduct elements, ejectors, high-velocity aerodynamic pipes) and provides certain results of such an investigation. It is found that the acoustic power is proportional (with an accuracy of up to an insignificant effect produced by the Reynolds number) to the cube of the excess pressure and to the square of the geometric dimensions. The noise has a statistical character and occupies a very wide frequency region. The directivity characteristic varies little when the pressure varies.

The concept of a dimensionless noise characteristic for an airduct element is introduced; the noise characteristics of certain types of airducts are experimentally obtained.

The magnitude of the air velocity in the ducts of ventilating units is often selected on the basis of unscientifically determined values of "allowable-noise" velocities which are not differentiated in accordance with the shape and dimensions of the duct, the attenuation of sound in it, the acoustical properties of the room in which the sound is radiated and the requirements governing the degree of acoustical comfort.

As a consequence of this, either the high cost of installations which is due to airducts with cross-sections that are too large is unjustified, or else undesirable noise often appears. In order to compute the allowable velocity of air motion it is necessary to know the acoustical power and the spectrum of the noise which is produced.

This paper is devoted to measurements of the relationship between the magnitude of the acoustic power and the frequency spectrum of the noise for several complex airduct elements, and the pressure differential in them, their geometric dimensions, and the acoustical conditions governing their operation. Since a diffuse sound field usually exists in rooms which are served by ventilation units, the directivity properties of the noise (which play a secondary role) have only been studied in a general way. The necessity of making specific measurements grew out of the requirements of industry.

The cause of the noise which arises when air moves along the ducts of ventilating units is the process by which vortices are created; this process is associated with the energy dissipation mechanism of the stationary (in the average sense) turbulent flow in the pipe. In view of the fact that the boundary perturbations (pulsations of velocity and pressure which are caused by the vortices) in airduct elements which have a complex shape are unknown at the present time, it is impossible to compute the sound field by analytical methods. Therefore, the basic method which we have used in this paper to investigate the above phenomena is the experimental method combined with the utilization of the similarity theory and dimensional analysis.

N. N. Andreev first proposed to use the methods of similarity and dimensional analysis in analyzing vortex noise. He came to the theoretical conclusion that the acoustic power of vortex noise is proportional to the fourth

power of the stream velocity, since when geometric and kinematic similarity are maintained, the pressure is determined by the Euler criterion, and the acoustic power is proportional to the square of the acoustic pressure. These concepts are valid for cases where the acoustic pressure is proportional to the amplitude of the pressure pulsations on the surface of the body around which the flow occurs (sound radiation with a fixed frequency when the stream velocity varies; such radiation is observed, for example, for pressure pulsations in aerodynamic pipes [5]). For the case of the external streamlining of bodies, where the Strouhal number remains constant and the sound is created by the presence of a head-on impedance associated with a pulsating transverse force and has the nature of dipole radiation, the author found that the acoustic power was proportional to the sixth power of the velocity and to the square of the geometric dimensions [2]. The sixth-power law is valid only for the case when the chief part in the formation of sound is played by pulsations of normal pressure and when the region to which the resultant pulsating force is applied is smaller than the dimensions of a sound wave. The general case of force radiation is examined by Lamb [14] and is the basis for the computation of the corresponding noise component for air propellers [1, 13].

If the pulsations of tangent stresses predominate (a jet emerging from a nozzle), then according to Lighthill [3], the acoustic power is proportional to the eighth-power of the velocity and the square of the geometric dimensions (quadruple radiation).*

All of the above-indicated papers touched upon cases of flow in an unbounded medium -- the external streamlining of bodies and the emergence of an immersed free jet. On the basis of the measurements which Stewart and Drake [4] made of noise in ventilation gratings, it is possible to conclude that the acoustic power is proportional to approximately the 5.5th power of the flow velocity and to the area of the grating.

The process of forming airduct noise and, in particular, the acoustic power and distribution of this power over the noise frequency spectrum (these are the most important acoustical characteristics of an airduct element) are determined by the geometric shape of the airduct, its dimensions, the flow parameters and the acoustical properties of the volume in which the sound is radiated.

The flow parameters in an airduct of specified geometric shape are determined by the static pressure differential p in it, the physical properties of the medium (the density ρ and the sound velocity c), and by the criteria

$$\mathrm{Re} = \frac{VD}{\nu} \quad \text{and} \quad M = \frac{V}{c},$$

where V is the time-averaged flow velocity at a characteristic point in the airduct; D is the determining geometric dimension; ν is the kinematic viscosity of the medium. The acoustical properties of the volume are determined by the dimensionless impedances $\bar{Z}$ of its boundaries and by the relationship between a sound wavelength and the dimensions of the volume λ/D.** In non-adiabatic streams the processes of heat exchange also play a part; these processes, however, are not examined in this paper.

*The first to indicate that the acoustic power was proportional to the eighth-power of the jet velocity when quadruple radiation occured was D. I. Blokhintsev [12].

**The frequency of the aerodynamic pulsations (and therefore, of the aerodynamically originating acoustic vibrations as well) is determined by the Strouhal number $\mathrm{Sh} = \frac{fD}{V} = \varphi_1$(the geometric shape, Re, M). Since the frequency is $f = c/\lambda$, then $\frac{\lambda}{D} = \frac{1}{M\,\mathrm{Sh}}$ and therefore, λ/D is not the determining criterion since in systems which are similar to aerodynamic systems $\lambda/D = \text{const}$ is automatically true under the condition $\bar{Z} = \text{const}$.

Thus the acoustic power of an airduct element is

$$W = \varphi_1\left(p, \rho, c, D, \mathrm{Re}, M, \overline{Z}, \frac{\lambda}{D}\right). \tag{1}$$

Here the acoustic power is determined as the integral of the sound intensity taken over the closed surface which surrounds the open end of the airduct in a free sound field.

An analogous expression can also be written for the acoustic power in any frequency band which has a constant relative pass band-width.

In accordance with the π-theorem of dimensional analysis, it is possible to write

$$W p^{\alpha} \rho^{\beta} c^{\gamma} D^{\delta} = \varphi_2 (\text{shape}\ \ \mathrm{Re}.\ M.\ \overline{Z}). \tag{2}$$

By performing computations which are usual for dimensional analysis, we find that

$$\beta = -1-\alpha,\ \gamma = \div 3-2\alpha,\ \delta = -2. \tag{3}$$

For any arbitrary law $W(p)$, the power is proportional to the square of the linear dimension provided that similarity is maintained.

From Equations (2) and (3) we obtain

$$\frac{W}{\rho c^3 D^2}\left(\frac{p}{\rho c^2}\right)^{\alpha} = \varphi_3 (\text{shape.}\ \ \mathrm{Re}.\ M.\ Z). \tag{4}$$

Formula (4) served as the working similarity formula in performing our experiments.

The purpose of the measurement was to clarify: a) the nature of the relationship between the acoustic power and the pressure differential in the airduct element (the exponent α); b) the relationship between the acoustic power and the size of the element, provided that geometric similarity is maintained (proportionality to the square of the linear dimension); c) the effect of the numbers Re and M, d) the effect of the acoustical properties of the room; e) the numerical value of the α-criterion for elements with various shapes, f) the frequency spectra in bands having a width of 1/3 of an octave. Since the investigation was limited to the case of airducts, the effect of the parameters of the medium (ρ and c) was not studied experimentally.

Various elements of metallic airducts were chosen in the capacity of test objects (certain of them are shown in Fig. 15), low- and high-pressure ejectors, layers of powdery granular material and aerodynamic velocity pipes. The investigations were performed both in acoustical and untreated rooms, and in open air.

The experimental unit which was used for investigating noise in airduct elements, ejectors and powdery materials at small velocities (Fig. 1) consisted of a pump-type ventilator 13 with input and output mufflers 14, a pumping chamber 1 and an output chamber 2. The ventilator 13 had a maximum pressure of 200 kg/m^2, and a maximum output of 3 m^3/sec. The design of the ventilator incorporated changes which guaranteed a lowering of the noise level. The pressure and output were regulated by changing the number of rpm of the electric motor 12. The air from the ventilator passed through the muffler into the pumping chamber 1 that simultaneously served both for decreasing and equalizing the air velocity and for measuring the noise at the

input to the investigated element 3. The latter was fastened to a wooden shield which was placed in the opening between the pumping chamber and the output chamber. In almost all cases a smooth collector 5(and in some cases a nozzle-sleeve 4) was stationed at the input to the element. Upon passing through the investigated element and through the output chamber, the air was thrown into the ventilated room through the muffler. The output chamber served for measuring the noise at the output of the element. The pressure differential across the investigated element was measured with a micromanometer 15. Two adjacent rooms with inclined ceilings

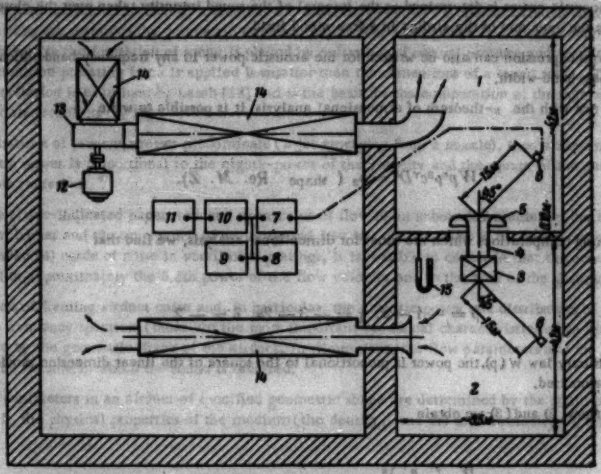

Fig. 1. Diagram of the experimental unit for investigating the formation of noise in airduct elements.

with a height of approximately 4 m were used in the capacity of the chambers. The dimensions of the rooms (in plan view) are given in Fig. 1. In order to diminish suction effects, the bounding surfaces of the rooms were painted with oil paint, the floors were covered with linoleum and the windows and doors were hermetically sealed. In order to equalize the frequency characteristics and to diminish the effects of the intrinsic frequencies of the rooms, the furniture present in the rooms(cabinets, tables, chairs, apparatus, etc.) was not removed during the measurements. When the chambers were properly adjusted, their reverberation characteristics were obtained for noise which covered bands 1/3 of an octave wide, the noise levels and noise frequency spectra were measured for several investigated elements for the purpose of clarifying whether or not the sound field in the chambers was uniform, the levels and spectra of the interference were measured, the acoustic insulation of the chambers was determined, and the values of the acoustic noise power were determined for one and the same source under various conditions in direct and diffuse sound in order to determine whether or not the results of the measurements performed in the chambers were applicable to other acoustical conditions. All-in-all, a large number of measurements with regard to levels and spectra were performed while the rooms were being adjusted. The following acoustical metering apparatus was used during the measurements: a n-52 noisemeter 7, an audio-frequency tone-spectrometer with 27 band filters 8, analyzers with a constant relative (16%) and absolute (50 and 2 cps) passbands 9, a loop oscillograph 11 with a dc amplifier 10, a "white noise" generator, a high-quality amplifier and speakers. The measurements of the reverberation characteristics of the rooms over noise bands which were 1/3 of an octave wide showed that deviations of the quantity $10 \log A$ from the mean value of 13 db did not exceed ± 1.5 db. The loudspeaker was located at the point where the investigated element was situated, and

the microphone was located successively at several points of the chamber in the diffuse sound region. For such insignificant nonuniformities, it is possible to assume with a sufficient degree of accuracy (for practical purposes) that the level of the acoustic power differs from the sound level in a diffuse field by the same amount regardless of the type of spectrum (of course, provided that a sufficiently large number of incoherent components are present in the spectrum so that it is possible to neglect the effect of standing waves). The introduction of corrections which account for the frequency responses of the chambers and the metering apparatus proved unnecessary in practice, since their effect upon the nature of the spectrum and upon the noise level lies within the limits of the accuracy of the measurements (Fig. 2).

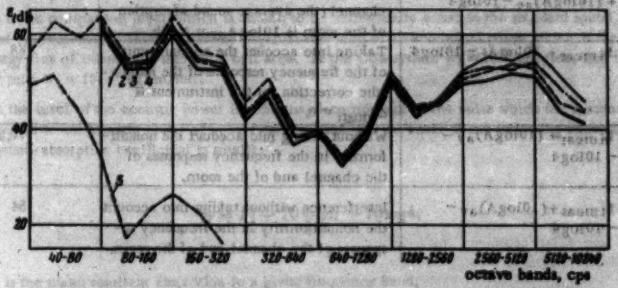

Fig. 2. The effect produced upon the measured spectrum and upon the magnitude of the noise when the frequency characteristics of the room and of the metering equipment are taken into account. The computed resultant noise level takes into account the corrections: $L = 10 \log \Sigma 10^{\frac{L_i \text{ meas} + L_i \text{ instr}}{10}} = 60.5$ db. The measured resultant noise level is: $L_{meas} = 63.5$ db. The measured interference level is $L_{meas} = 48$ db.

The results of the measurements made of the levels and of the spectra at various points in the chambers under the conditions of diffuse sound showed that the nonuniformity with respect to the resultant level is ± 3 db; the nonuniformity at the edges of the spectrum is ± 5 db and is ± 3 db in the center-frequency regions. The ability to duplicate measurements which are made at the same point at different times was fully satisfactory (Fig. 3). All the basic measurements of the acoustic power and of the spectra were performed at the points 6 of Fig. 1 which were located at a height 1.5 m above the floor and at a distance of 1.5 m from the center of the output cross-section of the investigated element. These points were selected on the basis of the following concepts: the level of the direct sound at these points was no less than 6-10 db below the level of the reflected sound and thus, the latter could be neglected*; the distance from the bounding surfaces of the chambers was

*The zone which is sufficiently close to the source so that reflected sound can be neglected and is sufficiently far so that the phase shift between the wave velocity and the acoustic pressure can be neglected (i. e., the zone in which the acoustic pressure is inversely proportional to distance) was determined by measuring the decrease in the noise level as the distance from the source increased (at radii which formed different angles with the axis of the airduct).

At low frequencies (below 100-200 cps) reflections from the floor and other relatively close boundaries could probably affect the accuracy of the measurements adversely. However, since the sounds which contained these frequencies formed a relatively small portion of the investigated noise, the error was not of any great importance.

Curve No.	Computation formula	Conditions	$\epsilon = 10\log \Sigma 10^{\frac{\epsilon_i}{10}}$ db
1	$\epsilon_i = L_{i\,meas} + \Delta L_{i\,instr} + 10\log A_i - 10\log 4$	Taking into account the nonuniformity of the frequency responses of the room and of the channel	68
2	$\epsilon_i = L_{i\,meas} + \Delta L_{i\,instr} + (10\log A)_{av} - 10\log 4$	Taking into account the nonuniformity of the frequency characteristics of the channel (the average sound absorption of the room is $10\log A_{av} = 13$ db.	67.5
3	$\epsilon_i = L_{i\,meas} + 10\log A_i - 10\log 4$	Taking into account the nonuniformity of the frequency response of the room (the correction for the instrument is $\Delta L_{instr} = 0$.	68
4	$\epsilon_i = L_{i\,meas} + (10\log A)_{av} - 10\log 4$	Without taking into account the nonuniformity in the frequency responses of the channel and of the room.	70.5
5	$\epsilon_i = L_{i\,meas} + (10\log A)_{av} - 10\log 4$	Interference without taking into account the nonuniformity in the frequency responses of the channel and of the room.	54

sufficient for one to neglect any local increase of acoustic pressure at a reflecting wall; the levels which were measured at these points corresponded to the averages of measurements made at other points in the majority of cases.

The basic source of interference in the chambers was ventilator noise that penetrated along the duct and also through the bounding surfaces. The level and spectrum of the interference were measured at various points in the chambers when air flow through the investigated element was absent, and for various speeds of the ventilator motor. During the measurements, we observed the condition which required that the level of the measured noise be not less than 5-20 db above the interference level. Measurements in the pumping chamber, in which the interference level was relatively high and in which the frequency of the interference predominantly corresponded to $f \leq 80$ cps, were performed with a high-frequency filter. Since the microphone was located outside of the free jet in the zone of small velocities, there was no need in protecting it from the air stream.

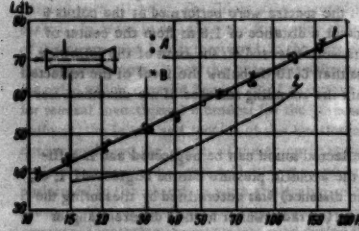

Fig. 3. The ability to duplicate measurements of the noise level which were made for airduct elements at one and the same point in the input chamber at various times. A "70" noise-meter characteristic was used.
1) $L = a + 30\log p$, 2) interference, A) April 4, 1954, B) April 29, 1954.

The frequency characteristics of the differences in chamber levels [these differences in levels were determined by means of measurements at the point 6 (Fig. 1) for a noise which was artificially created in the pumping chamber by a dynamic source while the investigated airduct element was present] showed that the " sound insulation " (approximately 25 db) was sufficient so that the penetration of noise from chamber to chamber could be neglected (taking into account the fact that the noise levels created in them when air flowed through the element were approximately identical).

For the purpose of clarifying the possibility of applying the measurements made of the acoustic power in

chambers to other acoustical conditions, we compared the values of acoustic power and noise spectrum obtained in direct sound and in a diffuse field.

Let us determine the level of the acoustic power by drawing an analogy with the noise level; we shall make use of the expression

$$\varepsilon = 10\log\frac{W}{W_0}, \tag{5}$$

where W_0 is the comparison level (which is chosen to be numerically equal to the standard sound level I_0 for the sake of convenience). Then W_0 has the physical meaning of an acoustical power which is equivalent to a sound energy flux of intensity I_0 through a unit area. In the CGS system $W_0 = 10^{-9}$ erg/sec, and in the engineering system of units $W_0 = 10^{-13}$ kg. m/sec.*

Then the level of the acoustic power in some band-component of the noise which has a measured level (or an acoustic sound pressure level) of L_1 in a diffuse field will be equal to the following expression (when the average sound-absorption coefficient is small):

$$\varepsilon_1 = L_1 + 10\log A_1 - 10\log 4, \tag{6}$$

where A_1 is the mean resultant absorption in a given frequency band.

The level of acoustic power is

$$\varepsilon_1 = 10\log\left(2\pi r^2\left[\int_0^{\pi} 10^{L_{1\,\text{meas}}}\sin\vartheta\,d\vartheta - 2\cdot 10^{L_{1\,\text{dif}}}\right]\right), \tag{7}$$

according to direct-sound measurements (when axial symmetry obtains), where r is the distance between the element and the microphone, ϑ is the angle between the axis of the element and a direction towards the microphone, $L_{1\,\text{meas}}$ is the level of the measured sound component, and $L_{1\,\text{dif}}$ is the level of the reflected sound component.

The over-all acoustic power level is

$$\varepsilon = 10\log\sum_1^n 10^{\frac{\varepsilon_1}{10}} \tag{8}$$

and the sound level in a diffuse field is

$$L = \varepsilon - 10\log A_{av} + 10\log 4. \tag{9}$$

* The numerical values of ε in various systems of units will not be identical due to the difference in the magnitudes of the units used for the area. In this paper we used the engineering system of units.

The results of manipulating the measured noise values according to Formulas (6)-(9) are shown in Fig. 4 for one of the tested elements. The agreement between the acoustic power spectra and levels as determined by the two indicated independent methods is satisfactory as far as engineering applications are concerned.

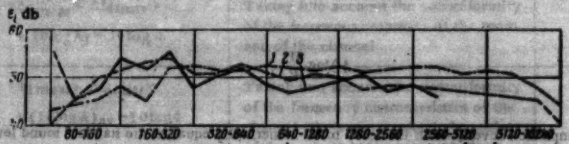

Fig. 4. Spectra of the acoustic power and the noise level of an element, as determined on the basis of measurements made in a diffuse sound field and under conditions where the direct sound predominates. In computing the noise levels according to measurements made in direct sound, corrections are introduced to compensate for the frequency response of the room.

Curve No. 1	Predominant type of sound	Distance from the microphone	Noise level in a diffuse field (db)		Level of the resultant acoustic power
			Measured value	Value computed on the basis of the directivity charac.	
1	Direct	0.5	—	58.5	64
2	Direct	0.75	—	59.5	64.5
3	Diffuse	1.5	59	—	65

High-pressure ejector noise measurements were performed on a unit whose diagram is shown in Fig. 5. The tested ejector had replaceable ejecting nozzles 1 with diameters of 8, 11, 14 and 18 mm; the stream of air passed from these nozzles into the mixing chamber 2 and the diffuser 3. A suction tube 4 with a metering collector 5 and a bank of restrictor diaphragms 6 for changing the grating coefficient are placed at the input to the ejector. Air was fed to the unit from a movable compressor through a flexible hose approximately 100 m long and a system of pipes. The pressure before the ejecting nozzle was controlled by means of a vane in the pipeline at a distance of approximately 5 m from the ejector. The pressure was measured by means of a standard spring manometer. The unit was placed in a laboratory room with dimensions of 17.5 × 7.5 m^2 and a height of 3.6 meters, which had a parquet floor and acoustically untreated walls and ceilings which were plastered and painted with adhesive paint; the room was sparsely filled with aerodynamic equipment made of plywood and metal. Measurements of the level and spectrum of the noise were performed at various points in the room, both in the zones where direct sound predominated, and in a diffuse field. The interference levels from the compressor and from airflow in the grating were determined in advance, and the measurements were performed only at levels which exceeded the interference level by no less than 5 db. In the direct-sound zone, the directivity characteristic * was measured, and the acoustic power was determined by integration over a sphere after subtracting the reflected sound as measured in a diffuse field.

The measurements of the noise in aerodynamic velocity pipes were performed both in open air at points located at various distances from the exhaust shaft and in the diffuse-sound region of rooms.

* After finding a radius which is such that the inverse proportionality between the intensity and the square of the distance is observed, the source could also be assumed to be a point source (this was indicated above).

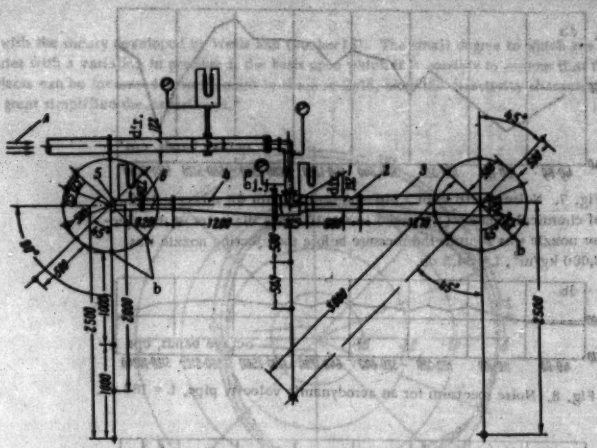

Fig. 5. Diagram of the experimental unit which is used for measuring the noise of a high-pressure ejector:
A) flow from the compressor, B) points at which the noise was measured.

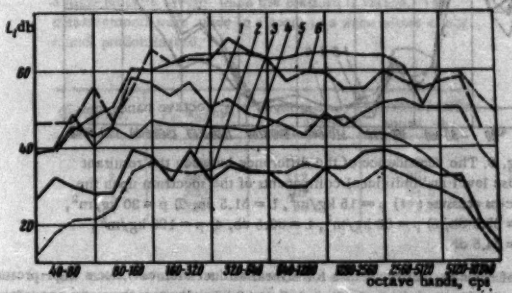

Fig. 6. Noise spectra for certain airduct elements, as measured in a chamber according to a " 70" noise-meter characteristic.

Curve No	Nomenclature of the elements	Pressure in kg/m²	Noise level in db
1	A round terminal funnel	30	48.5
2	A restrictor vane	30	46
3	A round terminal funnel	60	65
4	A restrictor vane	60	59
5	A cabin anemostat	120	75.5
6	A gastight cover	120	74.5

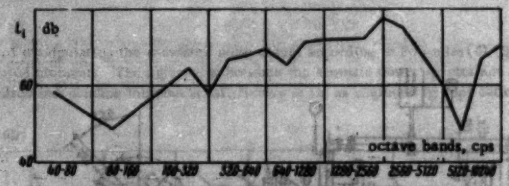

Fig. 7. Noise spectrum of a high-pressure ejector for the ventilation of chemical cabinets (measured in a hall). The diameter of the ejector nozzle was 14 mm, the pressure before the ejecting nozzle was 3,000 kg/m^2, L = 84.5 db.

Fig. 8. Noise spectrum for an aerodynamic velocity pipe, L = 188 db.

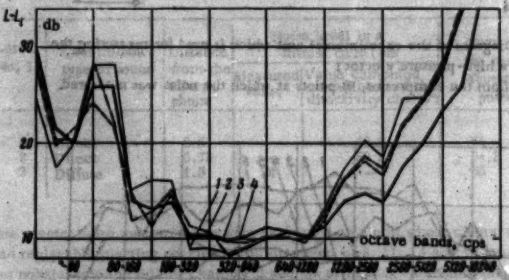

Fig. 9. The dependence of the difference between the resultant noise level and individual components of the spectrum upon the excess pressure: 1) p = 15 kg/m^2, L = 51.5 db, 2) p = 30 kg/m^2, L = 59.5 db, 3) p = 60 kg/m^2, L = 66.5 db, 4) p = 120 kg/m^2, L = 74.5 db.

Typical examples of noise frequency spectra for several airduct elements, for a high-pressure ejector and for an aerodynamic velocity pipe, are shown in Figs. 6, 7 and 8. In all cases the noise occupies an extremely wide region of frequencies, approximating a continuous spectrum with a very flat maximum; when measurements are made with an analyzer having a narrow pass band no substantial discrete components were detected. In almost all cases the noise is of a statistical nature. When the excess pressure p (and therefore, the flow velocity) varies, the energy distribution among the spectrum components varies only insignificantly. Therefore, the difference between the over-all noise level L and the levels of the components L_1 in the bands of the spectrum depend only weakly upon p (Fig. 9). Thus, a substantial variation of the sound level in the investigated objects is not accompanied by a substantial variation of tonality. This result was obtained in measurements which were

The smallness of the spectrum variation when the pressure is varied leads to the conclusion that the directivity characteristic of the noise emanating from the element or from the exhaust shaft of the unit varies little when the pressure varies (Fig. 10; the level at the axis is assumed to be zero). The statistical nature of the noise leads to the conclusion that the directivity (at least for the front hemisphere) is close to being spherical and is

in accord with the theory developed by Wells and Crocker [6]. The small degree to which the directivity characteristic varies with a variation in pressure is the basis upon which it is possible to assume that the acoustic power of such objects can be measured at some point in the free field, once the directivity characteristic has been plotted. This great simplified the experiment.*

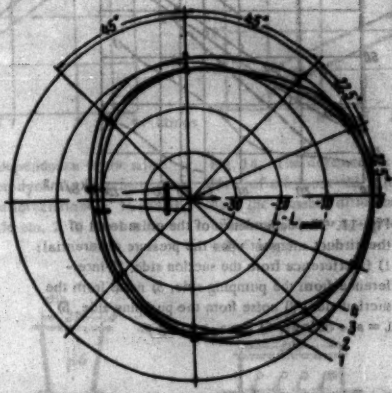

Fig. 10. Directivity characteristic of the noise produced by a high-pressure ejector when the pressure is varied. The measurements were made in a room in a zone where direct sounds predominated.

Curve No.	P_g kg/m²	Level at the L_{max} axis, db	Level of diffuse sound, db
1	7400	118.5	100.5
2	5400	112.5	95
3	3000	101	84.5
4	1800	95.5	77.9

Typical graphs for the noise level as a function of the excess pressure (measured in a diffuse field and in direct sound) for the test objects are given in Figs. 11-14. In the vast majority of cases, the proportionality between the acoustic power and the cube of the excess pressure is closely observed even when the latter quantity is very large (this corresponds to $\alpha = -3$ in Formula (4)). For small excess pressures in elements in which the flow depends upon the Reynolds number deviations from this law are observed in the direction of an increase in the exponent to -2.75 (the acoustic power is proportional to the 5.5-th power of the flow velocity; see Fig. 14). It should be noted that the law based upon the eighth power of the velocity and the fourth power of the pressure (this law assumes that the tangent stresses play the dominant role in producing sound radiation) were not observed in any case involving the investigated objects (see Fig. 11). Evidently, when vortices are formed due to the presence of a solid surface in the stream, or when vortices are formed in the vicinity of such a surface, the radiation of sound is caused by pulsations of normal pressure. A characteristic of such pulsations is

* The indicated concepts applied to objects in which the noise is due to airflow along the ducts and not due to the emergence of a free jet into the atmosphere. In the latter case the directivity characteristic and the other noise parameters may depend upon the velocity and the temperature of the jet [11].

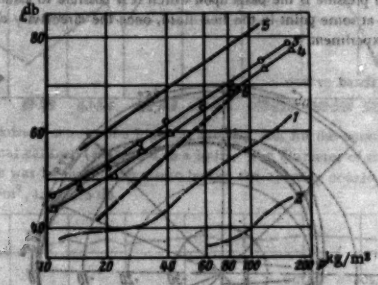

Fig. 11. The dependence of the noise level of the airduct element upon the pressure differential: 1) interference from the suction side, 2) interference from the pumping side, 3) noise from the suction side, 4) noise from the pumping side, 5) $L = a_1 + 30 \log p$, 6) $L = a_2 + 40 \log p$.

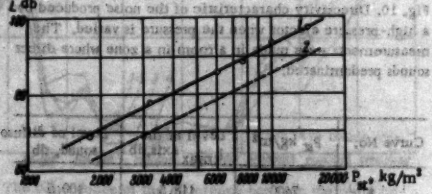

Fig. 12. The dependence of the noise level of a high-pressure ejector upon the excess pressure before the ejecting nozzle: 1) measured level p, 2) $L = a + 30 \log p$.

the proportionality of the acoustic power to the cube of the pressure; at small velocities the acoustic power is proportional to the 6.0-6.5-th power of the stream velocity, depending upon the nature of the streamlining and the Reynolds number (6.0 for autostimulating flow and approximately 5.5, when a dependence upon Re exists). This dependence is characteristic for vortex noise when external streamline flow around the body obtains [2, 8, 12], or for ventilator noise [7], and is often observed for reaction-motor noise when such motors operate in a regime of quiet combustion [10], although abroad the eighth-power velocity relationship [11] is considered to be more characteristic.

The predominant role of the pulsations of normal pressure which cause the acoustic power to be proportional to the cube of the pressure can be explained by the fact that the transverse pulsation forces which act upon the body when vortices are formed in its wake are of the order of the forces of head-on resistance [15] and are due to the normal pressure. The mechanism of the boundary layer (or of the frictional forces), which is due to the viscosity, only plays the role of a "valve" in the self-oscillatory process of forming vortices in the wake of the

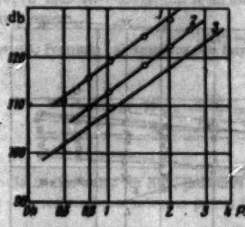

Fig. 13. The dependence of the noise level in an aerodynamic pipe upon the pressure in the forechamber: 1) nozzle No 1, 2) nozzle No. 2, 3) L = a + 30 log p.

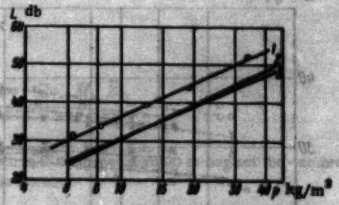

Fig. 14. The dependence of the noise level of a 3.3 cm-thick layer of gravel upon the pressure differential:) measured level, 2) L = a₁ + 30 log p, 3) L = a₂ + 27.5 log p.

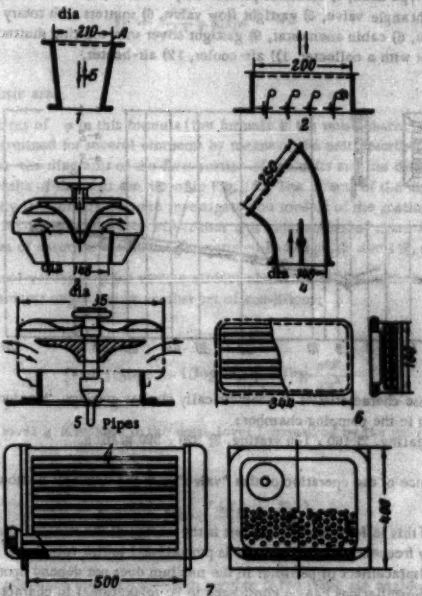

Fig. 15. Diagrams of the flow portion of certain of the tested airduct elements:
1) round terminal funnel, 2) hinged shutters, 3) "mushroom"-type head, 4) pitcher-shaped rotatable funnel, 5) anemostat, 6) gastight cover, 7) air-cooler, A) grating, B) direction of air motion.

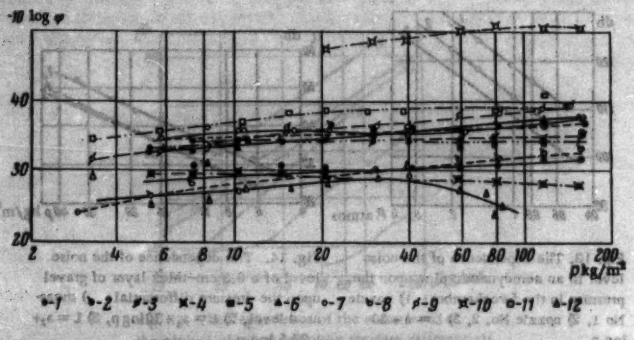

Fig. 16. Noise characteristics of certain tested elements of ventilation airducts: 1)" mushroom"-type head, 2) terminal pitcher-shaped funnel, 3) round terminal funnel, 4) gastight angle valve, 5) gastight flow valve, 6) shutters with rotary blades, 7) restrictor vane, 8) cabin anemostat, 9) gastight cover with rotating shutters, 10) rectilinear sector with a collector, 11) air-cooler, 12) air-heater.

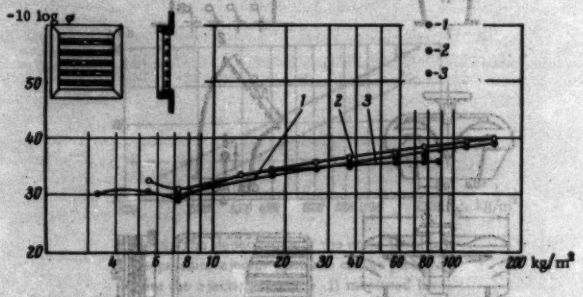

Fig. 17. Noise characteristics of geometrically similar gratings. Measurements taken in the pumping chamber: 1) 80 x 80 grating, 2) 160 x 160 grating, 3) 320 x 320 grating.

solid body.* The dependence of the operation of this "valve" upon the Reynolds number, in our opinion, is the

* The energy source of this self-oscillatory process is the energy of the stream. Since for a case of external streamlining the breakaway frequency for the vortices is proportional to the velocity of the stream at infinity, and the amplitude of the displacement of particles in the medium does not depend upon the velocity (neglecting the effect of Re), these self-oscillations can be considered to be relaxational in character. The part of a "reservoir" is played by the alternating circulation of the velocity vector around the streamlined body (for the case of a staggered vortex wake the amplitude of this circulation is equal to one-half of the circulation of the run-off vortices). An increase in the circulation leads to an increase in the pressure gradients on the surface of the body and in its vicinity (these gradients play the part of "feedback") which is such that periodic breakaways of the boundary layer occur alternately on the two sides of the body and a change in the form of flow occurs which is accompanied by a formation of vortices in accordance with the Thompson theorem.

cause of the above-indicated deviations from the law which states that the acoustical power is proportional to the cube of the pressure.

When $\alpha = -3$, Formula (4) acquires the form:

$$W = \frac{p^3 D^2}{\rho c^2} \varphi_3 \left(\text{shape}, \ \mathrm{Re}, \ M, \ \bar{Z} \right). \tag{10}$$

This formula is also valid for high pressures for which it is no longer possible to neglect the compressibility. Then ρ and c are referred to analogous points in similar systems.

Since the law stating that the acoustical pressure is proportional to the third power of the pressure is satisfactorily observed both at small pressures and at large pressures, and since the acoustical power is practically independent of the room in which the element operates, the dependence of the acoustical power upon Re, M and $\bar{Z}$ in Equation (10) can also be neglected for such autosimulating types of flow when making a number of practical computations:

$$W = \frac{p^3 F}{\rho c^2} \varphi \ \text{shape} \quad **, \tag{11}$$

where F is the characteristic area.

The similarity constants of φ in this formula (the formula is the noise characteristic of the airduct element) were experimentally determined for several elements by means of the unit described above. The elements had varying geometric shapes; the diagrams of the flow portion of the units and the dimensions of some of them are given in Fig. 15. The results of the tests are shown in Fig. 16. The effects of the dimensions of the element (when geometric similarity is maintained) were investigated on models of the gratings. The experiments verified (Fig. 17) the theoretical postulates to the effect that φ is independent of size. An analogous result was obtained for the vortex noise of external streamline flow around bodies [2, 3, and 12], and for ventilator noise [7].

Knowing the numerical values of φ for various airduct elements, it is possible to compute the level of noise created by such elements under one or another set of conditions:

$$L_s = 10 \log \varphi - 10 \log W_0 + 10 \log \frac{p^3 F}{\rho c^2}. \tag{12}$$

The acoustic power level L_s is related to the noise level L measured by the microphone by the following expression:

$$L \approx L_s + 10 \log \left(\frac{4K_1}{A} + \frac{K_2}{\Omega r^2} \right), \tag{13}$$

** Neglecting the dependence upon the Reynolds number is the same as neglecting the deviation of the exponent m from three. This yields an error of $\Delta L = 10 \log (p/p_0)^{3-m}$, in computing the sound level, where p_0 is the pressure for which φ was determined. For example, when $m = 2.75$ and when the variation in the pressure is equal to a factor of 10 the error is only ~3db (see Fig. 14).

where A is the average total absorption of the room; r is the distance from the observer to the output aperture of the pipeline; Ω is the angle of radiation in steradians; K_1 and K_2 are coefficients which respectively take into account the nonuniformity of the sound energy in a diffuse field and the directivity of the sound radiation.

Formulas (12) and (13) can be used for any noise band if φ is assumed to represent the noise characteristic as normalized to the given band.

The author is deeply indebted to N. N. Andreev for a number of very valuable comments which aided in the writing of this paper, to L. G. Rusakov for his advice in performing the experiments and to L. A. Grafskom for his help in doing the research.

LITERATURE CITED

[1] E. A. Nepomniashchii, Investigation and Computation of the Sound Produced by an Air Screw. Proceedings of the Central Aerodynamics Institute, No. 39, 1941.

[2] E. Ia. Iudin, "The vortex sound produced by rotating rods," J. Tech. Phys. (USSR) 14, 9 (1944).

[3] M. Y. Lighthill, "On sound generated aerodynamically," Proc. Roy. Soc. (London) A) I,. 211, 1107, 564 (1952); II, 222, 1148, 1 (1954).

[4] D. J. Stewart and G. F. Drake, "The noise characteristics of air supply outlets," Heating, Piping, Air Conditioning, 9, 1, 65-70 (1937).

[5] S. P. Strelkov et. al., Pulsations in Aerodynamic Pipes and Methods of Damping Them, Transactions of the Central Aerohydrodynamical Institute, No. 593, 1946.

[6] R. J. Wells and B. E. Crocker, "Sound radiation patterns of gas exhaust stocks," J. Acoust. Soc. Am. 25, 3, 433 (1953).

[7] E. Ia. Iudin, "Ventilator noise," Collection. Industrial Aerodynamics, S. A. Dovzhik, Editor (1944).

[8] E. Z. Stowell and A. F. Deming, Vortex Noise from Rotating Cylindrical Rods, NACA TN 1935, No. 619.

[9] Heating, Ventilating, Air Conditioning Guide, 29, (New York, 1951) p. 865.

[10] H. H. Hubbard and L. W. Lassiter, "Experimental studies of jet noise," J. Acoust. Soc. Am. 25, 3, 412 (1953).

[11] A. Powell, "A survey of experiments on jet noise," Aircraft Engr. 26, 299.2 (1951).

[12] D. I. Blokhintsev, The Acoustics of An Inhomogeneous Moving Medium (Moscow-Leningrad, 1946).

[13] L. Ia. Gutin, "The acoustic field of a rotating air screw" J. Tech. Phys. (USSR) 6, 5 (1936).

[14] G. Lamb, Hydrodynamics, sect. 291, 1947 (Translated from the 6th Edition, 1932).

[15] L. Kh. Bliumina and Iu. G. Zakharov "The investigation of the vibration of cylindrical bodies in an air stream," Collection Industrial Aerodynamics, No. 5, Central Aerohydrodynamical Institute 1954.

Affiliate of the N. E. Zhukovskii
Central Aerohydrodynamics Institute, Moscow

Received May 25, 1955

BIBLIOGRAPHY

E. G. Weaver and M. Lawrence, Physiological Acoustics (Princeton University Press, 1954). 454 pp.

Physiological Acoustics has been considerably developed during the last two decades as a part of biophysics. This is due to many causes of which we shall especially note three: the needs of medicine, the requirements of all kinds of auditory communication, and the development of the methodology of biophysical measurements (both in the field of physiology generally and in the physiology of hearing in particular).

This book is limited solely to one part of physiological acoustics: the human auditory organ. There is not a word about the speech organ; there is not a chapter on the auditory organs of various classes of animals and their organs of sound formation. Therefore, the title of this book proved to be broader than its contents.

There are seven parts to the book: the first part contains a description of the ear's structure, a development of the fundamentals of acoustics which the authors deem necessary for the subsequent parts of the book, and information concerning the sharpness of human hearing. In comparison with other similar books there is little new here; however, it must be noted that the presentation of the methods for measuring biopotentials of the cochlea was a welcome innovation (this was the most important achievement of metering methodology in this field during the past decade, and the former of the authors made a basic contribution to the creation of this methodology).

The second portion of the book examines the middle ear and views it as a transformer which receives pressures from an external medium. The authors strive to give not only a qualitative picture of the transformation, but also provide a physical computation of it; such an approach makes their book compare very favorably with many books which have been published previously.

The third portion analyzes the investigation of the distortion which is caused by the properties of the middle ear (the middle ear is again viewed as a mechanical transformer). The analysis is made in a long-established manner: linear distortion and the distortion due to intense sounds are assumed due to the nonlinearities of the middle-ear mechanism. The excellent papers by Bekeshe and the personal papers of the authors are widely utilized; the old works of Helmholtz have not been forgotten either.

In general, we must acknowledge the high quality and the modern approach which stand out in this book, both with regard to the selection of material and in the quality of presentation. It can be said that the authors have been able to deeply and critically survey those distortion theories (in particular, the appearance of modulation currents) which have reigned up to this time, in broad circles of otologists and which still remain under the aegis of Helmholtz's name. The authors clearly and definitively indicate that nonlinear distortion can be explained in terms of the nonlinearities of the middle ear only for cases of large pressure amplitudes; in order to explain nonlinear distortion for small pressures it is necessary to examine the processes which go on in the nerves.

Part IV is devoted to problems involving the functioning of the ear-drum musculature and to constant-pressure effects. Both problems are essential in practice.

Part V provides information on the behavior of the cochlea; in accordance with the essential significance of this organ almost one-fourth of the entire book is devoted to it; the basic material deals with the mechanical behavior of the organ, and only approximately 20 pages are devoted to an examination of the next-to-last stage — the stimulation of the auditory nerves. The last stage — the processing of arriving nerve pulses — is not examined at all in this book. However, the author of this book review is convinced that such fundamental auditory problems as the binaural effect, the sharpness of musical hearing and others, cannot be solved without taking into

account the processes which are carried out in the brain, nor without taking into account the synaptic connections between nerve fibers. We cannot blame the authors for not dealing with such problems: the study of them is only beginning.

In part VI the authors develop certain clinical applications of the material which they have presented in the preceding parts. This chapter is useful to otologists, especially because we find in it not only a description of the phenomena accompanying autosclerosis, but also an explanation of the recently introduced method of its surgical correction (fenestration).

Part VII contains information on modern theory concerning the auditory organ. At the present time there are many works which have been written along this direction and these works attempt (and successfully so) to perform a computation of at least the mechanical portion of the auditory organ. The authors have limited themselves solely to a general description of the principles which are used in these works; however, their presentation of this is masterful.

In the foreword, some very valuable material on physiological acoustics is given: data concerning all of the presently known parameters which characterize the mechanical section of the ear, as well as some information concerning the auditory nerve. A very complete bibliography is also given here.

In general we conclude that here we have a book which is a very high-quality monograph and which is very necessary. Undoubtedly it should be translated into Russian as soon as possible. The only book in Russian which is available on this subject is titled "Hearing and Speech in the Light of Modern Physical Research" and was written by S. N. Rzhevkin approximately 20 years ago. That book is thus extremely outdated, and the need for an up-to-date book of this nature in the USSR is great.

N. N. Andreev

CHRONICLE

ACOUSTICS CONFERENCE FOR 1956

The Acoustics Commission of the Acad. Sci. USSR is calling a regular expanded conference for 1956, at which there will be section sessions as weill as plenary sessions (the sections will include physical acoustics, ultrasonics, electroacoustics, physiological acoustics, et. al.)

The conference is scheduled to be held in Leningrad in the fall of 1956.

In order to have a more accurate idea of the number and composition of sections, the Acoustics Commission requests institutions and individuals desiring to present papers at this conference to inform the Commission of this (Moscow V-134, p/ia 1578) not later than April.1956.

accounts for processes which are carried out in the brain. Any attempt finding into so-called 'synaptic connections' between nerve fibers ... we cannot blame the authors for not dealing with such problems; the study of these is only beginning.

In part, I find a rather severe critical appraisal of the material which they have presented in the preceding pages. This character is easily recognizable in the volume we find to it is not only a description of the phenomena accompanying acoustomotor, but also an exploration of the recently introduced method of its objective observation (conditioning).

CHRONICLE

ACOUSTICS CONFERENCE FOR 1956

The Acoustics Committee of the Acad. Sci. USSR is calling a regular expanded conference for 1956 at which time will be devoted especially at plenary session (the location will include physical acoustics, ultrasonics, electroacoustics, physiological acoustics, et. al.)

The conference is scheduled to be held in January in the fall of 1956.

In order to have a more accurate idea of the number and composition of sections, the Acoustics Committee requests institutions and individuals desiring to present papers at this conference to inform the Committee of this (Moscow V-164, pl.Ia 15/6) not later than April 1956.

SOVIET PHYSICS – ACOUSTICS VOL. 1, Nos. 3, 4 July-December, 1955

(Published by the American Institute of Physics November, 1957).

CONTENTS Vol. 1, No. 3

	Page	Russian Page
N. N. Andreev (on his 75th birthday)	209	195
Motion Picture Theater Loudspeaker with Scattering Sound Lens. B. G. Belkin	214	200
On Surface Waves Launched in the Ocean by Underwater Earthquakes. Iu. L. Gazarian	217	203
Capacitive Analyzer for Sound Field. V. A. Zverev, V. M. Bokov and I. E. Lur'e	232	218
Solution of Inverse Problem of Geometric Acoustics. B. E. Kinber	235	221
Radiation of Sound from Vibrating Faces of an Arbitrary Wedge. Part II. G. D. Maliuzhinets	240	226
Investigation of the Propagation of Ultrasonic Waves in the Critical Region of a Liquid-Vapor System. V. F. Nozdrev	249	235
Devices to Protect Hearing Against Harmful Effects of Noise. I. M. Polkovskii	262	249
On the Design of a Ribbon Microphone. A. V. Rimskii-Korsakov	270	257
Temperature Dependence of Electrostriction and Elastic Properties of Ceramic Barium Titanate. N. A. Roi	278	264
Equivalent Circuits of Elements of Vibrating Systems with Distributed Constants. I. G. Rusakov	286	272
Production of Ultrasonic Radiation of Constant Intensity when Sounding in a Vessel with an Untuned Bottom. L. V. Skarda	288	274
Secondary Field in Sterophonic Twin-Channel Transmission and Certain Fixed Positions of the Source of Sound in the Primary Field. P. G. Tager	300	288
Chronicle		
Conference on Electroacoustics	308	294

CONTENTS Vol. 1, No. 4

Survey of Methods for Evaluating and Measuring the Diffuseness of a Sound Field. V. V. Furduev	312	299
The Measurement of Sound Attenuation in a Surface Isothermal Layer of Water. A. N. Barkhatov	327	315
The Intensity of Harmonic and Modulation Components when Waves of Complex Shape are Nonlinearly Distorted. V. M. Vol'f	334	321
On the Measurement of the Correlation Coefficient. S. G. Gershman and E. L. Feinberg	340	326

(continued on following page)

SOVIET PHYSICS - ACOUSTICS VOL. 1, Nos. 3, 4 July-December, 1955

CONTENTS (continued)

(Published by the American Institute of Physics November, 1957)

	Page	Russian Page
On the Problem of Mutual Interaction Between Soundwaves, A. G. Gorelik and V. A. Zverev	353	339
The Application of a Composite Piezoelectric Dipole in Investigating the Mechanical Properties of Polymers, I. G. Mikhailov and V. A. Solov'ev	358	343
An Electronic-Acoustical Transducer for the Visualization of Sound Images P. K. Oshchepkov, L. D. Rozenberg and Iu. B. Semennikov	362	348
The Dependence of the Coercive Force and the Permittivity of Ceramic Barium Titanate upon Mechanical Stresses, N. A. Roi	366	352
Method for Measuring the Mechanical Parameters of Rubber at Sonic and Ultrasonic Frequencies, V. V. Tiutekin	370	356
Method for Measuring Acoustical Impedance on the Basis of Measuring the Geometric Difference Between Sound Pressures, V. N. Fedorovich	374	360
The Acoustic Power of the Noise Created by Airduct Elements, E. Ia. Iudin	383	368
Bibliography	399	383
Chronicle		
Acoustics Conference for 1956	401	384

(continued on following page)

The expanded program of the American Institute of Physics comprises translation of four leading Soviet physics journals, as listed below. These translations, by competent, qualified scientists, will provide all research laboratories and libraries with accurate and up-to-date information of the results of research in the U.S.S.R.

Soviet Physics — Technical Physics

A translation of the "Journal of Technical Physics" of the Academy of Sciences of the U.S.S.R. The 1956 volume, which was originally announced as containing eighteen issues, is instead being issued monthly, in expanded issues. All issues of the original Russian journal for 1956 will be translated. Approximately 4,000 Russian pages. Annually, $80.00 domestic, $93.00 foreign.

Soviet Physics — Acoustics

A translation of the "Journal of Acoustics" of the Academy of Sciences of the U.S.S.R. Four issues per year, approximately 500 Russian pages. Annually, $20.00 domestic, $22.00 foreign. The 1955 issues of "Journal of Acoustics" U.S.S.R. will also be published. Will consist of two volumes, approximately 500 pages, and the subscription price will be $20.00 for the set.

Soviet Physics "Doklady"

A translation of the "Physics Section" of the Proceedings of the Academy of Sciences of the U.S.S.R. Six issues per year, approximately 900 Russian pages. Annually $25.00 domestic, $27.50 foreign.

Soviet Physics — JETP

A translation of the "Journal of Experimental and Theoretical Physics" of the Academy of Sciences of the U.S.S.R. Twelve issues per year, approximately 2,600 Russian pages. Annually $60.00 domestic, $64.00 foreign. Back issues of Volume 1 and 2 are available at a special price of $50.00 for both to subscribers to Volume 3.

Subscriptions should be addressed to the American Institute of Physics, 335 East 45th Street, New York 17, N. Y.